UNIVERSIDAD COMPLUTENSE DE MADRID
FACULTAD DE CIENCIAS QUÍMICAS
Departamento de Química Orgánica

SOBRE LA SÍNTESIS, ESTRUCTURA Y REACTIVAD DE COMPLEJOS METAL-CARBENO: UN ESTUDIO TEÓRICO-EXPERIMENTAL

TESIS DOCTORAL

ISRAEL FERNÁNDEZ LÓPEZ

Madrid, 2005

Sobre la Síntesis, Estructura y Reactividad de Complejos Metal-Carbeno: un Estudio Teórico-Experimental

MEMORIA que para optar al grado de

DOCTOR EN CIENCIAS QUÍMICAS

presenta

ISRAEL FERNÁNDEZ LÓPEZ

Madrid, 2005

D. Miguel Ángel Sierra Rodríguez, Profesor Titular de Química Orgánica, y **Dña. María José Mancheño Real**, Profesora Contratada-Doctora de Química Orgánica, de la Facultad de Ciencias Químicas de la Universidad Complutense de Madrid,

CERTIFICAN:

Que la presente Memoria, titulada: **SOBRE LA SÍNTESIS, ESTRUCTURA Y REACTIVAD DE COMPLEJOS METAL-CARBENO: UN ESTUDIO TEÓRICO-EXPERIMENTAL**, se ha realizado bajo su dirección en el Departamento de Química Orgánica de la Facultad de Ciencias Químicas de la Universidad Complutense de Madrid por el Licenciado en Ciencias Químicas **D. Israel Fernández López**, y autorizan su presentación para ser calificada como Tesis Doctoral.

Madrid, 20 de Enero de 2005

Fdo. D. Miguel A. Sierra

Fdo. Dª María J. Mancheño

A Laura, a mi familia.

A Juan Carlos.

“Con el conocimiento se acrecientan las dudas”

Goethe

Esta Tesis Doctoral se ha realizado en el Departamento de Química Orgánica de la Facultad de Ciencias Químicas de la Universidad Complutense de Madrid bajo la dirección del Prof. Miguel Ángel Sierra, a quien quiero agradecer su apoyo, disponibilidad, confianza en mí y sobre todo, lo mucho que me ha transmitido, tanto química como personalmente.

También quiero agradecer a la Prof. María José Mancheño, codirectora de este trabajo, por su entusiasmo en todo lo que hemos hecho y sobre todo, por el cariño con el que siempre me ha tratado. Por supuesto, agradezco a la Prof. Mar Gómez-Gallego y al Prof. Santiago Romano su entrega, disponibilidad y su constante interés en mi formación.

Esta Tesis Doctoral se ha llevado a cabo gracias a una beca predoctoral (FPU) del MEC desde abril de 2001 hasta abril de 2005. Durante este período he realizado una estancia corta en el laboratorio del Prof. Fernando P. Cossío (Universidad del País Vasco, UPV-EHU, San Sebastián-Donostia, junio-agosto 2002), a quien quiero agradecer, junto a las Profs. Ana Arrieta y Begoña Lecea y a todo su grupo de investigación, su cariñosa acogida, su estrecha colaboración con nosotros, el poco *euskara* que sé y la mucha química que me habéis enseñado. *Eskerrik asko!*.

Quiero agradecer al Dr. Jesús J. Barbero (CIB-CSIC), al Prof. Roberto Martínez (UCM), al Prof. W. Wulff (Michigan State University) y a la Dra. Susagna Ricart (CSIC) su colaboración en la realización de este trabajo.

Este trabajo está especialmente dedicado al Dr. Juan Carlos del Amo, una de las personas más buenas que jamás he conocido. Siempre estaré en deuda contigo por todo lo que me has enseñado y sobre todo, por tu amistad.

Agradezco sinceramente a todos mis compañeros de laboratorio, pasados y presentes, su amistad, su infinita paciencia y todos los ratos, tanto los buenos como los no tan buenos, que hemos pasado juntos. También quiero agradecer a Andrés su amistad y cariño desde que empezamos nuestro camino como químicos.

Por supuesto, quiero agradecer a Laura y a mi familia su apoyo, comprensión y constante preocupación por mí durante todo el tiempo.

El trabajo recogido en esta memoria ha sido financiado por los proyectos del MEC PB97-0323, del MCyT BQU2001-1283, del MEC y de la Comisión Europea 2FD97-0314 y de la CAM 07M/0043/2002, a los que quiero expresar nuestro agradecimiento. Asimismo, agradezco a Johnson Mathey PLC la aportación gratuita de catalizadores de paladio realizada a nuestro grupo de investigación.

Hasta el momento de redactar esta memoria, parte de los resultados aquí presentados se encuentran recogidos en las siguientes publicaciones:

"A Theoretical-Experimental Approach to the Mechanism of the Photocarbonylation of Chromium(0) (Fischer)-Carbene Complexes and Their Reaction with Imines"
A. Arrieta, F. P. Cossío, I. Fernández, M. Gómez-Gallego, B. Lecea, M. J. Mancheño, M. A Sierra, *J. Am. Chem. Soc*. **2000**, *122*, 11509.

"Synthesis of Cyclophanic Chromium(0) Bis(carbene) Complexes"
I. Fernández, M. A. Sierra, M. J. Mancheño, M. Gómez-Gallego, S. Ricart, *Organometallics* **2001**, *20*, 4304.

"New Rearrangement and Fragmentation Processes of Alkoxyalkynyl (Fischer) Carbene Complexes Induced by Aromatic Diamines"
M. A. Sierra, M. J. Mancheño, J. C. del Amo, I. Fernández, M. Gómez-Gallego, M. R. Torres, *Organometallics* **2003**, *22*, 384.

"Synthesis and Electrochemical Properties of Novel Tetrametallic Macrocyclic Fischer Carbene Complexes"
I. Fernández, M. J. Mancheño, M. Gómez-Gallego, M. A. Sierra, *Org. Lett.* **2003**, *5*, 1237.

"Unexpected Reaction Pathways in the Reaction of Alkoxyalkynylchromium(0) Carbenes with Aromatic Dinucleophiles"
M. A. Sierra, M. J. Mancheño, J. C. Del Amo, I. Fernández, M. Gómez-Gallego, *Chem. Eur. J*. **2003**, *9*, 4943.

"Light-Induced Aminocarbene to Imine Dyotropic Rearrangement in a Chromium(0) Center: An Unprecedented Reaction Pathway"
M. A. Sierra, I. Fernández, M. J. Mancheño, M. Gómez-Gallego, M. R. Torres, F. P. Cossío, A. Arrieta, B. Lecea, A. Poveda, J. Jiménez-Barbero*, J. Am. Chem. Soc*. **2003**, *125,* 9572.

"Structure and Conformations of Heteroatom-Substituted Free Carbenes and their Group 6 Transition Metal Analogues"
I. Fernández, F. P. Cossío, A. Arrieta, B. Lecea, M. J. Mancheño, M. A. Sierra, *Organometallics* **2004**, *23,* 1065.

"Chromium Imidate Complexes from the Metathesis-Like Reaction of Phosphinimines and Chromium(0) Fischer Carbene Complexes"

I. Fernández, M. J. Mancheño, M. Gómez-Gallego, M. A. Sierra, T. Lejon, L. K. Hansen, *Organometallics* **2004**, *23,* 1851.

"ESI Mass Spectrometry as a Tool for the Study of Electron Transfer in Nonconventional Media: The Case of Bi- and Polymetallic Carbene Complexes"

R. Martínez-Álvarez, M. Gómez-Gallego, I. Fernández, M. J. Mancheño, M. A. Sierra*,* *Organometallics* **2004***,* 23, 4647.

"Computational and Experimental Studies on the Mechanism of the Photochemical Carbonylation of Group 6 Fischer Carbene Complexes"

I. Fernández, M. A. Sierra, M. J. Mancheño, M. Gómez-Gallego, F. P. Cossío, *Chem. Eur. J.* enviado para su publicación.

"ESI Mass Spectrometry Study of the Intimate Mechanism of a Gas-Phase Organometallic Reaction by Selective Deuterium Labeling"

W. D. Wulff, K. A. Korthals, R. Martínez-Álvarez, M. Gómez-Gallego, I. Fernández, M. A. Sierra, *J. Org. Chem.* enviado para su publicación.

ÍNDICE

La presente memoria del trabajo de la Tesis Doctoral se ha escrito siguiendo el formato de publicaciones. Incluye, además de una introducción general detallada sobre el estado actual del área de investigación en la que se enmarca este trabajo, una discusión integradora de los resultados obtenidos. Los dos capítulos principales se han subdividido según las distintas publicaciones y apartados de resultados no publicados en el momento de la redacción de la memoria. Los capítulos publicados conservan su formato original en inglés mientras que el resto se ha escrito en castellano. Con el fin de respetar al máximo las diferentes publicaciones, se ha mantenido también la bibliografía y numeración originales de las mismas.

La memoria adjunta un CD en el que se han incluido todas las coordenadas cartesianas y energías totales de todos los puntos estacionarios mencionados en esta memoria, obtenidos mediante métodos computacionales.

INTRODUCCIÓN GENERAL

I. INTRODUCCIÓN

La bondad de las nuevas metodologías en síntesis orgánica se evalúa en la actualidad no sólo en términos de selectividad en todas sus facetas, sino también en términos de eficacia y economía molecular. En este sentido, los complejos de metales de transición se convierten en candidatos ideales para su aplicación a la síntesis orgánica del siglo XXI. La mayor parte de las reacciones organometálicas son altamente específicas, capaces de discriminar entre lugares con reactividades muy similares dentro de una misma molécula y adicionalmente, la elección cuidadosa del metal, de los ligandos y de los distintos sustratos permite realizar procesos en cascada, creando más de un enlace en la misma etapa de reacción con el consiguiente aumento de la complejidad molecular.

Los complejos metal-carbeno de tipo Fischer se han convertido, desde su descubrimiento,[1] en compuestos versátiles en síntesis orgánica. Esto se debe a la gran variedad de reacciones, tanto térmicas como fotoquímicas, que son capaces de experimentar.[2] Reacciones tales como la benzoanelación de Dötz (Esquema 1) o la generación fotoquímica de cetenas coordinadas a cromo (Esquema 2) son hoy en día herramientas habituales en síntesis.

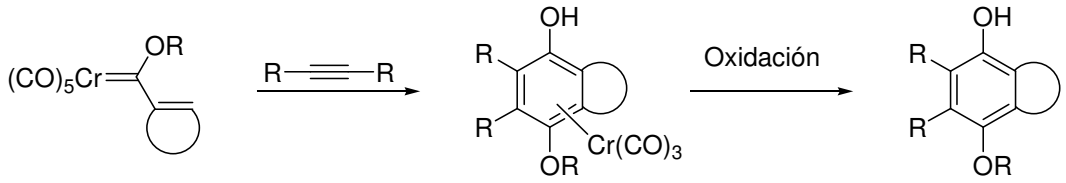

Esquema 1

[1] Fischer, E. O.; Maasböl, A. *Angew. Chem. Int. Ed. Engl.* **1964**, *3*, 580.

[2] (a) Casey, C. P. en *Transition Metal Organometallics in Organic Synthesis*, vol. 1, Alper H. Ed. Academic Press, New York, 1976, pág. 190. (b) Dötz, K. H. en *Transition Metal Carbene Complexes*, Fischer, H.; Hofmann, P.; Kreissl, F. R.; Schubert, U.; Weiss, K. Ed. Verlag Chemie: Weinheim, 1983. (c) Dötz, K. H. *Angew. Chem. Int. Ed. Eng.* **1984**, *23*, 587. (d) Wulff, W. D. en *Comprehensive Organic Synthesis*, Trost, B. M.; Fleming, I., Eds.; Pergamon Press: Oxford, 1991, vol. 5, pág. 1065. (e) Wulff, W. D. en *Comprehensive Organometallic Chemistry II*, Abel, E. W.; Stone, F. G. A.; Wilkinson, G., Eds.; Pergamon Press: Oxford, 1995, vol. 12, pág. 469. (f) Harvey, D. F.; Sigano, D. M. *Chem. Rev.* **1996**, *96*, 271. (g) Aumann, R.; Nienaber, H. *Adv. Organomet. Chem.* **1997**, *41*, 163. (h) de Meijere, A.; Schirmer, H.; Duetsch, M. *Angew. Chem. Int. Ed.* **2000**, *39*, 3964. (i) Aumann, R. *Eur. J. Org. Chem.* **2000**, 17. (j) Sierra, M. A. *Chem. Rev.* **2000,** *100*, 3591. (k) Barluenga, J.; Flórez, J.; Fañanás, J. *J. Organomet. Chem.* **2001**, *624*, 5. (l) Barluenga, J.; Santamaría, J.; Tomás, M. *Chem. Rev.* **2004**, *104*, 2259. (m) Gómez-Gallego, M.; Mancheño, M. J.; Sierra, M. A. *Acc. Chem. Res.* **2005**, en prensa.

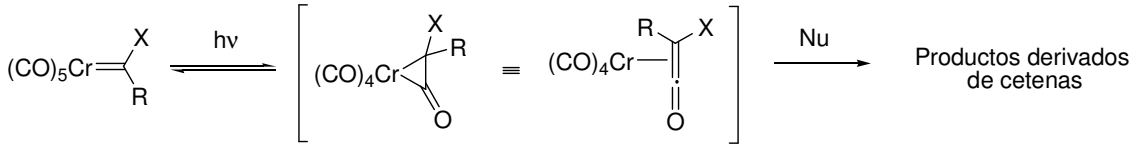

Esquema 2

I.1. Estructura y síntesis de complejos metal-carbeno

Se denomina carbeno a una especie carbonada divalente y neutra que sólo dispone de seis electrones en su capa de valencia, lo que le genera una deficiencia de carga. Los sustratos que poseen este grupo funcional son extraordinariamente reactivos por lo que se les considera intermedios sintéticos. Entre las reacciones más características de un carbeno destacan las ciclopropanaciones, las inserciones en enlaces C–H y la formación de iluros (Esquema 3). La reactividad de los carbenos está fuertemente influenciada por las propiedades electrónicas de sus sustituyentes. Así, estas especies se pueden estabilizar mediante la presencia de heteroátomos directamente unidos al carbono carbénico, que compensan su deficiencia de carga por deslocalización electrónica. Por otro lado, los carbenos pueden estabilizarse cuando se encuentran como ligandos en la esfera de coordinación de un metal de transición.

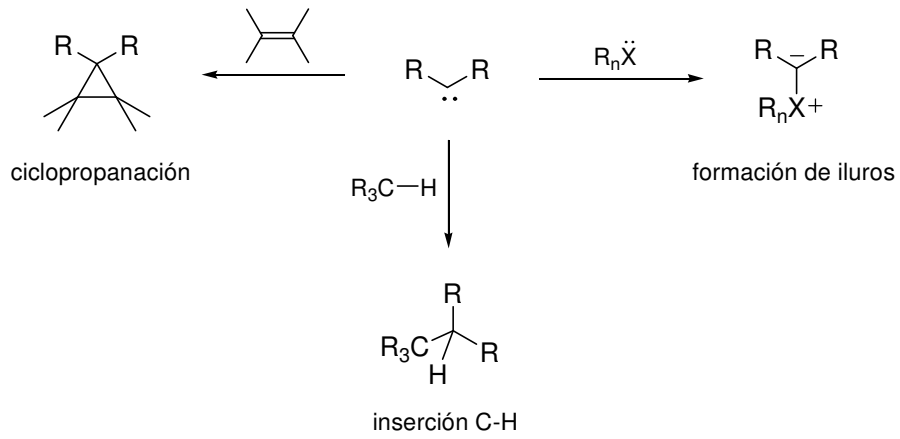

Esquema 3

I.1.1. Tipos de complejos metal-carbeno

Los complejos de metales de transición con un ligando carbeno en su estructura se denominan genéricamente complejos metal-carbeno. De modo general, la unión entre el metal y el ligando carbeno en un complejo metal-carbeno consiste en un enlace dador de tipo σ del ligando al metal y un enlace π, que se establece por retrodonación desde un orbital d ocupado del metal hacia el LUMO del ligando carbeno (Figura 1).

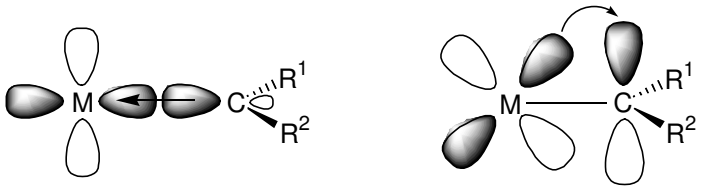

Figura 1

Así, los complejos metal-carbeno se pueden clasificar en varios grupos, en función de la capacidad del metal para aceptar electrones σ procedentes del ligando carbeno y de su capacidad de retrodonación π al orbital p vacío del carbono carbenoide. De este modo, se podrían considerar cuatro tipos de complejos metal-carbeno en función de las propiedades electrónicas del fragmento metálico:

1. Buen aceptor σ y buen retrodonador π
2. Pobre aceptor σ y buen retrodonador π
3. Buen aceptor σ y pobre retrodonador π
4. Pobre aceptor σ y pobre retrodonador π

Al primer tipo pertenecen los denominados carbenos de tipo Schrock, que se caracterizan por tener un enlace C=M fuerte y en el que el carbono carbenoide resulta ser nucleófilo. En el segundo tipo se encuentran los catalizadores de Grubbs, empleados en reacciones de metátesis de olefinas, que también tienen carácter nucleófilo aunque presentan un enlace C=M más débil. Dentro del tercer grupo se encontrarían los carbenos electrófilos. Los complejos metal-carbeno de tipo Fischer y los resultantes de la reacción de carboxilatos de Rh(II) y Pd(II) con diazoalcanos son ejemplos típicos de carbenos pertenecientes a este grupo. Al último grupo pertenecerían los complejos metal-carbeno que presentan una interacción muy débil entre el metal y el carbeno (Figura 2).

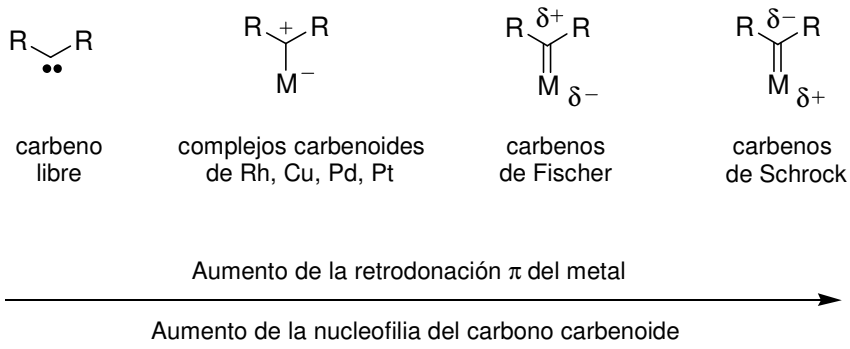

Figura 2

I.1.1.1. Complejos nucleófilos. Carbenos de Schrock

Los complejos metal-carbeno de tipo Schrock[3] se caracterizan por tener en su estructura un metal de transición temprana (Ta, Zr, Ti, etc.) en un alto estado de oxidación con ligandos dadores tales como grupos alquilo o ciclopentadienilo (Figura 3). El carbono carbenoide presenta carácter nucleófilo y reacciona por tanto con agentes electrófilos.

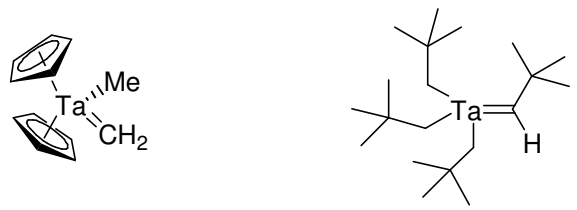

Figura 3

Las energías del HOMO y del LUMO para un complejo metal-carbeno vienen determinadas por la diferencia de energía entre el orbital 2p vacío del carbeno y un orbital d lleno del fragmento metálico con la simetría adecuada. Estudios teóricos[4] sugieren que la interacción entre estos orbitales en un complejo de tipo Schrock es muy eficaz al ser muy próximos en energía, lo que da lugar por solapamiento a un LUMO de alta energía, poco adecuado para la reacción con agentes nucleófilos (Figura 4). Por tanto, la nucleofilia de los carbenos de Schrock es el resultado de un enlace π C-M fuerte que permite la transferencia electrónica eficaz desde el metal al carbono carbenoide y de un LUMO de alta energía no accesible a los agentes nucleófilos.

[3] (a) Schrock, R. R. *Acc. Chem. Res.* **1979**, *12*, 98. (b) Schrock, R. R. *Acc. Chem. Res.* **1990**, *23*, 158. (c) Para una revisión véase: Stille, J. R. Transition Metal Carbene Complexes. Tebbe's Reagent and Related Nucleophilic Alkylidenes. En *Comprehensive Organometallic Chemistry II*; Abel, E. W.; Stone, F. G. A.; Wilkinson, G., Eds.; Pergamon: Oxford, UK, 1995; Vol. 12, págs. 577-600. (d) Schrock R. R.; Hoveyda, A. H. *Angew. Chem. Int. Ed.* **2003**, *42*, 4592.

[4] (a) Goddard, R. J.; Hoffmann, R.; Jemmis, E. D. *J. Am. Chem. Soc.* **1980**, *102*, 7667. (b) Cundari, T. R.; Gordon, M. S. *J. Am. Chem. Soc.* **1991**, *113*, 5231.

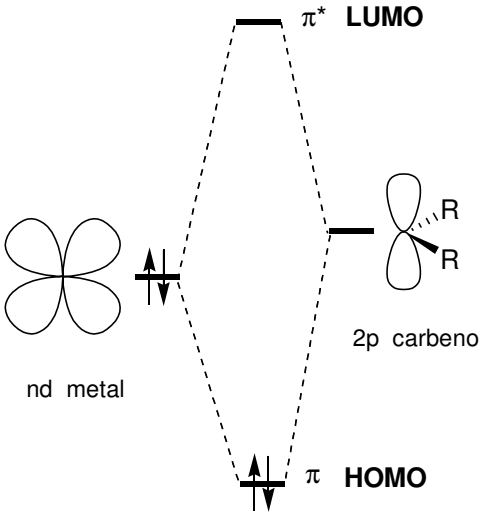

Figura 4

Dentro del grupo de complejos metal-carbeno nucleófilos se encuentran los carbenos de Grubbs que se emplean como catalizadores en las reacciones de metátesis de olefinas en fase homogénea (Figura 5). Este tipo de catalizadores ha tenido una enorme repercusión en el desarrollo de la síntesis orgánica a lo largo de la última década.[5]

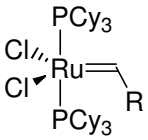

R = Ph, CH=CPh$_2$

Figura 5

Reacciones como la polimerización por metátesis de apertura de anillo (ROMP),[3b,6] la metátesis cruzada (CM)[7] y sobre todo la metátesis de cierre de anillo (RCM),[5b,8] son actualmente reacciones clásicas en ambos aspectos, organometálico y

[5] (a) Schuster, M.; Blechert, S. *Angew. Chem. Int. Ed.* **1997**, *36*, 2036. (b) Armstrong, S. K. *J. Chem. Soc., Perkin Trans. 1* **1998**, 371. (c) Grubbs, R. H.; Chang, S. *Tetrahedron* **1998**, *54*, 4413. (d) Maier, M. E. *Angew. Chem. Int. Ed.* **2000**, *39*, 2073. (e) Fürstner, A. *Angew. Chem. Int. Ed.* **2000**, *39*, 3012. (f) Buchmeiser, M. R. *Chem. Rev.* **2000**, *100*, 1565. (g) Louie, J.; Grubbs, R. H. *Organometallics* **2002**, *21*, 2153. (h) Grubbs, R. H. *Tetrahedron* **2004**, *60*, 7117.

[6] (a) Knoll, K.; Krouse, S. A.; Schrock, R. R. *J. Am. Chem. Soc.* **1988**, *110*, 4424. (b) Breslow, D. S. *Prog. Polym. Sci.* **1993**, *18*, 1141. (c) Schrock, R. R. *Pure & Appl. Chem.* **1994**, *66*, 1447. (d) Lynn, D. M.; Kanaoka, S.; Grubbs, R. H. *J. Am. Chem. Soc.* **1996**, *118*, 784. (e) Kanai, M.; Mortell, K. H.; Kiessling, L. L. *J. Am. Chem. Soc.* **1997**, *119*, 9931.

[7] (a) Giger, T.; Wigger, M.; Audétat, S.; Benner, S. A. *Synlett* **1988**, 688. (b) Boger, D. L.; Chai, W. Y. *Tetrahedron* **1998**, *54*, 3955.

[8] (a) Grubbs, R. H.; Miller, S. J; Fu, G. C. *Acc. Chem. Res.* **1995**, *28*, 446. (b) Fürstner, A.; Koch, D.; Langemann, K.; Leitner, W.; Six, C. *Angew. Chem. Int. Ed. Engl.* **1997**, *36*, 2466. (c) Nicolaou, K. C.; Winssinger, N.; Pastor, J.; Ninkovic, S.; Sarabia, F.; He, Y.; Vourloumis, D.; Yang, Z.; Li, T.; Giannakakou, P.; Hamel, E. *Nature* **1997**, *387*, 268.

sintético. El desarrollo de nuevas generaciones de estos catalizadores ha hecho de la metátesis de olefinas una herramienta fundamental en síntesis orgánica.

I.1.1.2. Complejos electrófilos. Carbenos de Fischer

Los complejos metal-carbeno de tipo Fischer[1,2] contienen en su estructura un metal de transición de los grupos 6 a 8 en un bajo estado de oxidación, unido al carbono carbenoide y estabilizado por una serie de ligandos con fuertes propiedades aceptoras (generalmente grupos CO). La polaridad del enlace carbono-metal es la contraria a la comentada anteriormente para los complejos de tipo Schrock. El carbono carbenoide ahora es electrófilo, por lo que el ataque de los nucleófilos se va a dar preferentemente en esa posición. Los complejos de tipo Fischer poseen un heteroátomo, que suele ser oxígeno, azufre o nitrógeno, directamente unido al carbono carbenoide y que es responsable de compensar la deficiencia de carga de éste por conjugación (Figura 6).

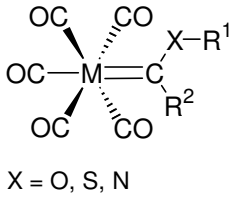

Figura 6

La interacción entre los orbitales d del fragmento metálico y el orbital 2p vacío del ligando carbeno en un complejo de tipo Fischer es poco eficaz al ser muy diferentes en energía, lo que da lugar, por solapamiento, a un LUMO de baja energía adecuado para la reacción con agentes nucleófilos (Figura 7).

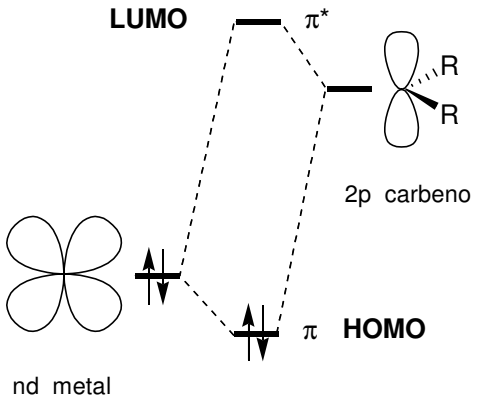

Figura 7

De este modo, el solapamiento poco eficaz entre los orbitales del metal y del ligando carbeno junto con la presencia de ligandos CO restringe la capacidad de retrodonación del metal, lo que justifica la electrofilia del carbono carbenoide. Esta deficiencia de carga en el átomo de carbono se compensa en parte por la cesión electrónica desde el heteroátomo. Por esta razón, la reactividad de los carbenos de Fischer frente a ataques nucleófilos aumenta al disminuir la capacidad de cesión electrónica del heteroátomo directamente unido al carbono carbenoide.

Se considera que el carbono carbenoide en los complejos de tipo Fischer posee una hibridación sp^2. Las estimaciones realizadas mediante cálculos teóricos, así como los datos obtenidos experimentalmente mediante difracción de rayos-X, indican que el orden de enlace entre el carbono carbenoide y el heteroátomo se corresponde con un valor intermedio entre un enlace sencillo y uno doble.[9] Por lo tanto, el complejo puede describirse como un híbrido de resonancia entre las estructuras **A**-**C** del esquema 4. La deslocalización electrónica se evidencia por la rotación restringida (14−25 kcal mol^{-1}) en torno al enlace carbono carbenoide-heteroátomo.

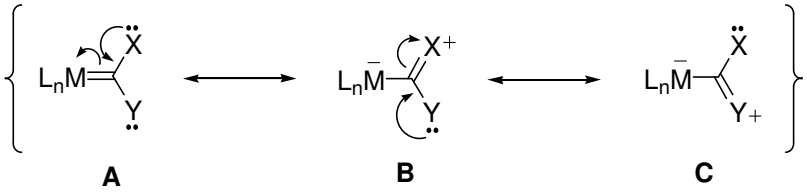

Esquema 4

I.1.2. Síntesis de complejos metal-carbeno de tipo Fischer

El procedimiento más general para la preparación de estos compuestos es el descrito por Fischer y Maasböl en 1964 (Esquema 5).[1] Este método parte del correspondiente carbonilo metálico que se hace reaccionar con un reactivo organolítico para formar un acilmetalato de litio denominado complejo *ate*. Debido a la fortaleza del par iónico formado por el oxígeno y el litio,[10] la *O*-alquilación de este complejo requiere el empleo de agentes alquilantes enérgicos, como sales de trimetiloxonio, sulfato de

[9] (a) Nakatsuji, H.; Ushio, J.; Han, S.; Yonezawa, T. *J. Am. Chem. Soc.* **1983**, *105*, 426. (b) Jacobsen, H.; Ziegler, T. *Organometallics* **1995**, *14*, 224. (c) Wang, C.-C.; Wang, Y.; Liu, H.-J.; Lin, K.-J.; Chou, L.-K.; Chan, K.-S. *J. Phys. Chem. A* **1997**, *101*, 8887. (d) Cases, M.; Frenking, G.; Durán, M.; Solá, M. *Organometallics* **2002**, *21*, 4182.
[10] Collman, J. P.; Finke, R. G.; Cawse, J. N.; Brauman, J. I. *J. Am. Chem. Soc.* **1977**, *99*, 2515.

dimetilo, triflato de metilo, fluorosulfonato de metilo o sales de difenilsulfonio, para dar lugar al correspondiente complejo alcoxicarbeno con excelentes rendimientos.[11]

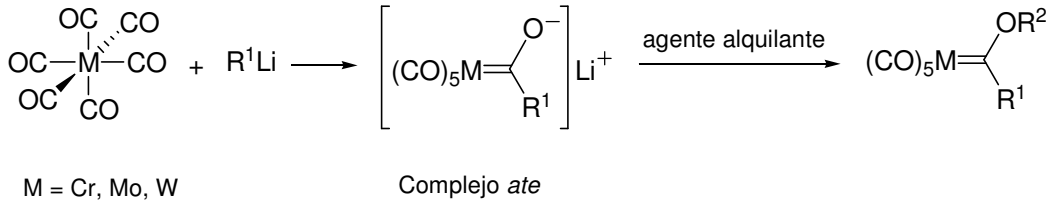

Esquema 5

El complejo *ate* se suele manejar mejor como su sal de tetrametilamonio, lo que además permite incrementar notablemente su reactividad. En este caso, el par iónico formado con el catión amonio, mucho más voluminoso, es más débil y el complejo puede acilarse fácilmente con haluros de ácido. Los aciloxicarbenos así formados suelen ser térmicamente inestables y los grupos aciloxi pueden ser desplazados por agentes nucleófilos tales como alcoholes, aminas o tioles para dar lugar a nuevos complejos metal-carbeno heterosustituidos (Esquema 6).[12]

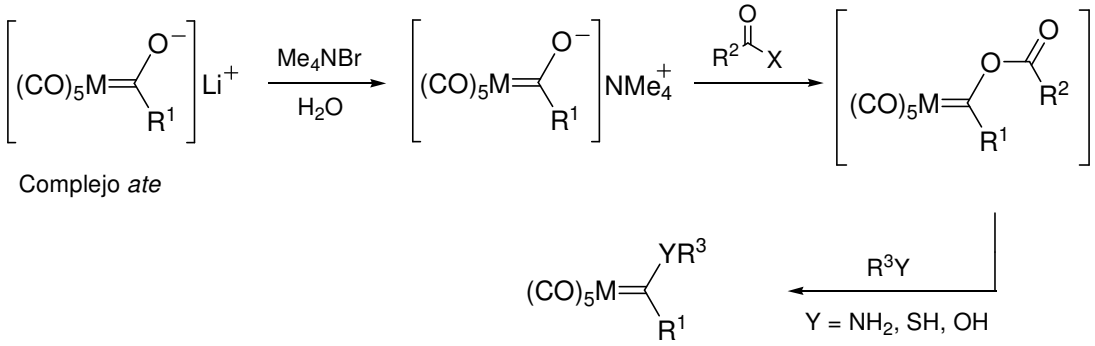

Esquema 6

Aunque la síntesis de complejos metal-carbeno de tipo Fischer utilizando reactivos organolíticos es la aproximación más comúnmente empleada para la obtención de estos compuestos, existen otros procedimientos, menos generales, que complementan esta metodología sintética. Entre ellos cabe destacar la reducción enérgica del correspondiente carbonilo metálico con C_8K[13] o naftalenuro sódico[14] y posterior

[11] (a) Casey, C. P.; Cyr, C. R.; Boggs, R. A. *Synth. Inorg. Met-Org. Chem.* **1973**, *3*, 249. (b) Harvey, D. F.; Brown, M. F. *Tetrahedron Lett.* **1990**, *31*, 2529. (c) Matsuyama, H.; Nakamura, T.; Iyoda, M. *J. Org. Chem.* **2000**, *65*, 4796.

[12] (a) Semmelhack, M. F.; Bozell, J. J. *Tetrahedron Lett.* **1982**, *23*, 2931. (b) Schwindt, M. A.; Miller, J. R.; Hegedus, L. S. *J. Organomet. Chem.* **1991**, *413*, 143.

[13] Schwindt, M. A.; Lejon, T.; Hegedus, L. S. *Organometallics* **1990**, *9*, 2814.

condensación del pentacarbonilmetalato bis-aniónico formado, con haluros de ácidos[15] o amidas (Esquema 7).[13,14,16] De este modo, el tratamiento del bis-anión carbonilmetalato con cloruros de ácido seguido de *O*-alquilación, conduce a complejos alcoxicarbeno, mientras que la reacción con amidas y TMSCl genera complejos aminocarbeno.

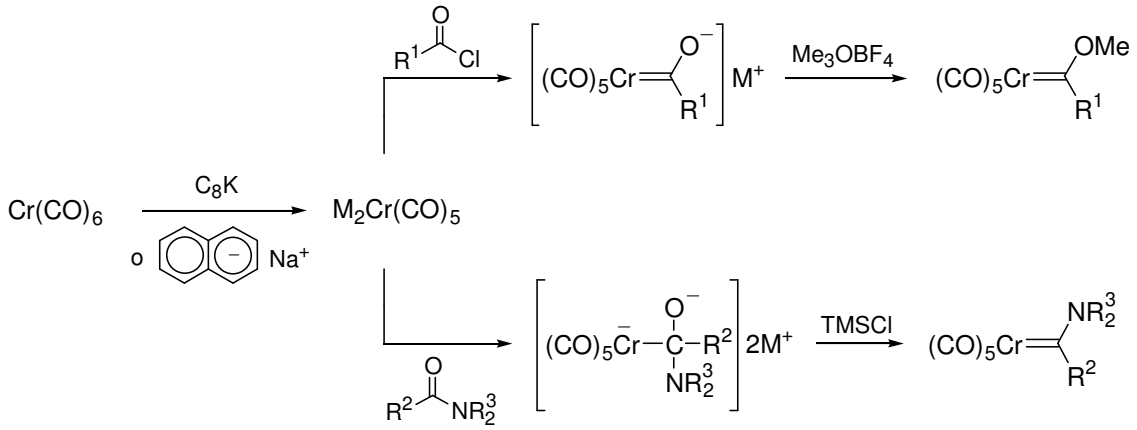

Esquema 7

Por otro lado, los complejos que tienen átomos de hidrógeno en posición α con respecto al carbono carbenoide son ácidos (pK_a = 8-12).[2a,17] La desprotonación por efecto de distintas bases origina el correspondiente anión, estabilizado por la deslocalización de la carga negativa en el fragmento metálico. Estos aniones reaccionan fácilmente con nitroalquenos,[18] aldehídos,[19] cetonas α,β-insaturadas[20] y con epóxidos en presencia de ácidos de Lewis,[21] dando lugar a carbenos con mayor complejidad estructural (Esquema 8).

---

[14] Imwinkelried, R.; Hegedus, L. S. *Organometallics* **1988**, *7*, 702.
[15] Semmelhack, M. F.; Lee, G. R. *Organometallics* **1987**, *6*, 1839.
[16] Hegedus, L. S.; Schwindt, M. A.; de Lombaert, S.; Imwinkelried, R. *J. Am. Chem. Soc.* **1990**, *112*, 2264.
[17] Referencias seleccionadas sobre medidas de la acidez de complejos metal-carbenoide con hidrógenos en posición α: (a) Bernasconi, C. F.; Sun, W. *J. Am. Chem. Soc.* **1993**, *115*, 12526. (b) Bernasconi, C. F.; Leyes, A. E. *J. Am. Chem. Soc*. **1997**, *119,* 5169. (c) Bernasconi, C. F.; Sun, W.; García-Río, L.; Yan, K.; Kittredge, K. *J. Am. Chem. Soc.* **1997**, *119,* 5583. (d) Bernasconi, C. F.; Leyes, A. E.; Ragains, M. L.; Shi, Y.; Wang, H.; Wulff, W. D. *J. Am. Chem. Soc.* **1998**, *120,* 8632. (e) Bernasconi, C. F.; Ali, M. *J. Am. Chem. Soc.* **1999**, *121,* 3039. (f) Bernasconi, C. F.; Sun, W. *J. Am. Chem. Soc*. **2002**, *124*, 2299.
[18](a) Licandro, E.; Maiorana, S.; Capella, L.; Manzotti, R.; Papagni, A.; Pryce, M.; Graiff, C.; Tiripicchio, A. *Eur. J. Org. Chem.* **1998**, 2127. (b) Licandro, E.; Maiorana, S.; Baldoli, C.; Capella, L.; Perdicchia, D. *Tetrahedron Asymmetry* **2000**, *11*, 975. (c) Licandro, E.; Maiorana, S.; Capella, L.; Manzotti, R.; Papagni, A.; Vandoni, B.; Albinati, A.; Chuang, S. H.; Hwu, J.-R. *Organometallics* **2001**, *20*, 485.
[19] (a) Aumann, R.; Heinen, H. *Chem. Ber.* **1987**, *120*, 537. (b) Wang, H.; Hsung, R. P.; Wulff, W. D. *Tetrahedron Lett.* **1998**, *39*, 1849l
[20] (a) Anderson, B. A.; Wulff, W. D.; Rahm, A. *J. Am. Chem. Soc.* **1993**, *115*, 4602. (b) Baldoli, C.; del Buttero, P.; Licandro, E.; Maiorana, S.; Papagni, A.; Zanotti-Gerosa, A. *J. Organomet. Chem.* **1995**, *486*, 279. (c) Shi, Y.; Wulff, W. D.; Yap, G. P. A.; Rheingold, A. L. *Chem. Commun.* **1996**, 2601.
[21] Lattuada, L.; Licandro, E.; Maiorana, S.; Molinari, H.; Papagni, A. *Organometallics* **1991**, *10*, 807.

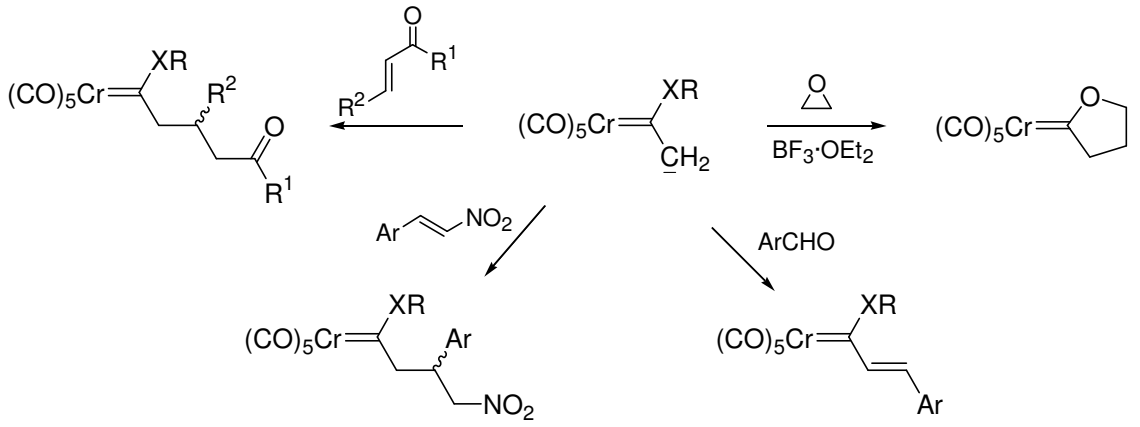

Esquema 8

I.2. Complejos metal-carbeno bi- y polimetálicos de tipo Fischer

Durante las últimas tres décadas, la química de complejos metal-carbeno de tipo Fischer se ha centrado en complejos que poseen un único enlace metal-carbeno. Aunque el uso de carbenos bi- y polimetálicos en síntesis orgánica es todavía reciente,[22] su empleo es cada vez más frecuente, debido al protagonismo creciente de la química organometálica en la química macromolecular, supramolecular y de dendrímeros,[23] y sobre todo, al interés en desarrollar nuevos catalizadores polimetálicos en los que los metales puedan cooperar entre sí de forma más eficiente que si se encontraran aislados.

Estrictamente hablando, el primer complejo metal-carbeno bimetálico de tipo Fischer, **1**, fue sintetizado por King en 1963, un año antes de que Fischer publicara la síntesis del primer complejo metal-carbeno.[24] Casey corrigió posteriormente la estructura **2** asignada inicialmente para este compuesto (Figura 8).[25] A pesar de esto, no

[22] (a) Huy, N. H. T.; Lefloch, P.; Robert, F.; Jeannin, Y. *J. Organomet. Chem.* **1987**, *327*, 211. (b) Macomber, D. W.; Hung, M.-H.; Verma, A. G.; Rogers, R. D. *Organometallics* **1988**, *7*, 2072. (c) Macomber, D. W.; Madhukar, P.; Rogers, R. D. *Organometallics* **1991**, *10*, 212. (d) Macomber, D. W.; Hung, M.-H.; Madhukar, P.; Liang, M.; Rogers, R. D. *Organometallics* **1991**, *10*, 737. (e) Macomber, D. W.; Madhukar, P. *J. Organomet. Chem.* **1992**, *433*, 279. (f) Geisbauer, A.; Mihan, S.; Beck, W. *J. Organomet. Chem.* **1995**, *501*, 61. (g) Dumas, S.; Lastra, E.; Hegedus, L. S. *J. Am. Chem. Soc.* **1995**, *117*, 3368. (h) Hsiao, Y.; Hegedus, L. S. *J. Org. Chem.* **1997**, *62*, 3586. (i) Kuester, E.; Hegedus, L. S. *Organometallics* **1999**, *18*, 5318. (j) Tomuschat, P.; Kröner, L.; Steckhan, E.; Nieger, M.; Dötz, K. H. *Chem. Eur. J.* **1999**, *5*, 700. (k) Aumann, R. *Eur. J. Org. Chem.* **2000**, 17. (l) Wynn, T.; Hegedus, L. S. *J. Am. Chem. Soc.* **2000**, *122*, 5034. (m) Puntener, K.; Hellman, M. D.; Kuester, E.; Hegedus, L. S. *J. Org. Chem.* **2000**, *65*, 8301. (n) Quast, L.; Nieger, M.; Dötz, K. H. *Organometallics* **2000**, *19*, 2179.

[23] (a) Tomalia, D. A.; Naylor, A. M.; Godart, W. A. S. *Angew. Chem.* **1990**, *102*, 119; *Angew. Chem. Int. Ed. Engl.* **1990**, *29*, 113. (b) Newcome, G. R.; Moorefield, C. N.; Vögtle, F. *Dendritic Molecules*; VCH: Weinheim, Germany, 1995. (c) Tomalia, D. A.; Dupont Durst, H. *Top. Curr. Chem.* **1993**, *165*, 193. (d) Bosma, A. W.; Janssen, H. M.; Meijer, E. W. *Chem. Rev.* **1999**, *99*, 1665. (e) Newcome, G. R.; He, E.; Moorefield, C. N. *Chem. Rev.* **1999**, *99*, 1689. (f) Lehn, J.-M. *Supramolecular Chemistry*; VCH: Weinheim, Germany, 1995.

[24] King, R. B. *J. Am. Chem. Soc*. **1963**, *85*, 1922.

[25] Casey, C. P. *J. Chem. Soc., Chem. Commun.* **1970**, 1220.

fue hasta 1982 cuando se sintetizó el primer complejo en el que coexistían más de una unidad metal-carbeno.[26]

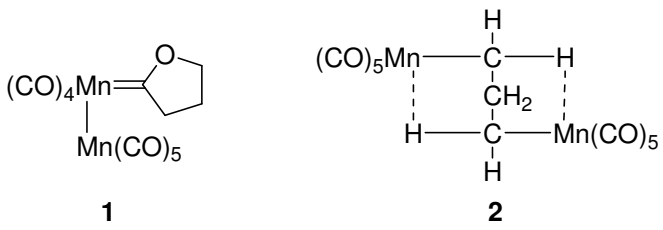

Figura 8

Existen tres posibilidades diferentes para unir nuevos centros metálicos a un complejo metal-carbeno preformado (Figura 9):

- Sobre el carbono carbenoide: directamente unido a dicho átomo (A) o a través de una cadena carbonada (B).
- A través del heteroátomo unido al carbono carbenoide (C y D).
- Directamente unido al centro metálico: mediante enlace metal-metal (E) o a través del empleo de un ligando bidentado que una ambos núcleos (F).

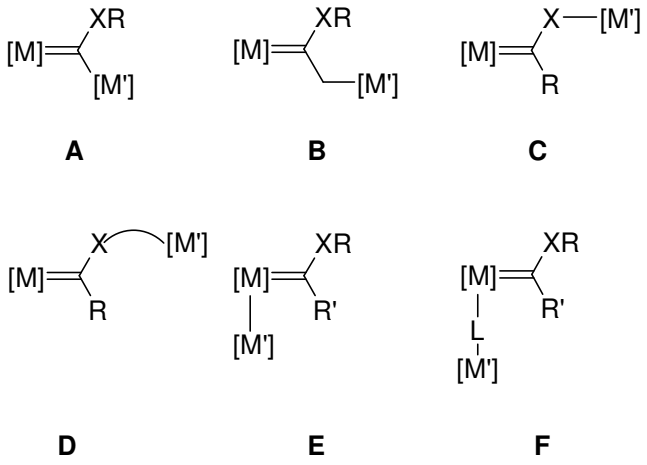

Figura 9

Cuando se comparan la reactividad y las aplicaciones en síntesis orgánica de los complejos metal-carbeno con un único centro metálico con los procesos que involucran a complejos con más de un centro metálico, se observa que la química de estos últimos se ha estudiado escasamente. Además, los compuestos de este tipo usados en síntesis, es decir, los que han funcionado con éxito en la formación de enlaces C-C, con o sin

[26] Fischer, E. O.; Röll, W.; Huy, N. H. T.; Ackermann, K. *Chem.Ber.* **1982**, *115*, 2951.

retención del fragmento metálico, son minoría. Por otra parte, se ha comprobado que los distintos centros metal-carbeno de un complejo polimetálico no se comportan de manera aislada en la molécula, sino que su reactividad se encuentra modulada por la presencia de los otros metales. Todos estos datos han convertido a esta familia de complejos organometálicos en excelentes compuestos para investigar las interacciones entre los distintos centros metálicos, así como para la búsqueda de nuevas formas de reactividad, tanto catalítica como estequiométrica.

I.3. Aplicaciones de complejos metal-carbeno a la síntesis de compuestos con estructuras restringidas

Como ya se ha dicho, las aplicaciones sintéticas de complejos metal-carbeno bi- y polimetálicos son prácticamente desconocidas.[2j] Por tanto, no es de extrañar que el empleo de este tipo de compuestos en la síntesis de moléculas con estructuras conformacionalmente restringidas sea todavía más escaso, a pesar de que estos complejos son, en principio, sustratos ideales para la producción de tales compuestos.

Entre los precedentes descritos en la bibliografía existen algunos ejemplos dignos de mención como los trabajos de Wulff encaminados a la síntesis de ciclofanos macrocíclicos (Esquema 9)[27] y, recientemente, a la síntesis de calixarenos utilizando reacciones de benzanulación (Esquema 10).[28] Esta reacción abre la posibilidad de preparar [n,m]-ciclofanos no simétricos desde la macrociclación de bis(carbenos) con diinos, o bien permite la síntesis regiocontrolada de calix[4]arenos no simétricos, en un proceso que construye de forma simultánea dos de los anillos bencénicos del calixareno, seguido de la macrociclación para construir el anillo final de 16 miembros.

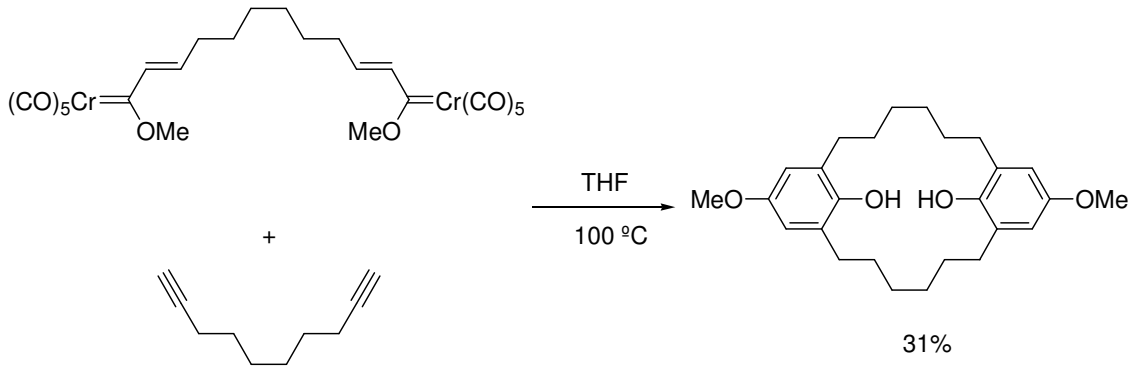

Esquema 9

[27] Wang, H.; Wulff, W. D. *J. Am. Chem. Soc.* **1998**, *120*, 10573.
[28] Gopalsamuthiram, V.; Wulff, W. D. *J. Am. Chem. Soc.* **2004**, *126*, 13936.

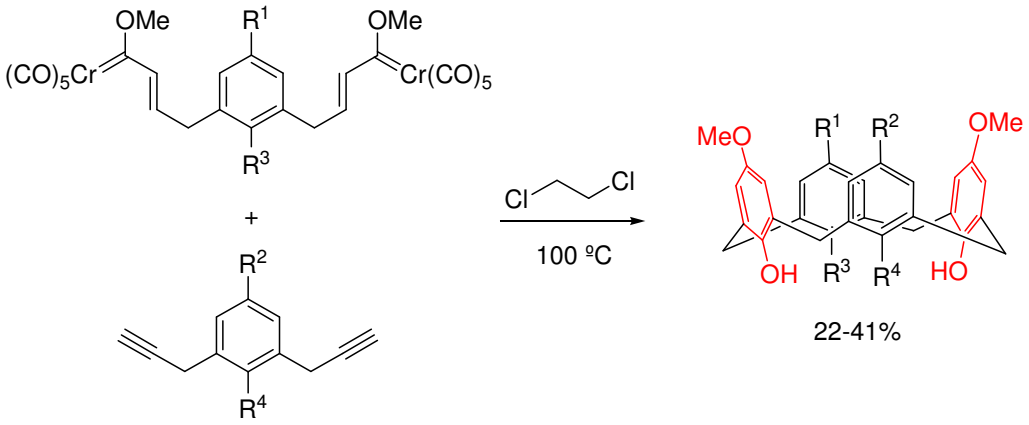

Esquema 10

Nuestro grupo de trabajo ha utilizado con éxito la reacción de transferencia intramolecular de ligando carbeno catalizada por reactivos de paladio para la síntesis de distintos tipos de compuestos macrocíclicos (Esquema 11).[2m,29] Este proceso transcurre a través de una doble transmetalación catalítica para generar la especie reactiva de naturaleza palada-carbeno bimetálico capaz de conducir a los productos de acoplamiento intramolecular.

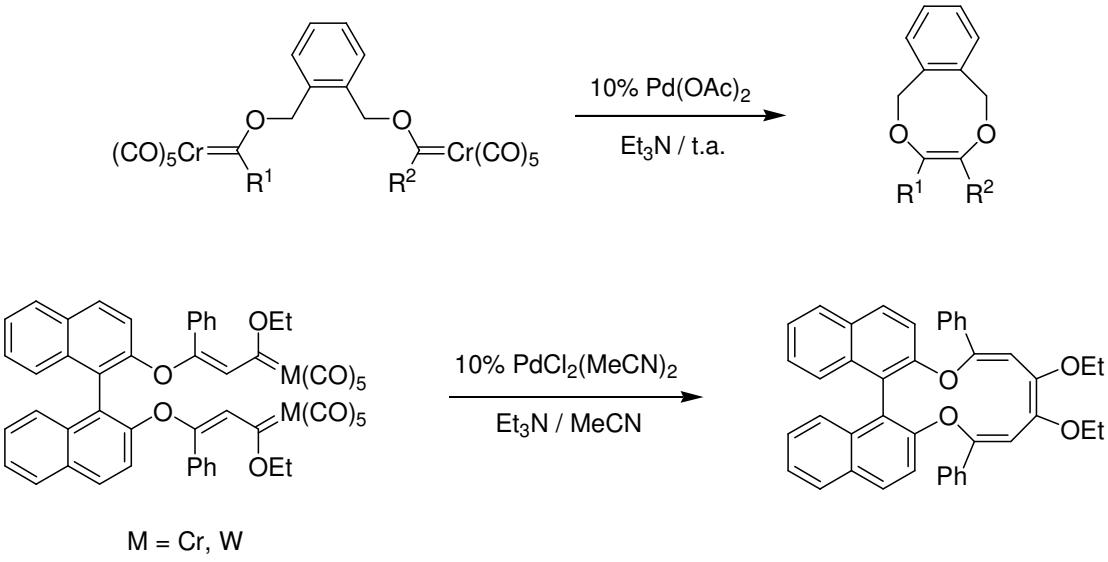

[29] (a) Sierra, M. A.; Mancheño, M. J.; Sáez, E.; del Amo, J. C. *J. Am. Chem. Soc*. **1998**, *120*, 6812. (b) Sierra, M. A.; del Amo, J. C.; Mancheño, M. J.; Gómez-Gallego, M. *J. Am. Chem. Soc*. **2001**, *123*, 6812. (c) Sierra, M. A.; del Amo, J. C.; Mancheño, M. J.; Gómez-Gallego, M.; Torres, M. R. *Chem. Commun*. **2002**, 1842. (d) del Amo, J. C.; Mancheño, M. J.; Gómez-Gallego, M.; Sierra, M. A. *Organometallics* **2004**, *23*, 5021.

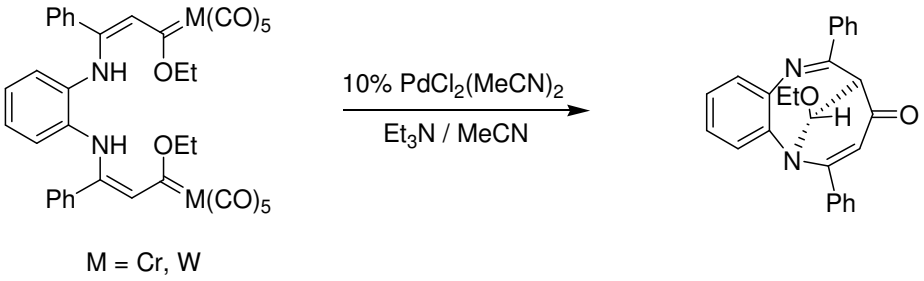

Esquema 11

Ninguno de los procesos anteriores ocurre con retención del fragmento metálico. De hecho, no existe ningún precedente bibliográfico en el que la nueva molécula formada conserve en su estructura alguna unidad metal-carbeno.

I.4. Procesos de transferencia electrónica en medios no convencionales

Los procesos de transferencia electrónica (TE) son esenciales en áreas tan diversas como la química, la biología, la física[30] y la electrónica molecular[31] y juegan un papel fundamental en procesos tan importantes para la vida como son la fotosíntesis y la respiración.[32,33] La transferencia electrónica entre un dador (D) y un aceptor (A) puede inducirse por métodos químicos, electroquímicos o fotoquímicos.[30,33]

Los procesos de TE que se han estudiado con mayor profusión son, sin duda alguna, aquellos que involucran interacciones electrónicas intramoleculares entre un grupo dador (D) y otro aceptor (A). La dependencia de la dinámica de la TE tanto de la naturaleza de D y A como de su separación y orientación relativa se ha discutido ampliamente. De hecho, todavía existe una gran controversia sobre si los procesos de

[30] (a) *Electron Transfer in Chemistry*; Balzani, V., Ed.; Wiley-VCH: Weinheim, 2001; Vols. 1-5. (b) Marcus, R. A.; Sutin, N. *Biochim. Biophys. Acta* **1985**, *811*, 265. (c) Marcus, R. A. *Rev. Mod. Phys.* **1993**, *65*, 599. (d) Barbara, P. F.; Meyer, T. J.; Ratner, M. A. *J. Phys. Chem.* **1996**, *100*, 13148. (e) También el número monográfico dedicado a transferencia electrónica en *Chem. Rev.* **1992**, *92*, 365.

[31] (a) Alivisatos, A. P.; Barbara, P. F.; Castleman, A. W.; Chang, J.; Dixon, D. A.; Klein, M. L.; McLendon, G. L.; Miller, J. S.; Ratner, M. A.; Rossky, P. J.; Stupp, S. I.; Thompson, M. E. *Adv. Mater.* **1998**, *10*, 1297. (b) Ratner, M. A.; Jortner J. en *Molecular Electronics: Some Directions*; Ratner, M. A., Jortner, J., Eds.; IUPAC, 1997.

[32] (a) *Anoxigenic Photosynthetic Bacteria*; Blankenship, R. E.; Madigan, M. T.; Bauer, C. E. Eds.; Kluwer Academic Publishing: Dordrecht, 1995. (b) Armstrong, F. A.; Kaim, W.; Schwederski, B. *Bioinorganic Chemistry: Inorganic Chemistry in the Chemistry of Life*; Oxford University, UK, 1995. (c) Kochi, J. K. *Acc. Chem. Res.* **1992**, *25*, 39. (d) Rathore, R.; Kochi, J. K. *Adv. Phys. Org. Chem.* **2000**, *35*, 193.

[33] (a) Fukuzumi, S. en *Advances in Electron-Transfer Chemistry*; Mariano P. S., Ed.; JAI Press: Greenwich, CT, 1992; págs. 67-175. (b) Fukuzumi, S.; Tanaka T. en *Photoinduced Electron Transfer*; Fox, M. A., Chanon, M., Eds.; Elsevier: Amsterdam, 1998; Parte C, Capítulo 10.

TE intramolecular ocurren a través de enlaces[34,35] o según un mecanismo a través del espacio mediado por el disolvente (Figura 10).[36,37]

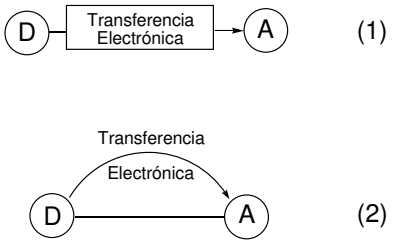

Figura 10

I.4.1. Procesos de TE en complejos metal-carbeno de Fischer

Los ejemplos de procesos de TE que implican a complejos metal-carbeno de tipo Fischer son escasos. Entre ellos, cabe destacar aquellos procesos inducidos químicamente por aleación de Na/K,[38] 1-metilnaftalenuro potásico,[39] SmI_2[40] o C_8K.[41]

Recientemente, nuestro grupo de investigación ha iniciado el estudio de procesos de TE en complejos metal-carbeno de Fischer del grupo 6 utilizando fuentes de electrones menos convencionales,[42] como la ionización electrónica por una fuente de electrospray en espectrometría de masas (ESI-MS).[43]

---

[34] (a) Johnson, R. C.; Hupp, J. T. *J. Am. Chem. Soc*. **2001**, *123*, 2053. (b) Closs, G. L.; Miller, J. R. *Science* **1988**, *240*, 440. (c) Closs, G. L.; Johnson, M. D.; Miller, J. R.; Piotrowiak, P. *J. Am. Chem. Soc*. **1989**, *111*, 3751.

[35] Para el efecto de enlaces de hidrógeno en TE, ver: (a) Fukuzumi, S.; Okamoto, K.; Yoshida, Y.; Imahori, H.; Araki, Y.; Ito, O. *J. Am. Chem. Soc*. **2003**, *125*, 1007. (b) Smitha, M. A.; Prasad, E.; Gopidas, K. R. *J. Am. Chem. Soc*. **2001**, *123*, 1159. (c) Prasad, E.; Gopidas, K. R. *J. Am. Chem. Soc*. **2000**, *122*, 3191.

[36] (a) Arimura, T.; Ide, S.; Suga, Y.; Nishioka, T.; Murata, S.; Tachiya, M.; Nagamura, T.; Inoue, H. *J. Am. Chem. Soc.* **2001**, *123*, 10744. (b) Bell, T. D. M.; Jolliffe, K. A.; Ghiggino, K. P.; Oliver, A. M.; Shephard, M. J.; Langford, S. J.; Paddon-Row, M. N. *J. Am. Chem. Soc.* **2000**, *122*, 10661 y referencias allí citadas.

[37] (a) Reek, J. N.; Rpowan, A. E.; de Gelder, R.; Beurskens, P. T.; Crossley, M. J.; de Feyter, S.; de Schryver, F.; Nolte, R. J. M. *Angew. Chem. Int. Ed.* **1997**, *36*, 361. (b) Hunter, C. A.; Hyde, R. K. *Angew. Chem. Int. Ed.* **1996**, *35*, 1936.

[38] Krusic, P. J.; Klabunde, U.; Casey, C. P.; Block, T. F. *J. Am. Chem. Soc.* **1976**, *98*, 2015.

[39] Lee, S.; Cooper, N. J. *J. Am. Chem. Soc.* **1990**, *112*, 9419.

[40] (a) Fuchibe, K.; Iwasawa, N. *Org. Lett.* **2000**, *2*, 3297. (b) Fuchibe, K.; Iwasawa, N. *Chem. Eur. J.* **2003**, *9*, 905.

[41] Sierra, M. A.; Ramírez-López, P.; Gómez-Gallego, M.; Lejon, T.; Mancheño, M. J. *Angew. Chem. Int. Ed.* **2002**, *41*, 3442.

[42] Sierra, M. A.; Gómez-Gallego, M.; Mancheño, M. J.; Martínez-Álvarez, R.; Ramírez-López, P.; Kayali, N.; González, A. *J. Mass. Spectrom.* **2003**, *38*, 151.

[43] (a) Van Berkel, G. J. en *Electrospray Ionization Mass Spectrometry. Fundamentals, Instrumentation and Applications.* Cole, R. B. Ed., Wiley, New York, 1997, pág. 65. Para un artículo reciente sobre el empleo de ESI-MS para la detección de intermedios reactivos, ver: (b) Meyer, S.; Koch, R.; Metzger, J. O. *Angew. Chem. Int. Ed.* **2003**, *42*, 4700.

ESI (Ionización por Electrospray) es una técnica que permite la transferencia de iones, desde una disolución a la fase gas como entidades aisladas, las cuales se pueden someter a análisis por espectrometría de masas. En todo experimento ESI se producen tres etapas en la generación de los iones-ESI: la producción de gotitas cargadas en el capilar ES ocurre en primer lugar; después, debido al alto voltaje aplicado, las gotitas merman en tamaño hasta convertirse en gotitas muy pequeñas fuertemente cargadas; la última etapa supone la formación de los iones en la fase gas a partir de las gotitas cargadas. El último paso de este mecanismo general es realmente difícil de establecer.[43,44]

El registro de un espectro de masas de un complejo metal-carbeno de Fischer es experimentalmente difícil puesto que estos complejos no son volátiles, son termolábiles y experimentan reacciones redox con facilidad. Las técnicas convencionales de ionización por impacto electrónico (EI) no son muy útiles para este tipo de compuestos organometálicos, puesto que la muestra necesita tener una presión de vapor significativa a temperaturas por debajo del punto de descomposición. De hecho, existen muy pocos casos de detección de complejos metal-carbeno mediante EI.[45] El empleo de la técnica ESI-MS es una buena alternativa a la técnica convencional puesto que evita tales problemas. De hecho, en ESI-MS la solubilidad, más que la volatilidad de la muestra, es el factor crítico de la técnica y, puesto que la ionización ocurre bajo condiciones muy suaves, ESI-MS es la técnica de elección para el registro del espectro de masas de analitos muy polares o particularmente lábiles.

A pesar de esto, los complejos cromo o wolframio-carbeno de tipo Fischer no se ionizan bajo las condiciones ESI de rutina. Las variaciones en el potencial de ionización usado, en el flujo de disolución o en el sistema de disolvente no producen cambios significativos en el proceso. Sin embargo, se puede conseguir la ionización de los complejos **3** y **4** gracias a la adición de un dador de electrones como la hidroquinona, HQ, o el tetratiafulvaleno, TTF, (Figura 11).[42]

[44] (a) Gaskell, S. J. *J. Mass. Spectrom.* **1997**, *32*, 677. (b) Kebarle, P. *J. Mass. Spectrom.* **2000**, *35*, 804.
[45] (a) Müller, J. *Angew. Chem. Int. Ed. Engl.* **1972**, *11*, 653. (b) Neidtein, R.; Gürtler, S.; Krieger, C. *Helv. Chim. Acta* **1994**, *77*, 2303. (c) Careri, M.; Mangia, A.; Manini, P.; Predieri, G.; Licandro, E.; Papagni, A. *Rapid Commun. Mass Spectrom.* **1997**, *11*, 51.

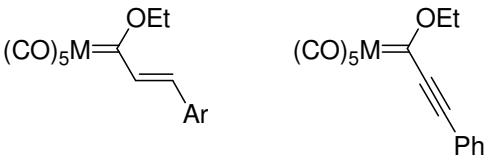

3 **4**

M = Cr, W
Ar= Ph, 2-furil, 2-tienil

a)

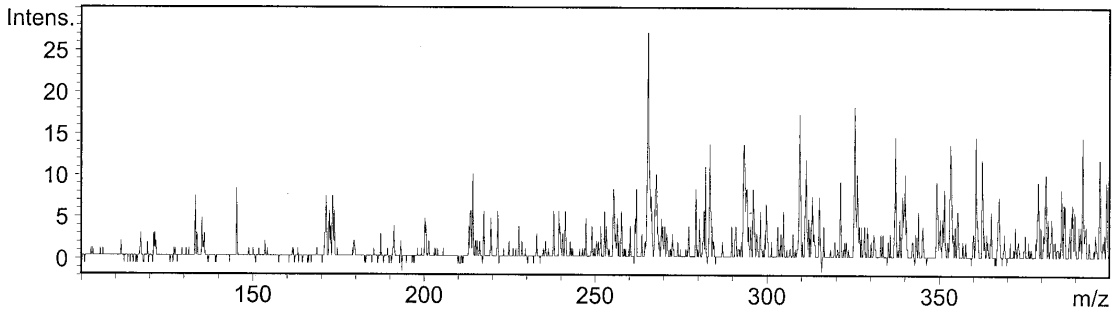

b)

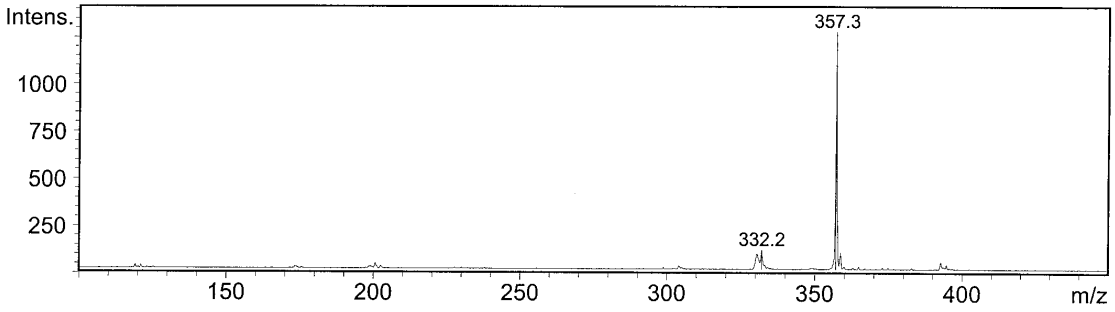

Figura 11. a) Espectro de masas del complejo **3** (M=Cr, Ar= 2-tienil) sin adición de HQ, b) espectro de masas del mismo complejo en presencia de HQ.

Nosotros hemos propuesto[42] que el proceso implica la captura de un electrón por parte de la HQ o TTF en la superficie del capilar. Las especies $HQ^{\bullet -}$ o $TTF^{\bullet -}$ así formadas provocan la formación del anión radical del carbeno, el cual pierde un radical $H^{\bullet}$ para formar los iones $[M - H]^-$ que son las especies que se detectan en el espectrómetro (Esquema 12).

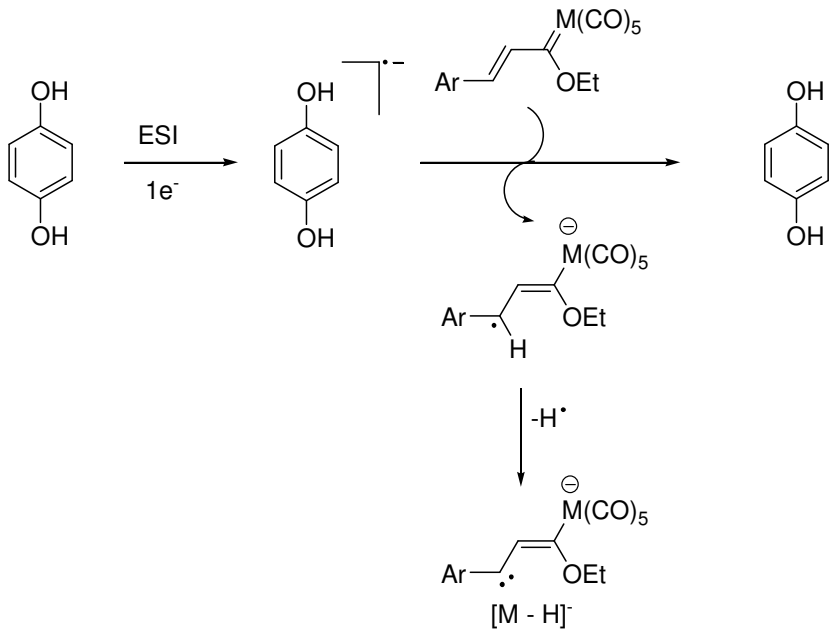

Esquema 12

Puesto que únicamente los complejos metal-carbeno que presentan conjugación son capaces de ionizarse en presencia de HQ o TTF, debe ser la estabilización que experimentan los aniones radicales intermedios por conjugación de la unidad carbeno con el anillo aromático, la causa por la que se forman tales especies. También se propone que el anión formado mediante ruptura homolítica del enlace C–H y posteriormente detectado como $[M - H]^-$, es un carbeno estabilizado por conjugación con el centro metálico. La capacidad de los carbenos metálicos para estabilizar carbenos centrados en sus carbonos en posición β se conoce bien.[46] Por tanto, la eliminación del radical $H^\bullet$ es la fuerza directora para estabilizar el anión radical formado inicialmente.

El proceso es similar en el caso del alquinil-complejo **4**, pero en este caso la TE desde la HQ forma el alenil-anión **5**.[47] En este caso, la ruptura homolítica ocurre en el anillo aromático para formar el anión altamente estabilizado **6** (Esquema 13).

[46] (a) Casey, C. P.; Kraft, S.; Powell, R. D. *J. Am. Chem. Soc*. **2000**, *122*, 3771. (b) Casey, C. P.; Kraft, S.; Powell, R. D. *J. Am. Chem. Soc*. **2002**, *124,* 2584.
[47] Este tipo de complejos se puede preparar fácilmente en disolución por tratamiento con C_8K, ver ref. 41.

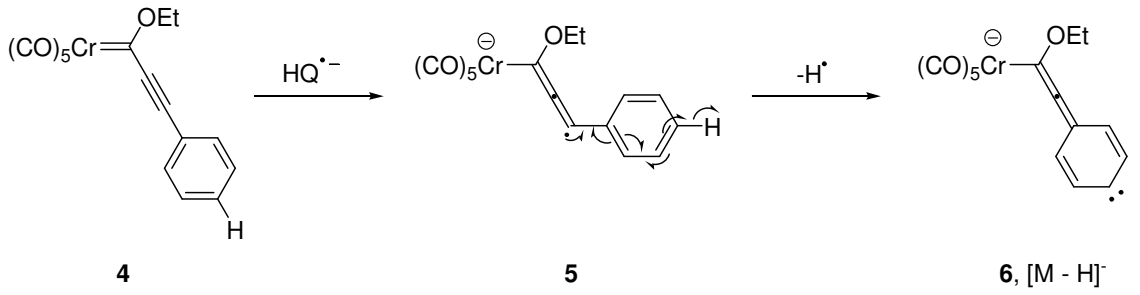

Esquema 13

También se han utilizado como aditivos compuestos aceptores de electrones como la tetraciano-*p*-benzoquinona (TCNQ) o azul de toluidina. Estos aditivos fueron inefectivos para provocar el proceso de ionización. Parece ser que bajo las condiciones ESI, tanto HQ como TTF (dadores de electrones) son forzados a aceptar un electrón, generándose de esta forma especies fuertemente reductoras responsables de la TE al complejo metal-carbeno.[48]

I.5. Fotoquímica de complejos metal-carbeno de Fischer

Como se ha comentado previamente, las reacciones térmicas de los complejos metal-carbeno de tipo Fischer se han estudiado en profundidad.[2] Al contrario, el potencial sintético y los mecanismos de sus reacciones fotoquímicas han sido mucho menos explorados.[49] Por esta razón, en el presente trabajo intentaremos arrojar "un poco más de luz" sobre los distintos factores que gobiernan los procesos fotoquímicos de este tipo de complejos.

El espectro UV-visible de los complejos metal-carbeno de tipo Fischer presenta tres absorciones bien diferenciadas:[50] una banda débil en torno a 500 nm correspondiente a la transferencia de carga metal-ligando (MLCT), una banda de intensidad moderada entre 350-450 nm correspondiente a una transición del campo del ligando de baja energía (LF), y una banda débil, generalmente solapada con la banda anterior, entre 300-350 nm correspondiente a una transición LF de alta energía. Estas bandas de absorción se corresponden con las transiciones electrónicas a los tres orbitales vacíos de simetría $2b_1$, $2a_1$ y $3a_1$, respectivamente, que podemos observar en el diagrama de orbitales moleculares de un complejo de tipo Fischer genérico (Figura 12).

[48] Como ejemplo en el que un buen dador de electrones es forzado a comportarse como un aceptor, ver: Redd, C. A.; Kim, K. C.; Bolskar, R. D.; Mueller, L. J. *Science,* **2000**, *289*, 101.
[49] (a) Hegedus, L. S. *Tetrahedron* **1997**, *53*, 4105. (b) Hegedus, L. S. en *Comprehensive Organometallic Chemistry II,* Abel, E. W.; Stone, F. G. A.; Wilkinson, G., Eds.; Pergamon: Oxford, 1995; vol. 12, pág. 549. (c) Schwindt, M. A.; Miller, J. R.; Hegedus, L. S. *J. Organomet. Chem.* **1991**, *413*, 143.
[50] Foley, H. C.; Strubinger, L. M.; Targos, T. S.; Geoffroy, G. L. *J. Am. Chem. Soc.* **1983**, *105*, 3064.

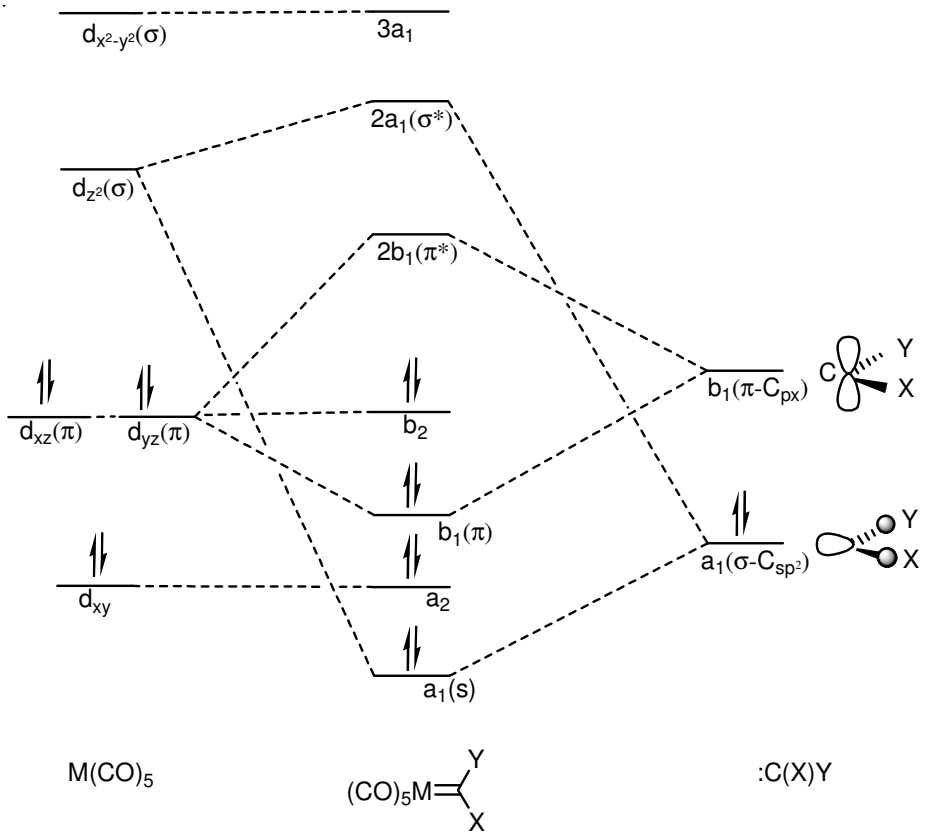

Figura 12. Diagrama de orbitales moleculares de un complejo metal-carbeno de tipo Fischer.

Según este diagrama, podemos ver que la banda MLCT corresponde a la promoción de un electrón desde un orbital no enlazante centrado en el metal (HOMO) a un orbital π^* centrado en el carbono carbénico (orbital *p* del carbeno, LUMO) (Figura 13), mientras que la banda LF resulta de la población del orbital $d_{x^2-y^2}$ del metal. Los complejos de Fischer son, por tanto, compuestos coloreados en un rango que abarca desde el amarillo hasta el rojo. La presencia de heteroátomos fuertemente dadores (N frente O) provoca desplazamientos hipsocrómicos en el espectro de absorción, mientras que sustituyentes π-aceptores (Ph frente a Me) dan lugar a desplazamientos batocrómicos.

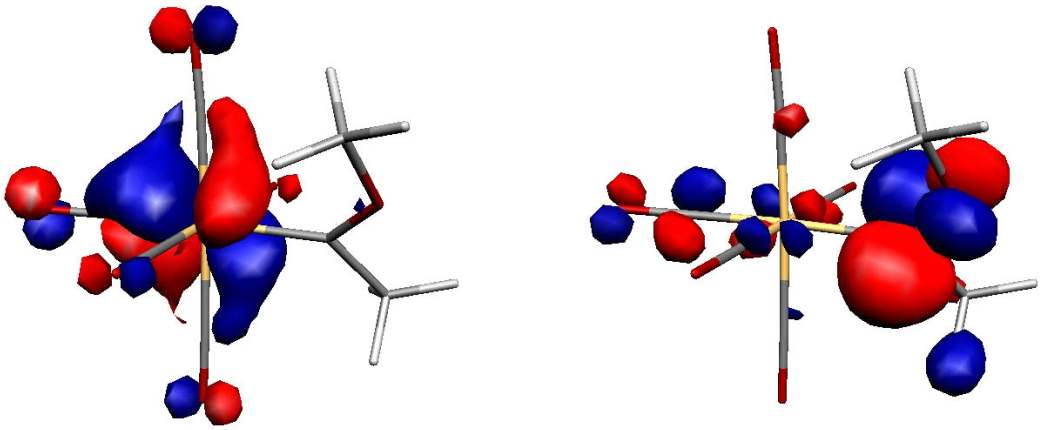

HOMO **LUMO**

Figura 13[51]

La mayoría de los estudios fotoquímicos llevados a cabo sobre complejos metal-carbeno de tipo Fischer se han centrado en los efectos producidos al irradiar en las bandas LF, observándose siempre la fotoexpulsión de uno de los ligandos carbonilo unido al metal. Así, la irradiación en la banda LF de alta energía del complejo $[(CO)_5W{=}C(OCH_3)Ph]$ provoca la disociación de uno de los ligandos CO-*cis*;[52] mientras que la irradiación en la banda LF de baja energía induce la pérdida del ligando carbeno o del CO-*trans*.[53] La fotoexpulsión de CO conduce a la formación de un intermedio con un tiempo de vida de varios microsegundos y con una estructura de tetracarbonil-carbeno (Figura 14).[54] Se propone que la vacante de coordinación de este intermedio está bloqueada por una interacción agóstica con el enlace C-H del sustituyente metoxi. En contraste, los resultados obtenidos con fotólisis en matriz sólida irradiando en la banda MLCT de los complejos $[(CO)_5\{W,Cr\}{=}(OCH_3)Ph]$ indican que

[51] Orbitales Moleculares HOMO y LUMO calculados (B3LYP/6-31G* & LanL2dz) para el complejo *anti*-$(CO)_5Cr{=}C(OCH_3)CH_3$. Para la representación se ha utilizado el programa MOLEKEL 4.3: MOLEKEL 4.3, Flükiger, P.; Lüthi, H. P.; Portmann, S.; Weber, J. Swiss Center for Scientific Computing, Manno (Switzerland), 2000-2002. Portmann, S.; Lüthi, H. P. MOLEKEL: An Interactive Molecular Graphics Tool. *Chimia*, **2000**, *54*, 766.

[52] Foley, H. C.; Strubinger, L. M.; Targos, T. S.; Geoffroy G. L. *J. Am. Chem. Soc.* **1983**, *105*, 3064.

[53] Servaas, P. C.; Stufkens, D. J.; Oskam, A. *J. Organomet. Chem.* **1990**, *390*, 61.

[54](a) Bechara, J. N.; Bell, S. E. J.; McGarvey, J. J.; Rooney, A. D. *J. Chem. Soc., Chem. Commun*. **1986**, 1785. (b) Bell, S. E. J.; Gordon, K. C.; McGarvey, J. J. *J. Am. Chem. Soc*. **1988**, *110*, 3107.

la fotorreacción primaria que tiene lugar es la isomerización del grupo OMe desde la forma más estable *anti* a la forma menos estable *sin* (Figura 14).[51,53,55]

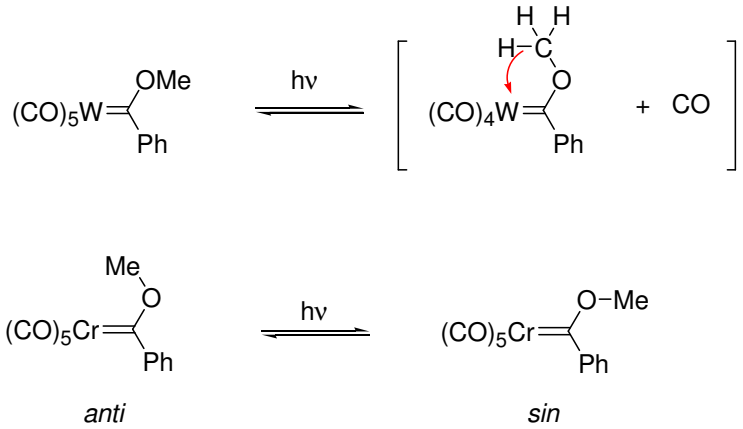

Figura 14

El equilibrio entre los confórmeros *anti-sin* en disolución fue descrito inicialmente por Kreiter y Fischer[56] en base a estudios de RMN, encontrándose una barrera de activación en torno a 12 kcal mol^{-1}. Nuestro grupo de trabajo ha abordado recientemente el estudio de este equilibrio para diversos complejos metal-carbeno mediante métodos computacionales.[57] En cualquier caso, ninguno de los procesos hasta ahora descritos parece ser útil en síntesis orgánica.

A pesar de esto, McGuire y Hegedus[58] encontraron que la irradiación en la banda MLCT de complejos metal-carbeno de tipo Fischer (de cromo y molibdeno pero no de wolframio) conduce a la generación de un intermedio con una reactividad similar a la de una cetena. De hecho, se propone que la irradiación de complejos cromo-carbeno en la banda MLCT provoca la inserción reversible de uno de los cuatro ligandos *cis*-CO en el enlace Cr-$C_{carbeno}$ para generar especies de tipo metalaciclopropanona/cetena coordinada a metal (Esquema 14).[59] Dichas especies, se consumen en presencia de cetenófilos, pero, en su ausencia, experimentan la desinserción térmica de CO para regenerar el complejo de partida.

---

[55](a) Rooney, A. D.; McGarvey, J. J.; Gordon, K. C.; McNicholl, R. A.; Schubert, U.; Hepp, W. *Organometallics* **1993**, *12*, 1277. (b) Rooney, A. D.; McGarvey, J. J.; Gordon, K. C. *Organometallics* **1995**, *14*, 107.

[56] (a) Kreiter, C. G.; Fischer, E. O. *Angew. Chem.* **1969**, *81*, 780; *Angew. Chem. Int. Ed. Engl.* **1969**, *8*, 761. (b) Kreiter, C. G.; Fischer, E. O. *Pure Appl. Chem.* **1971**, 151.

[57] Fernández, I.; Cossío, F. P.; Arrieta, A.; Lecea, B.; Mancheño, M. J.; Sierra, M. A. *Organometallics* **2004**, *23*, 1065.

[58] (a) McGuire, M. A.; Hegedus, L. S. *J. Am. Chem. Soc.* **1982**, *104*, 5538. (b) Hegedus, L. S.; McGuire, M. A.; Schultze, L. M.; Yijun, C.; Anderson, O. P. *J. Am. Chem. Soc*. **1984**, *106*, 2680.

[59] Hegedus, L. S.; deWeck, G.; D'Andrea, S. *J. Am. Chem. Soc.* **1988**, *110*, 2122.

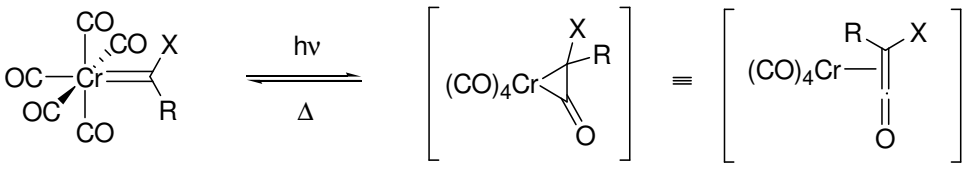

Esquema 14

En este contexto, la irradiación de uno de estos complejos supone la promoción de un electrón desde el orbital HOMO, centrado en el metal, al orbital LUMO, centrado en el carbono carbenoide, por lo que puede considerarse como una oxidación formal del metal que involucra a un electrón. Puesto que las oxidaciones de este tipo provocan la inserción de CO en enlaces metal-carbono,[60] este proceso parece ser bastante razonable. La formación de estas cromo-cetenas se ha deducido a partir de los fotoproductos (y de la estereoquímica de los mismos) obtenidos en la reacción fotoquímica de estos complejos con cetenófilos.[61] Sin embargo, todos los esfuerzos realizados hasta la fecha para detectar experimentalmente estos intermedios, mediante fotólisis de destello[62] o empleando matrices criogénicas,[63] han resultado infructuosos.[64]

I.5.1. Reactividad fotoquímica de complejos metal-carbeno de Fischer

Desde un punto de vista sintético, la generación fotoquímica de estas cetenas coordinadas a metal es muy útil ya que permite la formación de alcoxi-, amino- y tiocetenas ricas en electrones que no son fáciles de obtener por otras rutas convencionales. Todo ello ha permitido aplicar la reactividad fotoquímica de los complejos metal-carbeno a la síntesis de β-lactamas,[58,65] ciclobutanonas,[66] α-

[60] Collman, J. P.; Hegedus, L. S.; Norton, J. R.; Finke, R. G. *Principles and Applications of Organotransition Metal Chemistry*, Ed. University Science Books, Mill Vlley (CA), 1987, págs. 373-375.
[61] (a) Köbbing, S.; Mattay, J.; Raabe, G. *Chem. Ber.* **1993**, *126*, 1849. (b) Köbbing, S.; Mattay, J. *Tetrahedron Lett*. **1992**, *33*, 927. (c) Hegedus, L. S.; Montgomery, J.; Narukawa Y.; Snustad, D. C. *J. Am. Chem. Soc.* **1991**, *113,* 5784.
[62] Gut, H.; Welte, N.; Link, U.; Fischer, H.; Steiner U. E. *Organometallics*, **2000**, *19*, 2354.
[63] (a) Gallagher, M. L.; Greene, J. B.; Rooney, A. D. *Organometallics*, **1997**, *16*, 5260. (b) Doyle, K. O.; Gallagher, M. L.; Pryce, M. T.; Rooney, A. D. *J. Organomet. Chem.* **2001**, *617-618*, 269.
[64] Gröthjan ha descrito recientemente la isomerización cetena→carbeno sobre un núcleo de iridio, véase: (a) Gröthjan, D. B.; Bikzhanova, G. A.; Collins, L. S. B.; Concolino, T.; Lam, K. C.; Rheinhold, A. L. *J. Am. Chem. Soc.* **2000**, *122,* 5222. (b) Urtel, H.; Bikzhanova, G. A.; Gröthjan, D. B.; Hofmann, P. *Organometallics*, **2001**, *20*, 3938. (c) Gröthjan, D. B.; Collins, L. S. B.; Wolpert, M.; Bikzhanova, G. A.; Lo, H. C.; Combs, D.; Hubbard, J. L. *J. Am. Chem. Soc.* **2001**, *123,* 8260.
[65] (a) Hegedus, L. S.; Imwinkelried, R.; Alarid-Sargent, M.; Dvorak, D.; Satoh, Y. *J. Am. Chem. Soc.* **1990**, *112*, 1109. (b) Narukawa, Y.; Juneau, K. N.; Snustad, D. C.; Miller, D. B.; Hegedus, L. S. *J. Org. Chem.* **1992**, *57*, 5453.
[66] (a) Sierra, M. A.; Hegedus, L. S. *J. Am. Chem. Soc.* **1989**, *111*, 2335. (b) Soderberg, B. C.; Hegedus, L. S.; Sierra, M. A. *J. Am. Chem. Soc.* **1990**, *112*, 4364. (c) Hegedus, L. S.; Bates, R. W.; Söderberg, B. C. *J. Am. Chem. Soc.* **1991**, *113*, 923.

aminoácidos,[16] péptidos,[67] compuestos aromáticos[68] y lactonas[69] en procesos más eficientes que los que emplea la metodología sintética clásica (Esquema 15).

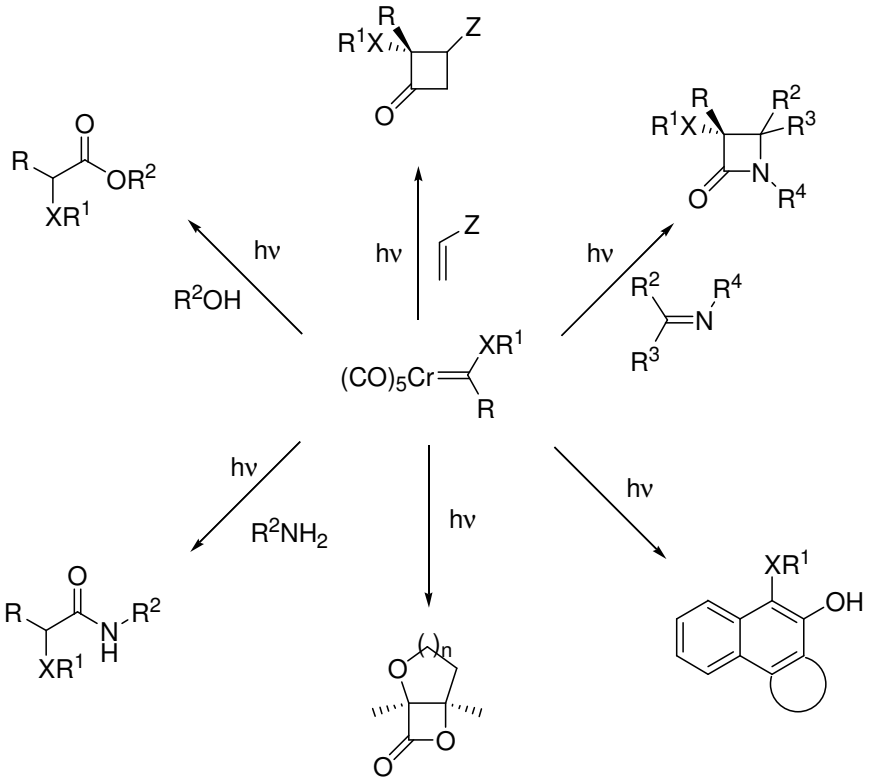

Esquema 15

I.5.1.1. Reacciones de cicloadición

- *Con iminas para generar β-lactamas*

La fotólisis de alcoxi-cromocarbenos en presencia de un amplio rango de iminas produce β-lactamas, con buenos rendimientos y libres de los productos secundarios que son típicos en reacciones con cetenas libres. El proceso es altamente diastereoselectivo, generándose normalmente un único diastereómero y no está restringido a iminas sencillas; de hecho, el empleo de iminas heterocíclicas produce de manera eficiente β-lactamas estructuralmente más complejas. (Esquema 16).

[67] Miller, J. R.; Pulley, S. R.; Hegedus, L. S.; DeLombaert, S. *J. Am. Chem. Soc.* **1992**, *114*, 5602.
[68] Merlic, C. A.; Xu, D. *J. Am. Chem. Soc.* **1991**, *113*, 7418.
[69] Colson, P. J.; Hegedus, L. S. *J. Org. Chem.* **1994**, *59*, 4972.

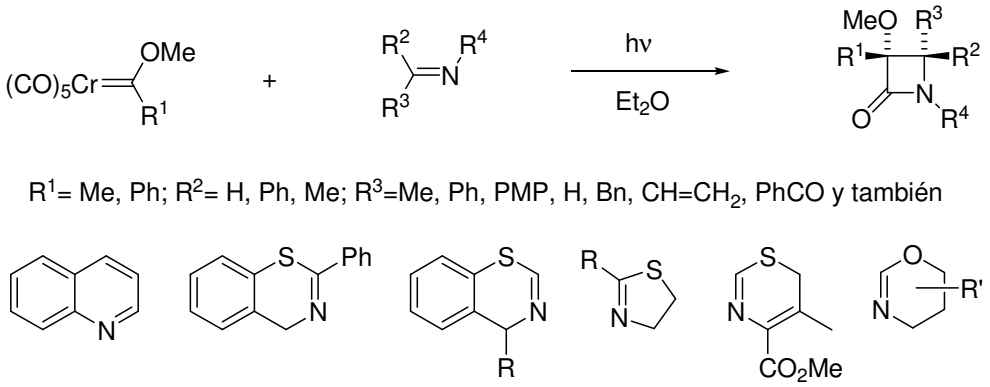

R^1= Me, Ph; R^2= H, Ph, Me; R^3=Me, Ph, PMP, H, Bn, $CH=CH_2$, PhCO y también

Esquema 16

Esta reacción se ha aplicado con éxito con complejos bis-carbénicos para la generación bis-azepenams (Esquema 17).[22g]

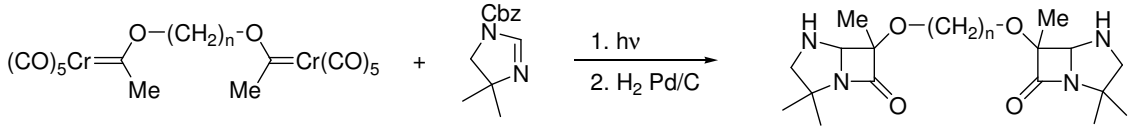

n = 2, 3, 4, 10

(1:1, mezcla de diastereoisómeros)

Esquema 17

Los intentos por inducir asimetría en esta reacción han conducido a resultados diversos. En la mayoría de los casos, el empleo de auxiliares quirales sobre el nitrógeno imínico no resulta efectivo ya que es poco estereoselectivo.[58] Existen excepciones si se utilizan iminas rígidas o cíclicas como tiazolinas (Esquema 18)[58] e imidazolinas,[70] con las que se llegan a obtener *ee* prácticamente del 100%.

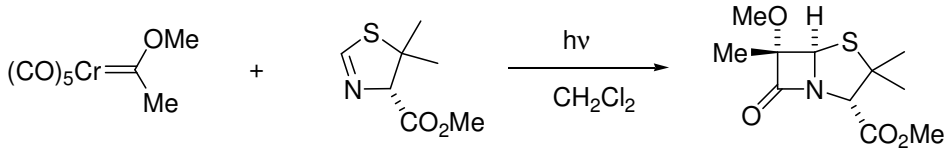

Esquema 18

También se ha colocado el auxiliar quiral en el complejo metálico. Así, el complejo **7** que incorpora una oxazolidina como agente de transferencia de quiralidad genera β-lactamas ópticamente activas con elevados rendimientos y altas diastereo- y enantioselectividades (Esquema 19).[65a]

[70] Betschart, C.; Hegedus, L. S. *J. Am. Chem. Soc*. **1992**, *114*, 5010.

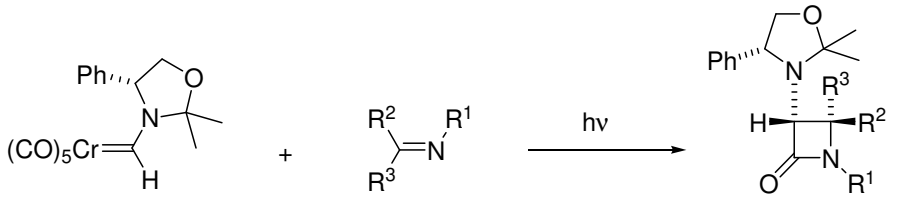

Esquema 19

Basado en una amplia evidencia teórica-experimental, se ha propuesto que la reacción entre cetenas e iminas para producir β-lactamas,[71,72] ocurre por un ataque perpendicular del nitrógeno de la imina sobre el carbono carbonílico de la cetena por el lado estéricamente menos impedido, seguido de un cierre conrotatorio del intermedio zwitteriónico formado (Esquema 20). Esto coloca al sustituyente más voluminoso de la cetena en posición *cis* respecto al sustituyente en *anti* de la imina.

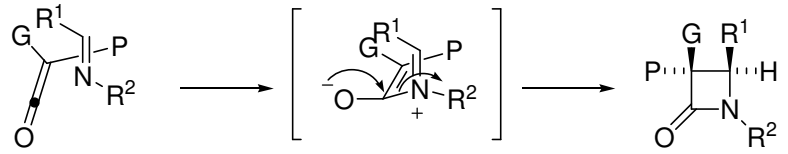

Esquema 20

En la reacción con cetenas derivadas de complejos metal-carbeno, la estereoquímica observada es exactamente la contraria a la esperada según estos criterios de tipo estérico. En principio, esta diferencia podría deberse a la presencia del metal durante el proceso de cicloadición, que supone la formación del producto contraestérico. Sin embargo, se asume[73] que la estereoselectividad observada se debe a la presencia del grupo dador alcoxi en la cetena, que disminuye la energía para el cierre del zwitterion resultante del ataque sobre el grupo más voluminoso, por la cara contraria a los grupos donadores, conduciendo al producto contraestérico (Esquema 21).

[71] *The Organic Chemistry of β-Lactams*, Georg, G. I., Ed., VCH Publishers, New York, 1993.
[72] Cossío, F. P.; Arrieta, A.; Lecea, B.; Ugalde, J. M. *J. Am. Chem. Soc*. **1994**, *116*, 2085.
[73] (a) Dumas, S.; Hegedus, L. S. *J. Org. Chem*. **1994**, *59*, 4967. (b) Cossío, F.; Ugalde, J. M.; López, X.; Lecea, B.; Palomo, C. *J. Am. Chem. Soc*. **1993**, *115*, 995. (c) López, R.; Sordo, T. L.; Sordo, J. A.; González, J. *J. Org. Chem*. **1993**, *58*, 7036. (d) Houk, K. N.; Spellmeyer, D. C.; Jefford, C. W.; Rimbailt, C. G.; Wang, Y.; Miller, R. D. *J. Org. Chem*. **1988**, *53*, 2129.

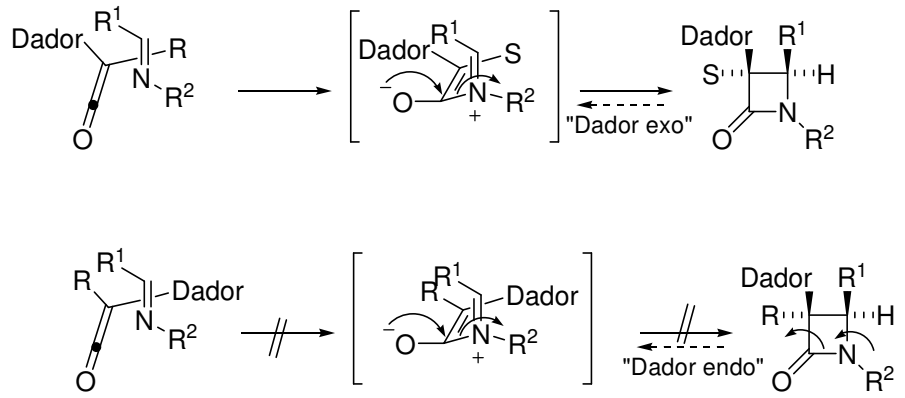

Esquema 21

La fotorreactividad de un complejo metal-carbeno de Fischer depende de los sustituyentes del ligando carbeno. En general, los mejores rendimientos se obtienen para complejos alcoxi-cromocarbenos y para amino-cromocarbenos con un átomo de hidrógeno unido al carbono carbenoide. Los rendimientos disminuyen drásticamente cuando se emplean aminocarbenos con sustituyentes distintos de hidrógeno (alquilo o arilo). Además, existen dos tipos de complejos cromo-carbeno que son fotoinertes:

a) Los complejos que poseen dos heteroátomos unidos al carbono carbenoide ($(CO)_5Cr=C(OMe)_2$, $(CO)_5Cr=C(OMe)(NR_2)$). Estos compuestos se caracterizan por ser incoloros e inertes a la irradiación, recuperándose inalterados después de una semana de irradiación.

b) Los complejos con buenos grupos π-aceptores unidos al carbono carbenoide (PhCH=CH-, PhC≡C-, etc.), caracterizados por ser de color rojo oscuro y por no dar ningún tipo de reacción fotoquímica cuando se someten a irradiación, a excepción de aquellas reacciones que implican la transferencia del ligando carbeno a olefinas pobres en electrones a bajas temperaturas (0 ºC).[74] Este proceso genera los correspondientes ciclopropanos *cis/trans* (cuya proporción relativa es muy sensible a la polaridad del disolvente utilizado) y productos de inserción C–H (Esquema 22).

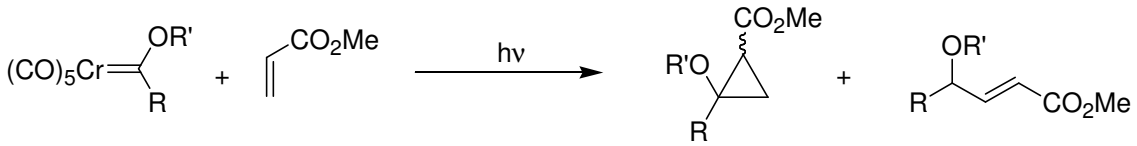

Esquema 22

[74] Sierra, M. A.; del Amo, J. C.; Mancheño, M. J.; Gómez-Gallego, M. *Tetrahedron Lett*. **2001**, *42*, 5345.

Por último, ningún complejo de wolframio de los estudiados hasta la fecha, independientemente de los sustituyentes sobre el carbono carbenoide o de su espectro UV-visible, es fotoquímicamente reactivo. La razón que justifica este hecho no se conoce.

I.6. Métodos computacionales

Muchos de los resultados presentados en esta memoria se han racionalizado en base a cálculos computacionales. Por esta razón, se ha incluido en esta Introducción un apartado dedicado a resumir los métodos computacionales empleados.

I.6.1. Teoría del funcional de la densidad (DFT)

Los métodos del funcional de la densidad (DFT) representan una alternativa para introducir la correlación electrónica en una función de onda monodeterminantal con un coste computacional relativamente bajo. Los físicos han empleado con éxito los métodos derivados de la Teoría del Funcional de la Densidad para el estudio del estado sólido, mientras que su aplicación al estudio de sistemas moleculares aislados es relativamente reciente.

La formulación original DFT nos dice que la energía de un sistema se puede expresar de manera exacta como un funcional de la densidad electrónica, ρ. Desafortunadamente, este funcional *universal*, $E[\rho]$, no se conoce, por lo que el objetivo a conseguir es obtener una buena aproximación de este funcional que se aplicará posteriormente sobre la densidad electrónica.

En principio, como la energía puede extraerse de la densidad electrónica, no es necesario introducir la aproximación orbital molecular en la metodología DFT. Sin embargo, en la metodología DFT más exitosa introducida por Kohn y Sham,[75] la densidad electrónica se expresa como un sumatorio sobre orbitales moleculares ocupados:

$$\rho = \sum_{i}^{N} \langle \chi_i | \chi_i \rangle$$

de esta manera se consigue un conjunto de ecuaciones monoelectrónicas análogas a las de la metodología Hartree-Fock (HF) empleando un Hamiltoniano análogo y llamado comúnmente Hamiltoniano de Kohn-Sham:

$$\hat{h}_{KS} | \chi_i \rangle = \varepsilon i | \chi_i \rangle; \forall i = 1, N$$

[75] Kohn, W.; Sham, L. J. *Phys. Rev*. **1965**, *140*, A1133.

para un modelo de partículas no interaccionantes, el Hamiltoniano de Kohn-Sham se puede expresar como:

$$\hat{h}_{KS}(r) = -\frac{1}{2}\nabla^2 + v(r) + \frac{1}{2}\int \frac{\rho(r')}{|r-r'|}dr' + v_{xc}(r)$$

donde el primer término representa la energía cinética del sistema; el segundo es un potencial externo debido a los núcleos; el tercer término representa la interacción culómbica entre los electrones y el último término representa el llamado potencial de intercambio-correlación. Este último término debe incluir el efecto real de la correlación electrónica, el intercambio sobre la energía cinética y parte de la repulsión electrón-electrón. Precisamente es en la forma de calcular este potencial en lo que difieren los distintos métodos DFT.

Desde un punto de vista práctico, un cálculo DFT es similar a uno HF (también es auto-consistente) con la salvedad de que debido a la complejidad del funcional de intercambio-correlación, las integraciones necesarias deben llevarse a cabo numéricamente.

Como se ha indicado, la elección del funcional para el intercambio-correlación es el punto clave en un cálculo DFT. Básicamente existen dos grandes familias de funcionales para el cálculo de la energía de intercambio-correlación: los basados en la Aproximación Local de la Densidad (LDA) y aquellos que incluyen correcciones de gradiente, como los metódos GGA (Generalized Gradient Approximation). El primer grupo tiene en cuenta sólo el valor de la densidad electrónica en cada punto del espacio, mientras que el segundo también tiene en cuenta variaciones en el gradiente de la densidad. Los funcionales GGA, en general, describen mejor el intercambio-correlación que los LDA.

En este trabajo, hemos empleado el funcional GGA conocido por B3LYP. Este funcional híbrido es una combinación del funcional de tres parámetros desarrollado por Becke para evaluar el intercambio[76] y el funcional desarrollado por Lee-Yang-Parr para evaluar la correlación electrónica.[77] El funcional así construido queda definido por:

$$E_{xc}^{B3LYP} = (1-a)E_x^{LDA} + aE_x^{HF} + b\Delta E_x^{B} + (1-c)E_c^{LDA} + cE_c^{LYP}$$

[76] (a) Becke, A. D. *Phys.Rev. A.* **1988**, *38*, 3098. (b) Becke, A. D. *J. Chem. Phys.* **1993**, *98*, 5648.
[77] Lee, C.; Yang, W.; Parr, R. G. *Phys. Rev. B* **1988**, *37*, 785.

donde el intercambio Hartree-Fock (E_x^{HF}) queda corregido por el de Becke (E_x^B), la correlación queda incluida en el funcional LYP (E_c^{LYP}) y donde a = 0.20, b = 0.72 y c = 0.81. B3LYP es quizás el funcional más ampliamente usado porque proporciona muy buenos resultados a pesar de que los parámetros a, b y c no están optimizados.

Los métodos DFT constituyen una mejora sustancial sobre los métodos HF o post-HF en el cálculo de complejos de metales de transición.[78] De hecho, este tipo de métodos constituyen el método de elección cuando tratamos con tales compuestos.

I.6.2. Materiales y métodos computacionales

Todos los cálculos se han llevado a cabo utilizando el conjunto de programas GAUSSIAN 98 y GAUSSIAN 03.[79] Hemos utilizado las funciones de base estándares 6-31G(d) ó 6-31+G(d)[80] según el caso, para describir los átomos de carbono, hidrógeno, oxígeno, nitrógeno y fósforo. Para los átomos de cromo y wolframio hemos recurrido al uso del potencial efectivo (ECP) desarrollado por Hay-Wadt[81] para describir los electrones internos incluyendo una función de base doble-zeta para describir a los electrones de valencia. En este esquema, y para el átomo de cromo, el pseudopotencial ECP incluye los diez electrones internos del metal, mientras que los electrones de

[78] Frenking, G.; Antes, I.; Böhme, M.; Dapprich, S.; Ehlers, A. W.; Jonas, V.; Neuhaus, A.; Otto, M.; Stegmann, R.; Veldkamp, A.; Vyboishchikov, S. F. en *Reviews in Computational Chemistry*, vol. 8, Lipkowitz, K. B. y Boyd, D. B. Eds., VCH: New York, 1996, pág. 63.

[79](a) Gaussian 98, Revision A.11.3, Frisch, M. J.; Trucks, G. W.; Schlegel, H. B.; Scuseria, G. E.; Robb, M. A.; Cheeseman, J. R.; Zakrzewski, V. G.; Montgomery Jr., J. A.; Stratmann, R. E.; Burant, J. C.; Dapprich, S.; Millam, J. M.; Daniels, A. D.; Kudin, K. N.; Strain, M. C.; Farkas, O.; Tomasi, J.; Barone, V.; Cossi, M.; Cammi, R.; Mennucci, B.; Pomelli, C.; Adamo, C.; Clifford, S.; Ochterski, J.; Petersson, G.; Ayala, A. P. Y.; Cui, Q.; Morokuma, K.; Rega, N.; Salvador, P.; Dannenberg, J. J.; Malick, D. K.; Rabuck, A. D.; Raghavachari, K.; Foresman, J. B.; Cioslowski, J.; Ortiz, J. V.; Baboul, A. G.; Stefanov, B. B.; Liu, G.; Liashenko, A.; Piskorz, P.; Komaromi, I.; Gomperts, R.; Martin, R. L.; Fox, D. J.; Keith, T.; Al-Laham, M. A.; Peng, C. Y.; Nanayakkara, A.; Challacombe, M.; Gill, P. M. W.; Johnson, B.; Chen, W.; Wong, M. W.; Andres, J. L.; González, C.; Head-Gordon, M.; Replogle, E. S.; Pople, J. A. Gaussian, Inc., Pittsburgh PA, 2002. (b) Gaussian 03, Revision B.04, Frisch, M. J.; Trucks, G. W.; Schlegel, H. B.; Scuseria, G. E.; Robb, M. A.; Cheeseman, J. R.; Montgomery Jr., J. A.; Vreven, T.; Kudin, K. N.; Burant, J. C.; Millam, J. M.; Iyengar, S. S.; Tomasi, J.; Barone, V.; Mennucci, B.; Cossi, M.; Scalmani, G.; Rega, N.; Petersson, G.; Nakatsuji, A. H.; Hada, M.; Ehara, M.; Toyota, K.; Fukuda, R.; Hasegawa, J.; Ishida, M.; Nakajima, T.; Honda, Y.; Kitao, O.; Nakai, H.; Klene, M.; Li, X.; Knox, J. E.; Hratchian, H. P.; Cross, J. B.; Adamo, C.; Jaramillo, J.; Gomperts, R.; Stratmann, R. E., Yazyev, O.; Austin, A. J.; Cammi, R.; Pomelli, C.; Ochterski, J. W.; Ayala, P. Y.; Morokuma, K.; Voth, G. A.; Salvador, P.; Dannenberg, J. J.; Zakrzewski, V. G.; Dapprich, S.; Daniels, A. D.; Strain, M. C.; Farkas, O.; Malick, D. K.; Rabuck, A. D.; Raghavachari, K.; Foresman, J. B.; Ortiz, J. V.; Cui, Q.; Baboul, A. G.; Clifford, S.; Cioslowski, J.; Stefanov, B. B.; Liu, G.; Liashenko, A.; Piskorz, P.; Komaromi, I.; Martin, R. L.; Fox, D. J.; Keith, T.; Al-Laham, M. A.; Peng, C. Y.; Nanayakkara, A.; Challacombe, M.; Gill, P. M. W.; Johnson, B.; Chen, W.; Wong, M. W.; González, C.; Pople, J. A. Gaussian, Inc., Pittsburgh PA, 2003.

[80] Hehre, W. J.; Radom, L.; Schleyer, P. v. R.; Pople, J. A. *Ab Initio Molecular Orbital Theory;* Wiley: New York, **1986**.

[81] Hay, P. J.; Wadt, W. R. *J. Chem. Phys.* **1985**, *82*, 299.

valencia $3s^2 3p^6 4s^1 3d^5$ quedan explícitamente descritos en términos de una función de base doble-zeta, como se encuentra implementado en el paquete Gaussian (keyword LANL2DZ).

Todos los puntos estacionarios se han caracterizado analizando sus frecuencias armónicas al mismo nivel de teoría,[82] encontrándose que todos los reactivos, intermedios y productos poseen Hessianos positivos mientras que todos los estados de transición (TSs) localizados muestran un único autovalor negativo en sus matrices de fuerza diagonalizadas, estando el autovector correspondiente asociado al movimiento a lo largo de la coordenada de reacción considerada y comprobado mediante cálculo IRC (Intrinsic Reaction Coordinate).[83] Las energías de vibración en el punto cero (ZPVE) también se han calculado al mismo nivel de teoría y no se han escalado.

Las interacciones dador-aceptor, cargas y órdenes de enlace se han calculado mediante el método NBO (Natural Bond Order).[84] Estas interacciones bielectrónicas se han calculado aplicando la ecuación:

$$\Delta E^{(2)}_{\phi\phi^*} = -n_\phi \frac{\langle \phi^* | \hat{F} | \phi \rangle}{\in_{\phi^*} - \in_\phi}$$

donde n_ϕ es el número de ocupación del dador NBO, $\hat{F}$ es el operador de Fock, y ϕ y $\phi*$ son los NBOs ocupado y vacío de energías $\in_\phi$ y $\in_{\phi^*}$ respectivamente.

[82] McIver, J. W.; Komornicki, K. *J. Am. Chem. Soc.* **1972**, *94*, 2625.
[83] González, C.; Schlegel, H. B. *J. Phys. Chem.* **1990**, *94*, 5523.
[84] (a) Foster, J. P.; Weinhold, F. *J. Am. Chem. Soc*. **1980**, *102*, 7211. (b) Reed, A. E.; Weinhold, F. J. *J. Chem. Phys*. **1985**, *83*, 1736. (c) Reed, A. E.; Weinstock, R. B.; Weinhold, F. *J. Chem. Phys*. **1985**, *83*, 735. (d) Reed, A. E.; Curtiss, L. A.; Weinhold, F. *Chem. Rev*. **1988**, *88*, 899.

CAPÍTULO I

Capítulo I. OBJETIVOS

Capítulo I: Objetivos

El trabajo recogido en esta parte de la memoria persigue como objetivo fundamental la síntesis de complejos metal-carbeno bi- y polimetálicos y la exploración preliminar de sus posibles aplicaciones a la síntesis orgánica.

- En este capítulo, se abordará la síntesis y caracterización estructural de nuevos complejos metal-carbeno bimetálicos con estructura conformacionalmente restringida. Para ello se prepararán distintos complejos bis(etinil)-metalcarbeno de estructura general I. Estos compuestos se usarán como moldes para la construcción de complejos bis-carbénicos ciclofánicos de estructura general II. Las reacciones llevadas a cabo serán el primer ejemplo de reacciones sobre complejos bimetálicos que transcurran con retención de la función metal-carbeno.

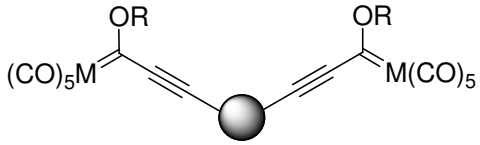

I

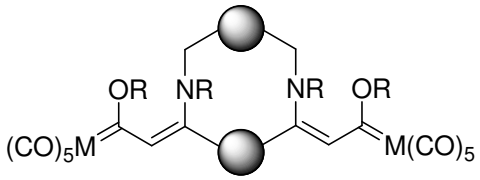

II

- Utilizando la metodología empleada en el objetivo anterior, abordaremos la síntesis de complejos tetrametálicos macrocíclicos, tanto homo- como heterometálicos, de estructura general III. Se estudiará su comportamiento electroquímico mediante voltamperometría cíclica y su capacidad para actuar como anfitriones para pequeñas moléculas huésped.

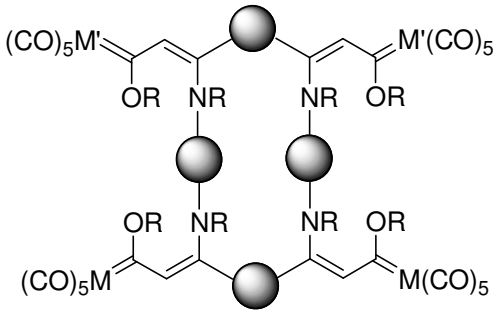

III

- Como tercer objetivo, se estudiarán procesos de transferencia electrónica (TE) en medios no convencionales (ESI-MS) en complejos metal-carbeno bi- y polimetálicos. Este trabajo nos permitirá determinar la participación de los distintos metales en reacciones de TE intramolecular bajo las condiciones ESI-MS optimizadas por nuestro grupo de investigación y también, determinar la influencia en el proceso del espaciador entre los metales.
- Como último objetivo de este capítulo, e íntimamente relacionado con el proceso de TE inducido por ESI, abordaremos un estudio teórico-experimental del mecanismo del proceso de generación de los iones detectados como $[M - H]^-$. Para ello, se sintetizarán distintos complejos cromo-carbeno α,β-insaturados deuterados selectivamente y serán sometidos al proceso ESI-MS.

1.1. Synthesis of Cyclophanic Chromium(0) Bis(carbene) Complexes

1.1. Synthesis of Cyclophanic Chromium(0) Bis(carbene) Complexes

The synthesis of chromium(0) bis(carbene) complexes as well as the study of their reactivity is far behind their mononuclear counterparts.[1] In fact, although the first of these compounds was reported by E. O. Fischer in 1982,[2] little work has been directed toward the transformation of simple bimetallic complexes into structurally more sophisticated bis(carbenes). Thus, some examples of this kind of transformations can be found in the aminolysis of group 6 alkoxy carbenes with different amines[3] or in the deprotonation and further alkylation of bis-(carbene) **1** with $[(CO)_3Fe(C_6H_7)BF_4]$ and $[(CO)_5Re(C_2H_4)BF_4]$ to yield tetranuclear derivatives **2a** and **2b**, respectively. Compound **3** was also obtained by oxidation of the bis-anion formed in the deprotonation process (Figure 1).[4] Aumann has also prepared an impressive array of complex chromium(0) bis(carbenes) while studying 1,4-nucleophilic additions to α,β-unsaturated chromium(0) and tungsten(0) carbene complexes[1a,i,5] and Macomber has prepared series of chromium(0) and tungsten(0) bis(carbene) complexes by reaction of the α-anions of group 6 carbene complexes and α,ω-dihaloalkanes.[6] Additionally, Hegedus has reported the preparation of different homo-bis(carbene) complexes in his approach to the synthesis of cyclams.[7]

---

[1] (a) Sierra, M. A. *Chem. Rev.* **2000**, *100,* 3591. (b) Barluenga, J.; Fañanás, F. J. *Tetrahedron* **2000**, *56*, 4597. For selected reviews on the chemistry of Fischer carbene complexes, see: (c) Dötz, K. H.; Fischer, H.; Hofmann, P.; Kreissel, R.; Schubert, U.; Weiss, K. *Transition Metal Carbene Complexes*, Verlag Chemie: Deerfield Beach, Florida, 1983. (d) Dötz, K. H. *Angew. Chem. Int. Ed. Eng.* **1984**, *23*, 587. (e) Wulff, W. D. in *Comprehensive Organometallic Chemistry II,* Abel, E. W.; Stone, F. G. A.; Wilkinson, G.; Eds. Pergamon: Oxford. 1995; vol. 12, p. 470. (f) Hegedus, L. S. in *Comprehensive Organometallic Chemistry II,* Abel, E. W.; Stone, F. G. A.; Wilkinson, G.; Eds. Pergamon: Oxford. 1995; vol. 12, p. 549. (g) Harvey, D. F.; Sigano, D. M. *Chem. Rev.* **1996**, *96*, 271. (h) Hegedus, L. S. *Tetrahedron* **1997**, *53*, 4105. (i) Aumann, R.; Nienaber, H. *Adv. Organomet. Chem.* **1997**, *41*, 163. (j) de Meijere, A.; Schirmer, H.; Duetsch, M. *Angew. Chem. Int. Ed.* **2000**, *39*, 3964.

[2] Fischer, E. O.; Röll, W.; Huy, N. H. T.; Ackermann, K. *Chem. Ber.* **1982**, *115*, 2951.

[3] Huy, N. H. T.; Lefloch, P.; Robert, F.; Jeannin, Y. *J. Organomet. Chem.* **1987**, *327*, 211.

[4] Geisbauer, A.; Mihan, S.; Beck, W. *J. Organomet. Chem*. **1995**, *501*, 61.

[5] Aumann, R. *Eur. J. Org. Chem*. **2000**, 17.

[6] (a) Macomber, D. W.; Madhukar, P. *J. Organomet. Chem*. **1992**, *433*, 279. For the preparation of *bis*(carbene) complexes by the Michael addition of group 6 metal carbene complexes derived α-carbanions to group 6 α,β-unsaturated metal carbenes, see: (b) Macomber, D. W.; Hung, M.-H.; Verma, A. G.; Rogers, R. D. *Organometallics* **1988**, *7*, 2072. (c) Macomber, D. W.; Hung, M.-H.; Madhukar, P.; Liang, M.; Rogers, R. D. *Organometallics* **1991**, *10*, 737. (d) Macomber, D. W.; Madhukar, P.; Rogers, R. D. *Organometallics* **1991**, *10*, 2121.

[7] (a) Wynn, T.; Hegedus, L. S. *J. Am. Chem. Soc*. **2000**, *122*, 5034. (b) Puntener, K.; Hellman, M. D.; Kuester, E.; Hegedus, L. S. *J. Org. Chem*. **2000**, *65*, 8301. (c) Kuester, E.; Hegedus, L. S. *Organometallics* **1999**, *18*, 5318. (d) Dumas, S.; Lastra, E.; Hegedus, L. S. *J. Am. Chem. Soc*. **1995**, *117*, 3368. (e) Hsiao, Y.; Hegedus, L. S. *J. Org. Chem*. **1997**, *62*, 3586.

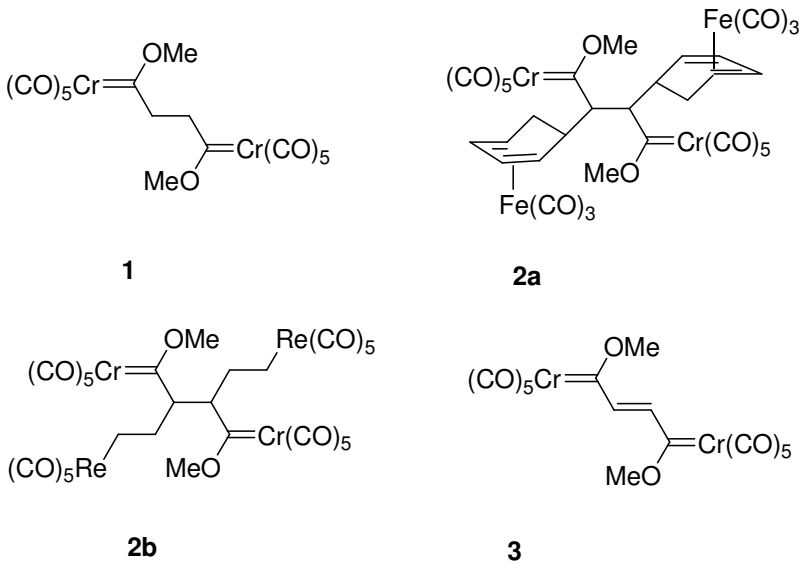

Figure 1

The chemistry of chromium(0) bis(carbene) complexes reported to this moment is that expected for both metal nuclei reacting as isolated centers,[8] although some anomalous results have been obtained in the regiochemistry of Dötz-type reactions[9] and during the Pd-catalyzed dimerization of alkylchromium(0) bis(carbenes).[10] These results may point to some kind of interaction between the metal centers during the reaction process. In this regard, tethered chromium(0) bis(carbene) complexes with a cyclophanic structure would be of interest. Should their preparation be viable, they would offer a good opportunity to study the reactivity of bimetallic alkoxychromium(0) carbene complexes having severe structural constraints. Here, we report the achievement of the first goal: a general procedure to prepare chromium(0) bis(carbene) complexes having a cyclophane structure.

1,3-Diethynylbenzene was the template selected to build the cyclophanic skeleton. This compound was transformed into the corresponding bis(carbene) complex **4** (26 % overall yield) by sequential reaction with BuLi and $[Cr(CO)_6]$ and final quenching of the lithium ate complex thus formed with Et_3OBF_4 (together with complex **4**, the corresponding mono(carbene) complex was obtained in a 21 % yield (see the Supporting Information for a detailed experimental procedure). The cyclophanic

[8] (a) Bao, J.; Wulff, W. D.; Fumo, M. J.; Grant, E. B.; Heller, D. P.; Whitcomb, M. C.; Yeung, S.-M. *J. Am. Chem. Soc*. **1996**, *118*, 2166. (b) Huy, N. H. T.; Lefloch, P. *J. Organomet. Chem*. **1988**, *344*, 303. (c) Tomuschat, P.; Kröner, L.; Steckhan, E.; Nieger, M.; Dötz, K. H. *Chem. Eur. J*. **1999**, *5*, 700. (d) Wang, H.; Wulff, W. D. *J. Am. Chem. Soc*. **1998**, *120*, 10573. See, also ref. 7.

[9] Wang, H.; Wulff, W. D.; Rheingold, A. L. *J. Am. Chem. Soc*. **2000**, *122*, 9862.

[10] (a) Sierra, M. A.; Mancheño, M. J.; Sáez, E.; del Amo, J. C. *J. Am. Chem. Soc*. **1998**, *120*, 6812. (b) Sierra, M. A.; del Amo, J. C.; Mancheño, M. J.; Gómez-Gallego, M. *J. Am. Chem. Soc*. **2001**, *123*, 851.

skeleton would be built on complex **4** through a double Michael addition. This assumption was based on the known fact that α,β-unsaturated complexes are exceptional Michael acceptors. However, the regiochemistry of their reaction with amines (namely the 1,4 *vs* 1,2-addition) is highly influenced by steric and electronic effects. This fact was early demonstrated by E. O. Fischer,[11] and it has been extensively studied recently by one of us.[12] In our case, the problem is exacerbated by the necessity to effect the ring closure into the second Michael acceptor, once the first addition has occurred. In fact, taking into account only regiochemical considerations, there are three different types of compounds that could be formed, with generic structures I-III (Figure 2). Nevertheless, we were confident that the double 1,4-adduct would be the main reaction product. This hypothesis was based on the known fact that usually 1,4-addition is obtained when the reaction is carried out at room temperature. As matters evolved, compounds having structures I and II were obtained in these reactions, depending on the nature of the diamine nucleophile.

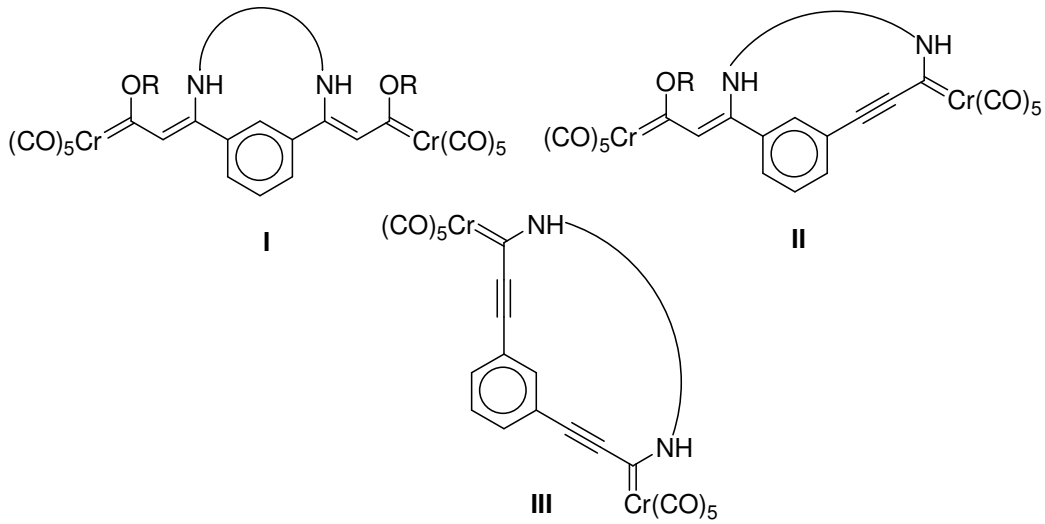

Figure 2

Complex **4** was reacted with 1,4-xylylenediamine in CH_2Cl_2 at room temperature. The violet solution of complex **4** became deep reed instantaneously upon addition of the diamine. After the solvent was removed, the ^{1}H NMR spectrum of the solid residue showed only the expected cyclophane bis(carbene) complex **5** formed as a single isomer. No further purification was required, since the product was obtained in

[11] (a) Fischer, E. O.; Kreissl, F. R. *J. Organomet. Chem.* **1972**, *35*, C45. (b) Fischer, E. O.; Kalder, H. J. *J. Organomet. Chem.* **1977**, *131*, 57.
[12] Moretó, J. M.; Ricart, S.; Dötz, K. H.; Molins, E. *Organometallics* **2001**, *20*, 62.

analytically pure form. The structure of complex **5** was determined by standard spectroscopic techniques. Since ^{1}H NMR spectra of complex **5** (and as a matter of fact ^{1}H NMR spectra of all the cyclophanic complexes obtained through this work) showed ill-resolved broad signals, the well resolved ^{13}C NMR spectra were decisive in establishing the cyclophane structure (this was also true for the remaining cyclophane complexes synthesized through this work). Thus, a single signal corresponding to the carbene carbon appeared at 297.6 ppm, with additional signals at 223.8 ppm (*trans*-CO) and 218.4 ppm (*cis*-CO) which unambiguously established the nature of alkoxycarbene complex for **5**. Therefore, a double 1,4-addition had occurred (Scheme 1).[13] Analogously, results were obtained with *m*-xylylendiamine and cadaverine (1,5-diaminopentane) that yielded complexes **6** and **7** almost instantaneously. However, in these cases the reactions were slightly dirtier and column chromatography was needed to obtain pure compounds. Complexes **6** and **7** were obtained in 61 and 53 % yields, respectively. The spectroscopic pattern in these cases was analogous to the observed with complex **5** with signals assignable to carbene carbons bearing alkoxy substituents at 297.9 and 294.1 ppm, respectively (Scheme 1). A *Z,Z* stereochemistry was assigned to complexes **5-7** by comparison of their spectroscopic data with their reported noncyclophane analogues.[12]

[13] The preparation of bimetallic cyclophane **5** is representative: To a solution of 750 mg (1.21 mmol) of complex **4** in dry CH_2Cl_2 was added *via cannula* at room temperature 164 mg (1.21 mmol) of *p*-xylylenediamine in 75 mL of dry CH_2Cl_2. The reaction mixture was stirred for about 30 min (all the reactions were monitored by T.L.C. until the disappearance of the starting material). An appreciable change of color to deep red was always observed in the reaction mixture. The solvent was removed under reduced pressure to obtain 916 mg (quantitative yield) of complex **5** as a red solid. No further purification was required. ^{1}H NMR ($CDCl_3$) δ 1.25 (m, 6H), 4.28 (s, 4H), 4.73 (q, 4H, J = 6.5 Hz), 6.20 (s, 2H), 7.13-7.46 (m, 8H), 9.04 (s, 2H). ^{13}C NMR ($CDCl_3$) δ 15.5, 49.5, 74.2, 119.6, 127.4, 128.2, 129.7, 135.4, 136.7, 151.5, 218.4, 223.8, 297.6. IR (KBr) 2050, 1896 cm^{-1}.

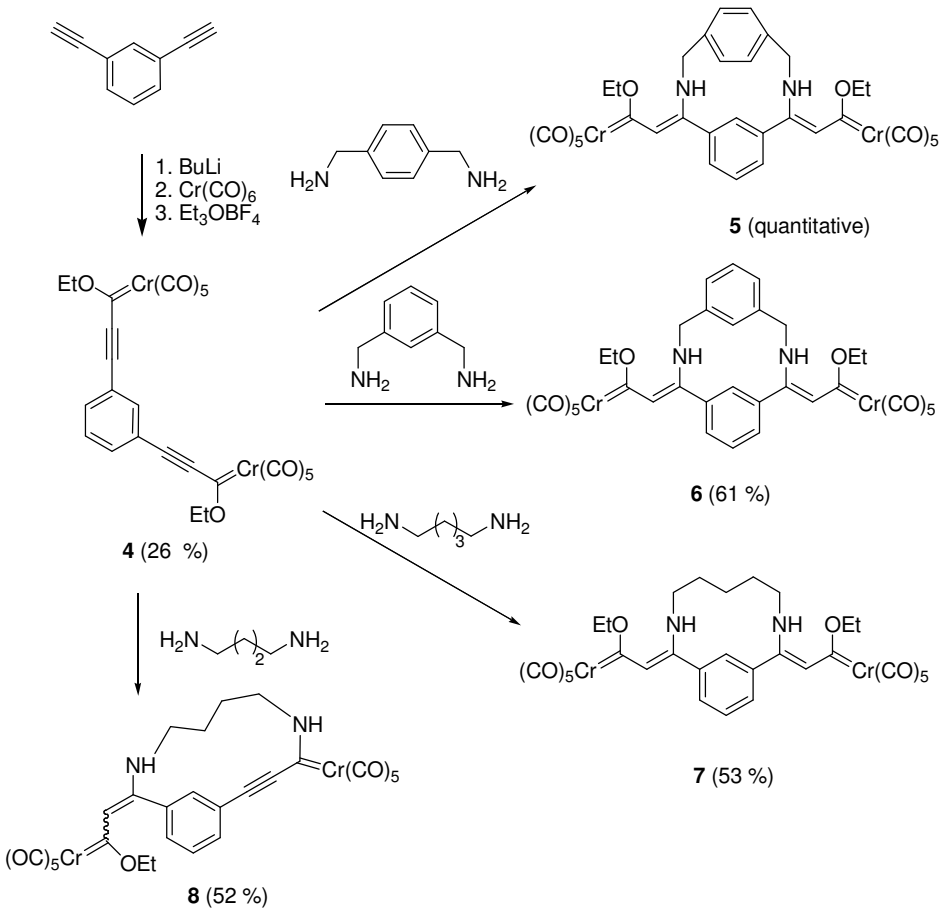

Scheme 1

The reaction between complex **4** and putrescine (1,4-diaminobutane) produced a different outcome. The starting complex was consumed quantitatively and the crude material was submitted to column chromatography, to yield a red solid having spectroscopic data clearly distinguishable from those discussed for complexes **5-7**. In fact, in this case the ^{13}C NMR spectra of the product showed two different signals at 297.8 ppm and 258.6 ppm, indicating that one of the alkoxychromium carbene nuclei had reacted with the amine to produce an aminochromium carbene (signal at 258.6 ppm), while the second amine group reacted as expected in a 1,4-fashion maintaining the second alkoxychromium carbene nucleus (signal at 297.8 ppm). Therefore, the alkoxyamino-bis(carbene) complex **8** (type II in Figure 2) was obtained in this case. This structure is fully consistent with the presence of two different sets of *cis*- and *trans*-CO ligands surrounding two different chromium nuclei. This results in four signals at 223.7, 222.9 (*trans*-CO), and 218.3, 217.0 (*cis*-CO) ppm. The two carbons of the intact triple bond appeared at 88.9 and 119.4 ppm in complex **8**. Furthermore, compound **8** was obtained as an inseparable 1:1 mixture of isomers around the newly

formed double bond. The reasons of this anomalous selectivity obtained with putrescine are not clear at this moment.

In conclusion, a new class of bimetallic bis(carbene) complexes having a cyclophanic structure has been prepared, taking advantage of the high Michael reactivity of bimetallic α,β-unsaturated alkoxychromium(0) carbene complex **4**. The double 1,4-addition occurrs easily with *p*- and *m*-xylylenediamines and cadaverine to form cyclophane bis(carbenes) of type I (Figure 2). However, the reaction with putrescine produces a different cyclophane complex derived from 1,2- + 1,4-addition (type II in Figure 2). The extension of this methodology to prepare other cyclophane bi- and polymetallic complexes as well as the study of their reactivity is actively underway in our laboratories.

Experimental Section

General. ^{1}H NMR and ^{13}C NMR spectra were recorded in $CDCl_3$, on a Varian XL-300S (299.94 MHz for ^{1}H and 75.43 MHz for ^{13}C), a Bruker AMX-500 (500.13 MHz for ^{1}H and 125.8 MHz for ^{13}C), a Bruker 250-AC (250.13 MHz for ^{1}H and 62.90 MHz for ^{13}C), a Bruker 200-AC (200.13 MHz for ^{1}H and 50.03 for ^{13}C MHz) and a Bruker Avance-300 (300.13 MHz for ^{1}H and 75.48 for ^{13}C MHz) spectrometers. Chemical shifts are given in ppm relative to TMS (^{1}H, 0.0 ppm), or $CDCl_3$ (^{13}C, 77.0 ppm). IR spectra were taken on a Perkin-Elmer 781 spectrometer. Flame-dried glassware and standard Schlenck techniques were used for all the reactions. Merck silica-gel (230-400 Mesh) was used as the stationary phase for purification of crude reaction mixtures by flash chromatography. Identification of products was made by TLC (Kiesegel 60F-254), UV light (λ = 254 nm), phosphomolibdic acid solution in 95% EtOH and iodine were also used to develop the plates. All commercially available compounds were used without further purification.

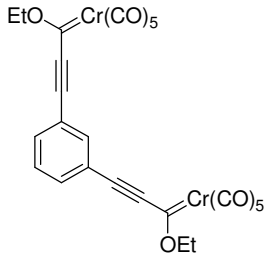

4

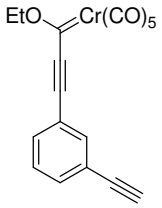

9

Complexes 4 and 9. To a solution of 1.0 g (8 mmol) of 1,3-diethynylbenzene in 75 mL of dry Et_2O at –78 ºC were added dropwise 11 mL (17.6 mmol) of *n*-butyllithium (1.6 M in hexanes). The mixture was stirred at –78 ˚C for 45 min and then, 3.48 g (15.8 mmol) of chromium hexacarbonyl at 0 ˚C were added. After stirring at this temperature for 15 min, 40 mL of dry THF were also added and the mixture was let to stir at room temperature overnight. Then, 6.08 g (32 mmol) of Et_3OBF_4 were added in one portion at –78 ˚C. The violet solution was stirred at this temperature for 15 min and then allowed to reach room temperature for an additional hour. Solvents were removed under reduced pressure and the residue was dissolved in Et_2O and filtered on silica gel. The solvent was evaporated and the residue was submitted to flash column chromatography (SiO_2, Hexane) to give 0.6 g (21%) of the corresponding mono(carbene) **9** and 1.28 g (26%) of the bis(carbene) **4**, both as deep green solids. **Bis(carbene) 4**: ^{1}H NMR δ 1.53 (t, 6H, *J* = 7.1 Hz), 4.70 (q, 4H, *J* = 7.1 Hz), 7.42-7.62 (m, 4H). ^{13}C NMR δ 15.4, 76.6, 91.9, 122.6, 130.0, 135.1, 135.6, 216.5, 226.1, 314.2. IR (KBr) 2152, 2062, 1996, 1963 cm^{-1}. $C_{26}H_{14}Cr_2O_{12}$: Calcd C 50.18, H 2.27, Found C 50.42, H 2.15. **Mono(carbene) 9**: ^{1}H NMR δ 1.51 (t, 3H, *J* = 7.1 Hz), 3.08 (s, 1H), 4.68 (q, 2H, *J* = 7.1 Hz), 7.19-7.58 (m, 4H). ^{13}C NMR δ 15.0, 76.0, 78.9, 81.9, 91.4, 121.4, 122.5, 129.0, 132.8, 134.7, 135.5, 137.1, 216.2, 225.7, 313.8. IR (KBr) 2150, 2062, 1961cm^{-1}.

General procedure for the synthesis of compounds 5-8.
To a solution of bis(carbene) complex **4** in dry dichloromethane was added *via* cannula at room temperature the corresponding bis(amine) dissolved in CH_2Cl_2. The reaction mixture was stirred for about 30 min (all the reactions were monitored by T.L.C. until the disappearance of the starting material). An appreciable change of color to deep red was always observed in the reaction mixture. The solvent was removed under reduced

pressure and the residue, when further purification was needed, was submitted to flash column chromatography (SiO_2, Hexane: AcOEt) under argon atmosphere to give pure compounds.

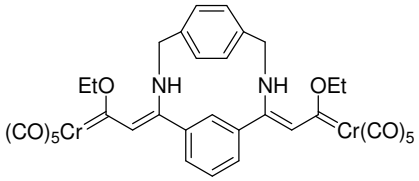

5

Complex 5. Following the general procedure, from 750 mg (1.21 mmol) of complex **4** and 164 mg (1.21 mmol) of *p*-xylylenediamine in 75 mL of dry CH_2Cl_2, was obtained **5** as a red solid (916 mg, quantitative yield). Complex **5** was obtained in analytically pure form and no further purification was required. ^{1}H NMR δ 1.25 (m, 6H), 4.28 (br s, 4H), 4.73 (q, 4H, *J* = 6.5 Hz), 6.20 (s, 2H), 7.13-7.46 (m, 8H), 9.04 (br s, 2H). ^{13}C NMR δ 15.5, 49.5, 74.2, 119.6, 127.4, 128.2, 129.7, 135.4, 136.7, 151.5, 218.4, 223.8, 297.6. IR (KBr) 2050, 1896, 1558 cm^{-1}. $C_{34}H_{26}Cr_2N_2O_{12}$: Calcd C 53.83, H 3.45, N 3.69, Found C 53.62, H 3.58, N 3.45.

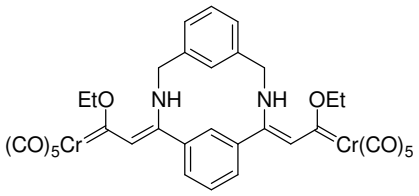

6

Complex 6. Following the general procedure, 400 mg (0.64 mmol) of complex **4** and 87.5 mg (0.64 mmol) of *m*-xylylenediamine were reacted in 40 mL of dry CH_2Cl_2. The crude material thus obtained was purified by flash column chromatography to yield 296 mg (61 %) of **6** as a red solid. ^{1}H NMR δ 1.19 (m, 6H), 4.29 (br s, 4H), 4.72 (br s, 4H), 6.21 (s, 2H), 7.19-7.45 (m, 8H), 9.01 (br s, 2H). ^{13}C NMR δ 15.8, 50.1, 74.6, 119.9, 127.2, 127.9, 130.2, 130.6, 135.7, 137.9, 151.9, 218.8, 224.3, 297.9. IR (KBr) 2050, 1904, 1545 cm^{-1}. $C_{34}H_{26}Cr_2N_2O_{12}$: Calcd C 53.83, H 3.45, N 3.69, Found C 54.04, H 3.61, N 3.47.

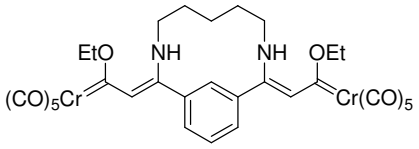

7

Complex 7. Following the general procedure, 300 mg (0.48 mmol) of complex **4** and 49.3 mg (0.48 mmol) of 1,5-diaminopentane were reacted in 30 mL of dry CH_2Cl_2. Purification of the crude material by crystallization in a mixture of CH_2Cl_2/Et_2O (1:2) at –50 ˚C yielded 186 mg (53%) of **7** as a red solid. ^{1}H NMR δ 1.58 (m, 12H), 3.12 (m, 4H), 4.86 (br s, 4H), 6.17 (br s, 2H), 7.17-7.55 (m, 4H), 8.88 (br s, 2H). ^{13}C NMR δ 15.9, 23.7, 30.0, 45.7, 74.1, 119.2, 126.9, 129.4, 135.0, 135.3, 152.6, 218.5, 223.9,

294.1. IR (KBr) 2048, 1908, 1556 cm^{-1}. $C_{31}H_{28}Cr_2N_2O_{12}$: Calcd C 51.39, H 3.90, N 3.87, Found C 51.20, H 3.81, N 3.62.

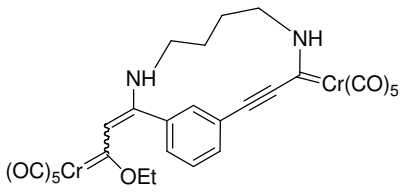

8

Complex 8. Following the general procedure, from 300 mg (0.48 mmol) of complex **4** and 42.5 mg (0.48 mmol) of 1,4-diaminobutane in 30 mL of dry CH_2Cl_2 were obtained after flash column chromatography 178 mg (52 %) of a red solid identified as a mixture of isomers *Z*/*E* (1:1 ratio) of **8**. ^{1}H NMR δ 1.54 (m, 14H), 3.16 (br s, 4H), 3.74 (br s, 4H), 4.78 (br s, 4H), 6.10 (s, 1H), 6.16 (s,1H), 7.19-7.52 (m, 8H), 8.76 (br s, 1H), 8.82 (br s, 1H). ^{13}C NMR δ 15.8, 26.7, 27.5, 29.6, 44.6, 45.3, 51.9, 52.4, 74.2, 88.9, 119.4, 122.2, 122.4, 126.8, 129.5, 129.8, 130.5, 130.8, 133.2, 133.5, 134.5, 135.1, 135.3, 151.4, 151.8, 217.0, 218.3, 222.9, 223.7, 258.6, 297.8. IR (KBr) 2174, 2050, 1909, 1554 cm^{-1}. $C_{28}H_{20}Cr_2N_2O_{11}$: Calcd C 50.61, H 3.03, N 4.22, Found C 50.79, H 3.23, N 4.11.

Una vez puesta a punto la síntesis de complejos ciclofánicos bis-carbénicos de cromo, decidimos extender la metodología empleada para comprobar la generalidad del proceso y sintetizar nuevos complejos bis-carbénicos con diferentes estructuras ciclofánicas. Con estos objetivos presentes, utilizamos los compuestos **12** y **13** como moldes (Esquema 2). Estos compuestos se prepararon fácilmente, mediante reacción de acoplamiento de Sonogashira,[14] a partir de sus correspondientes precursores dibromados **10** y **11**, respectivamente.

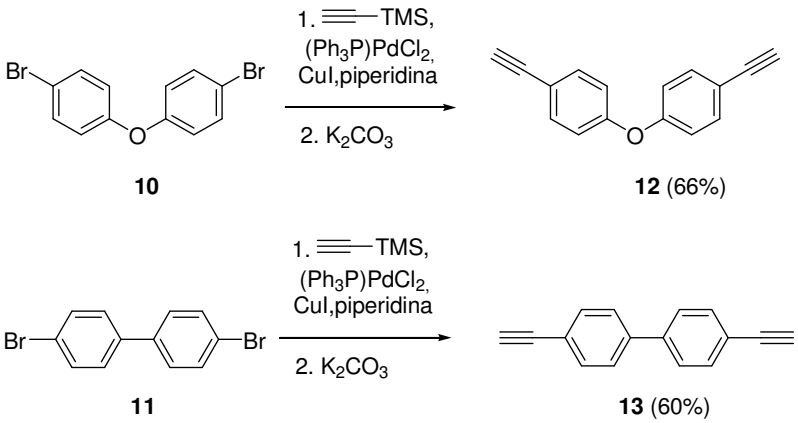

Esquema 2

El tratamiento secuencial de los diinos **12** y **13** con BuLi, $Cr(CO)_6$ y posterior alquilación de los correspondientes complejos *ate* formados con Et_3OBF_4, en las condiciones de reacción descritas anteriormente para la síntesis del complejo **4**, proporciona de manera eficaz los complejos bis-carbénicos **14** y **15** (Esquema 3). La misma metodología se empleó para preparar el complejo de wolframio **16** a partir de 1,3-dietinilbenceno.

[14] (a) Sonogashira, K.; Tohda, Y.; Hagihara, N. *Tetrahedron Lett*. **1975**, 4467. (b) Takahashi, S.; Kuroyama, Y.; Sonogashira, K.; Hagihara, N. *Synthesis* **1980**, 627. (c) Sonogashira, K. en *Comprehensive Organic Synthesis*; Trost, B. M., Fleming, T., Eds.; Pergamon Press: New York, 1991; Vol. 3, págs. 521-549.

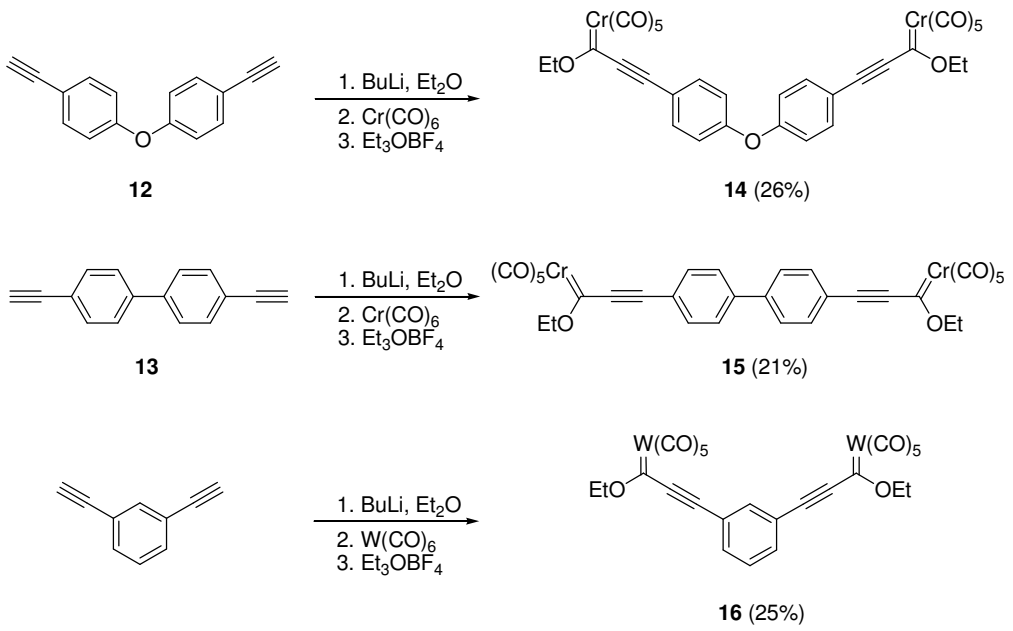

Esquema 3

La reacción de los complejos **14**-**16** con *p*-xililendiamina a temperatura ambiente y empleando CH_2Cl_2 como disolvente, conduce a los correspondientes complejos bis-carbénicos **17**-**19** de forma eficiente (Esquema 4).

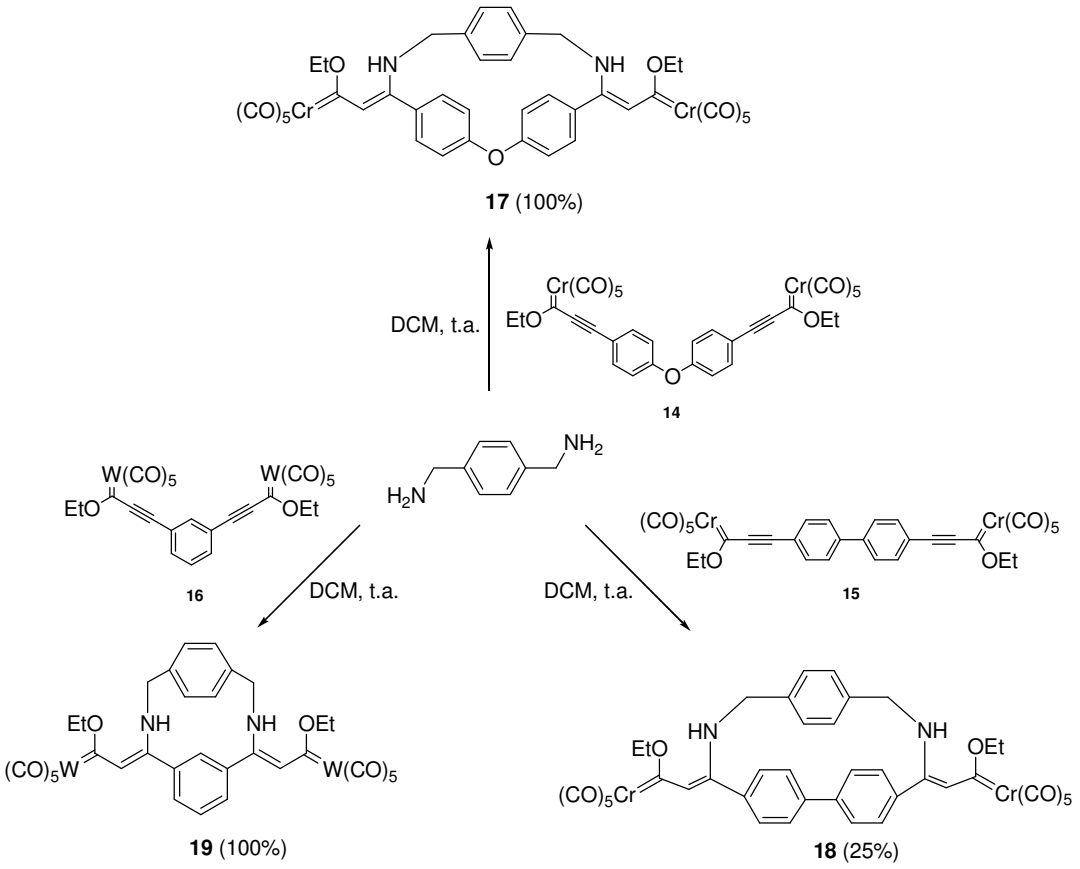

Esquema 4

De igual forma, se sintetizó el complejo **20** al hacer reaccionar el complejo **4** con *N*,*N'*-dimetil-*p*-xililendiamina con el objeto de estudiar la influencia de los sustituyentes en el nitrógeno de la bis-amina en el complejo formado (Esquema 5).

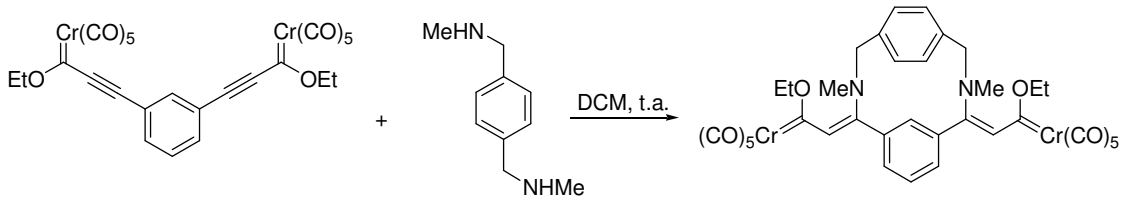

4 **20** (50%)

Esquema 5

Los diferentes espectros de ^{13}C-RMN de los complejos **17**-**20** muestran una única señal en el rango de δ = 295.2-298.8 ppm (δ = 275.4 ppm para el complejo de wolframio **19**) que corresponde de manera inequívoca a un carbono carbenoide con un sustituyente de tipo alcoxi. De nuevo, la estereoquímica de los dobles enlaces formados es también *Z*,*Z*, como se puede deducir a partir de la comparación de los datos espectroscópicos de dichos complejos y sus análogos no ciclofánicos.[12] Por tanto, en todos los casos estudiados siempre se obtiene el complejo ciclofánico correspondiente a una doble adición 1,4- de tipo Michael, lo que genera estructuras bimetálicas de tipo I (Figura 2) con rendimientos excelentes. El proceso es, por consiguiente, general para los distintos tipos de moldes, metales y bis-aminas empleados.

Aunque hasta el momento no se han conseguido monocristales de los complejos ciclofánicos sintetizados, lo que permitiría realizar una asignación estructural completa de los mismos, sí se ha conseguido dicha asignación para el complejo bis-carbénico **21**, análogo no ciclofánico de los complejos anteriores, mediante difracción de rayos-X (Figura 3). Dicho complejo se prepara fácilmente y de forma cuantitativa, mediante reacción del complejo **4** con dos equivalentes de 4-yodoanilina a temperatura ambiente y empleando THF como disolvente (Esquema 6).

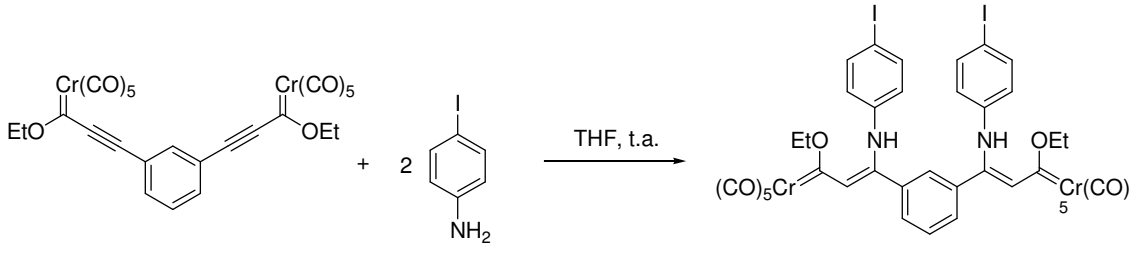

4 **21** (100%)

Esquema 6

Los datos espectroscópicos de **21** son similares a los datos obtenidos para los complejos con estructura ciclofánica **17**-**20**.

Como podemos apreciar en la Figura 3, existen dos enlaces de hidrógeno entre cada uno de los átomos de hidrógeno unido al átomo de nitrógeno y el oxígeno de cada grupo alcoxi, que fijan la estereoquímica de los dos dobles enlaces como *Z*,*Z*. Muy probablemente, ésta sea la causa de la facilidad y del elevado rendimiento con que transcurren las síntesis de los complejos ciclofánicos **5**-**8** y **17**-**20**. Si admitimos que estas interacciones se encuentran presentes en los complejos ciclofánicos análogos, entonces no sólo justifican la estereoquímica de los mismos sino también la excepcional reactividad de los moldes bimetálicos preparados.

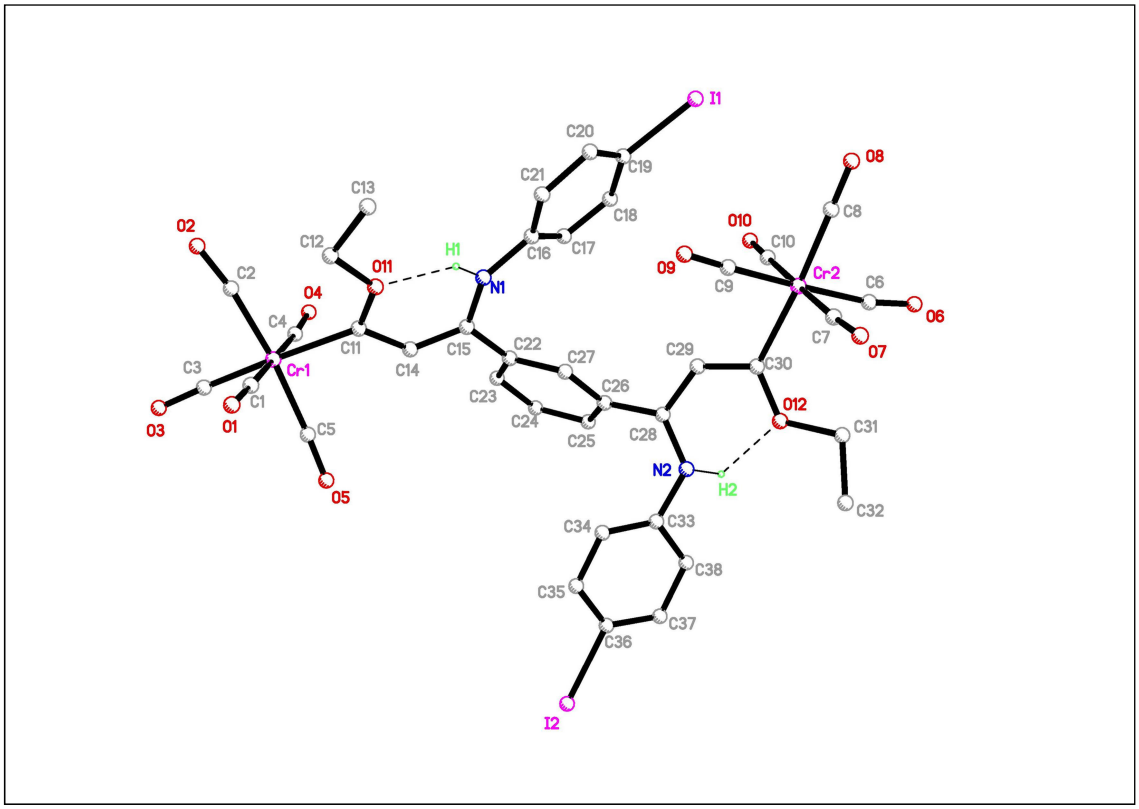

Figura 3

Parte Experimental

Procedimiento general para las reacciones de acoplamiento de Sonogashira. Síntesis de los compuestos 12 y 13.

A una disolución del dibromoderivado (**10**, **11**) y trimetilsililacetileno (2.4 equiv.) en piperidina (0.15 M), se le añade consecutivamente $(Ph_3P)PdCl_2$ (0.04 equiv.) y CuI (0.02 equiv.) y se calienta a reflujo durante 16 h. Después se deja alcanzar la temperatura ambiente y se elimina el disolvente a vacío. El crudo de reacción se disgrega en benceno y se filtra sobre un lecho de celita. El residuo resultante se purifica mediante cromatografía en columna (hexano/AcOEt, 10:1) para producir los correspondientes bis-etiniltrimetilsilil derivados (**22**, **23**), los cuales son tratados posteriormente con K_2CO_3 (5 equiv.) en MeOH/THF (2:1) durante 3h a temperatura ambiente para la desprotección de los grupos trimetilsililo. Tras extracción con CH_2Cl_2, secado con $MgSO_4$ y evaporación de los disolventes a vacío, se obtienen los compuestos moldes **12** y **13** puros.

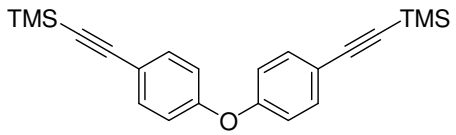

22

Compuesto 22. Siguiendo el procedimiento general, a partir de 2.0 g (6.1 mmol) de *p*-dibromo-difeniléter, **10**, 1.4 g (14.6 mmol) de trimetilsililacetileno, 0.17 g (0.24 mmol) de $PdCl_2(PPh_3)_2$ y 23 mg (0.12 mmol) de CuI en 45 mL de piperidina, se obtienen 1.46 g (66%) de **22** como un sólido blanco. ^{1}H RMN ($CDCl_3$) δ = 0.32 (s, 18H), 6.70 (d, J = 8.8 Hz, 4H, ArH), 7.25 (d, J = 8.8 Hz, 4H, ArH). ^{13}C RMN ($CDCl_3$) δ = 0.0, 93.7, 104.5, 118.4, 118.8, 133.7,156.9. IR (KBr) 2959, 2162, 1595, 1497, 1242, 1217, 1165, 858, 833 cm^{-1}. $C_{22}H_{26}OSi_2$, Calc.: C 72.87, H 7.23, Encontrado: C 73.05, H 7.02.

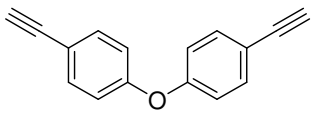

12

Compuesto 12. Siguiendo el procedimiento general, a partir de 1.46 g (4.0 mmol) de **22** en 110 mL de MeOH:THF (2:1) y 2.76 g (20.0 mmol) de K_2CO_3, se obtienen 878 mg (100%) de **12** como un sólido marrón claro. ^{1}H RMN ($CDCl_3$) δ = 2.90 (s, 2H), 6.80 (d, J = 8.7 Hz, 4H, ArH), 7.35 (d, J = 8.7 Hz, 4H, ArH). ^{13}C RMN ($CDCl_3$) δ =77.7, 83.1, 117.4, 118.9, 133.9, 157.1. IR (KBr) 3317, 3302, 2110, 1595, 1495, 1244, 1165, 835, 785, 762 cm^{-1}. $C_{16}H_{10}O$, Calc.: C 88.05, H 4.62, Encontrado: C 87.88, H 4.44.

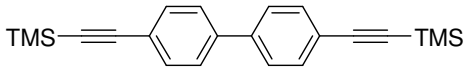

23

Compuesto 23. Siguiendo el procedimiento general, a partir de 2.5 g (8 mmol) de *p,p'*-dibromobifenilo, **11**, 1.9 g (19.2 mmol) de trimetilsililacetileno, 225 mg (0.32 mmol) de $PdCl_2(PPh_3)_2$, y 30 mg (0.16 mmol) de CuI en 55.5 mL de piperidina, se obtienen 1.69 g

(61%) de **23** como un sólido amarillo pálido. ^{1}H RMN ($CDCl_3$) δ = 0.00 (s, 18H), 7.26 (m, 8H, ArH). ^{13}C RMN ($CDCl_3$) δ =0.0, 95.2, 104.8, 122.4, 126.7, 132.4, 140.2. IR (KBr) 2954, 2153, 1489, 1254, 1242, 862, 847, 823, 758, 646 cm^{-1}. $C_{22}H_{26}Si_2$, Calc.: C 76.23, H 7.56, Encontrado: C 76.01, H 7.77.

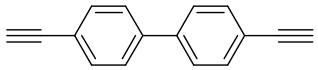

13

Compuesto 13. Siguiendo el procedimiento general, a partir de 1.69 g (4.88 mmol) de **23** en 50 mL de MeOH:THF (2:1) y 3.37 g (24.38 mmol) de K_2CO_3 se obtienen 965 mg (98%) de **13** como un sólido color crema. ^{1}H RMN ($CDCl_3$) δ = 3.09 (s, 2H), 7.46-7.52 (m, 8H, ArH). ^{13}C RMN ($CDCl_3$) δ = 78.1, 83.4, 121.4, 126.9, 132.6, 140.5. IR (KBr) 3273, 1489, 825 cm^{-1}. $C_{16}H_{10}$, Calc.: C 95.02, H 4.98, Encontrado: C 95.18, H 4.86.

Síntesis de los complejos 14-16.[15]

La síntesis se llevó a cabo siguiendo el procedimiento general descrito para la síntesis del complejo **4**.

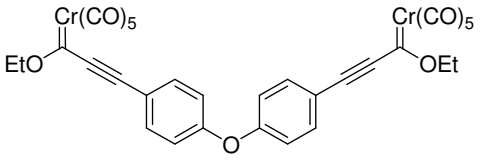

14

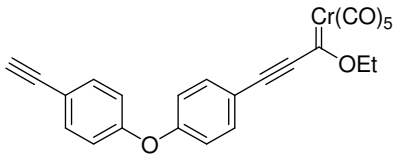

24

Bis(carbeno) 14. Sólido marrón (26%). ^{1}H RMN ($CDCl_3$) δ = 1.52 (t, *J* = 7.1 Hz, 6H, CH_3), 4.68 (q, *J* = 7.1 Hz, 4H, OCH_2), 7.04 (d, *J* = 8.5 Hz, 4H, ArH), 7.54 (d, *J* = 8.5 Hz, 4H, ArH). ^{13}C RMN ($CDCl_3$) δ = 14.9, 75.8, 92.2, 116.6, 119.5, 135.0, 158.9, 216.3, 225.6, 312.8. IR (KBr) 2150, 2060, 1954 cm^{-1}. $C_{32}H_{18}Cr_2O_{13}$, Calc.: C 53.79, H 2.54, Encontrado: C 54.01, H 2.72. **Mono(carbeno) 24**. Sólido marrón (20%). ^{1}H RMN ($CDCl_3$) δ = 1.48 (t, *J* = 7.1 Hz, 3H), 2.99 (s, 1H), 4.64 (q, *J* = 7.1 Hz, 2H), 6.92 (d, *J* = 8.5 Hz, 2H, ArH), 6.95 (d, *J* = 8.7 Hz, 2H, ArH), 7.45 (d, *J* = 8.5 Hz, 2H, ArH), 7.49 (d, *J* = 8.7 Hz, 2H, ArH). ^{13}C RMN ($CDCl_3$) δ = 14.9, 75.7, 77.3, 82.7, 92.3, 115.5, 118.4, 118.6, 119.7, 134.0, 135.0, 155.8, 160.1, 216.4, 225.6, 312.5. IR (KBr) 3300, 2150, 2058, 1938 cm^{-1}. $C_{24}H_{14}CrO_7$, Calc.: C 61.81, H 3.03, Encontrado: C 61.65, H 2.89.

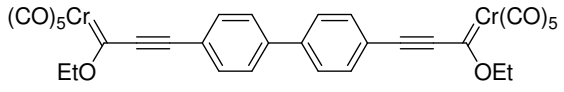

15

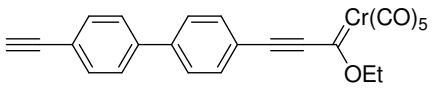

25

Bis(carbeno) 15. Sólido violeta (21%). ^{1}H RMN ($CDCl_3$) δ = 1.53 (t, *J* = 7.1 Hz, 6H), 4.71 (c, *J* = 7.1 Hz, 4H), 7.49-7.65 (m, 8H, ArH). ^{13}C RMN ($CDCl_3$) δ = 15.0, 75.9, 92.5, 120.9, 127.6, 133.3, 142.6, 216.3, 225.7, 313.3. IR (KBr) 2150, 2058, 1956, 1925 cm^{-1}. $C_{32}H_{18}Cr_2O_{12}$, Calc.: C 55.03, H 2.60, Encontrado: C 55.20, H 2.76. **Mono(carbeno) 25**. Sólido violeta (35%). ^{1}H RMN ($CDCl_3$) δ = 1.53 (t, *J* = 7.1 Hz, 3H), 3.10 (s, 1H), 4.71 (q, *J* = 7.1 Hz, 2H), 7.52 (m, 4H, ArH), 7.59 (m, 4H, ArH). ^{13}C RMN ($CDCl_3$) δ = 15.0, 75.8, 78.5, 83.2, 92.5, 120.2, 122.2, 127.0, 127.4, 132.8, 133.2,

[15] Para la síntesis del complejo **16** ver compuesto **2b** en capítulo 1.2.

139.9, 143.3, 216.3, 225.7, 313.2. IR (KBr) 2152, 2058, 1942 cm^{-1}. $C_{24}H_{14}CrO_6$, Calc.: C 64.01, H 3.13, Encontrado: C 63.85, H 3.01.

Procedimiento general para la síntesis de los complejos 17-21.
La síntesis se llevó a cabo siguiendo el procedimiento general descrito para la síntesis de los complejos ciclofánicos **5-8**.

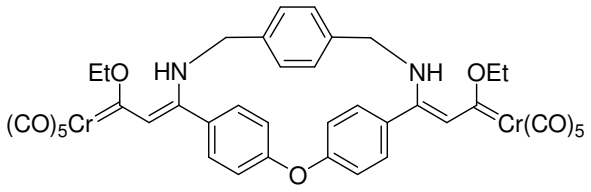

17

Complejo 17. Siguiendo el procedimiento general, a partir de 192 mg (0.27 mmol) del complejo **14** y 37 mg (0.27 mmol) de *p*-xililendiamina en 20 mL de CH_2Cl_2 anhidro, se obtienen, sin que sea necesaria purificación posterior, 229 mg (100%) de **17** como un sólido rojo. ^{1}H RMN ($CDCl_3$) δ = 1.23 (m, 6H), 4.31 (señal ancha, 4H), 4,71 (q, *J* = 6.3 Hz, 4H), 6.27 (s, 2H), 7.42–6.95 (m, 12H, ArH), 9.10 (señal ancha, 2H, NH). ^{13}C RMN ($CDCl_3$) δ = 15.4, 49.5, 73.9, 119.3, 119.7, 128.1, 130.1, 135.1, 137.0, 152.7, 158.1, 218.5, 223.9, 296.3. IR (KBr) 2048, 1904, 1547, 1479, 1227 cm^{-1}. $C_{40}H_{30}Cr_2N_2O_{13}$, Calc.: C 56.48, H 3.55, N 3.29, Encontrado: C 56.64, H 3.38, N 3.11.

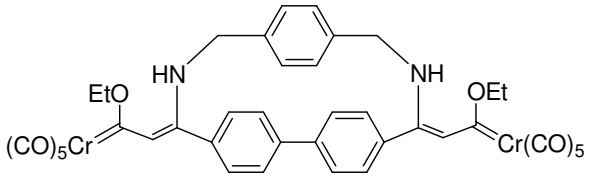

18

Complejo 18. Siguiendo el procedimiento general, a partir de 100 mg (0.24 mmol) del complejo **15** y 40 mg (0.29 mmol) de *p*-xililendiamina en 10 mL de CH_2Cl_2 anhidro, se obtienen, tras purificación por cromatografía en columna (hexano/AcOEt, 1:1), 32 mg (25%) de **18** como un sólido rojo (25%). ^{1}H RMN ($CDCl_3$) δ = 1.12 (t, *J* = 7.0 Hz, 6H), 3.83 (señal ancha, 4H), 4.71 (q, *J* = 7.0 Hz, 4H), 6.28 (s, 2H), 7.90–7.12 (m, 12H, ArH), 9.16 (s, 2H, NH). ^{13}C RMN ($CDCl_3$) δ = 14.1, 49.9, 73.9, 119.4, 126.9, 127.6, 128.2, 128.7, 129.0, 132.6, 153.0, 218.5, 223.9, 295.2. IR (KBr) 2066, 2048, 1919, 669, 658 cm^{-1}. $C_{40}H_{30}Cr_2N_2O_{12}$, Calc.: C 57.56, H 3.62, N 3.36, Encontrado: C 57.34, H 3.41, N 3.49.

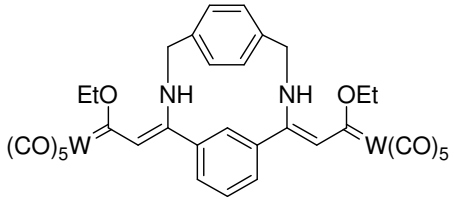

19

Complejo 19. Siguiendo el procedimiento general, a partir de 127 mg (0.14 mmol) del complejo **16** y 20 mg (0.14 mmol) de *p*-xililendiamina en 12 mL de CH_2Cl_2 anhidro, se

obtienen, sin que sea necesaria purificación posterior, 147 mg (100%) de **19** como un sólido rojo.^{1}H RMN ($CDCl_3$) δ 1.18 (señal ancha, 6H), 4.25 (señal ancha, 4H), 4.60 (señal ancha, 4H), 6.30 (s, 2H), 7.63-7.14 (m, 8H, ArH), 9.16 (señal ancha, 2H, NH). ^{13}C RMN ($CDCl_3$) δ 15.7, 50.1, 77.1, 122.8, 127.3, 128.0, 128.7, 130.0, 137.2, 141.6, 155.4, 199.5, 204.1, 275.4. IR (KBr) 2058, 1902 cm^{-1}. $C_{34}H_{26}N_2O_{12}W_2$, Calc.: C 39.95, H 2.56, N 2.74, Encontrado: C 39.74, H 2.69, N 2.96.

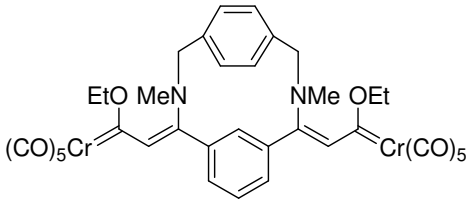

20

Complejo 20. Siguiendo el procedimiento general, a partir de 443 mg (0.70 mmol) del complejo **4** y 117 mg (0.70 mmol) de *N*,*N'*-dimetil-*p*-xililendiamina en 45 mL de CH_2Cl_2 anhidro, se obtienen tras purificación por cromatografía en columna, 278 mg del complejo **20** (50%) como un sólido rojo. ^{1}H RMN ($CDCl_3$) δ = 1.28 (señal ancha, 6H), 2.99 (señal ancha, 6H), 4.21 (señal ancha, 4H), 4.69 (señal ancha, 4H, OCH_2), 6.64 (s, 2H), 7.62–7.08 (m, 8H, ArH). ^{13}C RMN ($CDCl_3$) δ = 15.1, 29.7, 55.8, 73.8, 120.6, 126.7, 127.7, 129.1, 134.8, 135.2, 137.8, 152.0, 218.6, 224.0, 298.8. IR (KBr) 2048, 1908, 1508 cm^{-1}. $C_{36}H_{30}Cr_2N_2O_{12}$, Calc.: C 54.97, H 3.84, N 3.56, Encontrado: C 55.12, H 4.01, N 3.61.

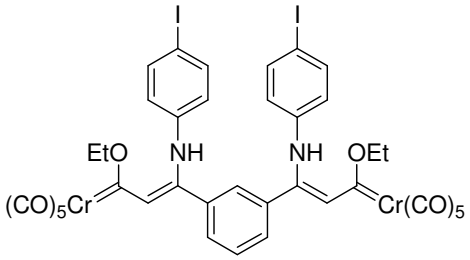

21

Complejo 21.A partir de 100 mg (0.16 mmol) del complejo **4** y 70 mg (0.32 mmol) de 4-yodoanilina en 10 mL de THF anhidro, se obtienen, sin purificación posterior, 170 mg del complejo **21** (100%) aislado como un sólido rojo. ^{1}H RMN ($CDCl_3$) δ = 1.60 (t, 6H, *J* = 7.0 Hz), 4.93 (q, 4H, *J* = 7.0 Hz), 6.27 (d, 4H, *J* = 8.4 Hz, ArH), 6.42 (s, 2H), 7.25–7.30 (m, 4H, ArH), 7.42 (d, 4H, *J* = 8.4 Hz, ArH), 10.05 (s, 2H, NH). ^{13}C RMN ($CDCl_3$) δ = 15.6, 74.8, 89.3, 122.7, 124.3, 128.9, 129.7, 130.7, 135.8, 128.0, 138.3, 143.2, 217.8, 224.0, 308.0. IR (KBr) 2050, 1973, 1915, 1541 cm^{-1}. $C_{38}H_{26}Cr_2I_2N_2O_{12}$: Calc.: C 43.04, H 2.47, N 2.64, Encontrado: C 42.85, H 2.81, N 2.50.

1.2. Synthesis and Electrochemical Properties of Novel Tetrametallic Macrocyclic Fischer Carbene Complexes

1.2. Synthesis and Electrochemical Properties of Novel Tetrametallic Macrocyclic Fischer Carbene Complexes

In the last few years, the use of transition metal centers in the construction of cyclophanes or macrocyclic structures has gained a lot of attention. [1] This is due to the fact that metal centers are an exceptional tool for constructing organic structures since they can be assembled easily with high efficiency.[2] Many of the metallocyclophanes known to date have been prepared using metals in low oxidation states I or II, in particular, square planar Cu^{II}, Pd^{II} or Pt^{II} centers or tetrahedral Cu^{I} centers.[3] Examples of cyclophanes containing octahedral W, Mo, Re, Ru and Rh centers have also been reported.[4] Recently, Re based chiral square molecular systems have been prepared by using chiral bridging ligands.[5]

Fischer carbene complexes have become an excellent tool in Organic Chemistry because of the impressive array of processes in which they can take part.[6] Nevertheless, the potential use of this type of compounds in the construction of macrocyclic and supramolecular structures remains unexplored.[7] Recently, our interest has focused on the design and development of new methods to the synthesis of cyclophanic structures

[1] (a) Fujita, M; Yakazai, J.; Ogura, K. *J. Am. Chem. Soc.* **1990**, *112*, 5645. (b) Stang, P. J.; Cao, D. H. *J. Am. Chem. Soc.* **1994**, *116*, 4981. (c) Stang, P. J.; Olenyuk, B. *Acc. Chem Res.* **1997**, *30*, 502. (d) Leininger, S.; Olenyuk, B.; Stang, P. J. *Chem. Rev*. **2000**, *100*, 853. (e) Fujita, M. *Chem. Soc. Rev.* **1998**, *27*, 417. (f) Holiday, B. J.; Mirkin, C. A. *Angew. Chem. Int. Ed.* **2001**, *40*, 2002. (g) Dinolfo, P. H.; Hupp, J. T. ; Guzei, I. A.; Rheingold, A. L. *Coord. Chem. Rev.* **1998**, *171*, 221. (h) Cotton, F. A.; Lin. C.; Murillo, C. A. *Acc. Chem. Res.* **2001**, *34*, 759. (i) Klausmeyer, K. K.; Rauchfuss, T. B.; Wilson, S. R. *Angew. Chem. Int. Ed.* **1998**, *37*, 1694. (j) Piotrowski, H., Polborn, K.; Hilt, G.; Severin, K. *J. Am. Chem. Soc.* **2001**, *123*, 2699.

[2] Lehn, J. M. *Supramolecular Chemistry: Concepts and Perspectives*, VCH Publishers: New York, 1995.

[3] Selected examples can be found in: (a) Maverick, A. W.; Klaveter, F. E. *Inorg. Chem.* **1984**, *23*, 4130. (b) Maverick, A. W.; Buckingham, S. C.; Yao, Q.; Bradbury, J. R.; Stanley, G. G. *J. Am. Chem. Soc.* **1986**, *108*, 7430. (c) ref. 1a and 1b. (d) Fujita, M.; Ogura, K. *Coord. Chem. Rev*. **1996**, *148*, 249.

[4] (a) Stricklen, P. M.; Volcko, E. J.; Verkade, J. G. *J. Am. Chem. Soc*. **1983**, *105*, 2494. (b) Derridge, T. E.; Jones, C. J. *Polyhedron* **1997**, *16*, 3695. (c) Slone, R. V.; Yoon, D. I.; Calhoun, R. M.; Hupp, J. T. *J. Am. Chem. Soc.* **1995**, *117*, 11813. (d) Sun, S.; Anspach, J. A.; Lees, A. J.; Zavalij, P. Y. *Organometallics* **2002**, *21*, 685. (e) Holliday, B. J.; Farrel, J. R.; Mirkin, C. A. *J. Am. Chem. Soc.* **1999**, *121*, 6316.

[5] Lee, S. J.; Lin, W. *J. Am. Chem. Soc.* **2002**, *124*, 4554.

[6] For recent reviews on carbene complexes in Organic Chemistry, see: (a) Wulff, W. D. *Comprenhensive in Organometallic Chemistry II*; Abel, E. W., Stone, F. G. A., Wilkinson, G. Eds.; Pergamon Press: Oxford, 1995, vol 12, p 470. (b) Hegedus, L. S. *Tetrahedron* **1997**, *53*, 4105. (c) Herdorn, J. W. *Coord. Chem. Rev.* **1999**, *181*, 177. (d) Dötz, K. H. ; Tomuschatt, P. *Chem. Soc. Rev.* **1999**, *28*, 187. (e) Dörwall, F. Z. *Metal Carbenes in Organic Synthesis*; Wiley-VCH: New York 1999. (f) de Meijere, A.; Schimer, H.; Duesch, M. *Angew. Chem. Int. Ed.* **2000**, 39, 3964. (g) Sierra, M. A. *Chem. Rev.* **2000**, *100*, 3591. (h) Barluenga, J.; Fañanás, F. J. *Tetrahedron* **2000**, *56*, 457. (i) Barluenga, J.; Flórez, J., Fañanás, F. J. *J. Organomet. Chem.* **2001**, *624*, 5.

[7] As far as we know only non-metallic cyclophanes had been prepared using Fischer carbene complexes, see: Wang, H.; Wulff, W. D. *J. Am. Chem. Soc.* **2000**, *122*, 9862.

using Fischer carbene complexes.[8] The incorporation of metal centers may be used to create further sophisticated structures by taking advantage of the chemistry of these complexes developed so far. Herein we report the synthesis, as well as the electrochemical properties of new metallomacrocyclic compounds containing four centers.

Tetrametallic macrocyclic compounds **1** were prepared by Michael addition of different amines to α,β-unsaturated Fischer carbene complexes **2**, according to Scheme 1.[9] Bis-carbene complexes **2a** and **2b** were selected as templates to build the macrocyclic structures. Reaction of these bis-carbene complexes **2** with diamines (2:1 ratio) in THF solution at room temperature afforded the binuclear carbene complexes **3** in high yields. These complexes were obtained as one single steroisomer (*Z*,*Z*) in accordance with the data reported in the literature.[8,10] Further reaction of the bis-enaminocarbene complexes **3,** with an equimolecular amount of the corresponding bis-carbene complex **2**, yielded cyclophane carbene complexes **1** in good yields.[11]

The tetranuclear macrocycles are quite stable, can be easily purified by flash column chromatography on silica and were characterized by spectroscopical and analytical methods. ^{1}H NMR and ^{13}C NMR spectra for all complexes exhibit the same features. Significantly the ^{13}C NMR spectra show a single signal in a range of 283.9-308.7 attributable to the carbene carbon, indicating the presence of one single steroisomer (all-(*Z*)). The stereochemistry was assigned by comparison of their spectroscopic data with reported analogue structures.[10] Chromium or tungsten

[8] Fernández, I.; Sierra, M. A.; Mancheño, M. J.; Gómez-Gallego, M.; Ricart, S. *Organometallics* **2001**, *20*, 4304.
[9] Aumann, R.; Nienaber, H. *Adv. Organomet. Chem.* **1997**, *41*, 163.
[10] Moretó, J. M.; Ricart, S.; Dötz, K. H.; Molins, E. *Organometallics* **2001**, *20*, 62.
[11] The preparation of tetrametallic macrocycic **1a** is representative: To a solution of chromium carbene complex **2a** in THF was added 1,4-diaminobenzene in one portion (2:1 molar ratio). The mixture was stirred at room temperature under argon until the dissappearance of the starting material (checked by T.L.C.). The solvent was removed under reduced pressure to yield compound **3a** (100%). **3a**: ^{1}H NMR (200 MHz, $CDCl_3$): δ 1.57 (t, 6H, *J* = 7.0 Hz), 3.61 (br s, 4H, NH_2), 4.85 (q, 4H, *J* = 7.0 Hz), 6.22 (s, 2H), 6.40-6.51 (m, 8H, ar), 7.19-7.24 (m, 4H, ar), 10.33 (s, 2H, NH). ^{13}C NMR (50 MHz, $CDCl_3$): δ 15.7, 74.2, 115.3, 116.7, 120.8, 124.7, 128.6, 129.0, 130.3, 135.6, 144.7, 147.1, 218.3, 224.2, 298.1. IR (KBr): ν 2048, 1909, 1541, 1514, 1198 cm^{-1}. $C_{38}H_{30}Cr_2N_4O_{12}$ Calcd C 54.42, H 3.61, N 6.68. Found C 54.55, H 3.76, N 6.51. The *bis*-enaminocarbene **3a**, was dissolved in dry THF and reacted with an equimolar amount of the chromium complex **2a**. The mixture was stirred for one hour. The solvent was reduced in *vacuo* and the macrocyclic purified by flash column chromatography under argon to yield pure tetranuclear complex **1a** (75% yield). **1a**: ^{1}H NMR (300 MHz, $CDCl_3$): δ 1.65 (t, 12H, *J* = 7.0 Hz), 4.95 (m, 8H), 6.38 (s, 8H, ar), 6.64 (s, 4H), 6.96 (m, 4H, ar), 7.74 (s, 2H, ar), 10.24 (s, 4H, NH). ^{13}C NMR (50 MHz, $CDCl_3$): δ 15.7, 74.8, 122.4, 122.9, 127.6, 127.7, 131.3, 135.0, 136.2, 142.7, 217.8, 224.1, 308.5. IR (KBr): ν 2052, 1975, 1931, 1535, 1371, 1350, 1192 cm^{-1}. $C_{64}H_{44}Cr_4N_4O_{24}$: Calcd C 52.61, H 3.04, N 3.83. Found C 52.85, H 3.26, N 3.68.

macrocyclic carbenes can be prepared in this way, and diverse diamines can be used as linkers to join the two bis-carbene moieties.

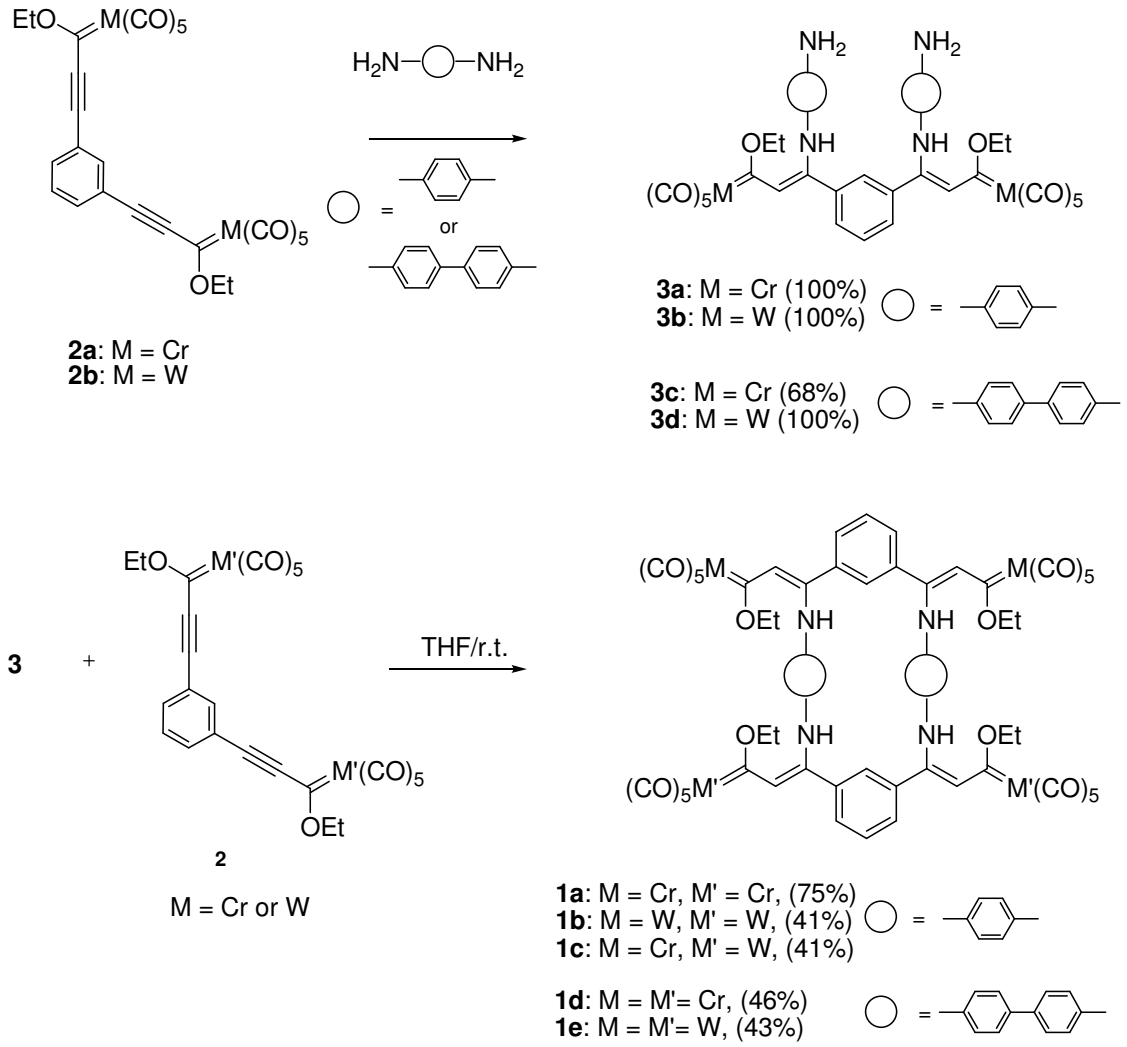

Scheme 1

The versatility of the method also enables the facile synthesis of heterotetrametallic complexes. This is an important aspect because the introduction of different metals in the same system may further control the reactivity and properties of the complexes formed. Thus, reaction of bis-tungsten enaminocarbene complex **3b** with chromium bis-carbene complex **2a**, in a stoichiometric ratio, afforded complex **1c** in 41% yield. Compound **1c** was isolated as an inseparable mixture of stereoisomers in the chromium moieties in a 1:2 ratio, as it can be deduced from the spectroscopic data. ^{13}C NMR spectrum of **1c** displays two signals at δ = 308.2 y 308.4 ppm attributable to different chromium moieties. However, the tungsten carbene carbons exhibit a single

signal at δ = 283.3 ppm. The stereochemistry of this mixture could not be assigned unequivocally.

It should be noted that this methodology allows control of the geometry and the size of the cavity of the cyclophane. They can be designed as a function of the bis-carbene complexes employed and the diamine used as linker. In order to evaluate the geometry and the size of the cavity created in tetranuclear macrocyclic complexes **1a-c**, a semiempirical PM3 calculation[12] was performed using the corresponding nonmetallic macrocyclic tetraethyl ester as a model. From the data obtained, the size of the cavity allows accommodation of molecules of about 6 Å.

Redox properties of compounds **1a**-**e** were also examined in order to evaluate the interaction among the metallic centers of the macrocyclic complexes, as well as the influence of the metal and the spacer in their electron donor and aceptor ability. Cyclic voltammograms of macrocycles **1a**-**d** in Bu_4NClO_4-CH_2Cl_2 are displayed in Figure 1.[13] The electrochemical properties are summarized in Table 1.

Table 1. Electrochemical data obtained for complexes **1**.

Compound	$1^{st}E_{pa}$	$2^{nd}E_{pa}$	$1^{st}E_{pc}$	$2^{nd}E_{pc}$
1a	0.88		-1.34	-1.60
1b	1.04		-1.28	-1.57
1c	0.92	1.05	-1.33	-1.59
1d	0.91	1.20	-1.33	-1.46
1e	1.03		-1.24	-1.44

[12] Calculation was carried out using the GAUSSIAN 98 suite of programs. *Gaussian 98*, revision A.5; Gaussian, Inc.: Pittsburgh, PA, 1998.

[13] Cyclic voltammetric experiments were performed in CH_2Cl_2 at room temperature with 0.1 M tetrabutyl ammonium perclorate as a supporting electrolyte and glassy carbon as a working electrode. A platinum wire was used as a counter electrode and Ag/Ag^+ as a reference electrode. All the measurements were performed with potentiostat/galvanostat Autolab PGSTAT30, and ferrocene was used as an internal standard.

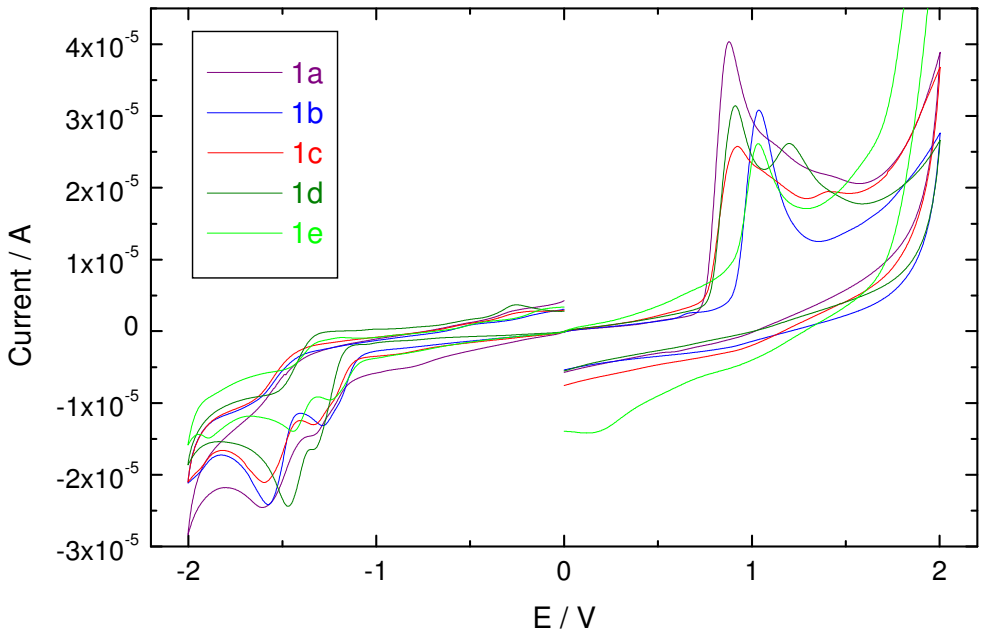

Figure 1. Cyclic Voltammograns of complexes **1** in 0.1 M Bu_4ClO_4-CH_2Cl_2 at scan rate of 0.1 V s^{-1} at 25ºC.

All homometallic chromium carbenes show an irreversible oxidation wave of the metal moieties in a range of E_{pa} = 0.88-0.92 V. The analogous homometallic tungsten carbene complexes behave in a similar way showing a further irreversible one step oxidation in a range of E_{pa} = 1.03-1.04 V. All tungsten carbene complexes in Table 1 exhibit higher oxidation potentials than the related chromium complexes, following the reported pattern for this kind of complexes.[14]

Bis-carbene **4** and mononuclear enaminocarbene **5** display the same features (E^1_{pa} = 0.83 V and E^1_{pa} = 0.95 V, respectively) (Figure 2). This means that the interaction among the metal centers of the cyclophane is practically nonexistent. [15]

[14] (a) Lloyd, M. K.; McCleverty, J. A.; Hall, M. B.; Hillier, I. H.; Jones, E. M.; McEwen, G. K. *J. Chem. Soc., Dalton Trans.* **1973**, 1743. (b) Casey, C. P.; Albin, L. D.; Saeman, M. C., D. H. *J. Organomet. Chem.* **1978**, *155*, C37. (c) Jayapraksh, K. N.; Ray, P. C., Matsuoka, I.; Bhadbhade, M. M.; Puranik, V. G.; Das, P. K.; Nishihara, H.; Sarkar, A. *Organometallics* **1999**, *18*, 3851. (d) Sierra, M. A.; Gómez-Gallego, M.; Mancheño, M. J.; Martínez-Álvarez, R.; Ramírez-López, P.; Kayali, N.; González, A. *J. Mass. Spectrom.* **2003**, *38*, 151.

[15] Hartbaum, C.; Mauz, E.; Roth, G; Weissenbach, K.; Fischer, H. *Organometallics* **1999**, *18*, 2619.

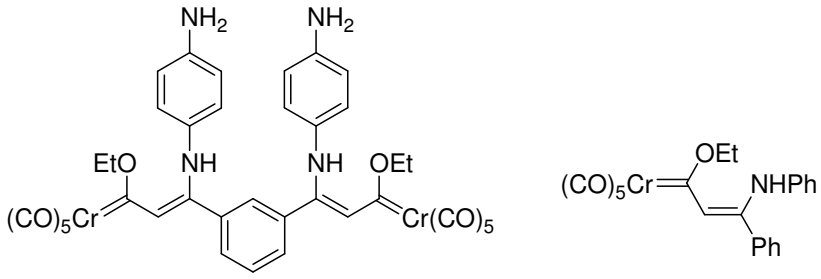

4 **5**

Figure 2

The voltammogram of cyclophane **1d** displays a second clear oxidation wave at 1.20 V that could be attributable either to the diamine used as a spacer or to a second oxidation step in the Fischer carbene moiety. Oxidation of the diamine bridge may be discarded because the corresponding tungsten carbene cyclophane **1e** voltammetry shows only the usual one oxidation step of the metal center. Moreover, the diamines used through this work have lower oxidation potentials that are not observed for macrocycles **1** (E^1_{pa} = 0.49 V and E^2_{pa} = 1.03 V for 1,4-diaminobenzene and E^1_{pa} = 0.57 V, E^2_{pa} = 0.75 V, E^3_{pa} = 1.00 V, E^4_{pa} = 1.17 V for benzidine).[16] These results suggest an important contribution of the resonance structures **6** in complexes **1** (Figure 3).[9]

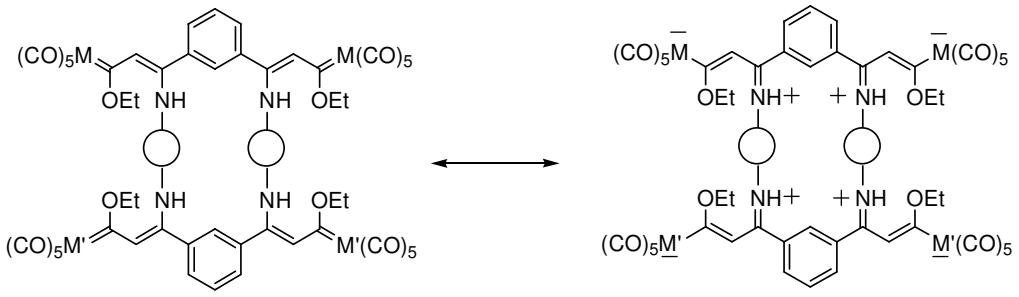

1 **6**

M = M' = Cr or W

Figure 3

Reduction potentials are a good measurement of the electron-accepting ability of these complexes.[17] Although there are no significant changes in the values obtained for

[16] Oxidation potentials of 1,4-diaminobenzene and benzidine were obtained under the same experimental conditions than macrocyclics **1.**

[17] (a) Krusic, P. J.; Klabunde, U.; Casey, C. P.; Block, T. F. *J. Am. Chem. Soc.* **1976**, *98*, 2015. (b) Lee, S.; Cooper, N. J. *J. Am. Chem. Soc.* **1990**, *112*, 9419. (c) Fuchibe, K.; Iwasawa, N. *Org. Lett*. **2000**, *2*, 3297. (d) Sierra, M. A.; Ramírez-López, P.; Gómez-Gallego, M; Lejon, T.; Mancheño, M. J. *Angew. Chem. Int. Ed.* **2002**, *41*, 3442.

all compounds, tungsten cyclophanes **1b** and **1e** present less negative E_{pc} values, which is in accordance with the higher polarizability of tungsten compared to chromium.[18]

In summary, a methodology for preparing a family of new polynuclear and heterometallomacrocyclic compounds is described. This methodology allows the design and synthesis of novel metallocyclophanic structures at will. Further work is in progress in order to study the reactivity and host properties of these compounds.

[18] Cotton, F. A.; Wilkinson, G.; Murillo, C. A.; Bochmann, M. *Advanced Inorganic Chemistry*, John Wiley & Sons, 6th Ed., New York 1999.

Experimental Section

Decacarbonyl[μ-1,3-Phenylenediethynyl)bis(ethoxycarbene)]dichromium(0) was prepared according to literature method.[19]

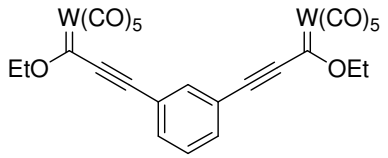

2b

Decacarbonyl[μ-1,3-Phenylenediethynyl)bis(ethoxycarbene)]ditungsten(0) 2b. To a solution of 1.0 g (7.9 mmol) of 1,3-diethynylbenzene in 75 mL of dry Et_2O at –78 ºC were added dropwise 10.9 mL (17.4 mmol) of *n*-butyllithium (1.6 M in hexanes). The mixture was stirred at –78 ˚C for 45 min and then, 5.58 g (15.9 mmol) of tungsten hexacarbonyl were added at 0 ºC. After stirring at this temperature for 15 min, 40 mL of dry THF were also added and the mixture was let to stir at room temperature overnight. Then, 6.02 g (31.7 mmol) of Et_3OBF_4 were added in one portion at -78 ºC. The solution was stirred at this temperature for 15 min and then allowed to reach room temperature for an additional hour. Solvents were removed under reduced pressure and the residue was dissolved in Et_2O and filtered on silica gel. The solvent was evaporated and the residue was submitted to flash column chromatography (SiO_2, Hexane) to give 195 mg (5%) of the corresponding monocarbene and 1.43 g (25%) of the bis-carbene **2b**, both as deep green solids. Bis-carbene **2b**: ^{1}H NMR (300 MHz, $CDCl_3$): δ 1.55 (t, 6H, *J* = 7.1 Hz), 4.64 (q, 4H, *J* = 7.1 Hz), 7.41-7.71 (m, 4H). ^{13}C NMR (75.4 MHz, $CDCl_3$): δ 15.1, 77.2, 97.5, 122.5, 129.8, 134.4, 135.6, 197.3, 205.6, 286.0. IR (CCl_4): ν 2154, 2069, 1992, 1958 cm^{-1}. $C_{26}H_{14}O_{12}W_2$: Calcd C 35.24, H 1.59, Found C 35.02, H 1.71.

Synthesis of macrocycles. General procedure:
In a typical experiment, 1,4-diaminobenzene or bencidine was added to a solution of chromium or tungsten bis-carbene complex (**2a**,**b**) in dry THF in one portion (2:1 molar ratio). The reaction mixture was stirred at room temperature under argon atmosphere until the disappearance of the starting material (checked by T.L.C.). An appreciable change of color to deep red was always observed in the reaction mixture after the addition of the diamine. The solvent was removed under reduced pressure and the crude reaction was purified by flash column chromatography on silica gel under argon pressure as specify below.
Then, the bis-enaminocarbene formed **3**, was dissolved in dry THF and reacted with an equimolar amount of the corresponding chromium or tungsten bis-carbene complex (**2a**,**b**) at room temperature under argon atmosphere until the disappearance of the starting material (checked by T.L.C.). The solvent was removed under reduced pressure and the crude reaction was purified by flash column chromatography on silica gel under argon pressure to give pure tetranuclear carbene complexes.

[19] Fernández, I.; Sierra, M. A.; Mancheño, M. J.; Gómez-Gallego M.; Ricart, S. *Organometallics* **2001**, *20*, 4304.

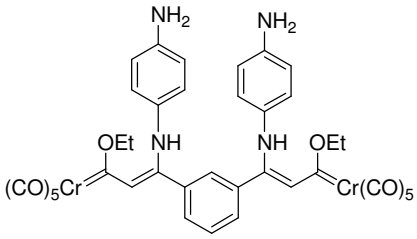

3a

Complex 3a. Following the general procedure, from 300 mg (0.48 mmol) of the bis-carbene complex **2a**, 105 mg (0.96 mmol) of 1,4-diaminobencene and 30 mL of THF were obtained 404 mg (quantitative yield) of the bis-carbene complex **3a** as a green solid. ^{1}H NMR (200 MHz, $CDCl_3$): δ 1.57 (t, 6H, *J* = 7.0 Hz), 3.61 (br s, 4H, NH_2), 4.85 (q, 4H, *J* = 7.0 Hz), 6.22 (s, 2H), 6.40-6.51 (m, 8H, ar), 7.19-7.24 (m, 4H, ar), 10.33 (s, 2H, NH). ^{13}C NMR (50 MHz, $CDCl_3$): δ 15.7, 74.2, 115.3, 116.7, 120.8, 124.7, 128.6, 129.0, 130.3, 135.6, 144.7, 147.1, 218.3, 224.2, 298.1. IR (KBr): ν 2048, 1909, 1541, 1514, 1198 cm^{-1}. $C_{38}H_{30}Cr_2N_4O_{12}$ Calcd C 54.42, H 3.61, N 6.68. Found C 54.55, H 3.76, N 6.51.

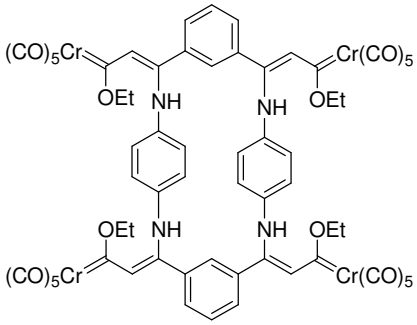

1a

Complex 1a. Following the general procedure, from 404 mg (0.48 mmol) of the complex **3a**, 300 mg (0.48 mmol) of bis-carbene complex **2a** and 30 mL of THF were obtained after purification by flash column chromatography 535 mg (75 %) of the *tetra*-carbene complex **1a** as a green solid. ^{1}H NMR (300 MHz, $CDCl_3$): δ 1.65 (t, 12H, *J* = 7.0 Hz), 4.95 (m, 8H), 6.38 (s, 8H, ar), 6.64 (s, 4H), 6.96 (m, 4H, ar), 7.74 (s, 2H, ar), 10.24 (s, 4H, NH). ^{13}C NMR (50 MHz, $CDCl_3$): δ 15.7, 74.8, 122.4, 122.9, 127.6, 127.7, 131.3, 135.0, 136.2, 142.7, 217.8, 224.1, 308.5. IR (KBr): ν 2052, 1975, 1931, 1535, 1371, 1350, 1192 cm^{-1}. $C_{64}H_{44}Cr_4N_4O_{24}$: Calcd C 52.61, H 3.04, N 3.83. Found C 52.85, H 3.26, N 3.68.

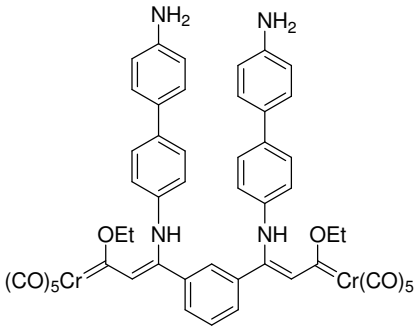

3c

Complex 3c. Following the general procedure, from 150 mg (0.24 mmol) of the bis-carbene complex **2a**, 89 mg (0.48 mmol) of bencidine and 15 mL of THF were obtained after purification by flash column chromatography 162 mg (68%) of the bis-carbene complex **3c** as a red solid. ^{1}H NMR (300 MHz, $CDCl_3$): δ 1.60 (t, 6H, *J* = 7.0 Hz), 3.67 (br s, 4H, NH_2), 4.90 (q, 4H, *J* = 7.0 Hz), 6.39 (s, 2H), 6.54 (d, 4H, *J* = 8.3 Hz), 6.63 (d, 4H, *J* = 8.3 Hz), 7.18-7.36 (m, 12H, ar), 10.29 (s, 2H, NH). ^{13}C NMR (50 MHz, $CDCl_3$): δ 15.6, 74.6, 115.4, 121.9, 123.1, 126.8, 127.6, 129.1, 129.7, 130.6, 135.9, 136.1, 138.4, 145.1, 146.1, 218.3, 224.1, 303.6. IR (KBr): ν 2050, 1909, 1541, 1500, 1198 cm^{-1}. $C_{50}H_{38}Cr_2N_4O_{12}$: Calcd C 60.61, H 3.87, N 5.65. Found C 60.50, H 3.99, N 5.78.

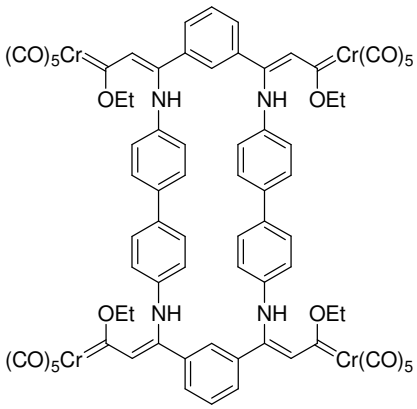

1d

Complex 1d. Following the general procedure, from 140 mg (0.14 mmol) of the complex **3c**, 88 mg (0.14 mmol) of bis-carbene complex **2a** and 10 mL of THF were obtained after purification by flash column chromatography 103 mg (46 %) of the *tetra*-carbene complex **1d** as a green solid. ^{1}H NMR (300 MHz, $CDCl_3$): δ 1.62 (t, 12H, *J* = 7.0 Hz), 4.94 (q, 8H, *J* = 7.0 Hz), 6.52 (d, 8H, *J* = 8.1 Hz), 6.56 (s, 4H), 7.28-7.37 (m, 16H, ar), 10.10 (s, 4H, NH). ^{13}C NMR (50 MHz, $CDCl_3$): δ 15.7, 74.8, 122.9, 123.2, 126.8, 128.6, 129.6, 130.6, 135.2, 136.9, 138.2, 143.4, 217.8, 223.9, 308.7. IR (KBr): ν 2052, 1909, 1541, 1375, 1350 cm^{-1}. $C_{76}H_{52}Cr_4N_4O_{24}$: Calcd C 56.58, H 3.25, N 3.47. Found C 56.84, H 3.01, N 3.65.

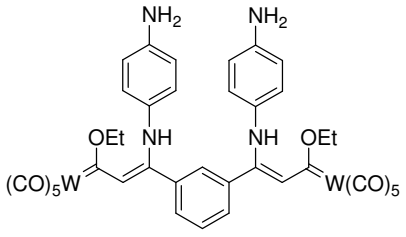

3b

Complex 3b. Following the general procedure, from 300 mg (0.34 mmol) of the bis-carbene complex **2b**, 73 mg (0.78 mmol) of 1,4-diaminobencene and 30 mL of THF were obtained 373 mg (quantitative yield) of the bis-carbene complex **3b** as a green solid. ^{1}H NMR (300 MHz, $CDCl_3$): δ 1.55 (t, 6H, *J* = 7.0 Hz), 3.60 (br s, 4H, NH_2), 4.70 (q, 4H, *J* = 7.0 Hz), 6.27 (s, 2H), 6.40-6.51 (m, 8H, ar), 7.20-7.29 (m, 4H, ar), 10.44 (s, 2H, NH). ^{13}C NMR (50 MHz, $CDCl_3$): δ 15.5, 76.9 115.3, 116.7, 123.6, 124.7, 128.5, 129.1, 130.1, 135.6, 144.8, 150.7, 199.0, 203.8, 275.0. IR (CCl_4): ν 2058, 1967, 1927,

1545, 1196 cm^{-1}. $C_{38}H_{30}N_4O_{12}W_2$: Calcd C 41.40, H 2.74, N 5.08. Found C 41.21, H 2.61, N 5.18.

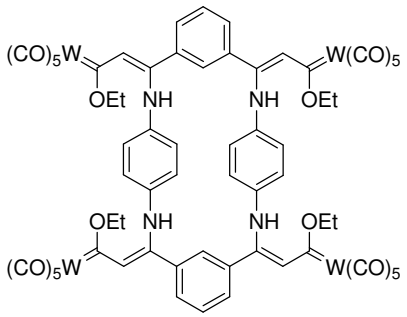

1b

Complex 1b. Following the general procedure, from 196 mg (0.18 mmol) of the complex **3b**, 158 mg (0.18 mmol) of bis-carbene complex **2b** and 16 mL of THF were obtained after purification by flash column chromatography 146 mg (41 %) of the *tetra*-carbene complex **1b** as a green solid. ^{1}H NMR (300 MHz, $CDCl_3$): δ 1.63 (t, 12H, *J* = 7.0 Hz), 4.78 (m, 8H), 6.41 (s, 8H, ar), 6.63 (s, 4H), 6.69-7.03 (m, 6H, ar), 7.73 (s, 2H), 10.36 (s, 4H, NH). ^{13}C NMR (50 MHz, $CDCl_3$): δ 15.5, 77.5, 122.4, 122.9, 125.6, 127.3, 127.8, 131.1, 135.1, 136.2, 146.4, 198.6, 203.7, 283.9. IR (KBr): ν 2060, 1900, 1533, 1514, 1369, 1192 cm^{-1}. $C_{64}H_{44}N_4O_{24}W_4$: Calcd C 38.66, H 2.23, N 2.82. Found C 38.85, H 2.40, N 2.71.

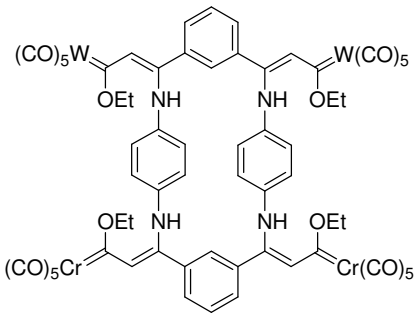

1c

Complex 1c. Following the general procedure, from 196 mg (0.18 mmol) of the complex **3d**, 158 mg (0.18 mmol) of bis-carbene complex **2a** and 16 mL of THF were obtained after purification by flash column chromatography 146 mg (41 %) of the *tetra*-carbene complex **1c** as a mixture of stereoisomers (2:1 ratio), green solid. ^{1}H NMR (300 MHz, $CDCl_3$): δ 1.63 (t, 6H, *J* = 7.0 Hz), 1.65 (t, 6H, *J* = 7.0 Hz), 4.78 (m, 4H), 4.96 (m, 4H), 6.38, 6.40 (s, s, 8H, ar), 6.64, 6.65 (s,s, 4H), 6.90-7.03 (m, 6H, ar), 7.73, 7.73 (s,s, 2H), 10.23, 10.24 (s,s, 2H, NH), 10.36, 10.37 (s, s, 2H, NH). ^{13}C NMR (50 MHz, $CDCl_3$): δ 15.4, 15.7, 74.8, 122.4, 123.0, 125.4, 127.3, 127.7, 131.1, 131.3, 134.9, 135.1, 135.2, 136.1, 142.7, 142.9, 146.7, 198.6, 203.8, 217.7, 224.1, 283.3, 308.2, 308.4. IR (KBr): ν 2052, 1904, 1533, 1514, 1369, 1192 cm^{-1}. $C_{64}H_{44}Cr_2N_4O_{24}W_2$: Calcd C 44.57, H 2.57, N 3.25. Found C 44.29, H 2.81, N 3.41.

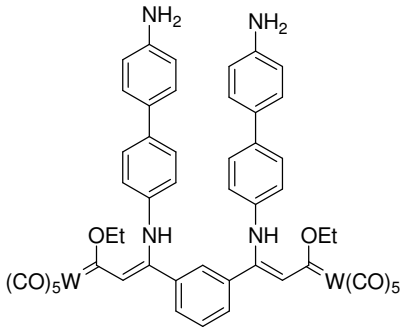

3d

Complex 3d. Following the general procedure, from 150 mg (0.17 mmol) of the bis-carbene complex **2b**, 62 mg (0.34 mmol) of bencidine and 15 mL of THF were obtained 213 mg (quantitative yield) of the bis-carbene complex **3d** as a red solid. ^{1}H NMR (300 MHz, $CDCl_3$): δ 1.58 (t, 6H, *J* = 7.0 Hz), 3.67 (br s, 4H, NH_2), 4.74 (q, 4H, *J* = 7.0 Hz), 6.43 (s, 2H), 6.54-6.66 (m, 8H), 7.18-7.28 (m, 12H, ar), 10.41 (s, 2H, NH). ^{13}C NMR (75.4 MHz, $CDCl_3$): δ 15.4, 77.2, 115.4, 123.2, 124.8, 126.8, 127.2, 127.6, 129.6, 130.4, 135.8, 136.0, 138.5, 144.9, 146.2, 148.8, 198.7, 203.8, 279.5. IR (KBr): ν 2058, 1904, 1541, 1375, 1196 cm^{-1}. $C_{50}H_{38}N_4O_{12}W_2$: Calcd C 47.87, H 3.05, N 4.47. Found C 48.02, H 3.22, N 4.35.

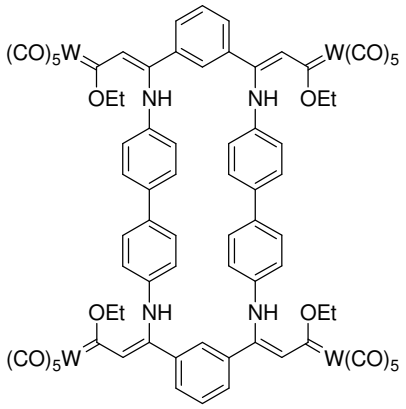

1e

Complex 1e. Following the general procedure, from 212 mg (0.17 mmol) of the complex **3d**, 150 mg (0.17 mmol) of bis-carbene complex **1e** and 15 mL of THF were obtained after purification by flash column chromatography 156 mg (43 %) of the *tetra*-carbene complex **3d** as a green solid. ^{1}H NMR (300 MHz, $CDCl_3$): δ 1.60 (t, 12H, *J* = 7.0 Hz), 4.77 (q, 8H, *J* = 7.0 Hz), 6.55 (d, 8H, *J* = 8.5 Hz), 6.60 (s, 4H), 7.29-7.40 (m, 16H, ar), 10.21 (s, 4H, NH). ^{13}C NMR (75.5 MHz, $CDCl_3$): δ 15.4, 77.2, 123.0, 126.2, 126.8, 129.7, 130.4, 135.2, 136.8, 138.1, 142.9, 147.1, 198.6, 203.6, 283.9. IR (KBr): ν 2060, 1904, 1541, 1373, 1196 cm^{-1}. $C_{76}H_{52}N_4O_{24}W_4$: Calcd C 42.64, H 2.45, N 2.62. Found C 42.45, H 2.59, N 2.77.

1.3. Chromium Imidate Complexes from the Metathesis-Like Reaction of Phosphinimines and Chromium(0) Fischer Carbene Complexes

1.3. Chromium Imidate Complexes from the Metathesis-Like Reaction of Phosphinimines and Chromium(0) Fischer Carbene Complexes

1.3.1. Introduction

The chemistry of Fischer carbene complexes has experienced a great development in the last years, mainly due to their unique reactivity. Today many efficient processes are based on these versatile synthons, which have become very valuable building blocks in organic synthesis.[1] In this context, the reactivity of Fischer carbene complexes with imines has been a subject of interest, as imines have both nucleophilic and electrophilic sites and are unsaturated, a combination of factors that could lead to different reaction pathways.

The thermal behavior of group 6 Fischer carbene complexes toward imines is strongly dependent on the structure of the reagents and the reaction conditions. Thus, the reaction of the methyl complex **1** with the *N*-methyl imine of benzaldehyde gives the α,β-unsaturated complex **2** as a result of a base-induced condensation between the relatively acidic compound **1** and the imine.[2] On the other hand, imino complexes **4** can be obtained from acyloxy- and alkoxycarbene complexes **3** and *N*-trimethylsilyl imines.[3] Additionally, heating alkoxycarbene complexes **5** and *N*-tosylimines forms β-methoxyallylamine derivatives **6** (Scheme 1).[4]

[1] Selected reviews in the chemistry and synthetic applications of Fischer carbene complexes: (a) Dötz, K. H.; Fischer, H.; Hoffmann, P.; Kreissel, F. R.; Schubert, U.; Weiss, K. *Transition Metal Carbene Complexes*, Verlag Chemie, Deerfield Beach, Florida, 1983. (b) Dötz, K. H. *Angew. Chem. Int. Ed. Engl.* **1984**, *23*, 587. (c) Wulff, W. D. in *Comprehensive Organometallic Chemistry II*; Abel, E. W.; Stone, F. G. A.; Wilkinson, G. Eds.; Pergamon: New York, 1995, Vol. 12, Chapter 5.3, p 469. (d) Hegedus, L. S. In *Comprehensive Organometallic Chemistry II*; Abel, E. W.; Stone, F. G. A.; Wilkinson, G. Eds.; Pergamon: New York, 1995, Vol. 12, Chapter 5.3, p 549. (e) Harvey, D. F.; Sigano, D. M. *Chem. Rev.* **1996**, *96*, 271. (f) Sierra, M. A. *Chem. Rev.* **2000**, *100*, 3591.

[2] Hegedus, L. S.; McGuire, M. A.; Schultze, L. S.; Yijun, C.; Anderson, O. P. *J. Am. Chem. Soc.* **1984**, *106*, 2680.

[3] Murray, C. K.; Warner, B. P.; Dragisich, V.; Wulff, W. D.; Rogers, R. D. *Organometallics* **1990**, *9*, 3142.

[4] Sangu, K.; Kagoshima, H.; Fuchibe, K.; Akiyama, T. *Org. Lett.* **2002**, *4*, 3967.

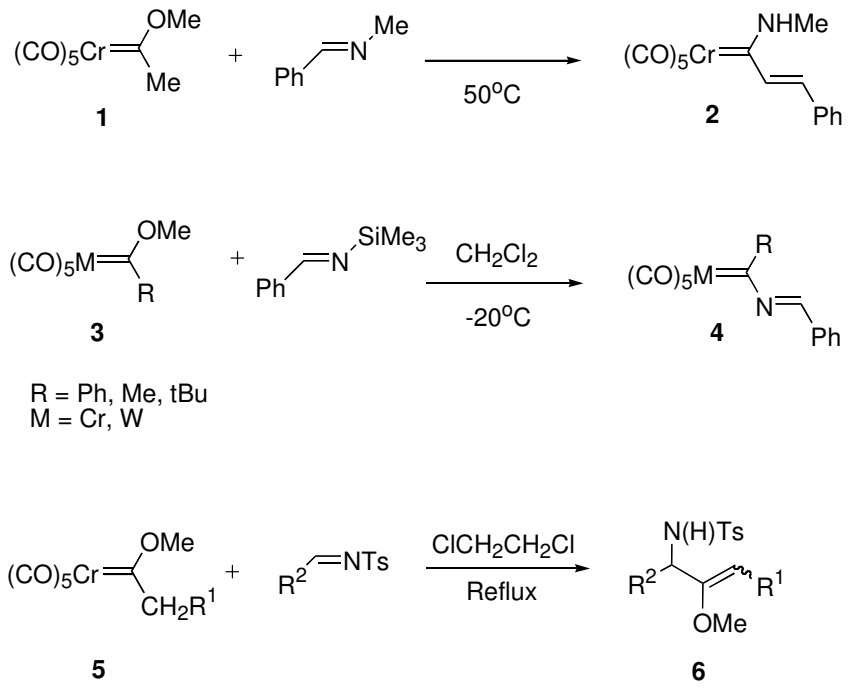

Scheme 1

The reactivity of imines, enamines, and azadienes with α,β-unsaturated group 6 carbene complexes has been thoroughly investigated by Barluenga's group, which has allowed them to describe a plethora of novel cycloaddition processes.[5] Finally, the photoinduced reaction of Fischer carbene complexes with imines to produce β-lactams has also been studied in depth. This reaction involves the reversible formation of chromium ketene complexes able to react with ketenophiles to yield ketene-derived products either on inter- or intramolecular reactions.[6] This type of processes has been profusely applied in synthesis[1d,6] and has been of longstanding mechanistic interest.[7]

---

[5] For reactions of Fischer carbene complexes with α,β-unsaturated imines, see: (a) Danks, T. N.; Velo-Rego, D. *Tetrahedron Lett.* **1994**, *35*, 9443. (b) Barluenga, J.; Tomás, M.; Ballesteros, A.; Santamaría, J.; López-Ortíz, F. *J. Chem. Soc., Chem. Commun.* **1994**, 321. (c) Barluenga, J.; Tomás, M.; López-Pelegrín, J. A.; Rubio, E. *J. Chem. Soc., Chem. Commun.* **1995**, 665. (d) Barluenga, J.; Tomás, M.; Rubio, E.; López-Pelegrín, J. A.; García-Granda, S.; Pertierra, P. *J. Am. Chem. Soc.* **1996**, *118*, 695. (e) Barluenga, J.; Tomás, M.; Ballesteros, A.; Santamaría, J.; Carbajo, R. J., López-Ortíz, F.; García-Granda, S.; Pertierra, P. *Chem. Eur. J.* **1996**, *2*, 88. (f) Barluenga, J.; Tomás, M.; Ballesteros, A.; Suárez-Sobrino, A. *J. Org. Chem.* **1997**, *62*, 9299. (g) Barluenga, J.; Tomás, M.; Rubio, E.; López-Pelegrín, J. A.; García-Granda, S.; Priede, M. P. *J. Am. Chem. Soc.* **1999**, *121*, 3065 and references therein. For other reactions, see: (h) Kagoshima, H.; Akiyama, T. *J. Am. Chem. Soc.* **2000**, *122*, 11741. (i) Kagoshima, H.; Okamura, T.; Akiyama, T. *J. Am. Chem. Soc.* **2001**, *123*, 7182.

[6] For reviews in the photochemistry of group 6 metal-carbene complexes, see: (a) Hegedus, L. S. *Tetrahedron* **1997**, *53*, 4105. (b) Schwindt, M. A.; Miller, J. R.; Hegedus, L. S. *J. Organomet. Chem.* **1991**, *413*, 143.

[7] (a) Hegedus, L. S.; de Weck, G.; D'Andrea, S. *J. Am. Chem. Soc.* **1988**, *110*, 2122. (b) Arrieta, A.; Cossío, F. P.; Fernández, I.; Gómez-Gallego, M.; Lecea, B.; Mancheño, M. J.; Sierra, M. A. *J. Am. Chem. Soc.* **2000**, *122*, 11509. (c) Sierra, M. A.; Fernández, I.; Mancheño, M. J.; Gómez-Gallego, M.; Torres, M. R.; Cossío, F. P.; Arrieta, A.; Lecea, B.; Poveda, A.; Jiménez-Barbero, J. *J. Am. Chem. Soc.* **2003**, *125*, 9572.

The reaction of Fischer carbene complexes with phosphines is a well-known process that leads to new carbene complexes formed by ligand exchange of the coordination sphere of the metal.[8] During our studies directed to discover novel processes in the chemistry of group 6 metal carbenes[7b,7c] the synthesis of chromium(0) carbene complexes having phosphinimine ligands was needed. Our results indicate that, instead of the expected CO-phosphine interchange, a new thermal process, the formation of imidate species coordinated to chromium, was observed. We report here a detailed study of the scope and limitations of this new type of reaction.

1.3.2. Results and Discussion

Imines **8** were prepared in quantitative yields from diphenylphosphinoamines **7** and the corresponding aldehyde in CH_2Cl_2 at room temperature (Scheme 2). Heating equimolecular amounts of [pentacarbonyl(ethoxymethyl)carbene] chromium(0), **9**, and imine **8a** in a mixture of hexane and benzene (1:1) yielded a new chromium complex lacking the carbene carbon (Scheme 3).

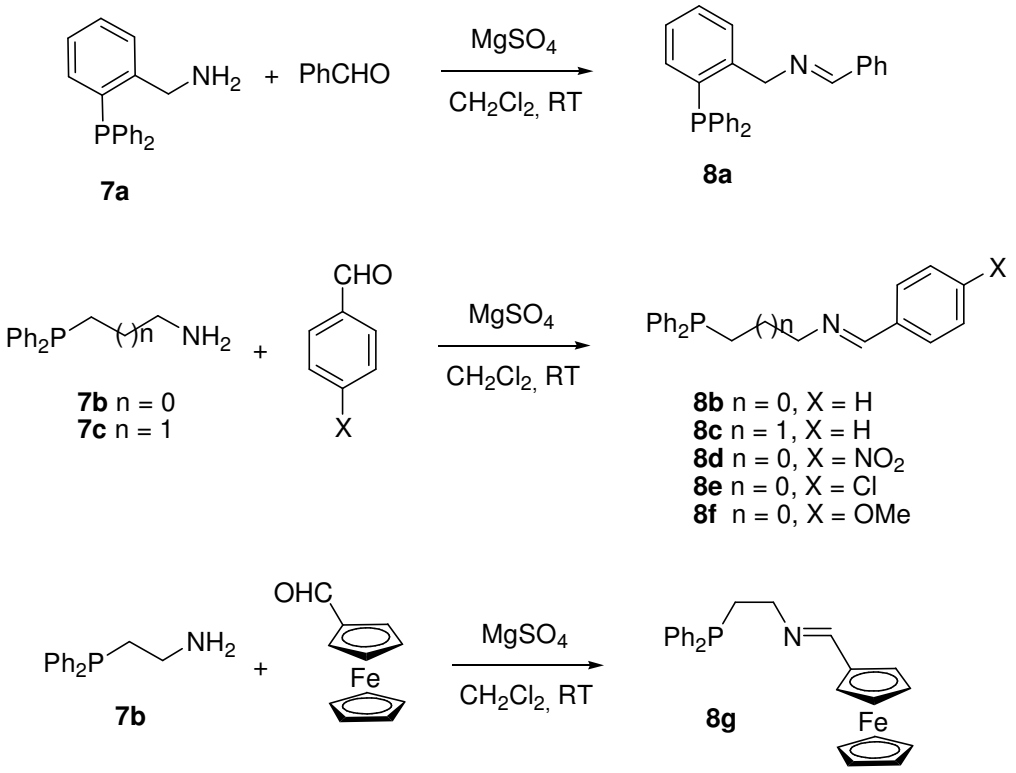

Scheme 2

[8] Fischer, E. O.; Fischer, H. *Chem. Ber.* **1974**, *107*, 657.

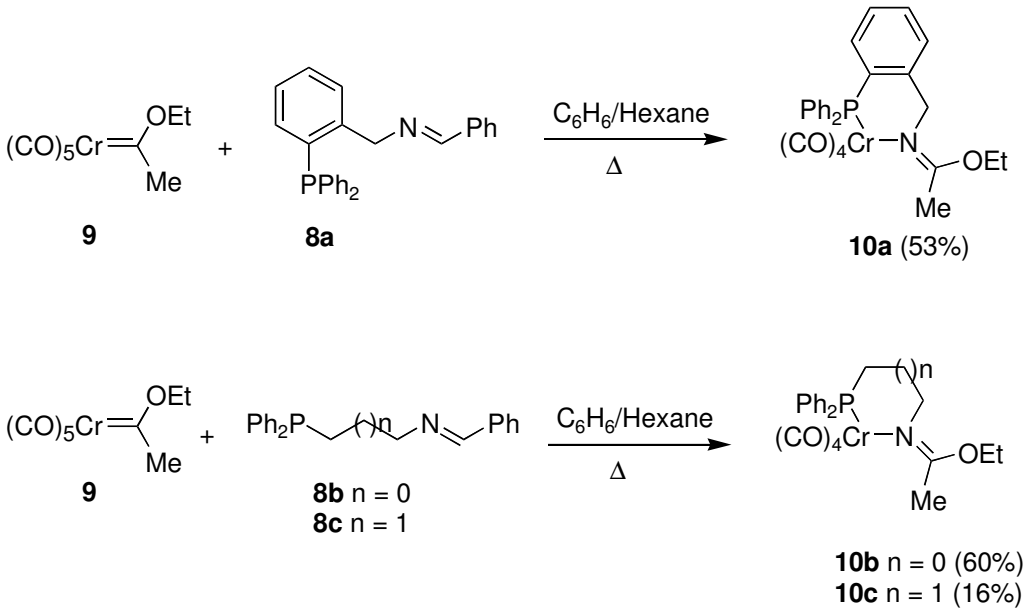

Scheme 3

The ^{13}C NMR spectrum of this complex exhibited three signals at 227.2, 227.0 and 219.0 ppm attributable to a $[(CO)_4Cr]$ moiety, together with a signal at 166.3 ppm that may correspond to a C=N bond. The ^{1}H NMR analysis showed the presence of a methyl group (δ = 2.44(*s*)) and an ethoxy group (δ = 1.33(*t*) and 4.05(*q*)) linked to an sp^2 carbon. A single crystal of this compound was submitted to X-ray diffraction analysis, and its structure was unambiguously established as the cyclic phosphinoimidate $(CO)_4Cr$ complex **10a** (Figure 1).[9] The reaction of complex **9** with imines **8b**,**c** under the same conditions as those above produced the analogous complexes **10b**,**c** in 60% and 16% yields, respectively. In this latter case, together with complex **10c** a new carbene complex was formed in 6% yield. This compound was identified as [pentacarbonyl(ethoxystyryl)carbene]chromium(0), by comparison of its spectroscopic data with those obtained from an authentic sample.[10] In all cases, the imidate complexes **10** were obtained as single isomers and their structures were established by comparison with the spectroscopic data of **10a**.

[9] Structure of **10a** was elucidated by X-ray crystallography. Crystal data: Mr = 573.51, monoclinic, space group = C2/c, a = 33.327(9) Å, b = 9.3291(14) Å, c = 19.595(8) Å; V = 5856(3) $Å^3$; Z = 8; Dz = 1.301 $Mg.m^{-3}$; Mo Kα (λ = 0.71069Å), μ = 0.484 mm^{-1}, R = 0.0131, Rw = 0.1434, 5135 reflections, 355 refined parameters; refinement on F^2. The data were collected with an Enraf-Nonius CAD-4 difractometer (T = 298(2) K). The structure and the refinement of the crystal structure were done with the SHELXL97 program.

[10] Aumann, R; Heinen, H. *Chem Ber.* **1987**, *120*, 537.

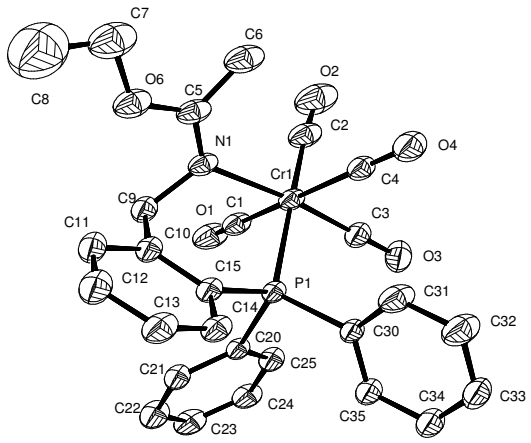

Figure 1. ORTEP-drawing of complex **10a**. Hydrogens atoms have been omitted for clarity.

To evaluate the role of the electrophilicity of the C=N double bond in the formation of the imidate complexes, the reactions of complex **9** with imines **8d-f** having electron-withdrawing or electron-donating groups in the aromatic ring were tested next. The results are compiled in Scheme 4. The most electrophilic imine, **8d**, yielded complex **10b** in 54% yield. Imine **8e** behaves in a similar way, affording complex **10b** in 46% yield, but the less electrophilic imine **8f** rendered a complex reaction mixture where [pentacarbonyl(ethoxy)(*p*-methoxystyryl)carbene]chromium(0) was the only product that could be isolated (Scheme 4).

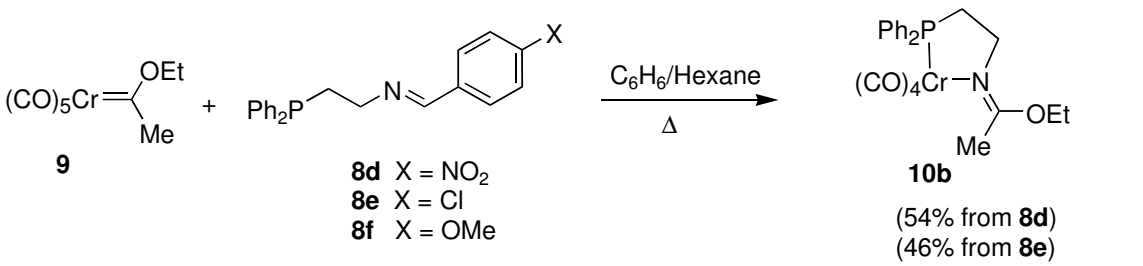

Scheme 4

The reactivity of ethoxyphenyl chromium carbene complex **11** with imine **8a** was tested next. This time, the imino complex **12a** was the sole identifiable reaction product and was obtained as *syn/anti* mixture of isomers across the double bond. The isomers were separated by column chromatography on silica gel, and their structures were established on the basis of NOE measurements. A similar behavior was found when complex **9** was treated with the bulky ferrocenylimine **8g**, yielding a *syn/anti* mixture of ferrocenylimino complexes **12b** as reaction products. As in the case of **12a**,

the isomers were separated by chromatography and their structures established on the basis of NOE measurements (Scheme 5).

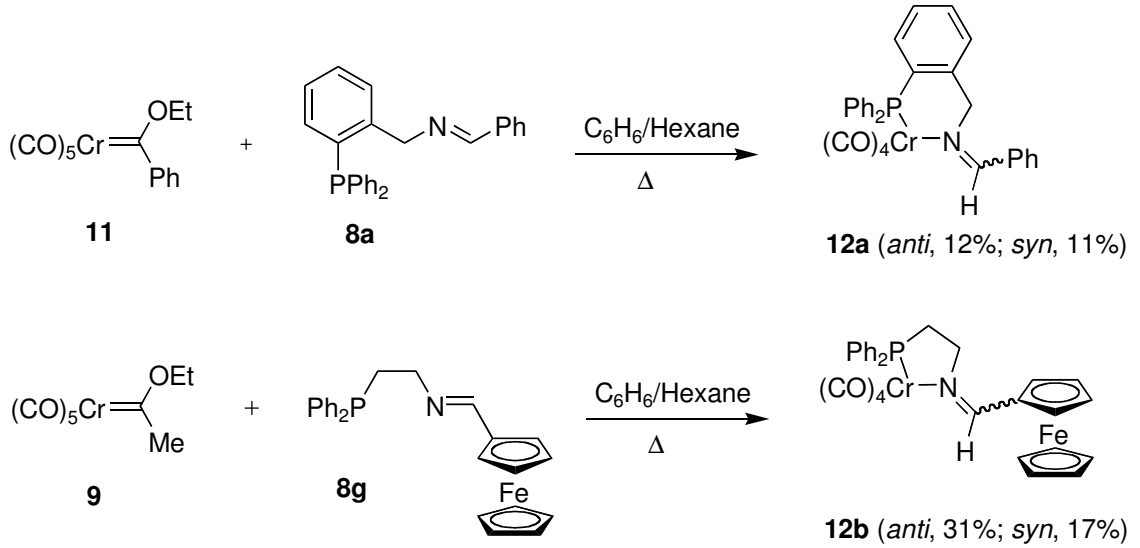

Scheme 5

Clear trends emerge from the data above: the formation of chromium(0) imidate complexes **10** from alkyl Fischer carbene complex **9** is favored with electrophilic phosphinimines **8**, while a less electrophilic carbene complex such as **11** or a bulky subtituent at the imine carbon (as in **8g**) leads exclusively to products **12**, in which the carbene and one of the CO ligands have been interchanged by the phosphinimine moiety. Considering all the experimental observations, the formation of imidate complexes **10** could be explained attending to a stepwise mechanism, which is illustrated in Scheme 6. The thermal CO-phosphine ligand exchange should form intermediate **13** in the first step. Nucleophilic attack of the imine moiety on the electrophilic carbene carbon may lead to zwitterion **14**, that evolves to azametallacycle **15** by attack of the nucleophilic chromium center at the iminium moiety. Finally, breakage of the metallacycle intermediate **15** should form the new carbene complex **16**, which evolves by extrusion of the arylcarbene moiety to compounds **10**.[11] This step may be induced by the metal-imidate coordination. Overall, the evolution of

[11] The detection of mixtures of *cis*- and *trans*-stylbenes in the reaction of acyloxy- and alkoxycarbene complexes and *N*-trimethylsilyl imines has been reported by Wulff.[3] We have carried out the reactions of complex **9** and imines **8b**,**d** with the goal of isolating the expected products of evolution of the corresponding intermediates **16**. Direct observation of stylbenes was hampered due to the presence of the diphenylphosphine moiety, which masked the aromatic region of the NMR spectra of the crude reaction mixtures. Chromatography led to pure imidate complex **10b**, together with mixtures of unidentified products. The sequence irradiation-light oxidation was used also in these reactions leading to total decomposition of complex **10b** together with very complex reaction mixtures.

phosphineimines **8** to complexed imidates **10** can be considered a metathesis-like reaction (Scheme 6).

The effect of the length of the tether on the yields of imidate-complexes **10** (60% for imine **8b** and 16% for imine **8c**) and the rigidity (53% yield for imine **8a** and only 16% for imine **8c**) supports the hypothesis that the coordination of the phosphine ligand should precede the metallacycle formation. Otherwise, the reactivity of imines **8a-c** should be comparable. As the formation of metallacycle **15** requires the attack of the chromium nucleus at the C=N bond, poorly electrophilic imines inhibit this reaction step, leading to decomposition products together with compounds derived from the normal acid-base reactivity reported earlier by Hegedus.[2] Other factors disfavoring the formation of this key intermediate **15** are bulky substituents on the imine (as in **8g**) or the choice of a less reactive Fischer carbene complex, such as **11**.

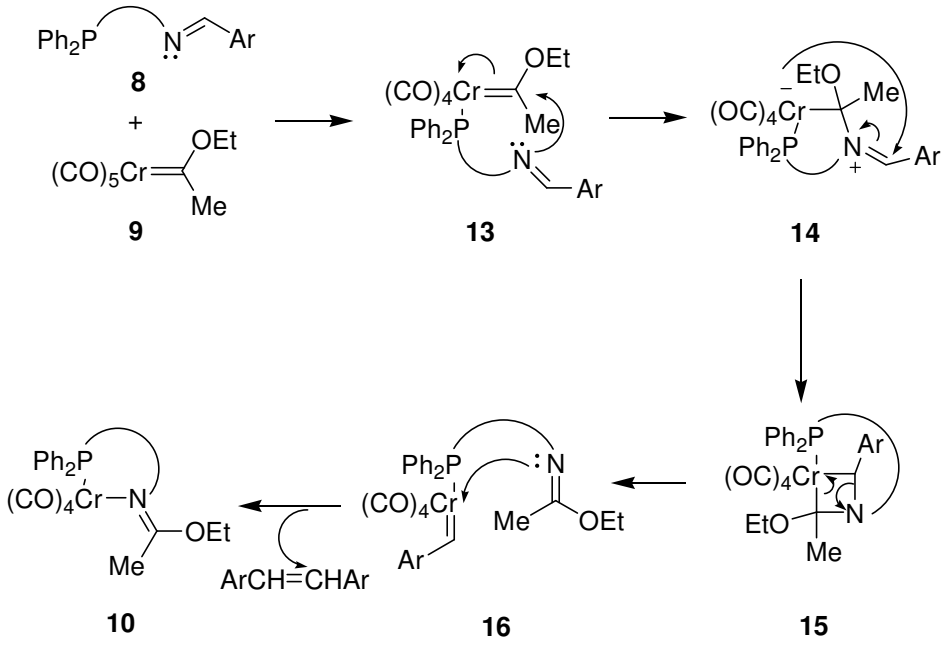

Scheme 6

Finally, to check the effect of the metal in the starting carbene on the reacion mechanism, imine **8a** was treated with [pentacarbonyl(ethoxymethyl) carbene]tungsten(0) under the same conditions used for complex **9**. In this case, the expected imidate was not formed and the reaction yielded a complex mixture of products from which only [pentacarbonyl(ethoxystyryl)carbene]tungsten(0) could be isolated. This result may be explained by the lower electrophilicity of the carbene carbon in tungsten Fischer carbene complexes, compared to their chromium analogues,

which is further diminished in this case by the electron-donating effect of the phosphine ligand.

In summary, a new thermal reaction of imines with chromium Fischer carbene complexes has been studied. Stable chromium imidate complexes are obtained in a metathesis-like process.[12,13] The formation of azametallacycle **15** from zwitterions **14** is the key to the reaction. The length of the phosphinimine tether, the electrophilicity of the C=N bond and the bulkiness of the imine substitutents determine whether or not the metathesis-like process occurs. Only those compounds having short or rigid tethers or electrophilic and moderately hindered C=N groups react with electrophilic carbene complexes. Otherwise, bulkier imines or less electrophilic carbene complexes are unable to form the key azametallacycles and either decompose or form the condensation products derived from acid-base reactivity.

[12] The examples of chromium imidate tetracarbonylphosphine complexes are scarce. See: (a) Raubenheimer, H. G.; Kruger, G. J.; Vijoen, H. W.; Hendrik, W.; Lotz, S. *J. Organomet. Chem.* **1986**, *314*, 281. The synthesis of imidate thioether chelates can be found in: (b) Raubenheimer, H. G.; Kruger, G. J.; Vijoen, H. W. *J. Organomet. Chem.* **1986**, *319*, 361. For earlier examples of the formation of chromium(0) imidate pentacarbonyl complexes, among other different products in the reaction of chromium(0) pentacarbonyl alkoxycarbene complexes and hydroxylamine, see: (c) Fischer, E. O.; Aumann, R. *Chem. Ber.* **1968**, *101*, 963. Dimethylhydrazine: (d) Raubenheimer, H. G.; Lotz, S.; Kruger, G. J.; Gafner, G. *J. Organomet. Chem.* **1979**, *173*, C1.

[13] The formation of metal-free imidates from group 6 metal carbene and different reagents is well-known. From aziridines: (a) Hegedus, L. S.; Kramer, A.; Yijun, C. *Organometallics* **1985**, *4*, 1747.(b) Curtis, M. D.; Hay, M. S.; Butler, W. M.; Kampt, J. *Organometallics* **1992**, *11*, 2884. From azobenzene: (c) Arndtsen, B. A.; Sleiman, H. F.; Chang, A. K.; McElwee-White, L. *J. Am. Chem. Soc.* **1991**, *113*, 4871. (d) Sleiman, H. F.; Mercer, S.; McElwee-White, L. *J. Am. Chem. Soc.* **1989**, *111*, 8007. (e) Hegedus, L. S.; Lundmark, B. *J. Am. Chem. Soc.* **1989**, *111*, 9194. (f) Hegedus, L. S.; Kramer, A. *Organometallics* **1984**, *3*, 1263. (g) Sleiman, H. F.; McElwee-White, L. *J. Am. Chem. Soc.* **1988**, *110*, 8700. (h) Maxey, C. T.; Sleiman, H. F.; Massey, S. T.; McElwee-White, L. *J. Am. Chem. Soc*. **1992**, *114*, 5153. From imines and *O*-acylchromium(0) carbene complexes: see reference 3. From nitrosobenzene: (i) Herndon, J. W.; McMullen, L. A. *J. Organomet. Chem.* **1989**, *368*, 83. (j) Pilato, R. S.; Williams, G. D.; Geoffroy, G. L.; Rheingold, A. L. *Inorg. Chem*. **1988**, *27*, 3665. From sulfilimines: (k) Alcaide, B.; Casarrubios, L.; Domínguez, G.; Sierra, M. A. *J. Org. Chem.* **1993**, *58*, 3886. (l) Alcaide, B.; Domínguez, G.; Plumet, J.; Sierra, M. A. *Organometallics* **1991**, *10*, 11.

1.3.3. Experimental Section

General Procedures. ^{1}H NMR and ^{13}C NMR spectra were recorded at 22 ºC on Bruker Avance 300 (300.1 and 75.4 MHz) or Bruker 200-AC (200.1 and 50 MHz) spectrometers. Chemical shifts are given in ppm relative to TMS (^{1}H, 0.0 ppm) and $CDCl_3$ (^{13}C, 77.0 ppm). IR spectra were taken on a Perkin-Elmer 781 spectrometer. Flame-dried glassware and standard Schlenk techniques were used for moisture sensitive reactions. Merck silica-gel (230-400 Mesh) was used as the stationary phase for purification of crude reaction mixtures by flash column chromatography. Identification of products was made by TLC (kiesegel 60F-254). UV light (λ = 254 nm) and 5% phosphomolybdic acid solution in 95% EtOH were used to develop the plates.
All commercially available compounds were used without further purification. 2-(Diphenyphosphino)benzylamine was prepared according to literature methods.[14]

General Procedure for the Synthesis of Phosphineimines 8a-g. A solution of 2-(diphenylphosphino)ethylamine, 3-(diphenylphosphino)propylamine or 2-(diphenyphosphino)benzyl amine and the corresponding benzaldehyde in stochiometric amounts and large excess of $MgSO_4$ in dry CH_2Cl_2 was stirred at room temperature for 24 hours. The mixture was filtered and solvent was removed under reduced pressure to yield the corresponding imines.

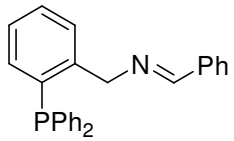

8a

Imine 8a. Following the general procedure, from 570 mg (1.96 mmol) of 2-(diphenylphosphino)benzylamine, **7a**, 208 mg (1.96 mmol) of benzaldehyde, 1.77 g (14.7 mmol) of $MgSO_4$ and 30 mL dry Et_2O were obtained 742 mg (quantitative yield) of the imine **8a** as a pale pink oil. ^{1}H NMR (300 MHz, $CDCl_3$): δ 4.97 (s, 2H), 6.82 (m, 2H), 7.18-7.51 (m, 18H), 8.16 (s, 1H). ^{13}C NMR (50 MHz, $CDCl_3$): δ 63.0 (d, J_{C-P} = 22.7 Hz), 127.1, 128.1, 128.4 (d, J_{C-P} = 3.5 Hz), 128.6 (d, J_{C-P} = 2.8 Hz), 129.0, 130.5, 132.0 (d, J_{C-P} = 9.6 Hz), 133.4, 133.9 (d, J_{C-P} = 19.9 Hz), 136.3 (d, J_{C-P} = 20.2 Hz), 136.4, 143.9 (d, J_{C-P} = 24.1 Hz), 162.3. IR (CCl_4): ν 3057, 2926, 2854, 1647, 1435 cm^{-1}. $C_{26}H_{22}NP$ Calcd C 82.30, H 5.84, N 3.69. Found C 82.51, H 5.69, N 3.84.

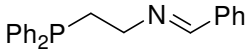

8b

Imine 8b. Following the general procedure, from 500 mg (2.18 mmol) of 2-(diphenylphosphino)ethylamine, **7b**, 213 mg (2.18 mmol) of benzaldehyde, 1.97 g (16.4 mmol) of $MgSO_4$ and 35 mL dry CH_2Cl_2 were obtained 692 mg (quantitative yield) of the imine **8b** as a pale yellow solid. ^{1}H NMR (300 MHz, $CDCl_3$): δ 2.41 (m, 2H), 3.06 (m, 2H), 7.24-7.40 (m, 13H), 7.58 (m, 2H), 8.15 (s, 1H). ^{13}C NMR (75.5 MHz, $CDCl_3$): δ 29.8 (d, J_{C-P} = 12.7 Hz), 58.4 (d, J_{C-P} = 21.1 Hz), 128.0, 128.5, 128.5 (d, J_{C-P} = 8.0 Hz), 128.7, 130.6, 132.7 (d, J_{C-P} = 18.8 Hz), 136.0, 138.3 (d, J_{C-P} = 12.4 Hz), 161.3. IR

[14] Brunner, A.; Kühnle, F. N. M.; Seebach, D. *Helv. Chem. Acta* **1996**, *79*, 319.

(CCl_4): ν 3057, 2841, 1643, 1433 cm^{-1}. $C_{21}H_{20}NP$ Calcd C 79.47, H 6.35, N 4.41. Found C 79.62, H 6.21, N 4.65.

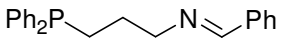

8c

Imine 8c. Following the general procedure, from 323 mg (1.33 mmol) of 2-(diphenylphosphino)propylamine, **7c**, 141 mg (1.33 mmol) of benzaldehyde, 1.20 g (9.96 mmol) of $MgSO_4$ and 25 mL dry CH_2Cl_2 were obtained, after vacuo distillation, 410 mg (93 %) of the imine **8c** as an orange solid. ^{1}H NMR (300 MHz, $CDCl_3$): δ 1,81 (m, 2H), 2.05 (m, 2H), 3.67 (td, 2H, J = 6.7 Hz, $J_{H\text{-}P}$ = 0.9 Hz), 7.23-7.37 (m, 13H), 7.63 (m, 2H), 8.19 (s, 1H). ^{13}C NMR (50 MHz, $CDCl_3$): δ 25.6 (d, $J_{C\text{-}P}$ = 11.7 Hz), 27.3 (d, $J_{C\text{-}P}$ = 16.3 Hz), 64.2 (d, $J_{C\text{-}P}$ = 13.1 Hz), 128.0, 128.4 (d, $J_{C\text{-}P}$ = 8.9 Hz), 128.4, 128.5, 130.5, 132.7 (d, $J_{C\text{-}P}$ = 18.4 Hz), 136.2, 138.6 (d, $J_{C\text{-}P}$ = 13.1 Hz), 161.2. IR (CCl_4): ν 3059, 2926, 2852, 1708, 1647, 1435 cm^{-1}. $C_{22}H_{22}NP$ Calcd C 79.74, H 6.69, N 4.23. Found C 79.55, H 6.84, N 4.50.

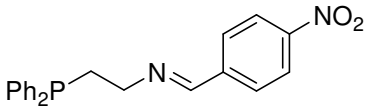

8d

Imine 8d. Following the general procedure, from 248 mg (1.08 mmol) of 2-(diphenylphosphino)ethylamine, **7b**, 163 mg (1.08 mmol) of *p*-nitrobenzaldehyde, 977 mg (8.11 mmol) of $MgSO_4$ and 18 mL dry CH_2Cl_2 were obtained 391 mg (quantitative yield) of the imine **8d** as an orange solid. ^{1}H NMR (300 MHz, $CDCl_3$): δ 2.39 (m, 2H), 3.70 (m, 2H), 7.19-7.37 (m, 10H), 7.65 (d, 2H, J = 8.8 Hz), 8.07 (d, 2H, J = 8.8 Hz), 8.14 (s, 1H). ^{13}C NMR (75.5 MHz, $CDCl_3$): δ 29.4 (d, $J_{C\text{-}P}$ = 13.1 Hz), 58.5 (d, $J_{C\text{-}P}$ = 20.3 Hz), 123.5, 128.2 (d, $J_{C\text{-}P}$ = 6.9 Hz), 128.4, 128.5, 132.6 (d, $J_{C\text{-}P}$ = 18.7 Hz), 138.0 (d, $J_{C\text{-}P}$ = 12.4 Hz), 141.3, 148.7, 158.8. IR (CCl_4): ν 3057, 2922, 2850, 1647, 1603, 1525, 1435, 1344 cm^{-1}. $C_{21}H_{19}N_2O_2P$ Calcd. C 69.61, H 5.29, N 7.73. Found C 69.84, H 5.14, N 7.94.

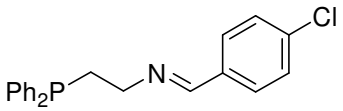

8e

Imine 8e. Following the general procedure, from 150 mg (0.65 mmol) of 2-(diphenylphosphino)ethylamine, **7b**, 92 mg (0.96 mmol) of *p*-chlorobenzaldehyde, 591 mg (4.9 mmol) of $MgSO_4$ and 11 mL dry CH_2Cl_2 were obtained 230 mg (quantitative yield) of imine **8e** as a pale yellow oil. ^{1}H NMR (300 MHz, $CDCl_3$): δ 2.36 (m, 2H), 3.62 (m, 2H), 7.18-7.67 (m, 14H), 8.02 (s, 1H). ^{13}C NMR (75.5 MHz, $CDCl_3$): δ 29.6 (d, $J_{C\text{-}P}$ = 12.5 Hz), 58.3 (d, $J_{C\text{-}P}$ = 20.8 Hz), 128.3 (d, $J_{C\text{-}P}$ = 6.8 Hz), 128.5, 128.6, 129.1, 132.6 (d, $J_{C\text{-}P}$ = 18.8 Hz), 134.4, 136.4, 138.2 (d, $J_{C\text{-}P}$ = 12.4 Hz), 159.8. IR (CCl_4): ν 3057, 2925, 2852, 1645, 1489, 1458 cm^{-1}. $C_{21}H_{19}ClNP$ Calcd C, 71.69, H 5.44, N, 3.98; Found C 71.84, H 5.51, N 4.12.

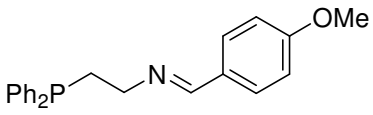

8f

Imine 8f. Following the general procedure, from 250 mg (1.09 mmol) of 2-(diphenylphosphino)ethylamine, **7b**, 149 mg (1.09 mmol) of anisaldehyde, 985 mg (8.2 mmol) of $MgSO_4$ and 18 mL dry CH_2Cl_2 were obtained 379 mg (quantitative yield) of the imine **8f** as a pale yellow solid. ^{1}H NMR (300 MHz, $CDCl_3$): δ 2.81 (m, 2H), 3.82 (s, 3H), 3.91 (m, 2H), 6.90-7.76 (m, 14H), 8.10 (s, 1H). ^{13}C NMR (50.0 MHz, $CDCl_3$): δ 29.9 (d, $J_{C\text{-}P}$ = 12.8 Hz), 55.3, 58.1 (d, $J_{C\text{-}P}$ = 20.2 Hz), 113.9, 128.3, 128.5 (d, $J_{C\text{-}P}$ = 4.3 Hz), 128.7, 129.8, 132.7 (d, $J_{C\text{-}P}$ = 18.8 Hz), 138.3 (d, $J_{C\text{-}P}$ = 12.4 Hz), 160.5, 161.7. IR (CCl_4): ν 3057, 2918, 2837, 1647, 1433, 1250 cm^{-1}. $C_{22}H_{22}NOP$ Calcd C 76.06, H 6.38, N 4.03. Found 76.26, H 6.47, N 3.94.

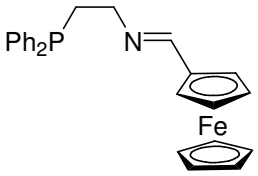

8g

Imine 8g. Following the general procedure, from 178 mg (0.78 mmol) of 2-(diphenylphosphino)ethylamine, **7b**, 167 mg (0.78 mmol) of ferrocenecarbaldehyde, 701 mg (5.8 mmol) of $MgSO_4$ and 15 mL dry CH_2Cl_2 were obtained 331 mg (quantitative yield) of the imine **8g** as an orange solid. ^{1}H NMR (300 MHz, $CDCl_3$): δ 2.34 (m, 2H), 3.48 (m, 2H), 4.08 (s, 5H), 4.27 (s, 2H), 4.46 (s, 2H), 7.24-7.70 (m, 10H), 8.00 (s, 1H). ^{13}C NMR (75.5 MHz, $CDCl_3$): δ 29.9 (d, $J_{C\text{-}P}$ = 12.6 Hz), 58.6 (d, $J_{C\text{-}P}$ = 21.2 Hz), 68.4, 69.0, 70.3, 80.3, 128.4 (d, $J_{C\text{-}P}$ = 6.7 Hz), 132.7 (d, $J_{C\text{-}P}$ = 18.6 Hz), 138.4 (d, $J_{C\text{-}P}$ = 12.5 Hz), 161.4. IR (CCl_4): ν 3057, 2923, 2852, 1645 cm^{-1}. $C_{25}H_{24}FeNP$ Calcd C 70.60, H 5.69, N, 3.29. Found C 70.41, H 5.81, N 3.08.

General procedure for the Synthesis of Phosphine-imidate Complexes, 10. A solution of the metal-carbene complex and the corresponding phosphineimine in degassed hexane-benzene (1:1) was heated at reflux 9 hours (unless otherwise specified). The solvents were removed under reduced pressure and the residue was submitted to flash column chromatography (SiO_2, Hexane: AcOEt) under argon atmosphere to give pure compounds.

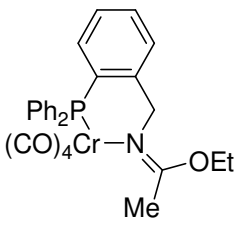

10a

Complex 10a. Following the general procedure, from 517 mg (1.96 mmol) of complex **9**[15] and 742 mg (1.96 mmol) of imine **8a** in 30 mL of hexane-benzene (1:1) were obtained after purification by flash column chromatography 549 mg (53 %) of complex **10a** as a yellow solid. ^{1}H NMR (300 MHz, $CDCl_3$): δ 1.33 (t, 3H, J = 7.0 Hz), 2.44 (s, 3H), 4.05 (q, 2H, J = 7.0 Hz), 4.36 (d, 2H, J = 3.3 Hz), 6.89 (t, 1H, J = 1.1 Hz), 7.22-7.41 (m,13H). ^{13}C NMR (75.5 MHz, $CDCl_3$): δ 14.9, 20.0, 58.4 (d, $J_{C\text{-}P}$ = 13.9 Hz), 66.0, 128.3 (d, $J_{C\text{-}P}$ = 9.1 Hz), 128.5, 129.6, 130.1, 130.5 (d, $J_{C\text{-}P}$ = 7.5 Hz), 132.8, 132.9 (d, $J_{C\text{-}P}$ = 11.0 Hz), 134.9 (d, $J_{C\text{-}P}$ = 35.7 Hz), 143.2 (d, $J_{C\text{-}P}$ = 17.5 Hz), 166.3, 219.0 (d, $J_{C\text{-}P}$ = 12.3 Hz), 227.0 (d, $J_{C\text{-}P}$ = 1.9 Hz), 227.2 (d, $J_{C\text{-}P}$ = 14.7 Hz). IR (KBr): ν 2009, 1900, 1886, 1852 cm^{-1}. $C_{27}H_{24}CrNO_5P$ Calcd C 61.72, H 4.60, N, 2.67. Found C 61.95, H 4.48, N 2.49.

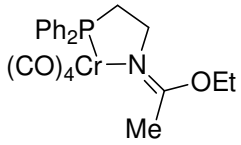

10b

Phosphine-imidate Complex 10b. Compound **10b** was obtained by reaction of Fischer carbene complex **9** with imines **8b**, **8d** and **8e** as specified bellow:

*From imine **8b***: Following the general procedure, from 278 mg (1.05 mmol) of complex **9** and 335 mg (1.05 mmol) of imine **8b** in 20 mL of hexane-benzene (1:1). Complex **10b** (294 mg, 60 %) was obtained as an orange solid. ^{1}H NMR (300 MHz, $CDCl_3$): δ 1.26 (t, 3H, J = 7.0 Hz), 2.25 (m, 2H), 2.45 (s, 3H), 3.53 (m, 1H), 3.61 (m, 1H), 4.03 (q, 2H, J = 7.0 Hz), 7.32-7.38 (m, 6H), 7.55-7.63 (m, 4H). ^{13}C NMR (75.5 MHz, $CDCl_3$): δ 14.7, 20.7, 29.0 (d, $J_{C\text{-}P}$ = 16.8 Hz), 48.2 (d, $J_{C\text{-}P}$ = 9.4 Hz), 65.8, 128.5 (d, $J_{C\text{-}P}$ = 9.1 Hz), 129.6 (d, $J_{C\text{-}P}$ = 0.7 Hz), 131.5 (d, $J_{C\text{-}P}$ = 11.1 Hz), 136.7 (d, $J_{C\text{-}P}$ = 34.7 Hz), 165.8 (d, $J_{C\text{-}P}$ = 2.3 Hz), 219.2 (d, $J_{C\text{-}P}$ = 14.3 Hz), 227.8 (d, $J_{C\text{-}P}$ = 2.0 Hz), 229.1 (d, $J_{C\text{-}P}$ = 14.7 Hz). IR (KBr): ν 2004, 1871, 1834, 1624 cm^{-1}. $C_{22}H_{22}CrNO_5P$ Calcd C 57.02, H 4.79, N 3.02. Found C 56.87, H 4.90, N 3.21.
*From imine **8d***: Following the general procedure, from 137 mg (0.52 mmol) of complex **9** and 188 mg (0.52 mmol) of imine **8d** in 9 mL of hexane-benzene (1:1). Complex **10b** (131 mg, 54 %) was obtained as an orange solid.
*From imine **8e***: Following the general procedure, from 173 mg (0.65 mmol) of complex **9** and 230 mg (0.65 mmol) of imine **8e** in 12 mL of hexane-benzene (1:1). Complex **10b** (139 mg, 46 %) was obtained after purification by flash column chromatography on silica-gel.

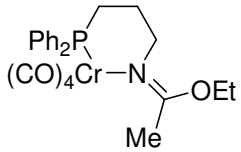

10c

[15] Hegedus, L. S.; McGuire, M. A.; Schultze, L. M. *Organic Syntheses*; Wiley: New York, Collect. Vol. VIII, p 217.

Complex 10c. Following the general procedure, from 526 mg (1.99 mmol) of complex **9**, and 660 mg (1.99 mmol) of imine **8c** in 30 mL of hexane-benzene (1:1). Complex **10c** (148 mg, 16 %) was obtained as an orange solid together with 40 mg (6%) of [pentacarbonyl(ethoxystyryl)carbene]chromium(0).[10] ^{1}H NMR (300 MHz, $CDCl_3$): δ 1.30 (t, 3H, J = 7.0 Hz), 1.50 (m, 2H), 2.29 (m, 2H), 2.43 (s,3H), 3.33 (m, 2H), 4.01 (q, 2H, J = 7.0 Hz), 7.31-7.45 (m,10H). ^{13}C NMR (75.5 MHz, $CDCl_3$): δ 14.4, 23.6, 23.6, 29.6 (d, $J_{C\text{-}P}$ = 20.2 Hz), 40.4 (d, $J_{C\text{-}P}$ = 14.7 Hz), 65.9, 128.4 (d, $J_{C\text{-}P}$ = 8.6 Hz), 129.6 (d, $J_{C\text{-}P}$ = 1.8 Hz), 131.7 (d, $J_{C\text{-}P}$ = 10.4 Hz), 136.9 (d, $J_{C\text{-}P}$ = 31.9 Hz), 167.2, 221.3 (d, $J_{C\text{-}P}$ = 14.7 Hz), 225.6 (d, $J_{C\text{-}P}$ = 5.5 Hz), 230.8 (d, $J_{C\text{-}P}$ = 12.9 Hz). IR (CCl_4): ν 2008, 1925, 1890 cm^{-1}. $C_{23}H_{24}CrNO_5P$ Calcd C 57.86, H 5.07, N 2.93. Found C 57.62, H 5.18, N 3.09.

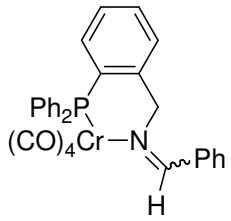

12a

Complex 12a. Following the general procedure, from 344 mg (1.05 mmol) of complex **11**[16] and 300 mg (0.48 mmol) of imine **8a** in 20 mL of hexane-benzene (1:1) and after chromatography on silica gel, 71 mg (12 %) of *anti*-**12a** and 65 mg (11%) of *syn*-**12a** were obtained as orange solids. **Complex 12a** (*anti* isomer): ^{1}H NMR (300 MHz, $CDCl_3$): δ 4.60 (s, 2H), 6.74 (m, 1H), 6.88 (m, 2H), 7.09-7.41 (m, 16H), 9.05 (s, 1H). ^{13}C NMR (75.5 MHz, $CDCl_3$): δ 62.6 (d, $J_{C\text{-}P}$ = 9.7 Hz), 127.3, 128.5 (d, $J_{C\text{-}P}$ = 9.1 Hz), 128.8, 129.0 (d, $J_{C\text{-}P}$ = 4.5 Hz), 129.8, 130.1, 130.3, 130.7, 131.1, 132.7, 133.0 (d, $J_{C\text{-}P}$ = 11.3 Hz), 134.5 (d, $J_{C\text{-}P}$ = 36.0 Hz), 141.5 (d, $J_{C\text{-}P}$ = 17.5 Hz), 172.4 (d, $J_{C\text{-}P}$ = 4.2 Hz), 219.6 (d, $J_{C\text{-}P}$ = 12.8 Hz), 225.9, 227.3 (d, $J_{C\text{-}P}$ = 13.9 Hz). IR (KBr): ν 2006, 1882, 1846 cm^{-1}. $C_{30}H_{22}CrNO_4P$ Calcd C 66.30, H 4.08, N 2.58. Found C 66.51, H 4.21, N 2.71. **Complex 12a** (*syn* isomer): ^{1}H NMR (300 MHz, $CDCl_3$): δ 4.80 (d, 2H, J = 2.3 Hz), 6.93 (m, 1H), 7.21-7.42 (m,18H), 8.80 (s, 1H). ^{13}C NMR (75.5 MHz, $CDCl_3$): δ 76.3 (d, $J_{C\text{-}P}$ = 12.5 Hz), 128.1, 128.4, 128.5 (d, $J_{C\text{-}P}$ = 9.2 Hz), 129.2 (d, $J_{C\text{-}P}$ = 3.7 Hz), 129.8, 130.4, 130.8, 130.9, 132.3, 133.0 (d, $J_{C\text{-}P}$ = 11.1 Hz), 134.4 (d, $J_{C\text{-}P}$ = 36.0 Hz), 136.2, 141.9 (d, $J_{C\text{-}P}$ = 18.2 Hz), 174.5 (d, $J_{C\text{-}P}$ = 2.1 Hz), 219.1 (d, $J_{C\text{-}P}$ = 12.7 Hz), 224.5 (d, $J_{C\text{-}P}$ = 1.8 Hz), 227.6 (d, $J_{C\text{-}P}$ = 14.5 Hz). IR (KBr): ν 2004, 1880, 1844 cm^{-1}. $C_{30}H_{22}CrNO_4P$ Calcd C 66.30, H 4.08, N 2.58. Found C 66.44, H 4.23, N 2.63.

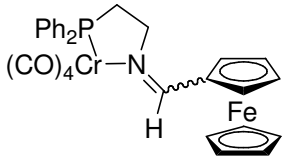

12b

[16] (a) Fischer, E. O.; Maasböl, A. *J. Organomet. Chem.* **1968**, *12*, P15. (b) Aumam, R.; Fischer, E. O. *Chem. Ber.* **1968**, *101*, 954.

Complex 12b. Following the general procedure, from 205 mg (0.78 mmol) of complex **9** and 330 mg (0.78 mmol) of imine **8g** in 13 mL of hexane-benzene (1:1). After chromatography on silica-gel 142 mg (31 %) of *anti*-**12b** and 79 mg (17%) of *syn*-**12b** were obtained as orange solids. Complex **12b** (*anti*-isomer): ^{1}H NMR (300 MHz, acetone-d_6): δ 2.66 (m, 2H), 3.63 (m, 1H), 3.71 (m, 1H), 4.20 (s, 5H), 4.50 (t, 2H, J = 1.9 Hz), 4.71 (t, 2H, J = 1.9 Hz), 7.33-7.38 (m,6H), 7.66-7.73 (m, 4H), 8.61 (s, 1H). ^{13}C NMR (75.5 MHz, $CDCl_3$): δ 30.7 (d, J_{C-P} = 16.7 Hz), 53.7 (d, J_{C-P} = 8.3 Hz), 69.7, 71.4, 72.2, 76.6, 128.7 (d, J_{C-P} = 9.1 Hz), 129.8, 131.6 (d, J_{C-P} = 11.6 Hz), 136.0 (d, J_{C-P} = 34.3 Hz), 168.9, 219.9 (d, J_{C-P} = 14.1 Hz), 227.4, 229.3 (d, J_{C-P} = 12.9 Hz). IR (KBr): ν 2002, 1877, 1830, 1608 cm-1. $C_{29}H_{24}CrFeNO_4P$ Calcd C 59.10, H 4.10, N 2.38. Found C 59.26, H 3.95, N 2.51. Complex **12b** (*syn*-isomer): ^{1}H NMR (300 MHz, $CDCl_3$): δ 2.45 (m, 2H), 3.71 (m, 1H), 3.80 (m, 1H), 4.13 (s, 5H), 4.52 (t, 2H, J = 1.9 Hz), 5.03 (t, 2H, J = 1.9 Hz), 7.35-7.37 (m, 6H), 7.58-7.64 (m, 4H), 8.40 (s, 1H). ^{13}C NMR (75.5 MHz, $CDCl_3$): δ 29.6 (d, = 16.2 Hz), 68.5 (d, J_{C-P} = 8.3 Hz), 69.8, 72.1, 72.2, 76.9, 128.7 (d, J_{C-P} = 8.8 Hz), 129.8 (d, J_{C-P} = 1.6 Hz), 131.5 (d, J_{C-P} = 11.1 Hz), 136.4 (d, J_{C-P} = 35.2 Hz), 171.7, 219.4 (d, J_{C-P} = 14.3 Hz), 227.3 (d, J_{C-P} = 2.7 Hz), 229.1 (d, J_{C-P} = 14.3 Hz). IR (KBr): ν 2004, 1878, 1834, 1618 cm^{-1}. $C_{29}H_{24}CrFeNO_4P$ Calcd C 59.10, H 4.10, N 2.38. Found C 59.01, H 3.98, N 2.43.

1.4. ESI Mass Spectrometry as a Tool for the Study of Electron Transfer in Nonconventional Media: The Case of Bi- and Polymetallic Carbene Complexes

1.4. ESI Mass Spectrometry as a Tool for the Study of Electron Transfer in Nonconventional Media: The Case of Bi- and Polymetallic Carbene Complexes

1.4.1. Introduction

Electron transfer (ET) processes are essential in chemistry, biology, physics,[1] and the emerging field of molecular electronics[2] and play a pivotal role in processes that have tremendous relevance to our life such as photosynthesis and respiration.[3,4] The electron transfer between a donor (D) and an acceptor (A) can be induced by chemical, electrochemical, or photochemical methods.[1,4] During the past decade, a considerable effort has been invested in determining the factors that control such processes, both from theoretical and experimental explorations. The understanding of ET processes can be done in light of Marcus theory,[5] which since was postulated, has been applied to a multitude of systems and it is still the subject of revision.[6]

Possibly, the most deeply studied ET processes are those involving the intramolecular electronic interactions between a donor (D) and an acceptor (A). The dependence of the ET dynamics on the nature of D and A and their relative separation and orientation have been thoroughly discussed. In fact, there is still a debate regarding the extent to which the intramolecular ET processes occur by a through-bond[7,8] or a through-space (solvent mediated)[9,10] mechanism (eqs 1 and 2 in Figure 1 respectively).

---

[1] (a) *Electron Transfer in Chemistry*; Balzani, V., Ed.; Wiley-VCH: Weinheim, 2001; Vols. 1-5. (b) Marcus, R. A.; Sutin, N. *Biochim. Biophys. Acta* **1985**, *811*, 265. (c) Marcus, R. A. *Rev. Mod. Phys.* **1993**, *65*, 599. (d) Barbara, P. F.; Meyer, T. J.; Ratner, M. A. *J. Phys. Chem*. **1996**, *100*, 13148. (e) See also the item dedicated to Electron Transfer, *Chem. Rev*. **1992**, *92*, 365.

[2] (a) Alivisatos, A. P.; Barbara, P. F.; Castleman, A. W.; Chang, J.; Dixon, D. A.; Klein, M. L.; McLendon, G. L.; Miller, J. S.; Ratner, M. A.; Rossky, P. J.; Stupp, S. I.; Thompson, M. E. *Adv. Mater.* **1998**, *10*, 1297. (b) Ratner, M. A.; Jortner J. in *Molecular Electronics: Some Directions;* Ratner, M. A.; Jortner, J., Eds.; IUPAC 1997.

[3] (a) *Anoxigenic Photosynthetic Bacteria*; Blankenship, R. E.; Madigan, M. T.; Bauer, C. E., Eds.; Kluwer Academic Publishing: Dordrecht, **1995**. (b) Armstrong, F. A.; Kaim, W.; Schwederski, B. *Bioinorganic Chemistry: Inorganic Chemistry in the Chemistry of Life*, Oxford University, UK, 1995. (c) Kochi, J. K. *Acc. Chem. Res*. **1992**, *25*, 39. (d) Rathore, R.; Kochi, J. K. *Adv. Phys. Org. Chem.* **2000**, *35*, 193

[4] (a) Fukuzumi, S. in *Advances in Electron-Transfer Chemistry*; Mariano P. S., Ed.; JAI Press, Greenwich, CT, **1992**, pp. 67-175. (b) Fukuzumi, S.; Tanaka T. in *Photoinduced Electron Transfer*; Fox, M. A.; Chanon M., Eds.; Elsevier, Amsterdam, 1998, Part C, Chapter 10.

[5] (a) Marcus, R. A. *J. Chem. Phys.* **1956**, *24*, 966. (b) Marcus, R. A. *J. Chem. Phys.* **1956**, *24*, 979. (c) Marcus, R. A. *Annu. Rev. Phys. Chem*. **1964**, *15*, 155. (d) Marcus, R. A. *Angew. Chem. Int. Ed.* **1993**, *32*, 1111.

[6] (a) Small, D. W.; Matyushov, D. V.; Voth, G. A. *J. Am. Chem. Soc.* **2003**, *125*, 7470.(b) Hartnig, C.; Koper, M. T. M. *J. Am. Chem. Soc.* **2003**, *125*, 9840.

[7] (a) Johnson, R. C.; Hupp, J. T. *J. Am. Chem. Soc.* **2001**, *123*, 2053. (b) Closs, G. L.; Miller, J. R. *Science* **1988**, 240, 440. (c) Closs, G. L.; Johnson, M. D.; Miller, J. R.; Piotrowiak, P. *J. Am. Chem. Soc.* **1989**, *111*, 3751.

[8] For the effect of hydrogen bonds in electron transfer reactions see: (a) Fukuzumi, S.; Okamoto, K.; Yoshida, Y.; Imahori, H.; Araki, Y.; Ito, O. *J. Am. Chem. Soc.* **2003**, *125*, 1007. (b) Smitha, M. A.;

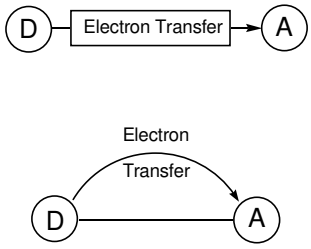

Figure 1

The chemistry of stabilized group 6 Fischer carbene complexes has reached a high level of maturity and these compounds have become very valuable building blocks in organic synthesis.[11] Despite this, studies of electron transfer processes involving this class of compounds are scarce. There are some reports about the behavior of chromium(0) and tungsten(0) Fischer carbene complexes in electron transfer processes chemically induced by Na/K alloy,[12] potassium 1-methylnaphthalenide,[13] SmI_2,[14] or potassium graphite (C_8K).[15] More recently, our research group has focused its interest on the study of ET reactions involving group 6 Fischer carbene complexes using other less conventional sources of electrons such as the electrospray ionization in mass spectrometry (ESI-MS).[16] ESI is a technique that allows the transfer of ions from solution to the gas phase as isolated entities, and these ions can be subjected to mass spectrometric analysis. There are three major steps in the production of ESI ions: first,

---

Prasad, E.; Gopidas, K. R. *J. Am. Chem. Soc.* **2001**, *123*, 1159. (c) Prasad, E.;. Gopidas, K. R *J. Am. Chem. Soc.* **2000**, *122*, 3191.

[9] (a) Arimura, T.; Ide, S.; Suga, Y.; Nishioka, T.; Murata, S.; Tachiya, M.; Nagamura, T.; Inoue, H. *J. Am. Chem. Soc.* **2001**, *123*, 10744. (b) Bell, T. D. M.; Jolliffe, K. A.; Ghiggino, K. P.; Oliver, A. M.; Shephard, M. J.; Langford, S. J.; Paddon-Row, M. N. *J. Am. Chem. Soc.* **2000**, *122*, 10661 and references therein.

[10] (a) Reek, J. N.; Rpowan, A. E.; de Gelder, R.; Beurskens, P. T.; Crossley, M. J.; de Feyter, S.; de Schryver, F.; Nolte, R. J. M. *Angew. Chem. Int. Ed.* **1997**, *36*, 361. (b) Hunter, C. A.; Hyde, R. K. *Angew. Chem. Int. Ed.* **1996**, *35*, 1936.

[11] Selected reviews on the chemistry of metal carbene (Fischer) complexes: (a) Dötz, K. H.; Fischer, H.; Hofmann, P.; Kreissel, F. R.; Schubert, U.; Weiss, K. *Transition Metal Carbene Complexes*, Verlag Chemie, Deerfield Beach, Florida, 1983. (b) Dötz, K. H. *Angew. Chem. Int. Ed. Eng.* **1984**, *23*, 587. (c) Wulff, W. D. in *Comprehensive Organic Synthesis, Vol. 5*; Trost, B. M.; Fleming, I., Eds.; Pergamon, Oxford, **1991**, p. 1065. (d) Hegedus, L. S. in *Comprehensive Organometallic Chemistry II, Vol. 12*; Abel, E. W.; Stone, F. G. A.; Wilkinson, G.; Pergamon, Oxford, 1995, p. 549. (e) Harvey, D. F.; Sigano, D. M. *Chem. Rev.* **1996**, *96*, 271. (f) Barluenga, J.; Fañanás, F. J. *Tetrahedron* **2000**, *56*, 4597. (g) Sierra, M. A. *Chem. Rev.* **2000**, *100*, 3591.

[12] Krusic, P. J.; Klabunde, U.; Casey, C. P.; Block, T. F. *J. Am. Chem. Soc.* **1976**, *98*, 2015.

[13] Lee, S.; Cooper, N. J. *J. Am. Chem. Soc.* **1990**, *112*, 9419.

[14] (a) Fuchibe, K.; Iwasawa, N. *Org. Lett.* **2000**, *2*, 3297. (b) Fuchibe, K.; Iwasawa, N. *Chem. Eur. J.* **2003**, *9*, 905.

[15] Sierra, M. A.; Ramírez-López, P.; Gómez-Gallego, M.; Lejon, T.; Mancheño, M. J. *Angew. Chem. Int. Ed.* **2002**, *41*, 3442.

[16] (a) Van Berkel, G. J., Electrospray Ionization Mass Spectrometry, Wiley, New York, 1997. For a recent article about the use of ESI-MS in the detection of reactive intermediates see: (b) Meyer, S.; Koch, R.; Metzger, J. O. *Angew. Chem. Int. Ed.* **2003**, *42*, 4700.

the production of charged droplets at the ES capillary; second, shrinkage of charged droplets (by the high voltage applied), leading to very small highly charged droplets and the last step where gas-phase ions are produced from the very small charged droplets. The last step of this general mechanism has proven to be very difficult to establish.[16,17]

We have recently reported that chromium and tungsten Fischer carbene complexes cannot be ionized under routine ESI conditions. Variations of the ionization potential, flow solution rate and solvent system (fundamental parameters of this technique) did not produce significant changes in the process. However, we found that the ESI-MS ionization of carbene complexes **1** and **2** (Figure 2) took place by addition of an electron donor such as hydroquinone (HQ) or tetrathiafulvalene (TTF) to the carbene solution.[18]

1 **2**

M = Cr, W
Ar = Ph, 2-furyl, 2-thienyl

Figure 2

The proposed mechanism for the ESI ionization process involves the capture of an electron by the addition of HQ or TTF at the surface of the capillary. The species $HQ^{\bullet -}$ or $TTF^{\bullet -}$ promotes the formation of a carbene radical anion, which loses a hydrogen radical to form the detected $[M-H]^-$ ions (Scheme 1). It is important to note that this reaction takes place only on the surface of the capillary during the ESI experiment and that no reaction is observed in solution when mixing carbenes **1** and **2** with the additives. As only conjugated carbene complexes **1** and **2** were ionized in the presence of HQ or TTF, we proposed that the stabilization of the intermediate radical anions produced by the conjugation of the carbene moiety with the aromatic rings is essential for the formation of such entities and hence for their subsequent detection by MS. Thus, pentacarbonyl[(ethoxy)(phenyl)carbene]chromium(0) did not ionize even in the presence of external additives. Although other compounds known as electron acceptors have been tested as additives (TCNQ, Toluidine Blue O), they were

[17] (a) Gaskell, S. J. *J. Mass. Spectrom.* **1997**, *32*, 677. (b) Kebarle, P. *J. Mass. Spectrom.* **2000**, *35*, 804.
[18] Sierra, M. A.; Gómez-Gallego, M.; Mancheño, M. J.; Martínez-Álvarez, R.; Ramírez-López, P.; Kayali, N.; González, A. *J. Mass. Spectrom.* **2003**, *38*, 151.

ineffective in promoting the ionization process. It seems that under ESI conditions HQ and TTF (both electron donors) can be forced to accept an electron, leading to a highly reductive species that is responsible for the ET to the carbene complex.[19]

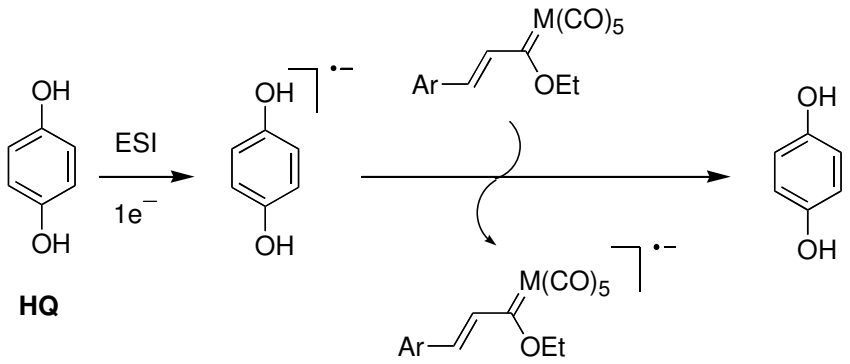

Scheme 1

In this context, we were interested in studying the ESI-induced electron transfer reactions in group 6 Fischer carbene complexes that incorporate in their structures an extra metallic center. This study will allow us to determine the participation of the two metals in intramolecular ET reactions under ESI-MS conditions, as well as the influence of the spacer between the two metallic moieties in the process. For the study, we have selected a series of bimetallic complexes **3-10**, with different spacers linking the two metals (M and M') (Figure 3). To establish the role of the metal in the intramolecular ET process, compounds **3-10** incorporate different metallic moieties. Thus, complexes **3-5** include in their structures a ferrocene, a well-known donor in electron transfer reactions.[20] The possible interaction between the two $M(CO)_5$ moieties (M = Cr, W) will be established in biscarbenes **6-8**, and finally, compounds **9** and **10** incorporate the good electron acceptor $Co_2(CO)_6$ moiety.

[19] For an example in which a good-electron acceptor compound is forced to behave as an electron donor see: Redd, C. A.; Kim, K. C.; Bolskar, R. D.; Mueller, L. J. *Science,* **2000**, *289*, 101.
[20] (a) Okamoto, K.; Imahori, H.; Fukuzumi, S. *J. Am. Chem. Soc.* **2003**, *125*, 7014. (b) Long, Y.-T.; Li, C.-Z.; Sutherland, T. C.; Chahma, M., Lee, J. S.; Kraatz, H. B. *J. Am. Chem. Soc.* **2003**, *125*, 8724. (c) Fukuzumi, S.; Yoshida, Y.; Okamoto, K.; Imahori, H.; Araki, Y.; Ito, O. *J. Am. Chem. Soc.* **2002**, *124*, 6794. (d) Creager, S.; Yu, C. J.; Bamdad, C.; O'Connor, S.; MacLean, T.; Lam, E.; Chong, Y.; Olsen, G. T.; Luo, J.; Gozin, M.; Kayyem, J. F. *J. Am. Chem. Soc.* **1999**, *121*, 1059.

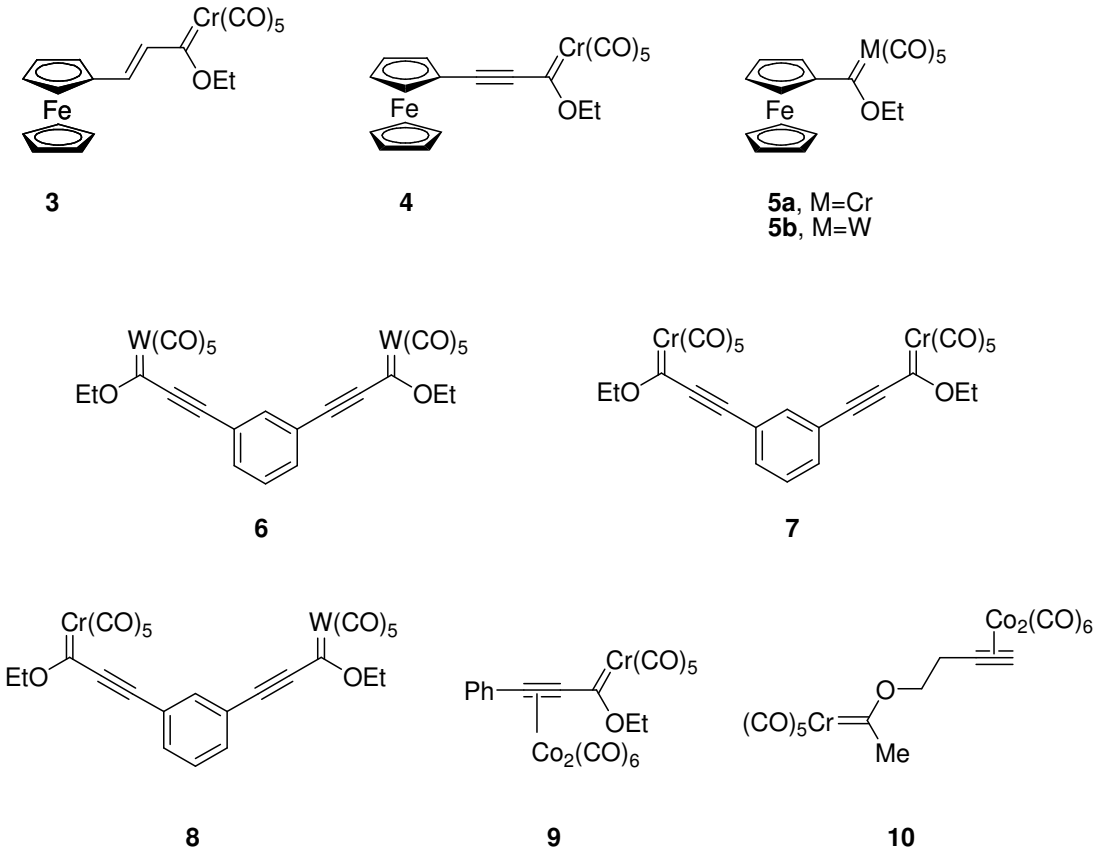

Figure 3

1.4.2. Results and Discussion

First we checked the behavior of ferrocenyl carbene complexes **3-5**. Solutions of carbene complexes **3** and **4** were directly sprayed under routine ESI conditions, and the corresponding quasimolecular ions $[M-H]^-$ or $[(M-H)-CO]^-$ were detected respectively in the mass spectra. The formation of quasimolecular ions of different compositions is a well-known process that is influenced by many factors such as the facility to form adducts with the solvent or the ability to lose ligands. Moreover, ligand fragmentation and ligand oxidation are also observed processes in the ESI of organometallic compounds, and it is not rare that structurally related compounds could lead to different quasimolecular ions. The ESI mass spectrum of **4** is displayed in Figure 4. The quasimolecular ions were also detected when the ESI-MS of **3** and **4** were done in the presence of HQ or TTF. These results contrast with those previously observed for the structurally related compounds **1** and **2** (Figure 2), which only could be ionized, and hence their mass spectra recorded, in the presence of HQ or TTF as additive.[18]

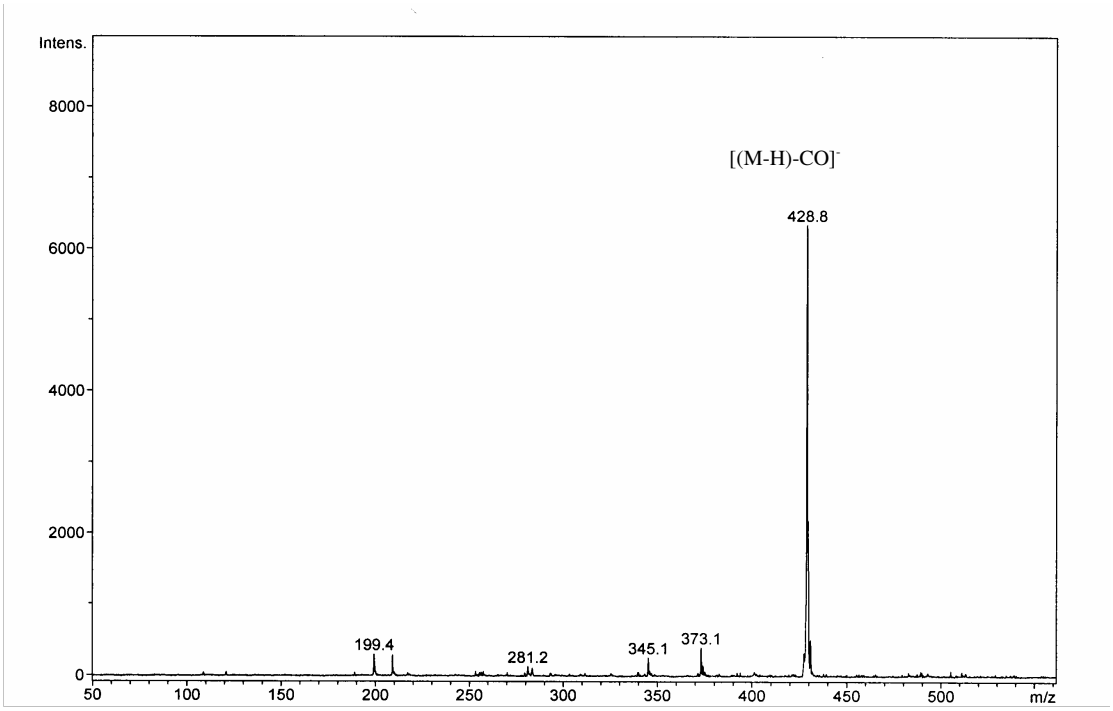

Figure 4. ESI mass spectrum of complex **4** showing the quasimolecular ion $[(M-H)-CO]^-$, (*m/z* 429).

A reasonable explanation to understand why compounds **3** and **4** do not need an additive to be ionized in the ESI source could be based on the ability of such complexes towards reduction. The reduction potentials of compounds **1-5** are summarized in Table 1. The comparison between the E_{pc} values of the different phenyl and ferrocenyl α,β-unsaturated carbene complexes displayed in Table 1 does not justify why carbenes **3** and **4** ionize directly under ESI conditions whereas their phenyl counterparts **1** and **2** require an additive for the ionization. Compounds **3** and **4** are push-pull complexes[21] in which the ferrocene is the donor and the $Cr(CO)_5$ group behaves like a large electron-depleted group since the five CO ligands are strong π-acceptors. It seems clear that during the ESI process the role of the ferrocene moiety in **3** and **4** is not just being a substituent conjugated with the metal carbene fragment. Ferrocene is a good electron donor that could be playing the same role as HQ or TTF in the ESI process (see above). In fact it could be considered as an *internal electron carrier* that makes possible the direct formation of the carbene radical anion in the ESI source (Scheme 2).

[21]Jayaprakash, K. N.; Ray, P. C.; Matsuoka, I.; Bhadbhade, M. M.; Puranik, V. G.; Das, P. K.; Nishihara, H., Sarkar, A. *Organometallics*, **1999**, *18*, 3851.

Table 1. Cyclic voltammograms in 0.1 M Bu_4NClO_4/CH_2Cl_2 at a scan rate of 0.1 V/s at 25 ^{0}C.

Compound	1st E_{pc}	2nd E_{pc}
1[b]	-1.25	
2[b]	-1.15	
3[c]	-1.22	
4	-1.29	
5a	-1.71	
5b	-1.61	
6	-0.92	-1.19
7	-0.99	-1.26
8	-1.00	-1.29

[b] See ref. 18
[c] See ref. 21

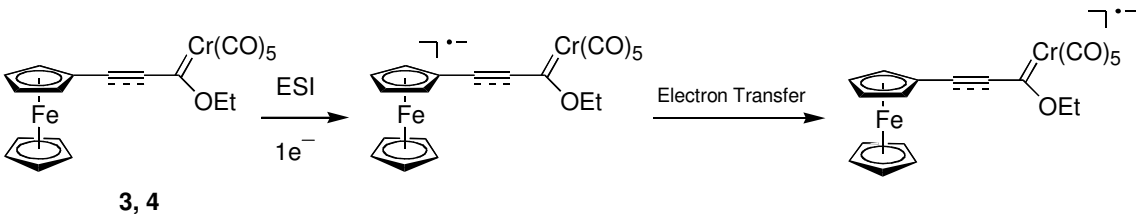

3, 4

Scheme 2

To evaluate the influence of the conjugation between the two metal centers in the ET process, nonconjugated carbene complex **5a** (M = Cr) was studied next. In this case, the direct electrospray ionization did not take place, but the quasimolecular ion $[(M-H)-CO]^-$ could be detected when HQ or TTF were added (Figure 5). Identical results were obtained when the experiments were carried out with **5b** (M = W). Again, the presence of a ferrocene moiety provokes a dramatic change on the behaviour of the carbene complexes **5** in ESI-MS, as their phenyl counterpart (pentacarbonyl[(ethoxy)(phenyl)carbene]chromium(0), E_{pc} = -1.78 V)[18] cannot be ionized even in the presence of additives.

a)

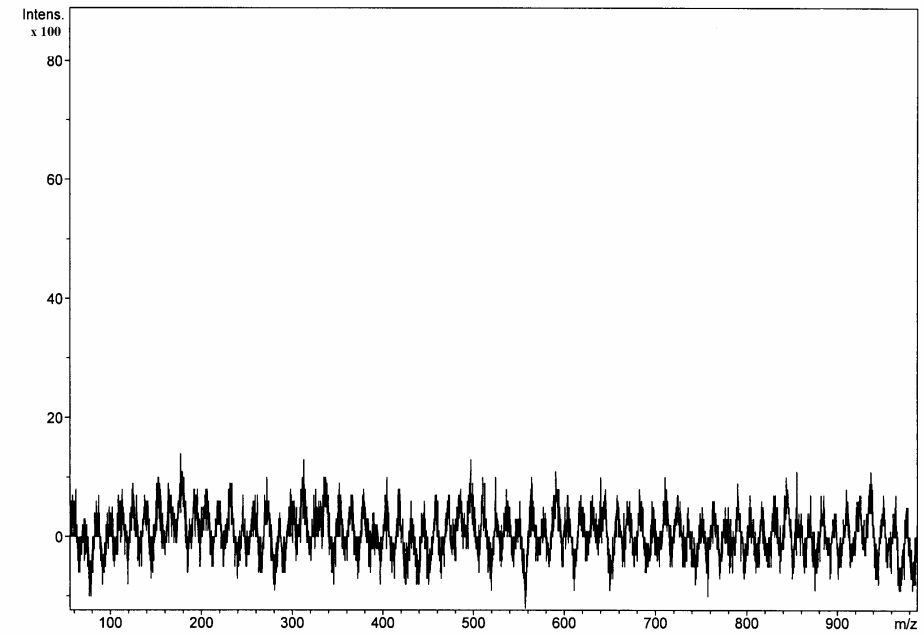

b)

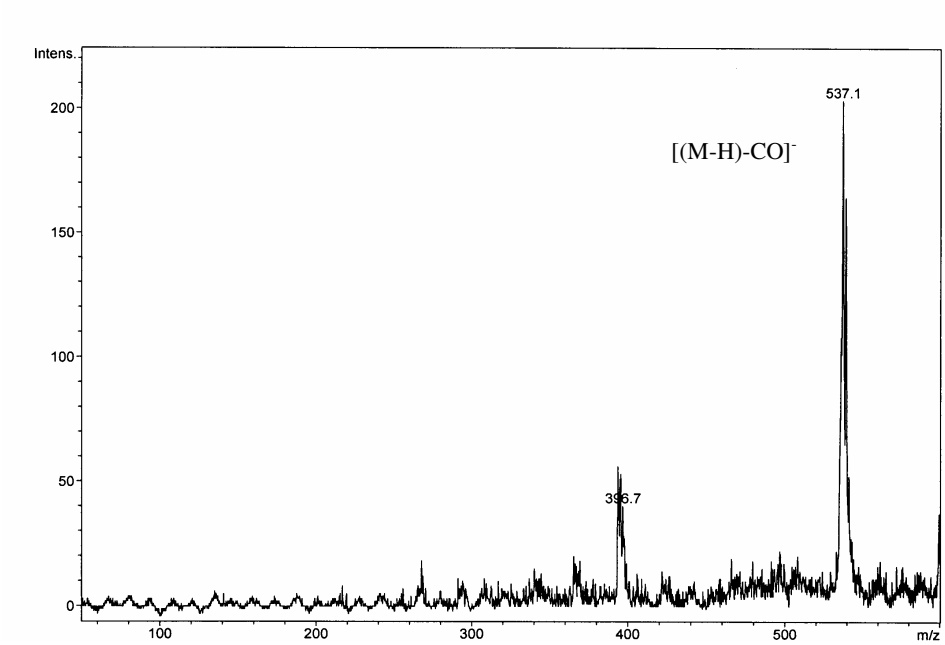

Figure 5. a) ESI mass spectrum of complex **5b**. Neither molecular peak nor fragments were observed. b) ESI mass spectrum of complex **5b** after addition of HQ showing the quasimolecular ion $[(M-H)-CO]^-$ (*m/z* 537) and a fragment at *m/z* 397.

The results obtained for compounds **5a**,**b** show that the ferrocene moiety is essential for the ESI-MS ionization process, but only when the ferrocenyl and the $Cr(CO)_5$ moieties are linked by a π-system is the efficient direct ET from the ESI source observed.

Once the ESI-MS spectra of ferrocenyl carbene complexes **3-5** were recorded, the corresponding quasimolecular ions were isolated and their fragmentations studied by the collision-induced dissociation (CID) technique. All of them undergo in the first fragmentation stage (MS^2) a double simultaneous decarbonylation process. This simultaneous removal of two CO ligands has been observed in organometallic complexes only in exceptional cases in electron-impact mass spectrometry (EI)[22]and was previously detected by us in ESI-MS for carbene complexes **1** and **2**.[18] The MS^3 fragmentation stage leads to a new monodecarbonylation process, and compound **3** also exhibits at this stage the loss of a cyclopentadiene molecule.

The behavior of compounds having two $M(CO)_5$ moieties (M = Cr, W) in ESI-MS conditions was studied next. Thus, biscarbenes **6**, **7** and **8** were obtained and their ESI mass spectra recorded. In all cases the direct ionization failed and the expected quasimolecular ions $[M-H]^-$ or $[(M-H)-CO]^-$ could only be detected in the presence of additives (HQ or TTF) (Figure 6). Therefore, biscarbenes **6-8** behave in ESI-MS like the parent monocarbene **2** (Scheme 3).

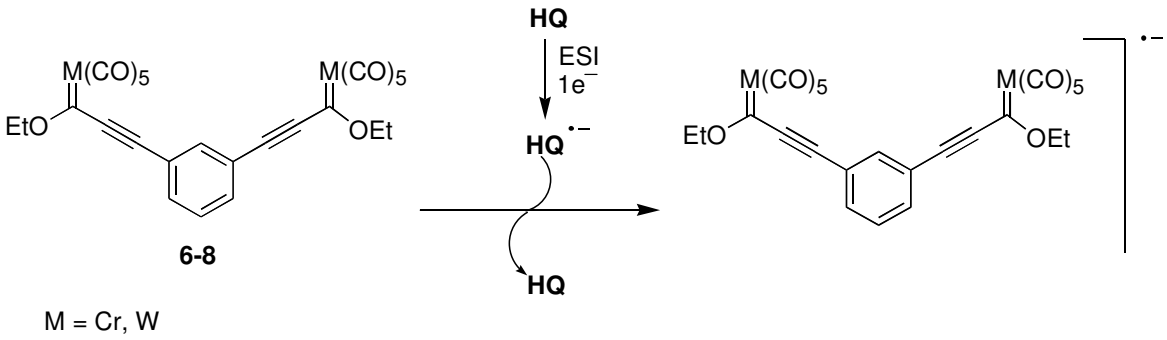

Scheme 3

[22] (a) Müller, J. *Angew. Chem. Int. Ed.* **1972**, *11*, 653. (b) Neidlein, R.; Gürtlen, S.; Krieger, C. *Helv. Chim. Acta*, **1994**, *77*, 2303.

a)

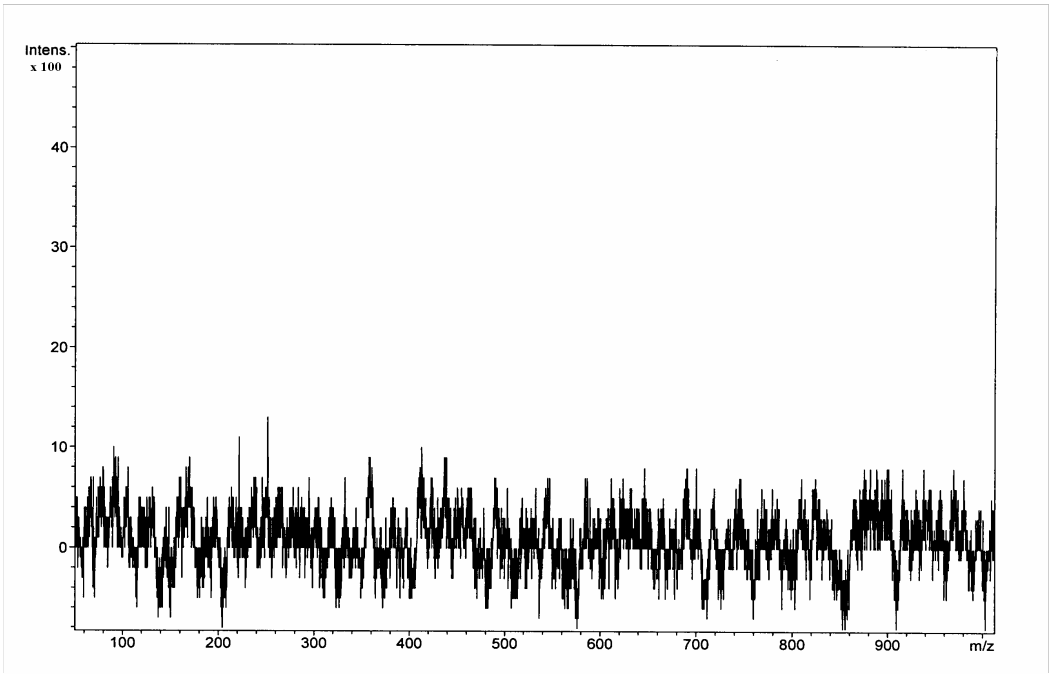

b)

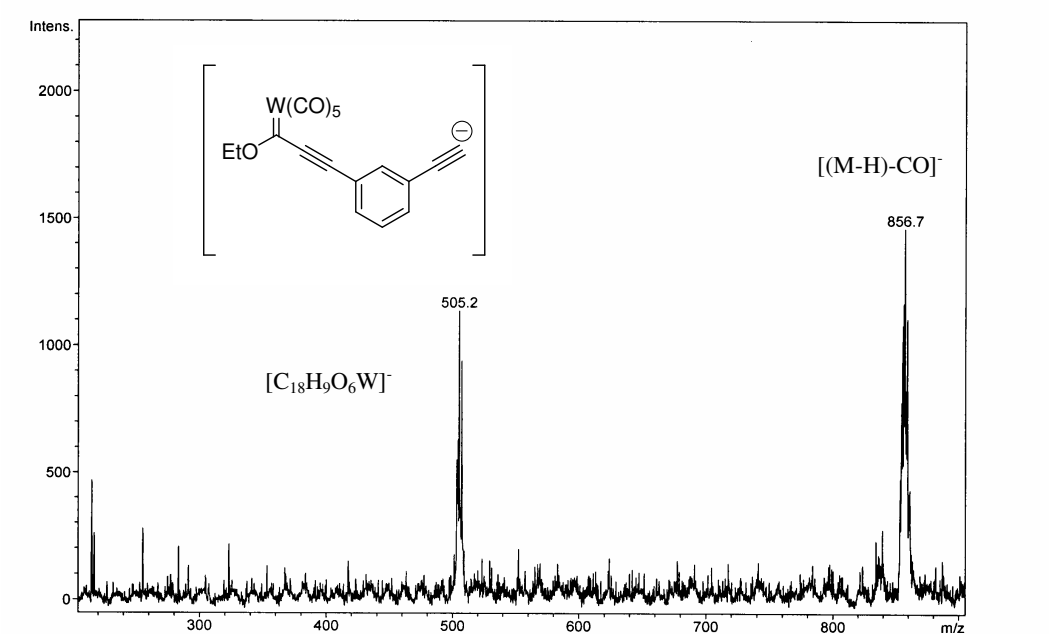

Figure 6. a) ESI mass spectrum of biscarbene **6**. Neither molecular peak nor fragments were observed. b) ESI mass spectrum of biscarbene **6** with HQ as additive, showing the quasimolecular ion $[(M-H)-CO]^-$ (*m/z* 857) and a fragment at *m/z* 505.

Spectroscopic studies on polymetallic π-bridged carbene complexes of the type M-π-M'-π-M'' suggested only a weak interaction between the carbene fragments and the central metal nucleus.[23] Similar conclusions were obtained for π-conjugated bisaminocarbene complexes, whereas π-bridged alkoxy amino biscarbene complexes

[23] Hartbaum, C.; Roth, G.; Fischer, H. *Eur. J. Inorg. Chem.* **1998**, 191.

showed a significant interaction between the two metallic fragments through the bridge.[24] The electrochemical properties of biscarbenes **6-8** are summarized in Table 1, and their cyclic voltammograms are included as Supporting Material.

The ESI-MS spectra of bimetallic complexes **6** and **7** reveal similar $[(M-H)-CO]^-$ quasimolecular ions whereas **8** leads to $[(M+CH_3OH-H) - 2CO]^-$ ion under the same conditions. However, the differences in the composition of quasimolecular ions are not induced by metallic interactions and can be assumed considering the stability of the different adducts formed in the gas phase reactions.[17,25] The observation of ions attributable to noncovalently bonded species only suggests the existence of associations between analyte and solvent. The species that appear in the mass spectra are not necessarily present in solution, and is also known that in some cases the effect of gas-phase proton transfer reaction can explain the formation of the different adducts.[25] The MS^2 spectra of biscarbenes **6, 7** and **8** reveal the formation of alkynyl monocarbene ions $[C_{18}H_9O_6M]^-$ which seem to be originated by the loss of an alkoxycarbene moiety. This fragmentation is independent of the nature of the metal (Cr or W) in symmetrical biscarbenes **6** and **7**, but two different fragments of similar abundance, corresponding to the elimination of the two possible metallic moieties, were detected for mixed biscarbene **8**. The double simultaneous decarbonylation process takes place in a further stage from the $[C_{18}H_9O_6M]^-$ ions, which behave in ESI-MS like the simple alkynyl monocarbene **2**.

The effect of the incorporation of a dicobalt hexacarbonyl moiety ($Co_2(CO)_6$) in the ESI ionization of group 6 Fischer carbene complexes was studied in complex **9**, obtained by coordination of the carbon-carbon triple bond of **2** with dicobalt octacarbonyl.

It is well known that metal carbonyls are easy to reduce due to the ability of carbonyl ligands to stabilize low oxidation states.[26] Octacarbonyl dicobalt $Co_2(CO)_8$ forms $Co(CO)_4^-$ in the presence of reducing agents such as SmI_2 (THF) or borohydrides, [26b,27] and being electron rich, most reactions of $Co(CO)_4^-$ result in the cobalt being

[24] (a) Hartbaum, C.; Manz, E.; Roth, G.; Weissenbach, K.; Fischer, H. *Organometallics* **1999**, *18*, 2619. (b) Fernández, I.; Mancheño, M. J.; Gómez-Gallego, M.; Sierra, M. A. *Org. Lett*. **2003**, *5*, 1237.
[25] Amad, M. H.; Cech, N. B.; Jackson, G. S.; Enke, C. E. *J. Mass Spectrom.* **2000**, *35,* 784.
[26] (a) Bates, R. W. in *Comprehensive Organometallic Chemistry II, Vol. 12*; Abel, E. W.; Stone, F. G. A.; Wilkinson, G., Eds.; Pergamon, Oxford, 1995, pp. 349-343. (b) Sweany, R. L. in *Comprehensive Organometallic Chemistry II, Vol. 8*; Abel, E. W.; Stone, F. G. A.; Wilkinson, G., Eds.; Pergamon, Oxford, 1995, pp. 1-114.
[27] Gibson, D. H.; Ahmed, F. U.; Phillips, K. R. *J. Organomet. Chem.* **1981**, *218*, 325.

oxidized. It has been reported that the one-electron electrochemical oxidation of $Co(CO)_4^-$ is irreversible, with formation of $Co_2(CO)_8$. On the other hand, electron transfer reactions have been presumed to lead to two molecules of $Co(CO)_4$ as disproportionation products of $Co_2(CO)_8$.[28]

Considering all these precedents, the introduction of the $Co_2(CO)_6$ moiety in a group 6 Fischer carbene complex should inhibit the electrospray ionization of this compound. In fact, treatment of alkynyl cobalt complex **9** under standard ESI-MS conditions did not produced the expected $[M-H]^-$ ion, either in the presence or absence of HQ as additive. Then, it seems clear that the cobalt moiety is behaving as an *electron-sink* that inhibits any possible electron transfer to the $Cr(CO)_5$ fragment. Very likely, the $Co_2(CO)_6$ moiety is initially reduced either in the ESI source or by means of the $HQ^{\bullet -}$ and subsequently oxidized without interacting with the Cr-C bond. This fact is confirmed by the detection of a peak (*m/z* 171) corresponding to $Co(CO)_4^{\bullet -}$ in the mass spectrum.

The redox properties of carbene complex **9** were also examined. Figure 7 shows the cyclic voltammograms of alkynyl complex **2**, alkynyl cobalt complex **9** and $Co_2(CO)_8$, all in Bu_4NClO_4-CH_2Cl_2. Whereas complex **2** shows a clear irreversible reduction wave of the $Cr(CO)_5$ moiety at E_{pc} = -1.15 V, in the voltammogram of alkynyl cobalt complex **9** appear two irreversible oxidation waves at E^1_{pa} = 0.11 V and E^2_{pa} = 1.16 V, together with an irreversible reduction wave at E_{pc} = -0.79 V, all of them attributable to the cobalt moiety. These results reveal that the redox properties of complex **9** are due to the complexation of the $Co_2(CO)_8$ fragment with the C-C triple bond. This point is further supported by the electrochemical study of alkynyl complex **2** in the presence of $Co_2(CO)_8$. The voltammogram (displayed in Figure 8) shows the two-step irreversible oxidation at E^1_{pa} = 0.12 V and E^2_{pa} = 1.24 V and irreversible reduction at E_{pc} = -0.51 V of the $Co_2(CO)_8$ together with the irreversible reduction of complex **2** at E_{pc} = -1.17 V. The electrochemical data are summarized in Table 2.

[28] (a) Absi-Halabi, M.; Atwood, J. D.; Forbus, N. P.; Brown, T. L. *J. Am. Chem. Soc.* **1980**, *102*, 6248. (b) Bockman, T. M.; Kochi, J. K. *J. Am. Chem. Soc.* **1989**, *111*, 4669.

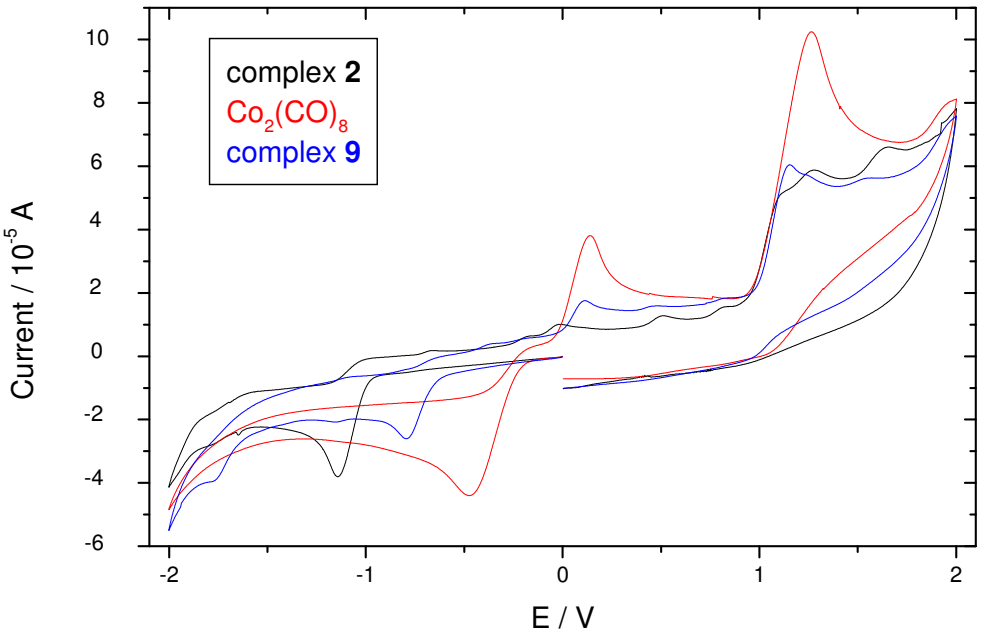

Figure 7. Cyclic voltammograms in 0.1 M Bu_4NClO_4/CH_2Cl_2 at a scan rate of 0.1 V/s at 25 ^{0}C.

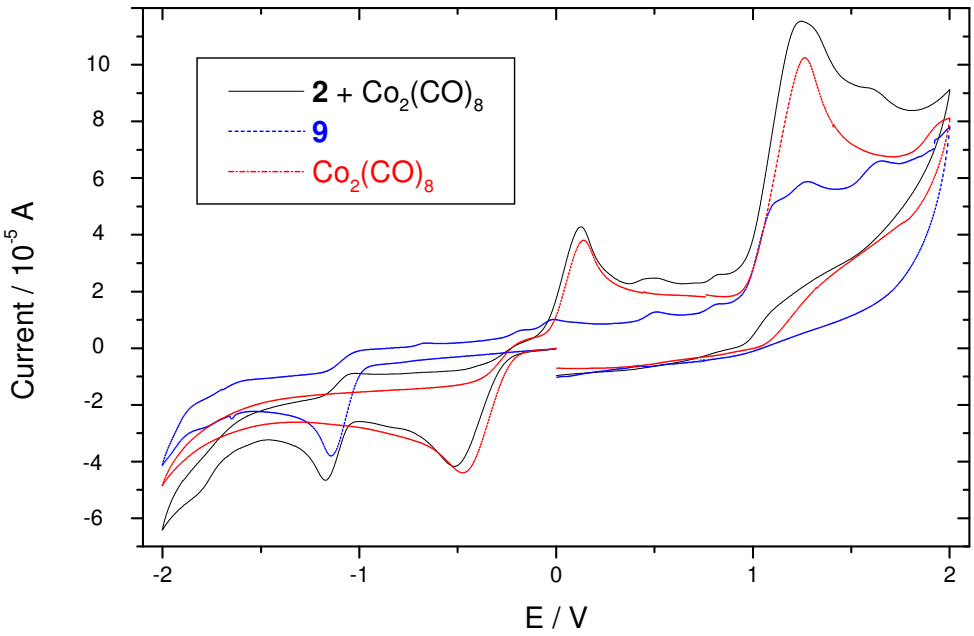

Figure 8. Cyclic voltammograms in 0.1 M Bu_4NClO_4/CH_2Cl_2 at a scan rate of 0.1 V/s at 25 ^{0}C.

Table 2.

Compound	1st E_{pc}	2nd E_{pc}	1st E_{pa}	2nd E_{pa}
2	-1.15			
$Co_2(CO)_8$	-0.47		0.14	1.26
9	-0.79		0.11	1.16
2 + $Co_2(CO)_8$	-0.51	-1.17	0.12	1.24

The ability of the $Co_2(CO)_8$ as an inhibitor of the ionization process was tested in an ESI-MS experiment with alkenyl carbene **1**, $Co_2(CO)_8$, and HQ as electron carrier.[29] The quasimolecular ions observed in the ESI-MS spectrum of a solution containing alkenyl carbene **1** and HQ disappear by addition of $Co_2(CO)_8$. This result confirms that the cobalt carbonyl moiety is easily reduced by the $HQ^{\bullet-}$ and behaves as an *electron-sink*, unable to take part in any electron transfer process to the M-C bond and hence responsible for the total inhibition of the ionization of the carbene complex in ESI-MS. The incorporation of a heteroatom in the spacer linking the $Co_2(CO)_6$ and the Cr-C moieties in Fischer carbene complex **10** did not produce any modifications in the previous results. This complex was also unable to show any molecular ions or fragments in the mass spectrum under standard ESI-MS conditions either in the presence or in the absence of additives.

In conclusion, electrospray ionization mass spectrometry (ESI-MS) has been revealed as a valuable tool in the study of ET reactions in bi- and polymetallic carbene complexes. Using the ESI as a nonconventional source of electrons we have shown that the direct ionization of these compounds requires both a good donor as the ferrocene group and a conjugated π-spacer as communication channel with the acceptor. The incorporation of the $Co_2(CO)_6$ cluster in the structure of a Fischer carbene complex inhibits the ionization even in the presence of external additives. In these cases the $Co_2(CO)_6$ moiety can be regarded as an *electron-sink*. An analogous effect is observed when the $Co_2(CO)_8$ is sprayed together with the conjugated complex in the ESI source. Further work directed to investigate the usefulness of the ESI-MS as a nonconventional source of electrons in the study of the reactivity of bi- and polymetallic complexes are currently under way in our laboratories.

[29] Before the experiment, the compatibility of the reagents was checked by keeping a dichloromethane solution of equimolar amounts of HQ and $Co_2(CO)_8$ 48h at room temperature. After this time both reagents remained unaltered.

1.4.3. Experimental Section

General procedures. ^{1}H NMR and ^{13}C NMR spectra were recorded at 22 ºC in $CDCl_3$, on a Varian XL-300S (300.1 and 75.4 MHz), Bruker Avance 300 (300.1 and 75.4 MHz) and Bruker 200-AC (200.1 and 50 MHz) spectrometers. Chemical shifts are given in ppm relative to TMS (^{1}H, 0.0 ppm) or $CDCl_3$ (^{13}C, 77.0 ppm). IR spectra were taken on a Perkin-Elmer 781 spectrometer. All solvents used in this work were purified by distillation and were freshly distilled immediately before use. Tetrahydrofuran (THF) and diethyl ether (Et_2O) were distilled from sodium-benzophenone and CH_2Cl_2 from CaH_2. Flame-dried glassware and standard Schlenk techniques were used for moisture sensitive reactions. Merck silica-gel (230-400 Mesh) was used as the stationary phase for purification of crude reaction mixtures by flash column chromatography. The identification of products was made by TLC (kiesegel 60F-254). UV light (λ = 254 nm) and 5% phosphomolybdic acid solution in 95% EtOH were used to develop the plates. All commercially available compounds were used without further purification. Compounds 3,[21] 4,[30] 5,[31] 6,[24b] 7,[32] 9[33] were obtained following the procedures reported in the literature.

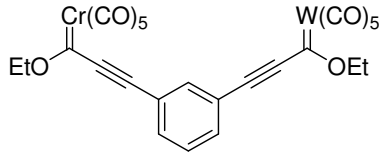

8

Preparation of compound 8. To a solution of ethynylferrocene (500 mg, 3.96 mmol) in dry Et_2O (38 mL) at –78 ºC was added dropwise *n*-butyllithium (1.6 M in hexanes, 5.5 mL, 8.7 mmol). The mixture was stirred at –78 ºC for 45 min and then chromium hexacarbonyl (0.87 g, 3.96 mmol) and tungsten hexacarbonyl (1.40 g, 3.96 mmol) were added in one portion at 0 ºC. The mixture was allowed to reach room temperature and stirred for 15 min. Afterwards, anhydrous THF (20 mL) was added and the mixture was let to stir at room temperature overnight. The reaction mixture was quenched by addition of Et_3OBF_4 (3.01 g, 15.9 mmol) in one portion at –78 ºC. The solution was stirred at this temperature for 15 min and then allowed to reach room temperature for an additional hour. Solvents were removed under reduced pressure and the residue was dissolved in Et_2O and filtered through silica gel. The solvent was evaporated and the residue was submitted to flash column chromatography under argon pressure (SiO_2, Hexane) to give **8** (251 mg, 8%) as a dark green solid. ^{1}H NMR (300 MHz, $CDCl_3$): δ 7.98 (s, 1H), 7.70-7.50 (m, 3H), 4.91 (q, *J* = 7.1 Hz, 2H), 4.70 (q, *J* = 7.1 Hz, 2H), 1.59 (t, *J* = 7.1 Hz, 3H), 1.53 (t, *J* = 7.1 Hz, 3H). ^{13}C NMR (75.5 MHz, $CDCl_3$): δ 313.7, 286.4, 225.6, 216.0, 202.9, 197.1, 136.9, 134.8, 129.7, 122.2, 91.5, 81.7, 79.4, 76.2, 73.0, 15.4, 15.0. IR (CCl_4): ν 2150, 2062, 2006, 1925 cm^{-1}. Elemental analysis calcd (%) for $C_{26}H_{14}CrO_{12}W$: C 41.40, H 1.87; found C 41.51, H 1.75.

[30] Sierra, M. A.; Mancheño, M. J.; del Amo, J. C.; Fernández, I.; Gómez-Gallego, M.; Torres, M. R. *Organometallics* **2003**, *22*, 384.
[31] Zora, M.; Yucel, B.; Peynircioglu, N. B. *J. Organomet. Chem*, **2002**, *656*, 11.
[32] Fernández, I.; Sierra, M. A.; Mancheño, M. J.; Gómez-Gallego, M.; Ricart, S. *Organometallics* **2001**, *20*, 4304.
[33] Wienand, A.; Reissig, H-U.; Fischer, H.; Pflumm, D.; Troll, C. *J. Organomet. Chem*, **1992**, *427*, C9.

Preparation of compound 10

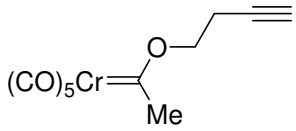

11

Pentacarbonyl[(1-butynoxy)(methyl)carbene]chromium(0) (11). This compound was synthesized following the method previously described by Hegedus.[34] A solution of pentacarbonyl[methyl(tetramethylammonium)carbene]chromium salt (1.5 g, 4.8 mmol) in dry CH_2Cl_2 (37.5 mL) under an argon atmosphere was cooled to –40 ºC with an acetone/dry ice bath. To the faint yellow solution was added acetyl bromide (4.8 mmol) by syringe. The reaction mixture was stirred at –35 ºC for 1 h and after this time a solution of 3-butyn-1-ol (0.34g, 4.8 mmol) in 10 mL of CH_2Cl_2 was added by syringe. The solution was stirred at –35 ºC for 3 h and allowed to slowly reach room temperature without removing the cold bath. To the resulting bright orange solution was added *ca*. 2 g of silica gel, and the solvent was removed under reducer pressure and the crude was submitted to flash column chromatography under argon pressure (Hexane) to give complex **11** (0.98 g, 71%) as an orange solid: ^{1}H NMR (300 MHz, $CDCl_3$): δ 4.93 (br s, 2H), 2.92 (s, 3H), 2.83 (br s, 2H), 2.03 (s, 1H). ^{13}C NMR (75.5 MHz, $CDCl_3$): δ 359.6 (Cr=C), 223.2 (CO *trans*), 216.2 (CO *cis*), 92.8, 78.5, 71.0, 49.4, 19.8. IR (CCl_4): ν 2064, 1982, 1944 cm^{-1}. Elemental analysis calcd (%) for $C_{11}H_8CrO_6$: C 45.85, H 2.80; found C 46.03, H 2.97.

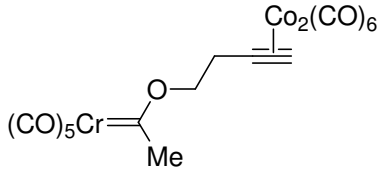

10

Complex 10. To a solution of complex **11** (150 mg, 0.52 mmol) in dry CH_2Cl_2 (10 mL) was added $Co_2(CO)_8$ (178 mg, 0.52 mmol) in one portion. The mixture was stirred at room temperature for 30 min and the solvent was removed under reduced pressure to yield complex **10** (298 mg, quantitative yield) as a brown solid. ^{1}H NMR (300 MHz, $CDCl_3$): δ 6.06 (s, 1H), 5.10 (br s, 2H), 3.47 (br s, 2H), 2.92 (s, 3H). ^{13}C NMR (75.5 MHz, $CDCl_3$): δ 359.8 (Cr=C), 223.1 (CO *trans*), 216.2 (CO *cis*), 199.3, 89.6, 80.4, 73.7, 49.6, 33.3. IR (CCl_4): ν 2095, 2056, 2031, 1985, 1944 cm^{-1}. Elemental analysis calcd (%) for $C_{17}H_8Co_2CrO_{12}$: C 35.57, H 1.40; found C 35.98, H 1.56.

Electrochemical Measurements

Cyclic voltammetric experiments were performed in CH_2Cl_2 at room temperature with 0.1 M tetrabutylammonium perchlorate as a supporting electrolyte and glassy carbon as a working electrode. A platinum wire was used as a counter electrode and Ag/Ag^+ as a reference electrode. All measurements were performed with potentiostat/galvanostat Autolab PGSTAT30, and ferrocene was used as an internal standard.

[34] Söderberg, B. C.; Hegedus, L. S.; Sierra, M. A. *J. Am. Chem. Soc*. **1990**, *112*, 4364.

ESI-MS experiments

All the ESI-MS experiments were carried out using an ESQUIRE-LC (Bruker Daltonic, Bremen, Germany) ion trap spectrometer in negative mode of detection. A syringe pump (Model 74900, Cole-Palmer, Vernon Hills, IL, USA) was used to deliver chloroform solutions (1.5x10-5 mol L^{-1}) of the corresponding Fischer carbene complex through a short length of 254mm i.d. PEEK tubing (Upchurch Scientific, Oak Harbor, WA, USA) with a flow rate of 3mL min^{-1}. The stainless-steel capillary was held at a potential of 5.0 kV. Nitrogen was used as nebulizer gas in a flow-rate of 3.98 L min^{-1} (nebulizer pressure 11 psi) at 150 ^{o}C. Solutions (chloroform-methanol, 1:1 v/v) containing 25mM hydroquinone (HQ), tetrathiafulvalene (TTF), ferrocene (Fc) or $Co_2(CO)_8$ were used. The spectra reported are the averages of 15 scans using 450 ms as the accumulation time. MS^n spectra were carried out using collision-induced dissociation (CID) with helium after isolation of the appropriate precursor ions. An isolation width of 0.4 *m/z* was used and the fragmentation amplitude was maintained at 0.60 V with a fragmentation time of 40 ms.

No differences were observed in the ESI mass spectra when HQ or TTF were used as additives. The HQ was detected as *m/z* 109 $[HQ-H]^-$ whereas TTF was observed as *m/z* 204 $[TTF]^{\cdot-}$ respectively.

Carbene 3: (ESI-MS) *m/z* MS^1 = 459 $[M-H]^-$; MS^2 = 403 [459-2 CO]$^-$; MS^3 = 375 [403- CO],$^-$ 337 [403- C_5H_6]$^-$; MS^4 = 319 [375- 2 CO].$^-$

Carbene 4: (ESI-MS) *m/z* MS^1 = 429 [(M-H)-CO]$^-$; MS^2 = 373 [429-2 CO].$^-$

Carbene 5a: (registered with additive) (ESI-MS) *m/z* MS^1 = 405 [(M-H)-CO]$^-$; MS^2 = 377 [405-CO]$^-$; MS^3 = 349 [377-CO]$^-$; MS^4 = 321 [349-CO]$^-$.

Carbene 5b: (registered with additive) (ESI-MS) *m/z* MS^1 = 537 [(M-H)-CO]$^-$; 397 [537-(5CO+C_2H_4]$^-$; MS^2 = 509 [537-CO]$^-$; MS^3 = 481 [509-CO].$^-$

Carbene 6: (registered with additive) (ESI-MS) *m/z* MS^1 = 857 [(M-H)-CO]$^-$; MS^2 = 505 [$C_{18}H_9O_6W$]$^-$; MS^3 = 449 [505-2CO].$^-$

Carbene 7: (registered with additive) (ESI-MS) *m/z* MS^1 = 593 [(M-H)-CO]$^-$; MS^2 = 373 [$C_{18}H_9O_6Cr$].$^-$

Carbene 8: (registered with additive) (ESI-MS) *m/z* MS^1 = 729 [(M+MeOH-H)-2 CO]$^-$; MS^2 = 505 [$C_{18}H_9O_6W$],$^-$ 373 [$C_{18}H_9O_6Cr$]$^-$; MS^3 = 449 [505-2 CO], 317 [373-2 CO].$^-$

Carbenes 9 and 10. No peaks were detected either directly or with addition of HQ.

1.5. ESI Mass Spectrometry Study of the Intimate Mechanism of a Gas-Phase Organometallic Reaction by Selective Deuterium Labeling

1.5. ESI Mass Spectrometry Study of the Intimate Mechanism of a Gas-Phase Organometallic Reaction by Selective Deuterium Labeling

1.5.1. Introduction

Electron spray ionization mass spectrometry (ESI-MS) is a standard tool for the analysis of the composition of solutions of organic, inorganic and bioorganic materials.[1] Different areas of chemistry ranging from host-guest chemistry[2] to structural biology,[3] benefit from the advantages of this powerful analytical technique that is the method of choice in the case of highly polar or labile compounds. The ESI-MS is also a useful tool in the detection of reactive intermediates of chemical reactions.[4] ESI is a technique that allows the transfer of ions from solution to the gas phase as isolated entities, and these ions can be subjected to mass spectrometric analysis. The production of ESI ions involves three key steps. The first event is the production of charged droplets at the ES capillary, which is followed by the shrinkage of the charged droplet due to the high voltage applied. These two sequential steps lead to very small, highly charged droplets in which the gas-phase ions are formed. This last step has proven to be very difficult to establish.[5] We have recently become aware of the potential of the electrospray ionization source to study electron-transfer processes in non-conventional media.[6] In fact, the behavior of mono- and polymetallic group 6 (Fischer) carbene complexes under ESI conditions clearly differs from that observed with conventional electron-transfer (ET) reagents such as Na/K alloy,[7] potassium 1-methylnaphtalenide,[8] SmI_2[9] or potassium graphite (C_8K).[10] Our results have shown that Fischer carbene complexes such as **1** can be ionized under ESI conditions in the presence of electron-carriers.[6] The process could be interpreted by initial capture of one electron to form intermediate **2** which would evolve to the $[M-H]^-$ detected ion by loss of a hydrogen radical. The

[1] Gaskell, S. J. *J. Mass Spectrom.* **1997**, *32*, 677.
[2] Vincenti, M. *J. Mass Spectrom.* **1995**, *30*, 925.
[3] Schiller, J.; Arnold, K. *Encyclopedia of Analytical Chemistry*; Meyers, R. A., Ed.; Wiley, Chichester, 2000.
[4] (a) Meyer, S.; Koch, R.; Metzger, J. O. *Angew. Chem. Int. Ed.* **2003**, *42*, 4700. (b) Traeger, J. C. *Int. J. Mass Spectrom.* **2000**, *200*, 387.
[5] Van Berkel, G. J., *Electrospray Ionization Mass Spectrometry*, Wiley, New York, 1997.
[6] (a) Martínez-Álvarez, R.; Gómez-Gallego, M.; Fernández, I.; Mancheño, M. J.; Sierra, M. A. *Organometallics* **2004**, *23*, 4647. (b) Sierra, M. A.; Gómez-Gallego, M.; Mancheño, M. J.; Martínez-Álvarez, R.; Ramírez-López, P.; Kayali, N.; González, A. *J. Mass. Spectrom.* **2003**, *38*, 151.
[7] Krusic, P. J.; Klabunde, U.; Casey, C. P.; Block, T. F. *J. Am. Chem. Soc.* **1976**, *98*, 2015.
[8] Lee, S.; Cooper, N. J. *J. Am. Chem. Soc.* **1990**, *112*, 9419.
[9] (a) Fuchibe, K.; Iwasawa, N. *Org. Lett.* **2000**, *2*, 3297. (b) Fuchibe, K.; Iwasawa, N. *Chem. Eur. J.* **2003**, *9*, 905.
[10] Sierra, M. A.; Ramírez-López, P.; Gómez-Gallego, M.; Lejon, T.; Mancheño, M. J. *Angew. Chem. Int. Ed.* **2002**, *41*, 3442.

nature of the $[M\text{-}H]^-$ ion is unknown and although it could have the structure of a carbene anion **3**[6,11] obtained by breakage of Hβ, the formation of allenyl anion **4** by the alternate Hα breakage should not be discarded (Scheme 1).

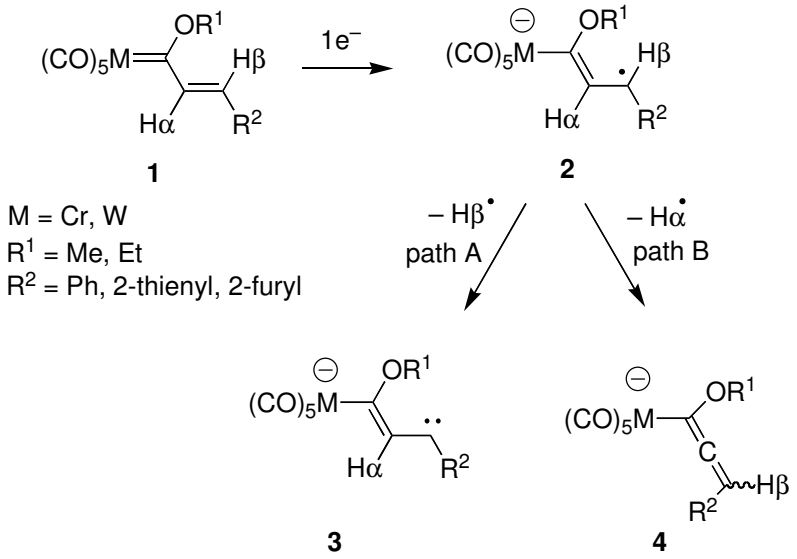

Scheme 1

The aim of this work is to understand the mechanism of ionization of group 6 Fischer carbene complexes mediated by electron carriers under ET-ESI (Electron Transfer-Electrospray Ionization) conditions. In this study we will use labeling experiments combined with DFT-calculations to unambiguously determine which of the two proposed mechanistic pathways in Scheme 1 is already occurring during the ESI process. An isotope tracer is one of the traditional mechanistic tools of physical organic chemistry that can also be applied to the investigation of organometallic reaction mechanisms.[12] This is an area of research of growing importance, as in most of the cases, we do not have a clear picture about how organotransition metal reactions work. On the other hand, the use of ESI combined with deuterium labeling experiments has been employed in the elucidation of fragmentation mechanisms[13] and in the investigation of reactive intermediates in organometallic reactions.[14]

[11] (a) Casey, C. P.; Kraft, S.; Powell, D. R. *J. Am. Chem. Soc.* **2000**, *122*, 3771. (b) Casey, C. P.; Kraft, S.; Powell, D. R. *J. Am. Chem. Soc.* **2002**, *124*, 2584.
[12] See, Blum, S. A.; Tan, K. L.; Bergman, R. G. *J. Org. Chem.* **2003**, *68*, 4127 and references therein.
[13] See for example: (a) Gatlin, C. J.; Turecek, F.; Vaisar, T. *J. Mass Spectrom.* **1995**, *30*, 1617 and *ibid* 1636. (b) Goodwin, L.; Startin, J. R.; Goodall, D. M.; Keely, B. J. *Rapid Commun. Mass Spectrom.* **2004**, *18*, 37. (c) Shoeib, T.; Hopkinson, A. C.; Siu, K. W. M. *J. Phys. Chem. B* **2001**, *105*, 12399. (d) Shoeib, T.; Cunje, A.; Hopkinson, A. C.; Siu, K. W. M. *J. Mass Spectrom.* **2002**, *38*, 408.
[14] Plattner, D. A. *Int. J. Mass Spectrom.* **2001**, *207*, 125.

1.5.2. Results and Discussion

Monodeuterated complex **5** was prepared from 2-tiophenecarbonyl chloride by reduction with superdeuteride to yield dideuterated alcohol **6**, Swern oxidation to aldehyde **7** and reaction of this compound with [ethoxymethylpentacarbonyl]chromium(0)carbene under Aumann conditions (Et_3N/TMSCl).[15] Complex **5** was determined to be 97% deuterated at the β-position (Scheme 2).

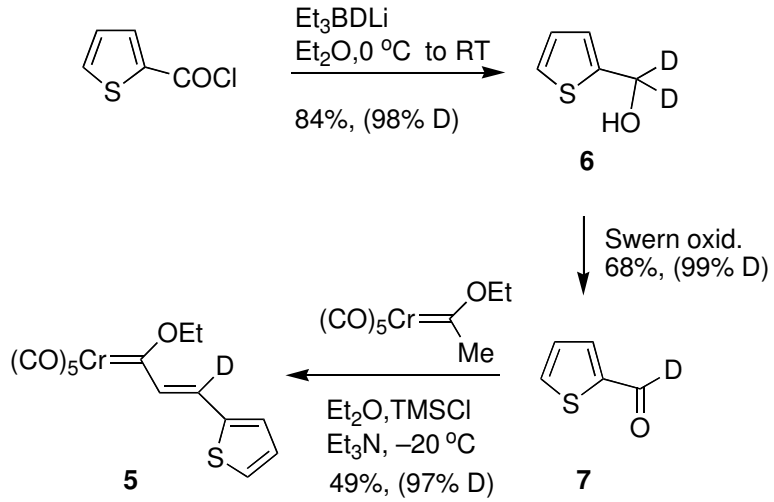

Scheme 2

ESI-MS spectra of complex **5** were recorded using an ESQUIRE-LC ion-trap spectrometer in negative mode of detection. To a sample of **5** in chloroform (1.5×10^{-5} mol L^{-1}) a methanolic solution of hydroquinone (HQ, 25 mM) was added following our previously reported methodology.[6] A pseudomolecular ion at *m/z* 358 corresponding to $[M\text{-}H]^-$ was observed (Figure 1). The isotopic cluster of this ion (Figure 1) reveals a composition related to $C_{14}H_8DO_6SCr$. Tandem mass spectrometry (MS^n) was used to determine the fragmentation pathway of this ion (Figure 2). Thus, the loss of two CO molecules affords a peak at *m/z* 302 $[M\text{-}H\text{-}(2CO)]^-$ ($C_{12}H_8DO_4SCr$) corresponding to MS^2, while MS^3 yields a peak at *m/z* 218 which corresponds to the elimination of another three CO molecules. This fragmentation pattern was identical to that observed for the non-deuterated compound **1** (M = Cr).[6b] These results suggested that the evolution of the initially formed radical-anion **8** occurs as proposed in path B in Scheme

[15] Aumann, R.; Heinen, H. *Chem. Ber.* **1987**, *120*, 537.

1, by loss of the Hα and formation of the allenyl anion **9** detected as $[M-H]^-$. Further extrusion of two CO ligands should provide the ion **10** (*m/z* 302) (Scheme 3).

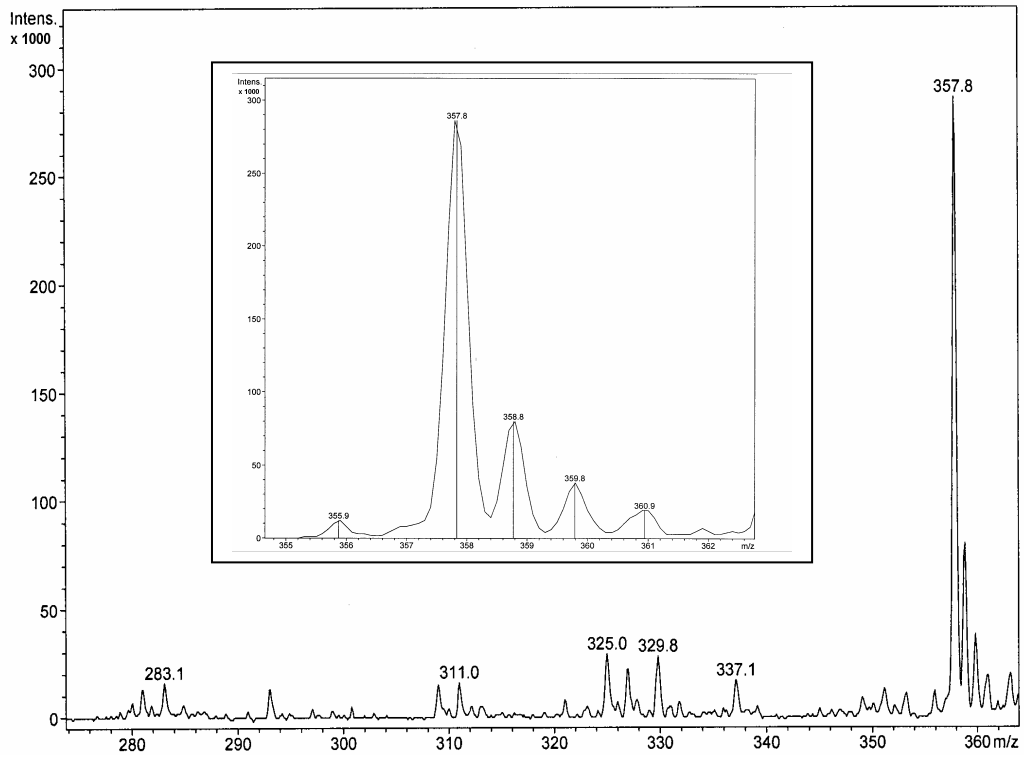

Figure 1. ESI mass spectrum of complex **5** showing the pseudomolecular ion $[M-H]^-$ at *m/z* 358. The magnified area corresponds to the isotopic cluster of the $[M-H]^-$ ion.

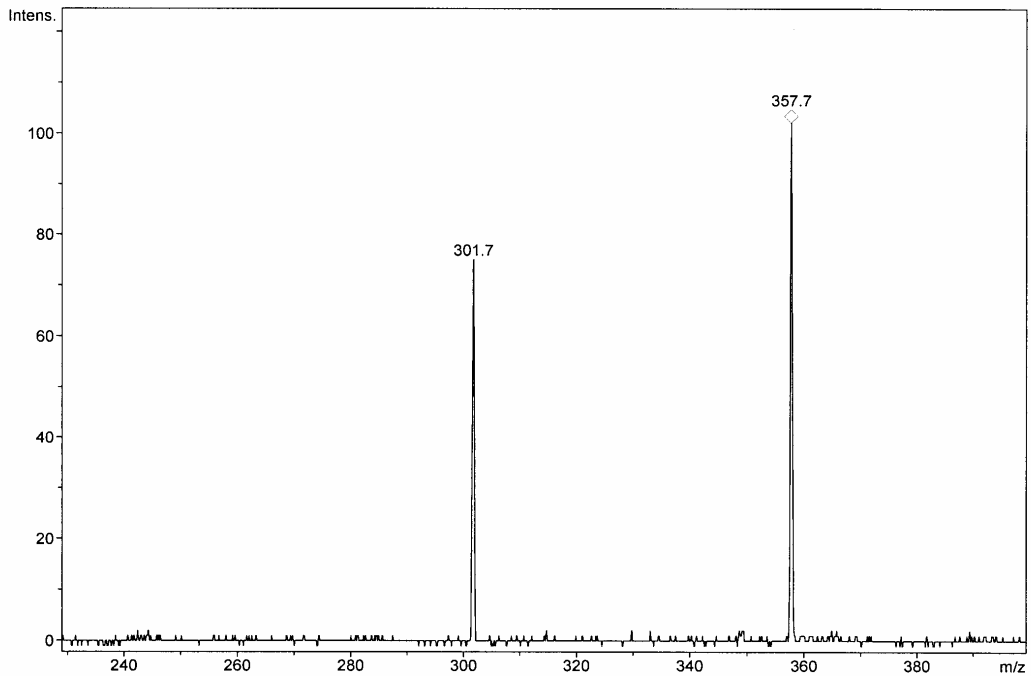

Figure 2. MS^2 spectrum of the $[M-H]^-$ ion at *m/z* 358 of the complex **5**. The daughter ion at *m/z* 302 is formed by loss of two CO molecules.

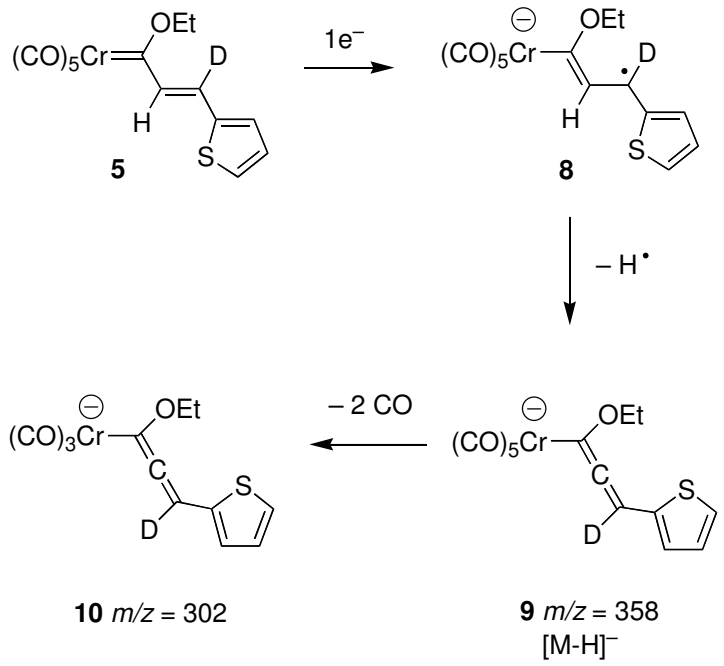

Scheme 3

To unambiguously confirm this ionization pattern, monodeuterated complex **11** was prepared. In this case, perdeuterated methyl chromium(0)carbene complex **12** (obtained from [ethoxymethylpentacarbonyl]chromium(0)carbene by treatment with NaOEt/EtOD, followed by quenching with $HCl_{(gas)}$/EtOD) was deprotonated with BuLi and condensed with 2-thiophene carbaldehyde to yield **11** in 17% yield. The degree of deuteration of this carbene complex in the α-position was 95% (Scheme 4).

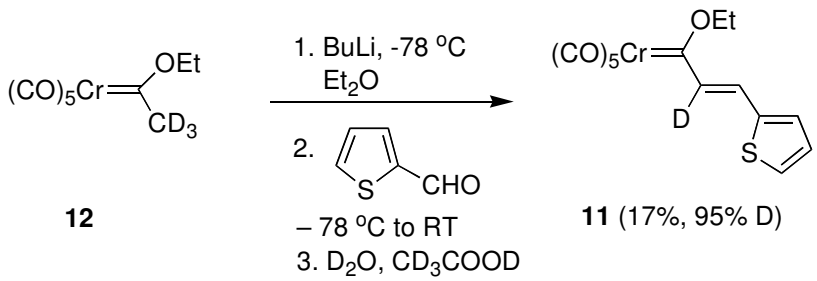

Scheme 4

Submission of complex **11** to the ESI-EM conditions used above resulted in a pseudomolecular $[M-D]^-$ ion **14** at *m/z* 357. No pseudomolecular $[M-H]^-$ ion (*m/z* 358) was observed in this case (Figure 3). The fragmentation of the $[M-D]^-$ ion (*m/z* 357) shows again the double simultaneous decarbonylation process characteristic of these compounds, affording exclusively an ion **15** at *m/z* 301 (Figure 4). By analogy with the reaction pattern depicted in Scheme 3, after the initial ET to **11**, the formation of

radical-anion **13** should lead to allenyl anion **14** by C-D bond breakage. Finally, the double elimination of CO would form **15** (Scheme 5).

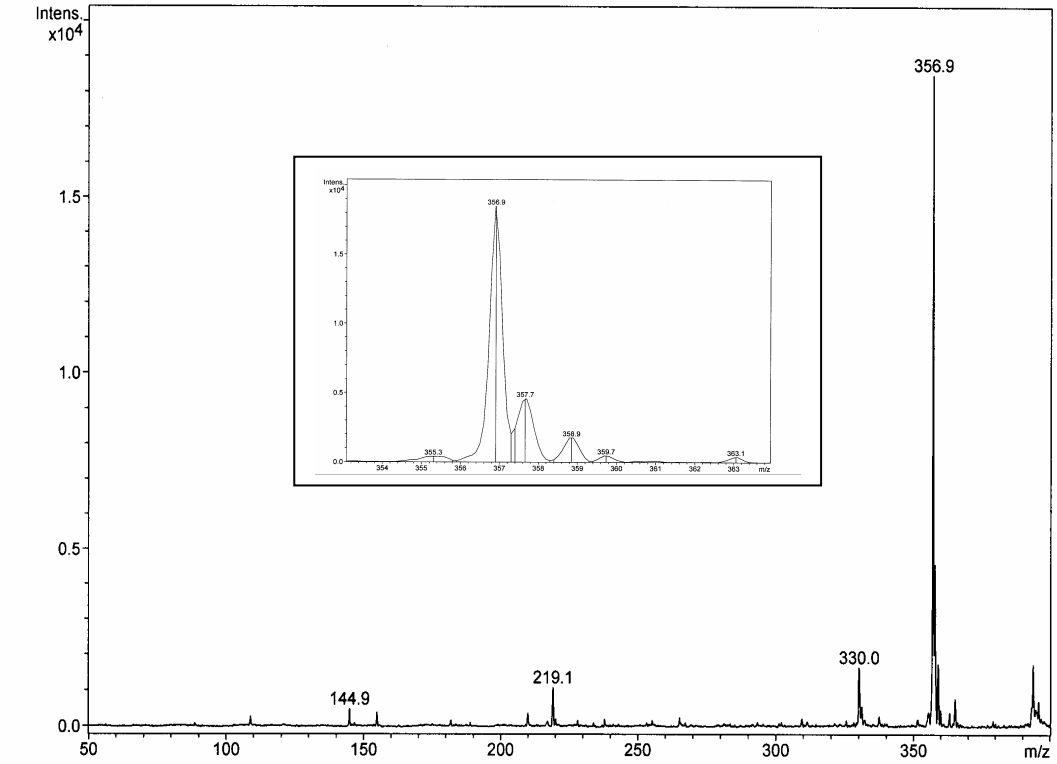

Figure 3. ESI mass spectrum of complex **11** showing the pseudomolecular ion $[M-D]^-$ at *m/z* 357. The magnified areas corresponds to the isotopic cluster of the $[M-D]^-$ ion.

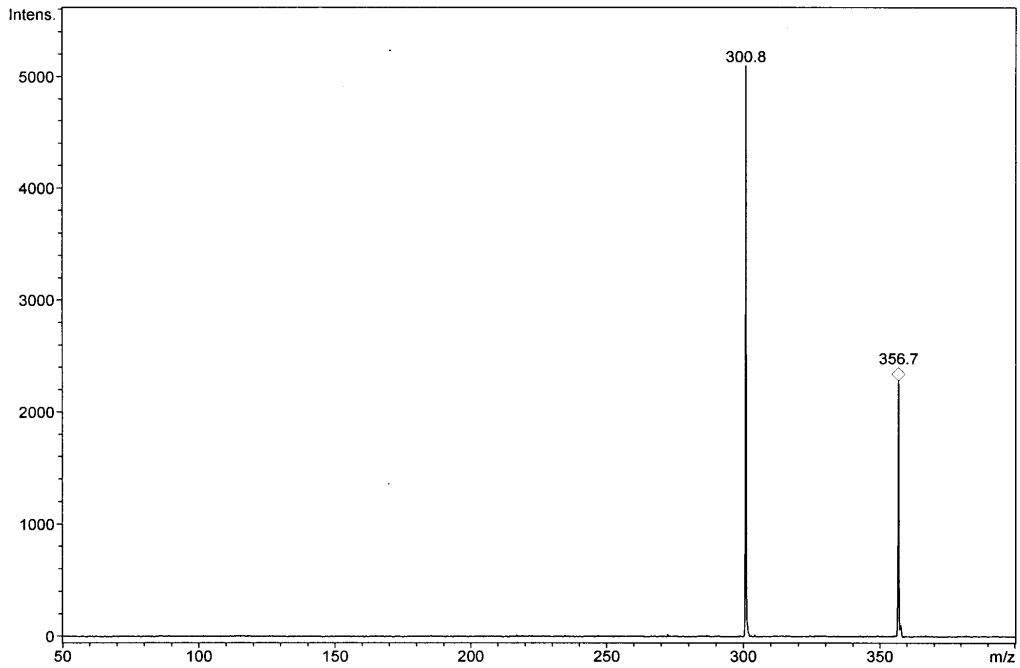

Figure 4. MS^2 spectrum of the $[M-D]^-$ ion at *m/z* 357 of the complex **11**. The daughter ion at *m/z* 301 is formed by loss of two CO molecules.

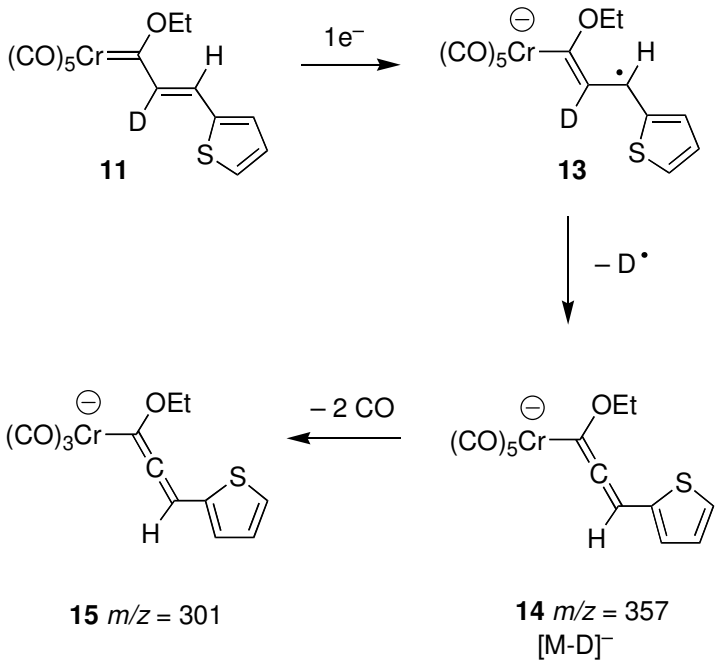

Scheme 5

As an additional confirmation of these results, and to discard any possibility of intermolecular H/D exchange during the experiment, the ESI-EM of an equimolar mixture of labeled complex **11** and compound **16** was recorded under the conditions used through this work. The resulting mass spectrum showed the expected peak $[M\text{-}D]^-$ **14** (*m/z* 357) of complex **11**, together with a $[M\text{-}H]^-$ pseudomolecular ion (*m/z* 351) for complex **16** (Figure 5). In both cases the intensities and the isotopic distribution of the peaks were identical to those observed for the single complexes, which discards any significant H/D scrambling in the process. Therefore, it can be concluded that the results obtained in the ESI-MS ionization of deuterated carbene complexes **5** and **11** indicate that the process occurs by the transfer of $1e^-$ to the organometallic compound, followed by extrusion of the α-hydrogen to form an allenyl anion which is the species detected in the MS spectrum.

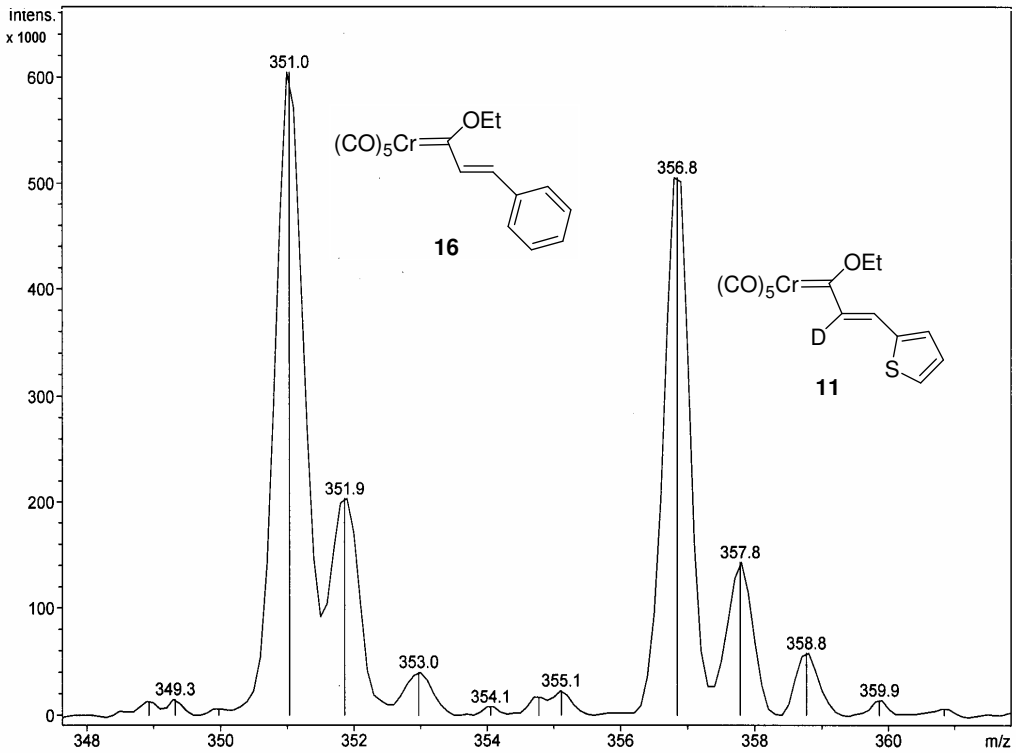

Figure 5. ESI mass spectra of the pseudomolecular ion zone of the mixture of complexes **11** and **16**. The ion at *m/z* 351 corresponds to the $[M-H]^-$ of **16** while the ion at *m/z* 357 corresponds to the $[M-D]^-$ of **11**.

The preference for the Hα breakage in the ionization process could be based on the higher stability of the allenyl anion **4** (path B, Scheme 1) compared to the carbene-anion **3** coming from the alternative Hβ fragmentation pathway (path A, Scheme 1). To support this explanation, we initially carried out DFT-calculations on the model complex pentacarbonyl[methoxyvinylcarbene]chromium(0), **17**. The S_0 geometries of radical-anion **18**, carbene-anion **19** and allenylchromium anion **20**, were optimized at the B3LYP/LANL2DZ&6-31+G(d) level and are represented in Figure 6. Our results showed that allenyl anion **20** was considerably more stable (42.02 kcal mol^{-1}) than carbene-anion **19**. Being aware that these results could be oversimplified by the fact that model complex **17** lacked an aromatic ring in the β-position. Additional calculations were carried out in phenyl substituted radical-anion **21** formed from carbine complex **16**, carbene-anion **22** and allenylchromium anion **23**. Again, the allenyl anion **23** resulted to be more stable than carbene-anion **22** (34.05 kcal mol^{-1}), even though this latter species benefits from the additional conjugative stabilization caused by the phenyl group. Nevertheless, it should be noticed that the difference in energies between these species is very high. As a matter of fact, this value of 34.05 kcal mol^{-1} is an estimation

of the stabilization of an allenyl-metal species compared to a vinyl-metal species (Figure 6). Furthermore, the charge on the chromium atom is nearly identical in species **21-23**, which points to the little effect of the metal in the evolution of the radical-anion formed after the initial electron transfer reaction.

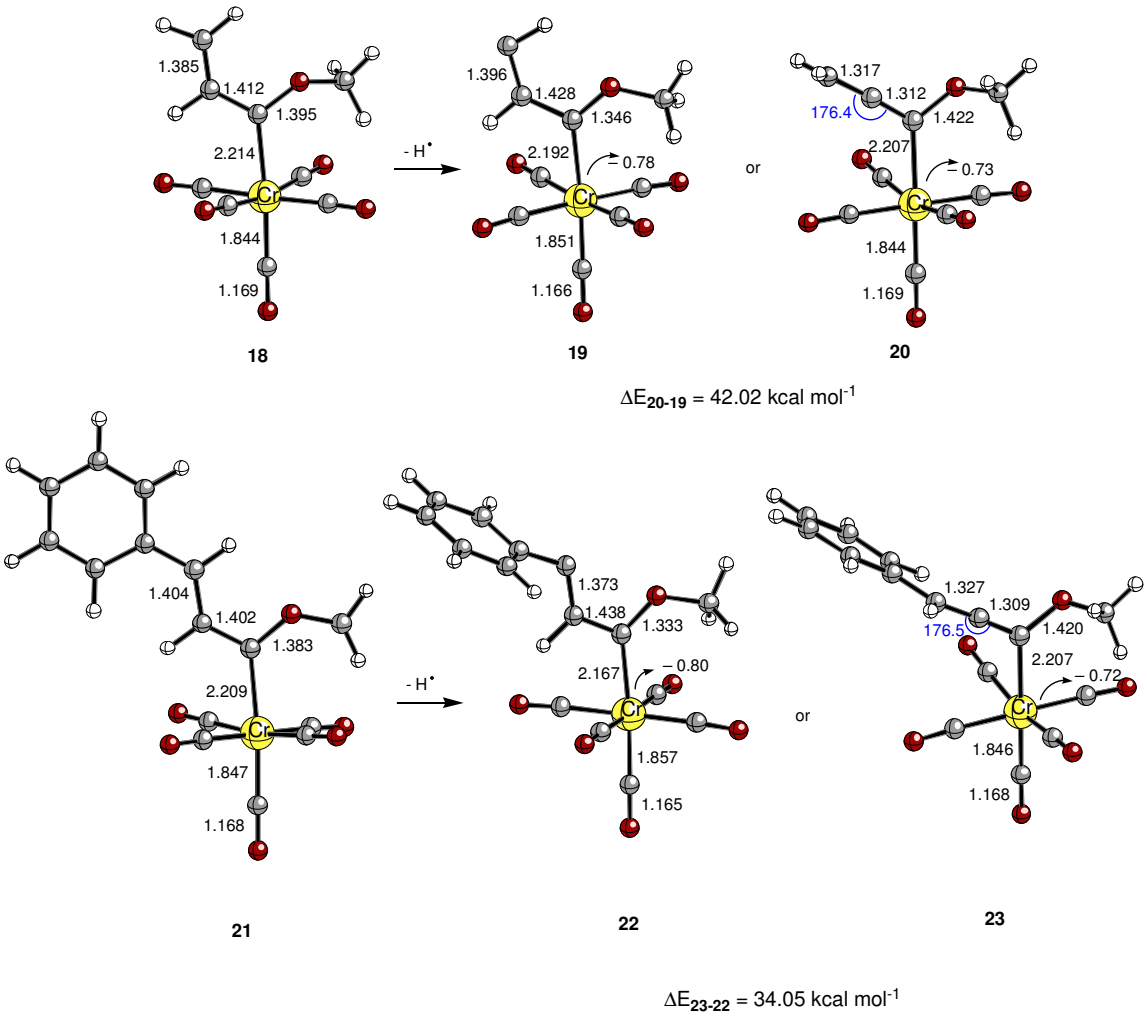

Figure 6

Having established the viability of the use of deuterium labeled substrates in the study of the behavior of Fischer carbene complexes under ESI conditions, we decided to employ this methodology to confirm the ionization pattern previously proposed by us for alkynyl carbene complexes **24**.[6b] In this case, the anion-radical **25** is formed after the capture of an electron, and this initial ionization is followed by the loss of a hydrogen radical to form the $[M\text{-}H]^-$ ion detected in the mass spectrum. We postulated that the cleavage of the aromatic C–H_A bond to yield the extended allene-anion carbene complex **26** was the most likely fragmentation pathway. However, an alternative reaction path may involve the intramolecular H_B transfer from the ethoxy group in the

radical anion **25** followed by the loss of a hydrogen radical to form allenyl anion **27**. This species will be also detected as $[M-H]^-$ ion in the ESI-MS spectrum (Scheme 6).

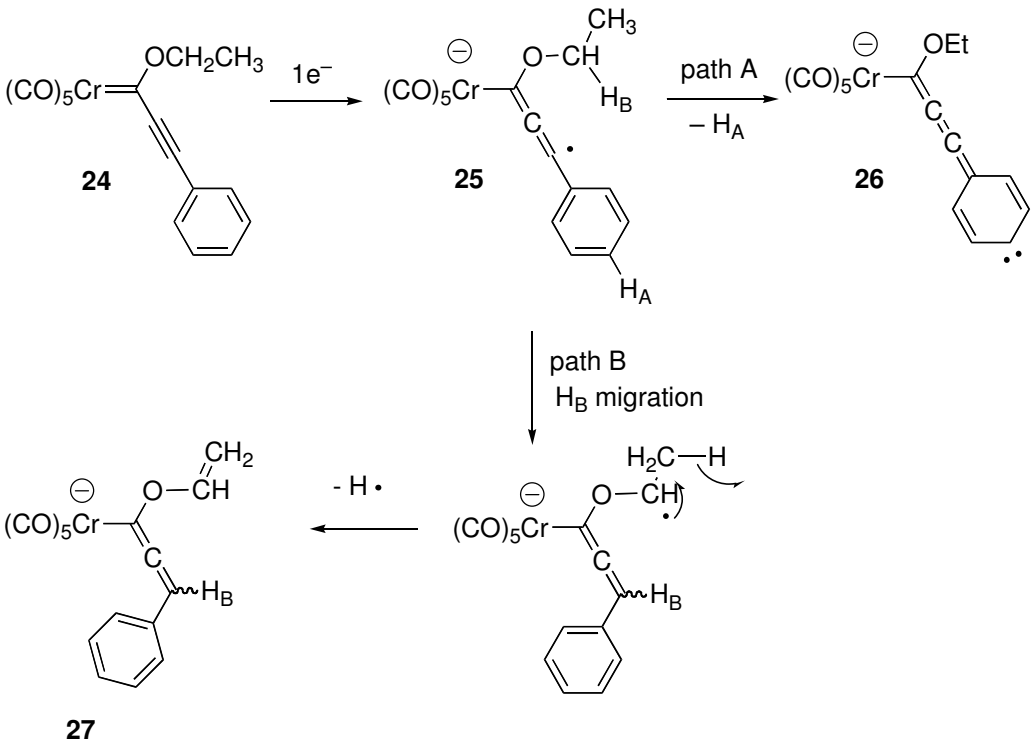

Scheme 6

Monodeuterated complex **28** was prepared from *p*-D-ethynylbenzene **29** following the standard procedure for the synthesis of Fischer carbene complexes ($Cr(CO)_6$/EtOTf). *p*-D-Ethynylbenzene **29** was made from **30** by Sonogashira coupling, D-halogen interchange and TMS-group removal. The desired complex **28** was prepared in 55% yield and ≥ 98 D-incorporation (Scheme 7).

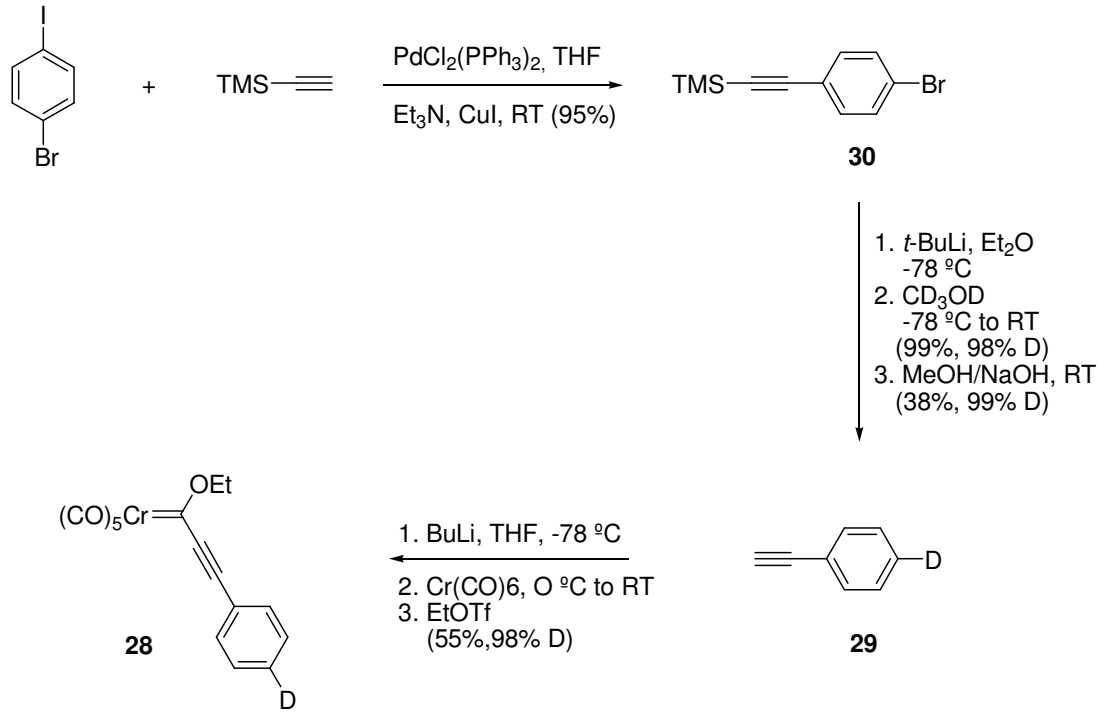

Scheme 7

The ionization of complex **28** takes place in presence of HQ under the standard conditions used through this work. A pseudomolecular $[M\text{-}D]^-$ ion (*m/z* 349) corresponding to $C_{16}H_9O_6Cr$ was observed. This result demonstrates that the ionization is promoted by loss of a deuterium radical as proposed in path A (Scheme 6). The second stage of fragmentation produces an ion at *m/z* 321 formed by loss of a CO molecule. No other peaks due to the fragmentation of a C–H bond and the extrusion of a hydrogen radical were observed (Figure 7).

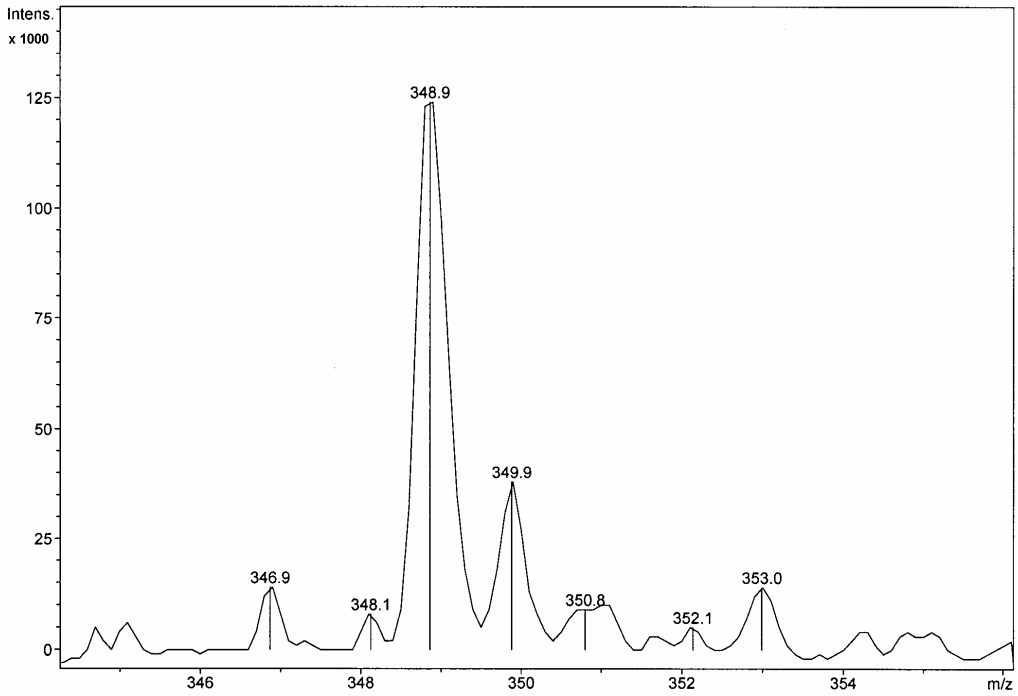

Figure 7. Isotopic cluster of the pseudomolecular ion $[M-D]^-$ at *m/z* 349 of complex **28**.

In conclusion, through this study we have used deuterium labeled compounds to establish the mechanism of ionization of conjugated Fisher carbene complexes under ESI conditions. The results indicate that in the ESI source, and after the initial hydroquinone mediated ET from the charged droplet to the carbene complex, an anion-radical is formed. These species evolve by extrusion of a radical hydrogen to form allenylchromium anion species that are detected in the mass spectrum as $[M-H]^-$ ions. A rationalization based on the higher stability of the allenylchromium anion species compared to the carbene-anion species previously postulated by us in these processes has been extracted from DFT-calculations. From the comparison of the energy values it can also conclude that the presence of the metal has little influence in the evolution of the radical anion formed after the initial electron transfer reaction.

1.5.3. Experimental Section

General procedures. Diethyl ether and tetrahydrofuran were distilled from sodium and benzophenone. Dimethyl sulphoxide (DMSO) was purified by standing overnight with CaH_2 and distillation over fresh CaH_2 at ~10 mm of Hg. DMSO was stored over 4 Å molecular sieves. The spectroscopic NMR data were acquired on Varian equipment for 300 and 500 MHz NMR. For ^{13}C NMR of deuterated compounds, the recycle delay (d1) was set to 10 seconds due to the relaxation of C-D. Infrared spectra were acquired on a Nicolet IR/42 spectrometer. EI-Mass spectroscopy of the volatile organic compounds were conducted on a Varian Chrompack Saturn 2000R 3800 Gas Chromatograph/MS with a CP Sil 8 CB low bleed/MS column. Reactions were conducted under a nitrogen or argon atmosphere unless otherwise stated. All glassware was either dried in an oven for at least 30 to 60 minutes or flame dried under vacuum (< 0.2 mm Hg). All the ESI-MS experiments were carried out using an ESQUIRE-LC (Bruker Daltonic, Bremen, Germany) ion trap spectrometer in negative mode of detection. A syringe pump (Model 74900, Cole-Palmer, Vernon Hills, IL, USA) was used to deliver chloroform solutions (1.5×10^{-5} mol L^{-1}) of the corresponding Fischer carbene complex through a short length of 254 mm i.d. PEEK tubing (Upchurch Scientific, Oak Harbor, WA, USA) with a flow rate of 3 mL min^{-1}. The stainless-steel capillary was held at a potential of 5.0 kV. Nitrogen was used as nebulizer gas in a flow-rate of 3.98 L min^{-1} (nebulizer pressure 11 psi) at 150 ^{o}C. The spectra reported are the averages of 15 scans using 450 ms as the accumulation time. MS^n spectra were carried out using collision-induced dissociation (CID) with He after isolation of the appropriate precursor ions. An isolation width of 0.4 *m/z* was used and the fragmentation amplitude was maintained at 0.60 V with a fragmentation time of 40 ms. In all the experiments the HQ was detected as $[HQ-H]^-$ (*m/z* 109).

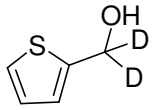

6

Synthesis of 2-dideuterothienylcarbinol 6. To a solution of 2-thiophenecarbonyl chloride (1.03 g, 7.00 mmol) in 5 mL of diethyl ether, Super deuteride (20 mL, 20.0 mol, 1 M solution) was added dropwise at 0 °C. The contents of the flask were warmed to RT for 3 h. Column chromatography (26 cm x 3 cm, silica gel) with 30 % ethyl acetate / hexane gave 0.68 g of **7** as yellow oil, $R_f = 0.31$ (30 % EtOAc/hexane) (84 % yield, 98 % deuterium incorporation). The deuterium incorporation was determined by ^1H NMR. The spectral data of compound **6** are identical with those previously reported for this compound.[16] Spectral data for **6**: ^1H NMR ($CDCl_3$) δ: 2.66 (s, 1 H), 6.90 - 7.05 (m, 2 H), 7.22 - 7.30 (m, 1 H); ^{13}C NMR ($CDCl_3$) δ: 124.99, 125.39, 126.49, 126.73 (one carbon missing due to the relaxation of C-D bond); MS *m/z* (% rel intensity): 116 M^+ (53), 115 (19), 99 (100), 86 (13), 83 (18) 55 (5).

[16] (a) Fetizon, M.; Henry, Y.; Moreau, N.; Moreau, G.; Golfier, M.; Prange, T. *Tetrahedron* **1973**, *29*, 1011. (b) Macco, A. A.; Brouwer, R. J. D.; Nossin, P. M. M.; Godefroi, E. F.; Buck, H. M. *J. Org. Chem.* **1978**, *43*, 1591.

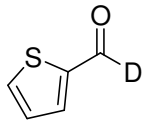

7

Synthesis of Deuterothienyl carbaldehyde 7. To a solution of DMSO (2.20 mL, 41.7 mmol) in 175 mL of dichloromethane, oxalyl chloride (1.30 mL, 14.6 mmol) was added dropwise. The solution was stirred 10 min., and **6** (1.70 g, 14.60 mmol) in 20 mL of dichloromethane was added dropwise. Column chromatography (21 cm x 3 cm, silica gel) with 60 % dichloromethane / hexane gave 1.12 g of aldehyde **7** as yellow oil, R_f = 0.36 (60 % CH_2Cl_2/hexane) (68 % yield, 99 % deuterium incorporation). The deuterium incorporation was determined by ^{1}H NMR. The spectral data of **7** were identical to those previously reported for this compound.[17] Spectral data for **7**: ^{1}H NMR ($CDCl_3$) δ: 7.21 (t, 1 H, J = 4.3 Hz), 7.73 - 7.84 (m, 2 H); ^{13}C NMR ($CDCl_3$) δ: 128.08, 134.82, 136.16, 143.54 (t, due to C-C-D coupling, ^2J = 5.1 Hz), 182.45 (t, due to C-D coupling, ^1J = 26.8 Hz).

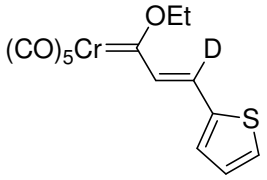

5

Preparation of 5. In a 50 mL round bottom flask where the 14/20 glass joint was replaced with a threaded high-vacuum Teflon stopcock, 30 mL of diethyl ether, compound **7** (0.59 g, 5.22 mmol), [ethoxymethylpentacarbonyl]chromium(0)carbene[18] (1.35 g, 5.11 mmol), triethyl amine (3.0 mL, 21.5 mmol) and TMSCl (2.0 mL, 15.8 mmol) were added.[15] Three freeze thaw cycles were done to remove oxygen. The solution was stirred 23 h at RT and then stored 24 h at -20 °C. The contents of the flask were poured onto silica gel and the solvent removed under reduced pressure. Column chromatography (24.5 cm x 4 cm, silica gel) with 30 % dichloromethane / hexane gave 0.89 g of **5** as a black solid, R_f = 0.51 (30 % CH_2Cl_2/hexane), mp 86 - 87 °C, (49 % yield, 97 % deuterium incorporation) along with 0.44 g (33 %) of recovered [ethoxymethylpentacarbonyl]chromium(0)carbene. The deuterium incorporation was determined by ^{1}H NMR by comparison of the integration of the signals at 7.16 ppm (d) and 7.08 ppm (dd). Spectral data for compound **5**: ^{1}H NMR ($CDCl_3$) δ: 1.67 (t, 3 H, J = 7.1 Hz), 5.07 (q, 2 H, J = 7.1 Hz), 7.08 (dd, 1 H, J = 3.7, J = 5.1 Hz), 7.38 (dd, 1 H, J = 1.0, J = 3.7Hz), 7.47 (dd, J = 1, J = 4.9 Hz); ^{13}C NMR ($CDCl_3$) δ: 15.15, 75.85, 123.49 (t, ^1J = 22.5 Hz, very weak) 128.73, 130.45, 133.54, 138.35, 139.93, 216.80, 224.38, 328.60; IR (thin film) 3080w, 3026w, 2963m, 2901w, 2108s, 1480m cm^{-1}; Anal calcd for $C_{14}H_9DCrO_6S$: C, 46.80; H, 3.09. Found; C, 46.72; H, 2.81.

[17] (a) Hoskovec, M.; Luxova, A.; Svatos, A.; Boland, W. *Tetrahedron* **2002**, *58*, 9193. 8b) Chadwick, D. J.; Chambers, J.; Hargrave.He; Meakins, G. D.; Snowden, R. L. *J. Chem. Soc., Perkin Trans. 1* **1973**, 2327. (c) Chadwick, D. J.; Chambers, J.; Meakins, G. D.; Snowden, R. L. *J. Chem. Soc., Perkin Trans. 2* **1975**, 604.

[18] Fischer, E. O.; Maasböl, A. *J. Organomet. Chem.* **1968**, *12*, P15.

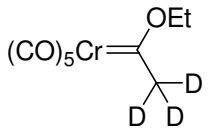

12

Preparation of 12. To [ethoxymethylpentacarbonyl]chromium(0)carbene[18] (4.57 g, 17.3 mmol) was added 10 mL of ethanol-d_1 with pre-dissolved sodium metal < 4 mg. The solution was stirred for 15 min and acidified with conc. HCl / ethanol-d_1 (1:3, v/v). The solution was then taken up in Et_2O and filtered through Celite 503. The organic solvent was removed under reduced pressure. This procedure was repeated four times, resulting in 2.94 g of **12** as orange oil at RT, yellow solid at -20 ºC, R_f = 0.42 (9:1 hexane/EtOAc) (64 % yield, 96 % deuterium incorporation). The spectral data were consistent with the known literature compound.[19] The deuterium incorporation was determined by ^{1}H NMR by comparison of the integration of the signals at 2.88 ppm and 1.65 ppm. Spectral data for **12**: ^{1}H NMR ($CDCl_3$) δ: 1.64 (t, 3 H, *J* = 7.1 Hz), 2.88 (br s, 0.15 H, from non-deuterated compound), 5.01 (bs, 2 H); ^{13}C NMR ($CDCl_3$) δ: 14.93, 49.27 (broad and weak), 216.49, 223.40, 357.81 (deuterated carbon missing due to the relaxation time of C-D); IR (thin film) 2991.97m, 2945.68m, 2905.17w, 2064.10vs, 1917.49vs, 1469.94m, 1367.76s, 1250.03vs, 1128.50s, 1030.12s, 978.03s 812.13m, 640.45vs cm^{-1}.

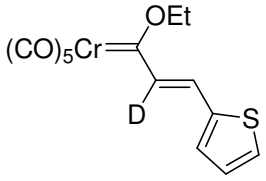

11

Preparation of 11. To a solution of **12** (1.0 g, 3.8 mmol) in Et_2O (25 mL) at -78 °C was added 2.4 mL of *n*-butyllithium (1.6 M in hexanes, 3.8 mmol). The solution was stirred for 20 min and then 2-thiophenecarbaldehyde (0.7 mL, 7.7 mmol) was added at -78 °C. The solution was stirred for 45 min at -78 °C, then was warmed to RT and stirred for four additional hours. The reaction was extracted with 10 mL of D_2O and the D_2O layer was adjusted to a pH < 7 with acetic acid-d_4. The D_2O layer was extracted with CH_2Cl_2 (3 x 50 mL), the organic extracts were combined and dried over sodium sulfate and the solvent was removed under reduced pressure. Column chromatography (2.8 cm x 26 cm, silica gel) with 5 % CH_2Cl_2 to 10 % CH_2Cl_2/hexane gave 0.24 g of **11** as red solid, mp 86 - 88 °C,[13] R_f = 0.30 (hexane), (17 % yield, 95 % deuterium incorporation). The deuterium incorporation was determined by ^{1}H NMR by comparison of the integration of the signals at 7.70 ppm (d) and 7.36 ppm (d). Spectral data for **11**: ^{1}H NMR ($CDCl_3$) δ: 1.66 (t, 3 H, *J* = 7.0 Hz), 5.04 (q, 1 H, *J* = 7.2 Hz), 7.08 (dd, 1 H, *J* = 3.8, J = 5.0 Hz), 7.11 (s, 1 H), 7.36 (d, 1 H, *J* = 3.8 Hz), 7.47 (d, 1 H, *J* = 5.0 Hz), 7.70 (d, 0.05 H, *J* = 15.0 Hz, from non-deuterated compound); ^{13}C NMR ($CDCl_3$) δ: 15.19, 75.86, 123.03, 128.74, 130.49, 133.64, 137.90 (t, ^1J = 23.7 Hz, weak), 139.94, 216.78, 224.39, 328.33; IR (thin film) 3112w, 2994m, 2056s, 1916s 1561s cm^{-1}; Anal calcd for $C_{14}H_9DCrO_6S$: C, 46.80; H, 3.09. Found; C, 46.86; H, 2.82.

[19] Chelain, E.; Parlier, A.; Audouin, M.; Rudler, H.; Daran, J. C.; Vaissermann, J. *J. Am. Chem. Soc.* **1993**, *115*, 10568.

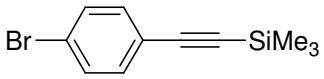

30

Preparation of 30. The following procedure is adapted from one that has been reported for this compound.[20,21] A magnetic stirring bar was placed into a flame-dried single neck 50 mL flask that had been modified by replacement of the 14/20 joint with a threaded high vacuum Teflon stopcock. The flask was charged with 1-bromo-4-iodobenzene (4.05 g, 14.3 mmol), TMS acetylene (2.0 mL, 14.2 mmol), THF (25 mL), triethyl amine (8 mL), dichloropalladium (II) bis(triphenylphosphine) (0.20 g, 2.0 mol %), and copper (I) iodide (0.14 g, 5 mol %). Three freeze thaw cycles were performed to remove oxygen. The contents of the flask were stirred for three days at RT under Argon. The contents of the flask were filtered through silica gel with ethyl acetate (3 x 170 mL) and the solvent was removed under reduced pressure. The filtration procedure through silica gel was repeated once after the solvent was removed. Column chromatography (20 cm x 3.8 cm, silica gel) with hexane gave 3.44 g (95 % yield) of **30** as white solid (hexane), mp 60 - 61 °C, R_f = 0.50 (hexane). The spectral data were identical to those previously reported.[20,21] Spectral data for **30**: ^{1}H NMR ($CDCl_3$) δ: 0.25 (s, 9 H), 7.31 (d, 2 H, *J* = 8.6 Hz), 7.42 (d, 2 H, *J* = 8.6 Hz); ^{13}C NMR ($CDCl_3$) δ: -0.15, 95.53, 103.81, 122.00, 122.72, 131.42, 133.35; MS *m/z* (% rel intensity) 254 M^+ (96, ^{81}Br), 252 M^+ (100, ^{79}Br), 240 (21), 239 (19, ^{81}Br), 238 (18), 237 (17, ^{79}Br), 144 (25), 129 (16), 115 (35), 75 (25); Anal calcd for $C_{11}H_{13}BrSi$: C, 52.18; H, 5.17. Found; C, 52.18; H, 5.34.

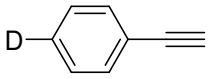

29

Preparation of 29. The following procedure is adapted from one that has been reported for this compound.[22] To a solution of **30** (3.44 g, 13.5 mmol) in 100 mL Et_2O at -78 °C was added *t*-butyllithium (1.7 M in pentane, 16.4 mL, 27.9 mmol). The solution was stirred for 25 min. after adding *t*-butyllithium at -78 °C. Then, methanol-d_4 (1.2 mL, 29.6 mmol) was added at -78 °C. The solution was allowed to warm over four hours to RT. A cloudy white solution resulted. The solution was extracted with 50 mL of water and the water layer was back extracted with 3 x 50 mL Et_2O. The organic layers were combined and dried over sodium sulfate. The solution was filtered and the solvent removed under reduced pressure. This gave 2.36 g of 4-D-trimethylsilylethynylbencene as a clear oil, R_f = 0.38 (hexane), (>99 % yield, 98 % deuterium incorporation). The deuterium incorporation was determined by ^{1}H NMR by comparison of the integration of the signals at 7.28 ppm and 7.28 ppm. The spectral data were identical to those previously reported.[22] Spectral data for 4-D-trimethylsilylethynylbencene: ^{1}H NMR ($CDCl_3$) δ: 0.25 (s, 9 H), 7.28 (d, 2 H, *J* = 8.0 Hz), 7.47 (d, 2 H, *J* = 8.0 Hz); ^{13}C NMR ($CDCl_3$) δ: -0.03, 94.04, 105.12, 123.13, 128.06, 128.17 (t, ^1J = 25.6 Hz), 131.94; IR (thin film) 3079s, 3029s, 2961vs, 2899s, 2101vs, 1595m, 1480m, 1406m, 1250m,

[20] Schafer, L. L.; Nitschke, J. R.; Mao, S. S. H.; Liu, F. Q.; Harder, G.; Haufe, M.; Tilley, T. D. *Chem. Eur. J.* **2002**, *8*, 74.
[21] Weil, T.; Reuther, E.; Beer, C.; Mullen, K. *Chem. Eur. J.* **2004**, *10*, 1398.
[22] Evans, A. G.; Evans, J. C.; Phelan, T. J. *J. Chem. Soc., Perkin. Trans. 2* **1974**, 1216.

1219m, 841s cm^{-1}; MS *m/z* (% rel intensity) 175 M^+ (3), 174 (11), 161 (20), 160 (100), 144 (5), 103 (4), 89 (8), 61 (21); Anal calcd for $C_{11}H_{13}DSi$: C, 75.36; H, 8.62. Found; C, 75.32; H, 8.54.

Following the previously reported procedure,[22,23] **4-D-trimethylsilylethynylbencene** (6.07 g, 34.6 mmol) was dissolved in methanol (20 mL). Sodium hydroxide (1.51 g, 37.8 mmol) was added. The reaction was stirred for 3 h at RT. The solution was extracted with water and the water was back extracted with 3 x 50 mL of hexane. The organic layers were combined and dried over sodium sulfate. The volume of solvent was reduced to 35 mL under reduced pressure and the remaining solvent was removed by distillation leaving 1.35 g of **29** (38 % yield, ≥ 98 % deuterium incorporation) that was used without further purification in the next step. The deuterium incorporation was measured by setting the region of integration of 7.50 ppm (d) to 2 and noting the difference of the integration of the region of 7.31 ppm (d). This difference was calibrated to the undeuterated compound. The spectral data of **29** were identical to those previously reported.[22,23] ^{1}H NMR ($CDCl_3$) δ: 3.07 (s, 1 H), 7.31 (d, 2 H, *J* = 7.6 Hz), 7.50 (d, 2 H, *J* = 8.0 Hz); MS *m/z* (% rel intensity) 103 M^+ (100), 88 (5), 77 (16), 61 (11), 50 (14).

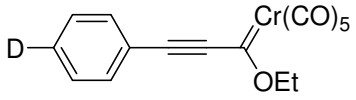

28

Preparation of 28. To a solution of **29** (0.37 g, 3.6 mmol) at -78 °C in 20 mL THF was added *n*-butyllithium (1.6 M in pentane, 2.25 mL, 3.6 mmol). The solution was warmed to 0 °C and stirred for 45 min which gave a yellow-brown solution. At this point, chromium hexacarbonyl (0.80 g, 3.6 mmol) was added at 0 °C and the orange solution was allowed to warm to RT over 45 minutes. The solution was cooled to 0 °C and ethyl triflate (0.94 mL, 7.3 mmol) was added. The solution was stirred for 35 min, which resulted in a blood-red solution. The contents of the flask were poured onto brine (50 mL) and extracted with three portions of Et_2O (20 mL, 2 x 75 mL). The organic layers were combined and dried with sodium sulfate. The solvent was removed under reduced pressure with care taken to maintain a temperature of 0 to 10 °C for the water bath. Column chromatography (30 cm x 3.8 cm, silica gel) first with hexane and then with 5 % EtOAc/hexane resulted in 0.69 g of **28** as a black solid (hexane), mp 61-63 °C, R_f = 0.18 (hexane), R_f = 0.34 (5 % EtOAc/hexane)[24] (55 % yield, ≥ 98 % deuterium incorporation). Again, care was taken to maintain a temperature of 0 to 10 °C of the water bath when the solvent was removed. The deuterium incorporation was determined by ^{1}H NMR by setting the region of integration of 7.58 ppm (d) to 2 and noting the difference of the integration of the region of 7.45 ppm (d). This difference was calibrated to the undeuterated compound. Spectral data for **29**: ^{1}H NMR ($CDCl_3$) δ: 1.58 (t, 3 H, *J* = 7.1 Hz), 4.74 (q, 2 H, *J* = 6.9 Hz), 7.45 (d, 2 H, *J* = 7.8 Hz), 7.58 (d, 2 H, *J* = 7.3 Hz); ^{13}C NMR ($CDCl_3$) δ: 14.97, 75.83, 91.78, 121.02, 128.80, 131.32 (t, ^1J = 22.8 Hz, weak), 132.67, 135.67 (weak), 216.30, 225.71, 313.84; IR (thin film) 2999wb, 2155m, 2060s, 1935s, 1294m, 1196m, 1146w, 1109w, 1036m, 862m, 681m, 650m, 608m, 594m cm^{-1}; Anal calcd for $C_{16}H_9DCrO_6$: C, 54.71; H, 3.16. Found; C, 54.40; H,

[23] (a) Suydam, I. T.; Boxer, S. G. *Biochemistry* **2003**, *42*, 12050. (b) Berger, S.; Diehl, B. W. K. *Tetrahedron Lett.* **1987**, *28* , 1243.
[24] Fischer, E. O.; Kreissl, F. R. *J. Organomet. Chem.* **1972**, *35*, C47.

3.00. Attempts to make compound **28** by treatment of **4-D-trimethylsilylethynylbencene** with MeLi-LiBr complex were unsuccessful to produce yields greater than 0.1 % of the carbene complex.

CAPÍTULO II

CAPÍTULO II. OBJETIVOS

En este capítulo se abordará sistemáticamente, de forma teórico-experimental, la estructura y reactividad fotoquímica de complejos metal-carbeno de tipo Fischer del grupo 6. Los objetivos concretos son los siguientes:

- Estudio teórico sobre la preferencia que muestran los complejos alcoximetal-carbeno por adoptar una disposición *anti* tanto en su forma cristalina como en disolución.
- Estudio de la reacción de fotocarbonilación de complejos metal-carbeno del grupo 6. Se estudiará en profundidad el proceso de carbonilación, con especial interés en las distintas especies que se forman tras la excitación inicial del complejo metal-carbeno (Esquema 1).

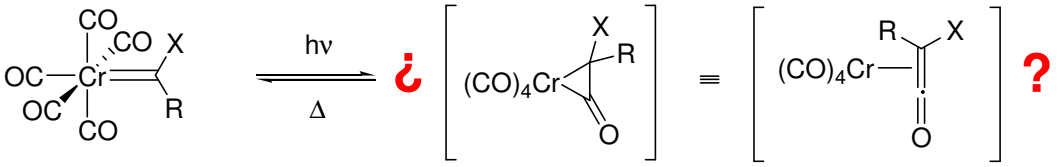

Esquema 1

- Una vez conocida la etapa de fotocarbonilación en complejos metal-carbeno, se estudiará la reacción de estas especies con cetenófilos. Concretamente, se usará como reacción a estudiar, tanto teórica como experimentalmente, la formación de β-lactamas. Asimismo, se intentará explicar la diastereoselectividad encontrada en este proceso.
- Como objetivo complementario se estudiará la reacción de complejos metal-carbeno en los que se ha sustituido un ligando carbonilo de la esfera de coordinación del metal por un ligando σ-dador (Esquema 2). Estos últimos complejos nos servirán como sonda experimental en el estudio del mecanismo de esta reacción.

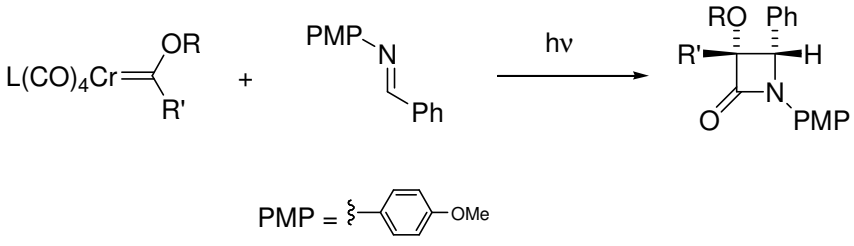

Esquema 2

- El último objetivo de este capítulo persigue la búsqueda e interpretación teórica de nuevas formas de reactividad fotoquímica de complejos metal-carbeno de tipo Fischer diferentes a la fotocarbonilación. De nuevo, se empleará una combinación de métodos computacionales y experimentación para determinar los mecanismos de los posibles nuevos procesos descubiertos.

2.1. Structure and Conformations of Heteroatom-Substituted Free Carbenes and Their Group 6 Transition Metal Analogues

2.1. Structure and Conformations of Heteroatom-Substituted Free Carbenes and Their Group 6 Transition Metal Analogues

2.1.1. Introduction

The first tungsten(0)-carbene complex was prepared by Fischer and Maasböl in 1964.[1] Almost 40 years after this seminal discovery, these reagents have a widespread use in Organic Synthesis.[2] Among them, group 6 metal-carbene complexes are specially well suited for structural and mechanistic studies because of the easiness of their preparation and the amazing number of different reactivities they can experience. The nature of the metal–carbon double bond has attracted a continuous and still unabated interest, from both the experimental and theoretical points of view. In fact, the first crystal and molecular structure of [pentacarbonyl(methoxyphenyl)chromium(0)] carbene, **2**, was reported in 1968 by Mills and Redhouse[3] showing a partial double bond character of the [O–C]=Cr bond. This was explained from the interaction between a lone pair on the oxygen and the empty p_z orbital orbital of the carbene carbon. This interaction would be competitive with the back-donation from the metal and therefore would result in the consequent lessening of the double bond character of the O-[C=Cr] double bond. One remarkable feature of this structure was that the methyl group is directed toward the chromium (an orientation we shall denote *anti* throughout this work; see below).

[1] Fischer, E. O.; Maasböl, A. *Angew. Chem. Int. Ed. Eng.* **1964**, *3*, 580.
[2] Reviews: (a) Dötz, K. H.; Fischer, H.; Hofmann, P.; Kreissel, R.; Schubert, U.; Weiss, K. *Transition Metal Carbene Complexes*, Verlag Chemie: Deerfield Beach, Florida, 1983. (b) Dötz, K. H. *Angew. Chem. Int. Ed. Eng.* **1984**, *23*, 587. (c) Wulff, W. D. in *Comprehensive Organic Synthesis,* Trost, B. M.; Fleming, I., Eds. Pergamon: Oxford, 1991; vol. 5, pp. 1065. (d) Schwindt, M. A.; Miller, J. R.; Hegedus, L. S. *J. Organomet. Chem.* **1991**, *413*, 143. (e) Rudler, H.; Audouin, M.; Chelain, E.; Denise, B.; Goumont, R.; Massoud, A.; Parlier, A.; Pacreau, A.; Rudler, M.; Yefsah, R.; Álvarez, C.; Delgado-Reyes, F. *Chem. Soc. Rev.* **1991**, *20*, 503. (f) Grotjahn, D. B.; Dötz, K. H. *Synlett.* **1991**, 381. (g) Wulff, W. D. in *Comprehensive Organometallic Chemistry II,* Abel, E. W.; Stone, F. G. A.; Wilkinson, G.; Eds. Pergamon: Oxford. 1995; vol. 12, pp. 470. (h) Hegedus, L. S. in *Comprehensive Organometallic Chemistry II,* Abel, E. W.; Stone, F. G. A.; Wilkinson, G.; Eds. Pergamon: Oxford. 1995; vol. 12, pp. 549. (i) Harvey, D. F.; Sigano, D. M. *Chem. Rev.* **1996**, *96*, 271. (j) Hegedus, L. S. *Tetrahedron* **1997**, *53*, 4105. (k) Aumann, R.; Nienaber, H. *Adv. Organomet. Chem.* **1997**, *41*, 163. (l) Alcaide, B.; Casarrubios, L.; Domínguez, G.; Sierra, M. A. *Curr. Org. Chem.* **1998**, *2*, 551. (m) Sierra, M. A. *Chem. Rev.* **2000**, *100*, 3591. (n) de Meijere, A.; Schirmer, H.; Duetsch, M. *Angew. Chem., Int. Ed.* **2000**, *39*, 3964. (o) Barluenga, J.; Flórez, J.; Fañanás, F. J. *J. Organomet. Chem.* **2001**, *624*, 5.
[3] Mills, O. S.; Redhouse, A. D. *J. Chem. Soc. (A)* **1968**, 642.

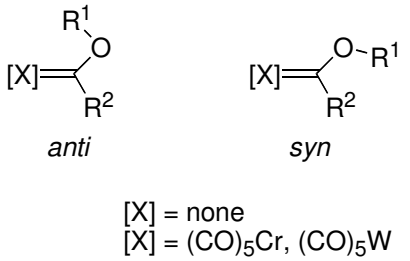

Figure 1. *Syn* and *anti* conformations of free and Fischer carbenes.

Since this original crystallographic study many, other structures of group 6 alkoxy metal-carbene complexes have been reported.[4,5] Except for complexes having linear substituents linked to the carbene carbon such as [pentacarbonyl(phenylethynylmethoxy)chromium(0)], **4**,[12] [pentacarbonyl(phenylethynylethoxy)chromium(0)], **5**,[5t] and the allenylethoxy derivative,[5s] the remaining alkoxy-complexes, whose structures have been reported, systematically have the alkoxy substituent in an *anti* disposition (Figure 1). Furthermore, the [C–C]-O–C=Cr distance in the crystals is in many cases considerably

[4] *anti*-Methoxy carbenes: (a) Jayaprakash, K. N.; Ray, P. C.; Matsuoka, I.; Bhadbhade, M. M.; Puranik, V. G.; Das, P. K.; Nishihara, H.; Sarkar A. *Organometallics* **1999**, *18*, 3851. (b) Dötz, K. H.; Kuhn, W.; Thewalt, U. *Chem. Ber.* **1985**, *118*, 1126. (c) Macomber, D. W.; Hung, M-H.; Madhukar, P.; Liang, M.; Rogers, R. D. *Organometallics* **1991**, *10*, 737. (d) Ulrich, K.; Guerchais, V.; Dotz, K. H.; Toupet, L.; Le Bozec, H. *Eur. J. Inorg. Chem.* **2001**, 725. (e) Dötz, K. H.; Ehlenz, R.; Straub, W.; Weber, J. C.; Airola, K.; Nieger, M. *J. Organomet. Chem.* **1997**, *548*, 91. (f) Geisbauer, A.; Polborn, K.; Beck, W. *J. Organomet. Chem.* **1997**, *542*, 205. (g) Breimair, J.; Weidmann, T.; Wagner, B.; Beck, W. *Chem. Ber.* **1991**, *124*, 2431. (h) Wienand, A.; Reissig, H.-U.; Fischer, H.; Pflumm, D.; Troll, C. *J. Organomet. Chem.* **1992***, 427*, C9. (i) Kretschik, O.; Nieger, M.; Dötz, K. H. *Chem. Ber.* **1995**, *128*, 987. (j) Jahr, H. C.; Nieger, M.; Dötz, K. H. *J. Organomet. Chem.* **2002***, 641*, 185. Exceptions (*syn*-methoxy carbenes): (k) Dötz, K. H.; Tomuschat, P.; Nieger, M. *Chem. Ber.* **1997**, *130*, 1605. (l) Longen A.; Nieger, M.; Vogtle, F.; Dötz, K. H. *Chem. Ber.* **1997**, *130*, 1105. (m) Lattuada, L.; Licandro, E.; Papagni, A.; Maiorana, S.; Villa, A. C.; Guastini, C. *Chem. Commun.* **1988**, 1092.

[5] *anti*-Ethoxy carbenes: (a) Aumann, R.; Roths, K. B.; Kossmeier, M.; Fröhlich, R. *J. Organomet. Chem*. **1998**, *556*, 119. (b) Duetsch, M.; Stein, F.; Lackmann, R.; Pohl, E.; Herbst-Irmer, R.; de Meijere, A. *Chem. Ber.* **1992**, *125*, 2051. (c) Barluenga, J.; Montserrat, J. M.; Flórez, J.; García-Granda, S.; Martín, E. *Angew. Chem. Int. Ed. Engl.* **1994**, *33*, 1392. (d) Streubel, R.; Hobbold, M.; Jeske, J.; Jones, P. G. *Chem. Commun.* **1994**, 2457. (e) Landman, M.; Gorls, H.; Lotz, S. *J. Organomet. Chem*. **2001***, 617*, 280. (f) Aumann, R.; Fröhlich, R.; Kotila, S. *Organometallics* **1996**, *15*, 4842. (g) Aumann, R.; Hinterding, P.; Krüger, C.; Betz, P. *Chem. Ber.* **1990,** *123*,1847. (h) Aumann, R.; Jasper, B.; Goddard, R.; Krüger, C. *Chem. Ber.* **1994***, 127*, 717. (i) Terblans, Y. M.; Roos, H. M.; Lotz, S. *J. Organomet. Chem.* **1998**, *566*, 133. (j) Landman, M.; Gorls, H.; Lotz, S. *Eur. J. Inorg. Chem.* **2001***,* 233. (k) Tran-Huy, N. H.; Lefloch, P.; Robert, F.; Jeannin, Y. *J. Organomet. Chem.* **1987***, 327*, 211. (l) Aumann, R.; Hinterding, P.; Krüger, C.; Goddard, R. *J. Organomet. Chem.* **1993***, 459*, 145. (m) Moldes, I.; Ros, J.; Torres, M. R.; Perales, A.; Mathieu, R. *J. Organomet. Chem.* **1994**, *464*, 219. (n) Aumann, R.; Jasper, B.; Fröhlich, R.; Kotila, S. *J. Organomet. Chem*. **1995**, *502***,** 137. (o) Aumann, R.; Fröhlich, R.; Kotila, S. *Organometallics* **1996**, *15*, 4842. (p) Aumann, R.; Göttker-Schnetmann, I.; Fröhlich, R.; Meyer, O. *Eur. J. Org. Chem.* **1999**, 2545. (q) Sierra, M. A.; Ramírez-López, P.; Gómez-Gallego, M.; Lejon, T.; Mancheño, M. J. *Angew. Chem. Int. Ed*. **2002**, *41*, 3442. Even *bis*-carbenes complexes: (r) Fischer, E. O.; Roll, W.; Schubert, U.; Ackermann, K. *Angew .Chem. Int. Ed. Engl.* **1981***, 20*, 611. (s) Tran-Huy, N. H.; Pascard, C.; Tran-Huu Dau E.; Dötz, K. H. *Organometallics* **1988***, 7*, 590. *Syn*-ethoxy carbenes (t) Aumann, R.; Jasper, B.; Lage, M.; Krebs, B. *Chem. Ber.* **1994**, *127*, 2475 (this paper contains also crystallographic data for two *anti*-carbene complexes). (u) Lorenz, H.; Huttneer, G. *Chem. Ber.* **1975**, *108*, 1864. (v) Mathur, P.; Ghosh, S.; Sarkar, A.; Satyanarayana, C. V. V.; Rheingold, A. L.; Liable-Sands, L. M. *Organometallics* **1997***, 16*, 3536.

shorter than the expected for a single bond, like for example in CH_3–CH_2–OH. One clear exception to this rule is observed in [pentacarbonyl(ethoxymethyl)chromium(0)]carbene, **1**,[6] albeit in this case the measurement was effected by neutron-diffraction (Table 1).

Table 1. Selected experimental and calculated bond distances (Å) and angles (deg.) for complexes **1**-**5**.

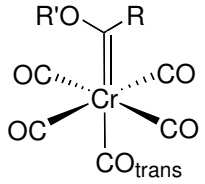

[Cr]=C(OR')R[a]	dCr-C	dCr-CO_{trans}	dC-R	dC-O	dO-C_1	dC_1-C_2	C-O-C_1	R-C-O
R = Me, R'=Et[6]	2.053 (2.064)	1.894 (1.892)	1.511 (1.515)	1.314 (1.313)	1.461 (1.454)	1.509 (1.517)	124.1 (124.1)	106.1 (105.9)
R=Ph, R'=Me[3]	2.04 (2.084)	1.87 (1.889)	1.47 (1.493)	1.33 (1.323)	1.40 (1.436)		121 (124.3)	104 (105.3)
R = CH=CHPh R'=Et[b]	2.054 (2.057)	1.884 (1.896)	1.478 (1.483)	1.299 (1.322)	1.449 (1.435)	1.452	123.4 (123.4)	108.6 (107.5)
R=C≡CPh, R'=Me[12]	1.9990 (2.005)	1.897 (1.908)	1.416 (1.426)	1.3233 (1.329)	1.447		(121.7)	(115.5)
R=C≡CPh, R'=Et[5t]	2.00	1.86	1.37	1.32	1.51	1.50	121	116

a. Calculated data are given in parentheses. See text. The C_1 and C_2 atoms refer to the ethoxy groups.

b. Data provided by Prof. Lars K. Hansen (University of Tromsø, Norway). The full crystallographic data for compound **2** will be reported in due time.

From a theoretical point of view the nature of the metal-carbene bond has been repeatedly discussed. Early work by Block[7] using semiempirical methods showed a correlation between the site of nucleophilic attack and the location of the LUMO in the metal complexes. In this work the effect of complexation on the electronic distribution of the ligands was also studied by comparison of the nature of the free and coordinated carbenes, although they were directed toward the comparative effect of coordination between CH_3CO^- and CH_3COMe. Subsequently the problem of the nature of the metal-

[6] Krüger, C.; Goddard, R.; Claus, K. H. *Z. Naturforsch*. **1983**, *B38,* 1431.
[7] Block, T. F.; Fenske, R. F.; Casey, C. P. *J. Am. Chem. Soc*. **1976**, *98*, 441.

carbon double bond was approached using semiempirical,[8] Hartree-Fock (HF),[9] post-HF,[10] and most recently density functional theory (DFT) calculations.[11] A landmark in these works is the study by Wang,[12] who demonstrated by a combination of X-ray diffraction and molecular orbital (MO) calculations that the π-bond character of the metal-carbene can be best represented by a Cr–C–X three-centered four electron bond, with the π-electron density mainly located at either the d_{yz} orbital of Cr or the p_z orbital of X in the carbene ligand. This makes the carbene an electrophilic site in the p_π direction. An extensive DFT study by Frenking and Solá[13] reported, while this work was under progress, that stronger π electron donors attached to the carbene carbon lead to larger Cr=C lengths, shorter Cr–CO_{trans} and larger C–O_{trans} bond distances. An additional effect of these stronger π electron donors is to produce smaller Cr=C bond dissociation energies. Surprisingly, all these calculations were effected on the *syn* orientation, that is not the usually encountered in the solid structures of group 6 alkoxy carbenes.

Despite the extensive studies resumed above no additional effort has been exerted to compare the free and coordinated ligands to extract information about the nature of the M=C bond, except the pioneering work by Block.[7] Reported herein is a systematic DFT study of different conformations of free and Cr- and W-coordinated alkoxy-carbenes that shows that coordination to the metal does not change the structure of the free carbenes and their conformational trends. Furthermore, the preference of the

---

[8] (a) Block, T. F.; Fenske, R. F. *J. Am. Chem. Soc*. **1977**, *99*, 4321. (b) Goddard, R. J.; Hoffmann, R.; Jemmis, E. D. *J. Am. Chem. Soc*. **1980**, *102*, 7667. (c) Volatron, F.; Eisenstein, O. J. *J. Am. Chem. Soc*. **1986**, *108*, 2173.

[9] (a) Nakatsuji, H.; Ushio, J.; Han, S.; Yonezawa, T. *J. Am. Chem. Soc*. **1983**, *105*, 426. (b) Ushio, J.; Nakatsuji, H.; Yonezawa, T. *J. Am. Chem. Soc*. **1984**, *106*, 5892. (c) Marynick, D. S.; Kirkpatrick, C. M.; *J. Am. Chem. Soc*. **1985**, *107*, 1993. (d) Cundari, T. R.; Gordon, M. S. *J. Am. Chem. Soc*. **1991**, *113*, 5231. (e) Cundari, T. R.; Gordon, M. S. *J. Am. Chem. Soc*. **1992**, *114*, 539. (f) Cundari, T. R.; Gordon, M. S. *Organometallics* **1992**, *11*, 55.

[10] (a) Taylor, T. E.; Hall, M. B.; *J. Am. Chem. Soc*. **1984**, *106*, 1576. (b) Carter, E. A.; Goddard, W. A., III. *J. Am. Chem. Soc*. **1986**, *108*, 4746. (c) Márquez, A.; Fernández Sanz, J. *J. Am. Chem. Soc*. **1992**, *114,* 2903.

[11] (a) Jacobsen, H.; Schreckenbach, G.; Ziegler, T. *J. Phys. Chem.* **1994**, *98*, 11406. (b) Jacobsen, H.; Ziegler, T. *Organometallics* **1995**, *14*, 224. (c) Ehlers, A. W.; Dapprich, S.; Vyboishchikov, S. F.; Frenking, G. *Organometallics* **1996**, *15*, 105. (d) Jacobsen, H.; Ziegler, T. *Inorg. Chem.* **1996**, *35*, 775. (e) Fröhlich, N.; Pidun, U.; Stahl, M.; Frenking, G. *Organometallics* **1997**, *16*, 442. (f) Frenking, G.; Pidun, U. *J. Chem. Soc.*, *Dalton Trans.* **1997**, 1653. (g) Torrent, M.; Durán, M.; Solá, M. *Organometallics* **1998**, *17*, 1492. (h) Vyboishchikov, S. F., Frenking, G. *Chem. Eur. J.* **1998**, *4*, 1428. (i) Beste, A.; Krämer, O.; Gerhard, A.; Frenking, G. *Eur. J. Inorg. Chem.* **1999**, 2037. (j) Frenking, G. *J. Organomet. Chem*. **2001**, *635*, 9.

[12] Wang, C.- C.; Wang, Y.; Liu, H.-J.; Lin, K.-J.; Chou, L.-K.; Chan, K.-S. *J. Phys. Chem. A* **1997**, *101*, 8887.

[13] Cases, M.; Frenking, G.; Durán, M.; Solá, M. *Organometallics*, **2002**, *21*, 4182.

free and coordinated carbenes for the *anti*-geometry is explained by means of a simple model based upon second-order perturbation theory.

2.1.2. Computational Details

All the calculations reported in this paper were obtained with the GAUSSIAN 98 suite of programs.[14] Electron correlation has been partially taken into account using the hybrid functional usually denoted as B3LYP[15] and the standard 6-31G* basis set[16] for hydrogen, carbon, oxygen and nitrogen and the Hay-Wadt small-core effective core potential (ECP) including a double-ξ valence basis set[17] for chromium or tungsten (LanL2DZ keyword). Zero-point vibrational energy (ZPVE) corrections have been computed at the B3LYP/6-31G* level and have not been corrected. Stationary points were characterized by frequency calculations[18] and have positive defined Hessian matrixes. Transition structures (TSs) show only negative eigenvalue in their diagonalized force constant matrixes, and their associated eigenvectors were confirmed to correspond to the motion along the reaction coordinate under consideration. Nonspecific solvent effects have been taken into account by using the self-consistent reaction field (SCRF) approach.[19] Donor-acceptor interactions and atomic charges have been computed using the Natural Bond Order (NBO)[20] method. The energies associated with these two-electron interactions have been computed according to the following equation:

[14] Gaussian 98, Revision A.5: Frisch, M. J.; Trucks, G. W.; Schlegel, H. B.; Scuseria, G. E.; Robb, M. A.; Cheeseman, J. R.; Zakrzewski, V. G.; Montgomery, J. A., Jr.;. Stratmann, R. E.; Burant, J. C.; Dapprich, S.; Millam, J. M.; Daniels, A. D.; Kudin, K. N.; Strain, M. C.; Farkas, O.; Tomasi, J.; Barone, V.; Cossi, M.; Cammi, R.;. Mennucci, B.; Pomelli, C.; Adamo, C.; Clifford, S.; Ochterski, J.; Petersson, G. A.; Ayala, P. Y.; Cui, Q.; Morokuma, K.; Malick, D. K.; Rabuck, A. D.; Raghavachari, K.; Foresman, J. B.; Cioslowski, J.; Ortiz, J. V.; Stefanov, B. B.; Liu, G.; Liashenko, A.; Piskorz, P.; Komaromi, I.; Gomperts, R.; Martin, R. L.; Fox, D. J.; Keith, T.; Al-Laham, M. A.; Peng, C. Y.; Nanayakkara, A.; Challacombe, M.; Gill, P. M. W.; Johnson, B.; Chen, W.; Wong, M. W.; Andres, J. L.; González, C.; Head-Gordon, M.; Replogle, E. S.; Pople, J. A. Gaussian, Inc., Pittsburgh, PA, 1998.

[15] (a) Becke, A. D. *J. Chem. Phys*. **1993**, *98*, 5648. (b) Lee, C.; Yang, W.; Parr, R. G. *Phys. Rev. B* **1988**, *37*, 785. (c) Vosko, S. H.; Wilk, L.; Nusair, M. *Can. J. Phys*. **1980**, *58*, 1200.

[16] Hehre, W. J.; Radom, L.; Scheleyer, P. v. R.; Pople, J. A. *Ab Initio Molecular Orbital Theory*; Wiley: New York, 1986, page 76 and references therein.

[17] Hay, P. J.; Wadt, W. R. *J. Chem. Phys*. **1985**, *82*, 299.

[18] McIver, J. W.; Komornicki, A. K. *J. Am. Chem. Soc*. **1972**, *94*, 2625.

[19] (a) Onsager, L. *J. Am. Chem. Soc.* **1936**, *58*, 1486. (b) Wong, M. W.; Wiberg, K. B.; Frisch, M. J. *J. Am. Chem. Soc.* **1992**, *114*, 523. (c) Wong, M. W.; Wiberg, K. B.; Frisch, M. J. *J. Am. Chem. Soc.* **1992**, *114*, 1645.

[20] (a) Foster, J. P.; Weinhold, F. *J. Am. Chem. Soc*. **1980**, *102*, 7211. (b) Reed, A. E.; Weinhold, F. J. *J. Chem. Phys*. **1985**, *83*, 1736. (c) Reed, A. E.; Weinstock, R. B.; Weinhold, F. *J. Chem. Phys*. **1985**, *83*, 735. (d) Reed, A. E.; Curtiss, L. A.; Weinhold, F. *Chem. Rev*. **1988**, *88*, 899.

$$\Delta E^{(2)}_{\phi\phi^*} = -n_\phi \frac{\langle \phi^* | \hat{F} | \phi \rangle}{\in_{\phi^*} - \in_{\phi}}$$

where $\hat{F}$ is the DFT equivalent of the Fock operator and ϕ and ϕ^* are two filled and unfilled Natural Bond Orbitals having $\in_\phi$ y $\in_{\phi^*}$ and energies, respectively; n_ϕ stands for the occupation number of the filled orbital.

2.1.3. Results and Discussion

Both free carbenes and their organometallic group 6 metal-carbene analogs may exist in two conformations, *syn* and *anti*, interchangeable by rotation through the C-heteroatom bond. Our study was initiated studing the comparative stability of free carbenes **6-9** and their pentacarbonylchromium(0) analogs **2**, **10**, **11** and **12**. Table 2 compiles the calculated energies for both classes of compounds. The optimized geometries of both isomers of complexes **2**, **10**, **11** and **12** are depicted in Figure 2. Except for the alkynyl-substituted carbene complex **12**, in all cases the *anti*-isomer was the more stable of both isomers. The difference in energies between the *anti*- and *syn*-isomers is considerably higher in the free carbenes **6-9** than in the metalla-carbenes **2**, **10**, **11** and **12**. These results are in full agreement with the reported X-ray structural data for complexes **1-3** (see Table 1).[4] The calculated preference of alkynyl-substituted carbene complex for the *syn*-isomer form is also concordant with the observed X-ray structure for [pentacarbonyl(phenylethynylmethoxy)carbene]chromium(0), **4**.[12]

Table 2. Relative energies ($\Delta E^{a,b}$, kcal mol^{-1}) of *anti* and *syn* conformations of carbenes **2**, **6-12**.

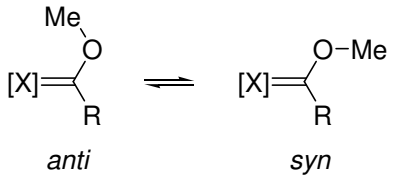

anti *syn*

ΔE / kcal mol^{-1}			
[X] = none		**[X] = $(CO)_5$Cr**	
6 R = Me	+7.3	**10** R = Me	+1.8
7 R = Ph	+9.7	**2** R = Ph	+1.3
8 R = CH=CH_2	+6.2	**11** R = CH=CH_2	+4.0
9 R = C≡CH	+2.9	**12** R = C≡CH	-1.6

[a]ΔE values computed as $\Delta E = E_{syn} - E_{anti}$. [b]All values have been calculated at the B3LYP/LANL2DZ&6-31G*+ΔZPVE level.

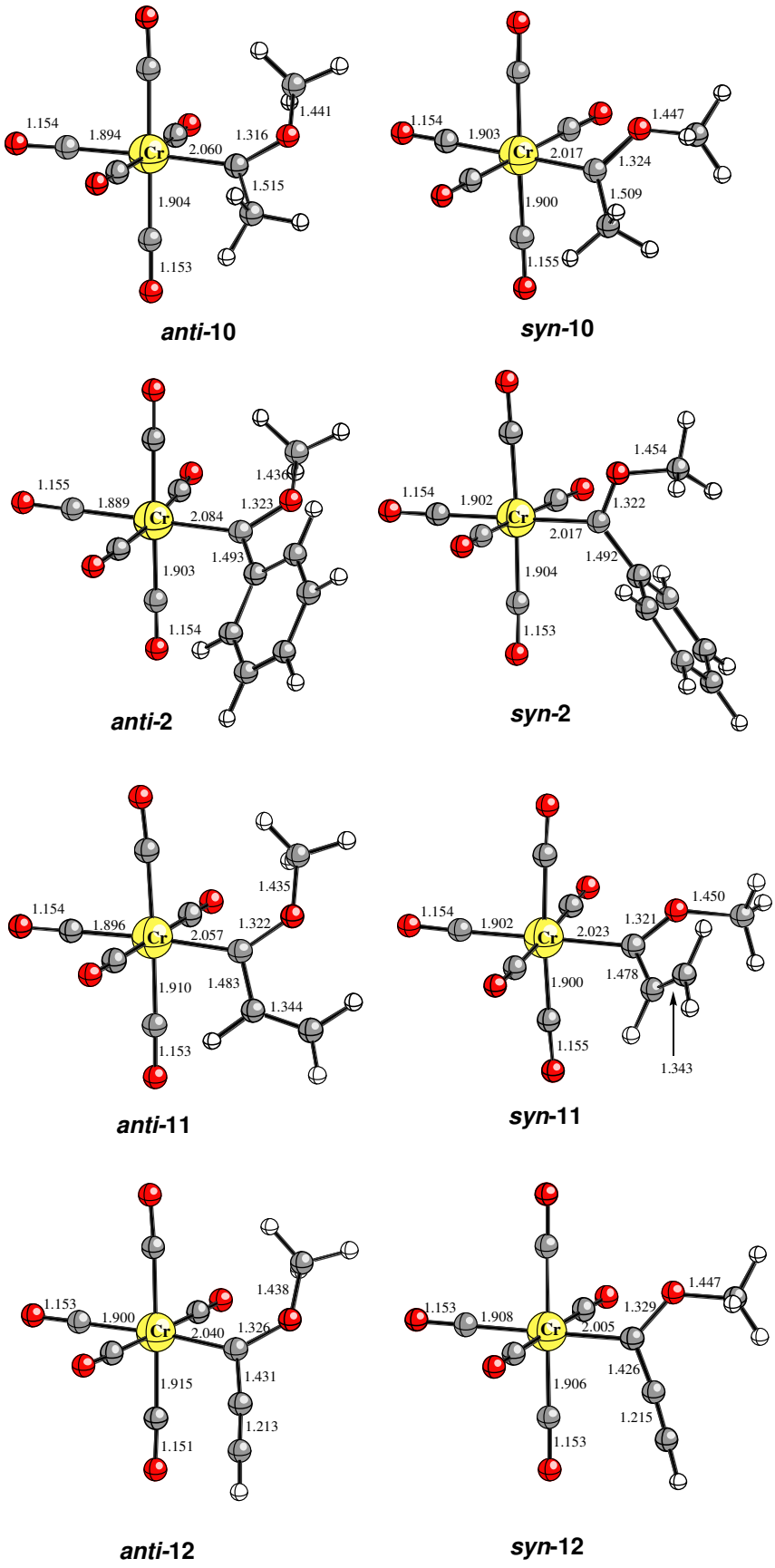

Figure 2. Chief geometrical data (B3LYP/LANL2DZ&6-31G* fully optimized structures) of *syn* and *anti* conformations of Fischer carbenes **2** and **10**-**12**. Bond distances are given in Å. Carbon, oxygen and hydrogen atoms are represented in grey, red and white, respectively.

The preference of both free **6**-**9** and complexed carbenes **2**, **10** and **11** for the *anti*-isomer may be explained on the basis of two additive effects. The *syn*-isomer has two unfavorable interactions. Free carbenes have a staggered interaction between the methyl group bonded to oxygen and the substituent in the carbene carbon. Additionally, free carbenes are also affected by the strong repulsive interaction between the carbene electron pair and the two nonbonding electron pairs of the oxygen (Figure 3). Clearly, this last interaction is not present in complexed carbenes**;** therefore the differences in energy between both isomers is reduced.

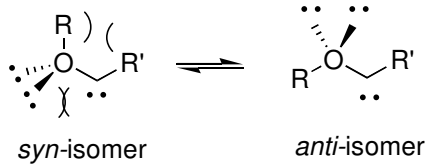

Figure 3. Conformational equilibrium in free singlet carbenes.

This reduction of the energy differences between both isomers would be exacerbated by the repulsive steric interaction that exists between the methyl group and the "CO-wall".[21] Nevertheless, there are three factors that minimize this interaction. The first one is the enlargement of the bond distance between the metal and the sp^2-hybridized atom of the carbene in the *anti* conformation (see Figure 2). The second factor is the staggered disposition of the carbene group and two CO-*cis* ligands flanking it. This staggered disposition is maintained in all complexes studied, independently of the isomer considered with dihedral angles OC–Cr–C–OMe having absolute values between 25.1˚ (complex ***syn*-11**) and -58.0˚ (complex ***anti*-2**). The conformational staggering should minimize the steric repulsion. The exception is complex ***syn*-2** which is in a nearly eclipsed conformation (dihedral angle OC–Cr–C–OMe = 8.4˚). In addition, the NBO analysis of compound **10** shows a two electron stabilizing interaction between the O-Me group hydrogens and the CO ligand *cis*-to the carbene moiety. Thus, the two electron donation from the σ_{CH} orbital of the O-Me group to the π^*_{CO} orbital of the CO-ligand (-0.21 kcal mol^{-1}) coupled to the feed-back donation of the π_{CO} orbital to the σ^*_{CH} orbital (-0.67 kcal mol^{-1}) results in a significant stabilizing contribution in the *anti*-isomer that is not present in the *cis*-isomer (Figure 4). The additive effect of all the contributions mentioned above (at least two contributions for each interaction mode)

[21] Hegedus, L. S. *Transition Metals in the Synthesis of Complex Organic Molecules 2nd Ed.* University Science Books, Sausalito, California, 1999.

renders the *anti*-isomer more favorable than the *syn*-isomer for chromium(0) alkoxy carbenes, in full agreement with experimental X-ray data. Even bulky substituents as menthyl groups linked to the oxygen maintain the *anti*-disposition despite the expected increased steric destabilization expected in these cases.[5c]

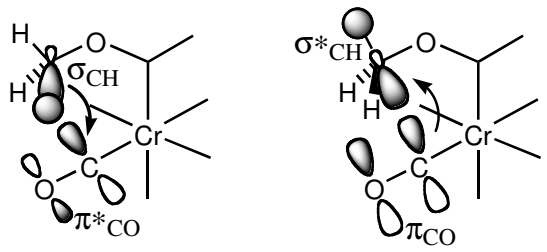

$\Delta E(2)$=-0.21 kcal mol^{-1} $\Delta E(2)$=-0.67 kcal mol^{-1}

Figure 4. Two-electron interactions and associated second-order perturbational energies between a methyl group and a CO ligand in *syn*-Fischer carbenes.

Alkynyl-substituted carbene complex **12** is the exception to the rule. In fact, in this case, according to our calculations, the *syn*-isomer is preferred by 1.6 kcal mol^{-1}. This result is supported by experimental data since complex **4** crystallized as the *syn*-isomer.[12] A considerable decrease in the difference of energies between *syn* and *anti*-isomers is also observed in the free carbene **9**, but in this case there is still a clear bias favoring the *anti*-isomer. The reasons for this change in behavior should be found in the linear structure of the triple bond. In this case, and according to our model, the decrease in the steric interaction between the triple bond and the methyl group of the carbene may approach the energies of both isomers. In fact, this may serve as a probe to evaluate the relative participation between the steric repulsion and the electronic destabilization. Clearly, and according to the relative energies shown in Table 1, it is the steric repulsion between the groups attached to the carbene carbon rather than the electronic repulsion that is responsible for the bias toward the *anti-isomer*. This trend is also maintained in compounds having linear allene substitutents linked to the carbene carbon.[5s] Coordination of the triple bond to a $Co_2(CO)_6$ fragment results in the recovering of the usual *anti*-disposition.[4h,5m]

X-ray data for the structures of ethoxy-substituted complexes show in some cases a significant shortening of the [C–C]-O bond that could be as short as 1.45 Å.[5k,5n,5p] Our calculated optimized structures for *syn*- and *anti*-conformations of complexes **1** and **15** are depicted in Figure 5.

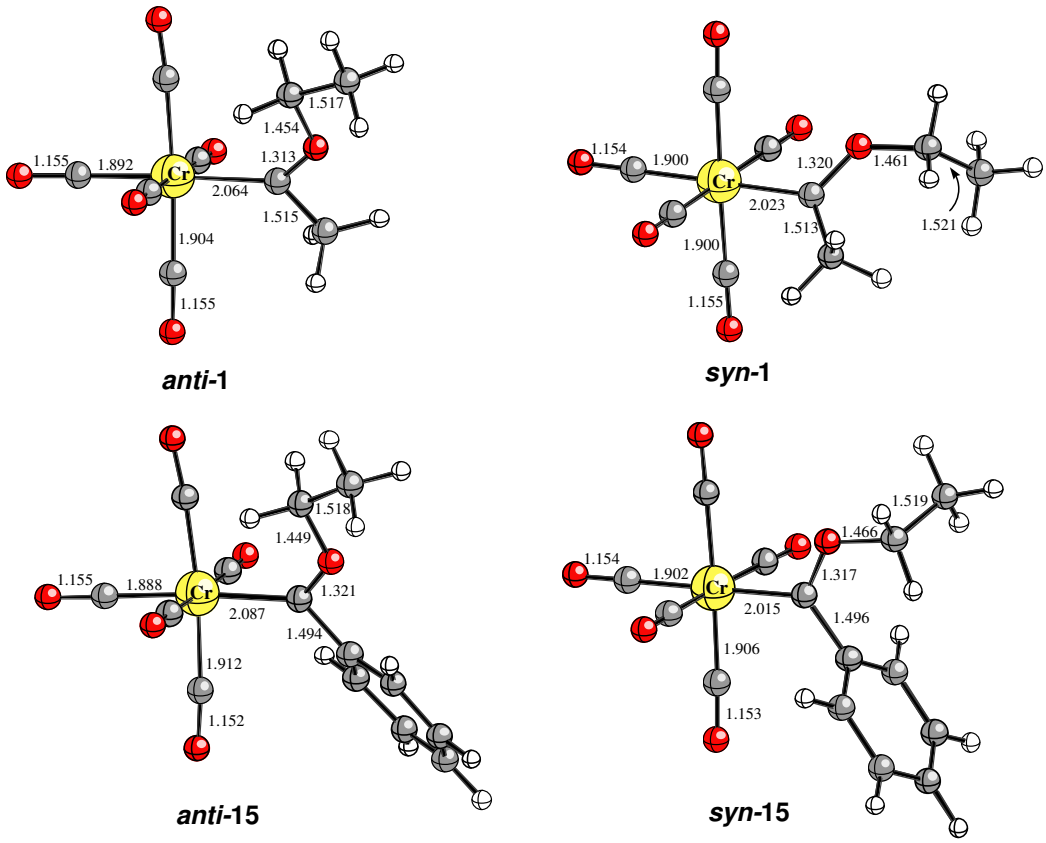

Figure 5. Chief geometrical data (B3LYP/LANL2DZ&6-31G* fully optimized structures) of *syn*- and *anti*-conformations of Fischer carbenes **1** and **15.** See Figure 2 caption for additional details.

Our model again explains the bias for the *anti*-isomer both in the free and coordinated carbenes (Table 3). These results are also confirmed by neutron diffraction measurements.[6] However, the calculated [C–C]-O distances (1.517 and 1.518 Å for complexes **1** and **15**, respectively) are the expected for a single $\sigma_{C\text{-}C}$ bond. The dihedral angles OC–Cr–C–OEt of complexes **1** and **15** follow the same trend as their methoxy analogues. Again, with the exception of ***syn*-15** (OC–Cr–C–OEt = 4.5˚), which is close to an eclipsed conformation, the remaining compounds are in a staggered disposition.

Table 3. Relative energies (ΔE,[a,b] kcal mol^{-1}) of *anti* and *syn* conformations of carbenes **1**, **13**-**15**.

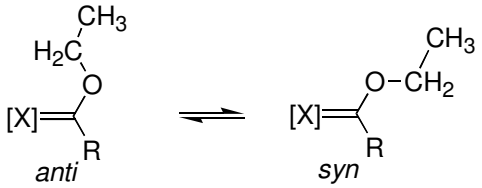

ΔE (kcal mol^{-1})			
[X] = none		**[X] = $(CO)_5$Cr**	
13 R = Me	+7.5	**1** R = Me	+2.9
14 R = Ph	+10.0	**15** R = Ph	+1.7

[a]ΔE values computed as $\Delta E=E_{syn}-E_{anti}$. [b]All values have been calculated at the B3LYP/LANL2DZ&6-31G*+ΔZPVE level.

There are, in principle, two alternative hypotheses to explain the shortening effect of the $\sigma_{O\text{-}C\text{-}C}$. It might be a consequence of a stereolectronic effect involving donation of electron density from the σ_{CH} orbital to the σ^*_{CO} orbital placed in an antiperiplanar disposition (Table 4). This donation would result in the shortening of the [C–C]-O bond while elongating the C–H bond. This model is a simple orbital description of the inductive effect exerted by the oxygen onto the adjacent C–C bond. Within this hypothesis higher positive charges onto the oxygen should result in shorter adjacent C–C bonds. The magnitude of this donation was evaluated on the basis of the donor-acceptor interactions in the NBO analysis using ethanol, ethylmethyl ether, *O*-ethylformaldehyde, and complexes **1** and **15**. Table 4 compiles the results obtained in these calculations.

Table 4. C-C Bond distances[a] ($d_{C\text{-}C}$, Å) and second-order perturbational energies[a,b] ($\Delta E(2)$, kcal mol^{-1}) associated with two-electron interactions between σ_{CH} and σ^*_{CO} localized orbitals in several ethoxy derivatives.

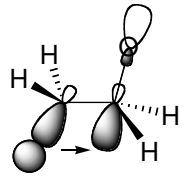

		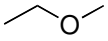	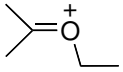	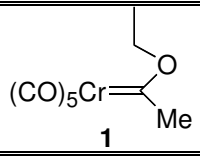 **1**	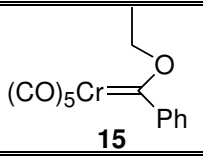 **15**
$\Delta E(2)$	-3.99	-3.91	-7.06	-4.69	-4.65
$d_{C\text{-}C}$	1.519	1.520	1.508	1.517	1.519

[a]Properties computed at the B3LYP/LANL2DZ&6-31G* level. [b]Calculated by means of eq. 1.

Data in Table 4 show clearly the stronger donation from the ethyl group in formaldehyde with a positive charge on the oxygen ($\Delta E(2)$ = –7.06 kcal mol^{-1}) compared to either the alcohol or the ether ($\Delta E(2)$ = –3.99 and –3.91 kcal mol^{-1}, respectively). Complexes **1** and **15** are closer in the value of $\Delta E(2)$ to neutral alcohols than to ethylated formaldehyde. In any case, the expected shortening of the [C–C]-O bond was observed. To obtain more accurate geometries, the basis set for the explicit electrons of chromium was augmented with a set of f-polarization functions.[22] The ethoxy [C–C]-O distance remained invariant also in these conditions.

This failure to explain the observed bond shortening by applying an inductive model led us to consider an alternative explanation. In fact, the bond shortening is clearly seen in X-ray diffraction structural determinations,[5] but it is not present in the structure of [pentacarbonyl(ethoxymethyl)carbene]chromium(0) obtained by neutron diffraction.[6] Therefore, it can be thought that the anomalous shortening seen in some ethoxy-carbene complexes may be due to the packing in the crystal. To simulate the condensed phase[19] we repeated the calculations carried out on complex **15** but now using a dielectric constant ε = 7, conditions that would favor the contribution of the corresponding polar hyperconjugative forms. Again, our efforts meet no success. The [C–C]-O was not affected by these new conditions. Therefore, although crystal packing may be responsible for this effect, we have been so far unable to model the shortening of the [C–C]-O bond experimentally observed in some cases.

[22] Ehlers, A. W.; Böhme, M.; Dapprich, S.; Gobbi, A.; Höllwarth, A.; Jonas, V.; Köhler, K. F.; Stegman, R.; Veldkam, A.; Frenking, G. *Chem. Phys. Lett.* **1993**, *208*, 111.

The question of the *syn/anti* isomerization was addressed next. The experimental activation energy for this transformation in methoxymethylchromium(0)-carbene complex resulted to be 12.4±1 kcal mol^{-1}.[23] Figure 6 represents the calculated coordinate of reaction for the ***anti*-10** to ***syn*-10** isomerization. According to our calculations, the activation energy associated with this process has a value of 14.3 kcal mol^{-1} for complex **10** and decreases to 11.1 kcal mol^{-1} for complex **2**. The dihedral angle Me–C(Cr)–O-Me changes from an initial value of –178.2˚ in the *anti*-isomer to a –91.9˚ in the transition structure **TS1**. It should be noted that the staggered conformation of the carbene moiety and the *cis*-CO ligands is maintained in the transition state. The final dihedral for the *syn*-isomer is 0.0˚, which is again in a staggered conformation. The behavior of phenyl-substituted carbene complex is similar, although in this case the dihedral Ph–C(Cr)–O-Me on the transition state **TS2** is slightly larger (-103.8º) than in the methyl substituted analogue. This is maintained in the *syn*-isomer. It is worthy to note that the staggered disposition of the carbene is maintained during the *syn-anti* isomerization process that occurs by rotation across the C(Cr)–O-Me without affecting the Cr=C bond and therefore the coordination sphere of chromium. Our calculated energies for the *syn-anti* isomerization barrier match those experimentally determined by NMR.

Experimentally, the solvent has a strong effect on the *anti-syn* isomer ratio of alkoxy Fischer carbenes.[23] Thus, this ratio changes from 50:50 (acetone-d_6) to 90:10 in Cl_3CD in complex **10**. This points to a strong difference in the polarity of both forms, with the *syn*-isomer being more polar. Therefore, this is the preferred isomer in the more polar acetone solvent. The calculated ΔE(*anti-syn)* for both isomers in different solvents ranging from gas phase ($\varepsilon = 1$) to MeOH ($\varepsilon = 32.63$)[24] are compiled in Table 5, together with the ΔE_a for the isomerization process. Clearly, the effect of the solvent change on ΔE_a is not significant. The *syn*-isomer is more stable in polar solvents than in apolar solvents, in full agreement with the NMR data. Since the calculated dipolar moment of the *ant*- isomer of complex **10** has a value of 4.14 D and that of its *syn*-isomer is 6.36 D, with the value for **TS1** being 3.84 D, the small effect of the polarity on the ΔE_a derives from its decreased polarity compared to the *anti* isomer, while the preference for the *syn*

[23] (a) Kreiter, C. G.; Fischer, E. O. *Angew. Chem.* **1969**, *81*, 780; *Angew. Chem. Int. Ed. Engl.* **1969**, *8*, 761. (b) Kreiter, C. G.; Fischer, E. O. *Pure Appl. Chem.* **1971**, *6*, 151. A theoretical value of 18.3 kcal*mol^{-1} has been previously calculated for this isomerization, see: (c) Marynick, D. S.; Kirkpatrick. C. M. *J. Am. Chem. Soc.* **1985**, *107*, 1993.

[24] Reichardt, C. *Solvents and Solvents Effetcs in Organic Chemistry*, VCH Publishers, Weinheim, 1990.

form in polar solvents may be explained through a Coulombic stabilization of this more polar isomer. Even more, the conditions in the crystal should resemble those of the vacuum since only the *anti*-isomer is mainly observed in the different examples reported in the literature.[4]

Table 5. Calculated Δ*E*(*anti-syn)* for both isomers in different solvents ranging. All values have been calculated at the B3LYP/LANL2DZ&6-31G*+ΔZPVE level.

ε (solvent)	**ΔE_a / kcalmol^{-1}**	**Δ*E*(*anti-syn*) /kcalmol^{-1}**	**Relative amounts of *anti-syn*[23]**
1 (gas phase)	14.3	1.8	–
4.9 ($CHCl_3$)	14.5	0.2	90:10
5.621 (chlorobenzene)	14.5	0.1	84:16
20.7 (acetone)	14.6	-0.4	50:50
32.63 (MeOH)	14.6	-0.5	61:39

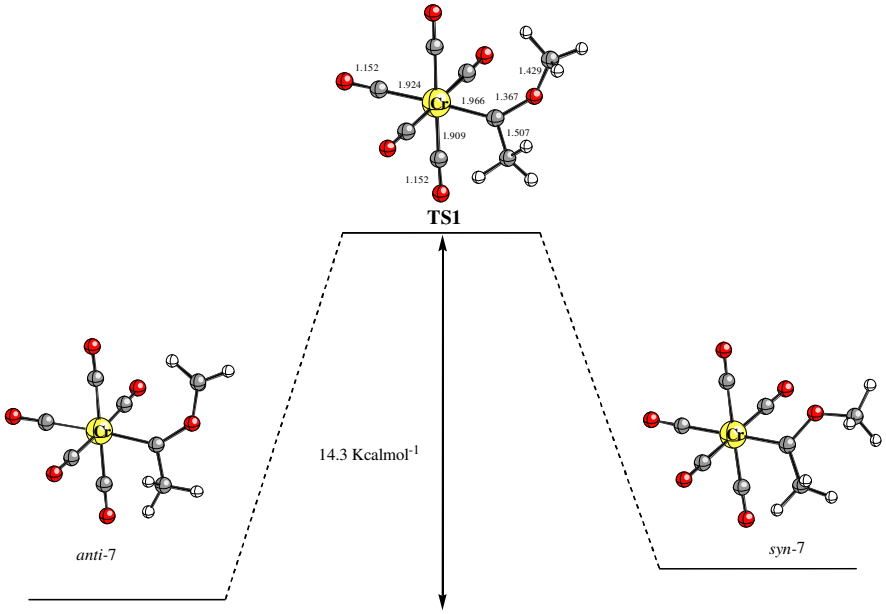

Figure 6. Main geometric features and relative energy of transition structure **TS1** associated with *syn-anti* isomerization of Fischer carbene **10**. All values have been obtained at the B3LYP/LANL2DZ&6-31G*(+ΔZPVE) level. See Figure 2 caption for additional details.

To conclude this study, the pentacarbonyl[ethoxymethyltungsten(0)]carbene, **16**, was studied. The optimized structures for both *syn* and *anti*-isomers are depicted in Figure 7. The bias for the *anti*-isomer (2.8 kcal mol^{-1}), as well as the staggered conformation of the carbene ligand and the *cis*-CO ligands, is maintained also in these cases, thus indicating that the model reported above can be extended to other Fischer carbenes.

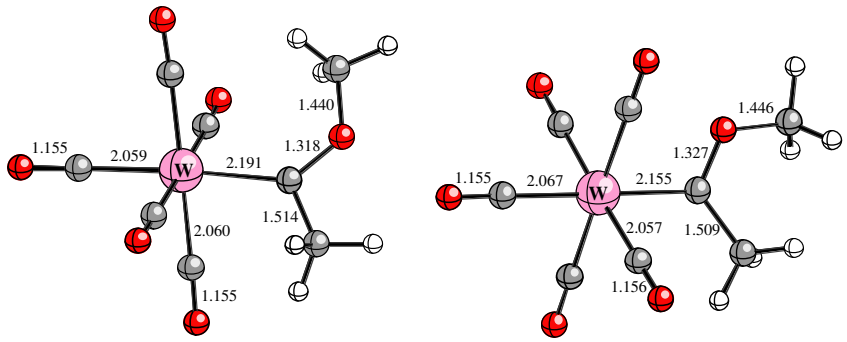

Figure 7. Main geometrical features of *syn*- and *anti*-conformations of tungsten Fischer carbene **16**. See Figure 2 caption for additional details.

2.1.4. Conclusions

A systematic DFT study of free and Cr- and W-coordinated alkoxy-carbenes has shown that the structure of the free carbenes does not vary significantly by coordination to the metal. Although of lower magnitude than in their free analogues, a clear bias for the *anti*-isomer is observed in the free and coordinated carbenes with the exception of complexes having alkynyl substituents. In this latter case, the metal complex prefers the *syn*-disposition. According to our model, the observed bias for the *anti*-conformer in Fischer alkoxy carbenes can be explained in terms of the stabilizing contribution of a stereoelectronic effect due to the two electron donation from the σ_{CH} orbital of the O-Me group to the π^*_{CO} orbital of the CO-ligand and feedback donation of the π_{CO} orbital to the σ^*_{CH} orbital and the destabilizing repulsion between the groups linked to the carbene carbon. This latter factor is the determinant one since the linear triple bond produces a clear bias for the *syn*-isomer only in the coordinated carbene, showing that the steric contribution rather than the electronic repulsion is responsible for the structure of group 6 Fischer carbenes. Finally, the *anti-syn* isomerization in chromium(0)-carbene complexes occurred by simple rotation around the C-O bond without affecting the carbene ligand.

2.2. Computational and Experimental Studies on the Mechanism of the Photochemical Carbonylation of Group 6 Fischer Carbene Complexes

2.2. Computational and Experimental Studies on the Mechanism of the Photochemical Carbonylation of Group 6 Fischer Carbene Complexes

2.2.1. Introduction

Nowadays Fischer carbene complexes are reagents of general use in organic and organometallic chemistry.[1] The scope of the extremely rich thermal reactivity of these complexes has been recently widened by the report from ourselves[2] and from other groups[3] on the possibility to effect the catalytic transmetallation from group 6 metal-carbene complexes to other transition metals, opening opportunities to explore new reactivity based on these compounds. Our recently reported[4] photochemically induced dyotropic rearrangements of chromium(0) aminocarbene complexes, unambiguously demonstrate that there are also opportunities to discover new photo-processes of these complexes. However, despite the enormous amount of work dedicated to the chemistry of these complexes their reaction mechanisms have been barely studied. This is an important point, since even apparently simple processes like the addition of

---

[1] Selected reviews in the chemistry and synthetic applications of Fischer carbene complexes: (a) K. H. Dötz, H. Fischer, P. Hofmann, R. Kreissel, U. Schubert, K. Weiss, *Transition Metal Carbene Complexes*, Verlag Chemie: Deerfield Beach, Florida, 1983; (b) K. H. Dötz, *Angew. Chem. Int. Ed. Eng.* **1984**, *23*, 587; (c) W. D. Wulff, in *Comprehensive Organic Synthesis,* B. M. Trost, I. Fleming, Eds.. Pergamon: Oxford, 1991; vol. 5, pp. 1065; (d) M. A. Schwindt, J. R. Miller, L. S. Hegedus, *J. Organomet. Chem.* **1991**, *413*, 143; (e) H. Rudler, M. Audouin, E. Chelain, B. Denise, R. Goumont, A. Massoud, A. Parlier, A. Pacreau, M. Rudler, R. Yefsah, C. Álvarez, F. Delgado-Reyes, *Chem. Soc. Rev.* **1991**, *20*, 503; (f) D. B. Grötjahn, K. H. Dötz, *Synlett* **1991**, 381; (g) W. D. Wulff, in *Comprehensive Organometallic Chemistry II,* Abel, E. W.; Stone, F. G. A.; Wilkinson, G.; Eds. Pergamon: Oxford. 1995; vol. 12, pp. 470; (h) L. S. Hegedus, in *Comprehensive Organometallic Chemistry II,* Abel, E. W.; Stone, F. G. A.; Wilkinson, G.; Eds. Pergamon: Oxford. 1995; vol. 12, pp. 549; (i) D. F. Harvey, D. M. Sigano, *Chem. Rev.* **1996**, *96*, 271; (j) L. S. Hegedus, *Tetrahedron* **1997**, *53*, 4105; (k) R. Aumann, H. Nienaber, *Adv. Organomet. Chem.* **1997**, *41*, 163; (l) B. Alcaide, L. Casarrubios, G. Domínguez, M. A. Sierra, *Curr. Org. Chem.* **1998**, *2*, 551; (m) M. A. Sierra, *Chem. Rev.* **2000**, *100*, 3591; (n) J. Barluenga, F. J. Fañanás, *Tetrahedron* **2000**, *56*, 4597.

[2] (a) M. A. Sierra, M. J. Mancheño, E. Sáez, J. C. del Amo, *J. Am. Chem. Soc.* **1998**, *120*, 6812; (b) M. A. Sierra, J. C. del Amo, M. J. Mancheño, M. Gómez-Gallego, *J. Am. Chem. Soc.* **2001**, *123*, 851; (c) M. A. Sierra, J. C. del Amo, M. J. Mancheño, M. Gómez-Gallego, M. R. Torres, *Chem. Commun.* **2002**, 1842; (d) J. C. del Amo, M. J. Mancheño, M. Gómez-Gallego, M. A. Sierra, *Organometallics* **2004**, *23*, 5021.

[3] (a) H. Sakurai, K. Tanabe, K. Narasaka, *Chem. Lett*. **1999**, 309; (b) H. Sakurai, K. Tanabe, K. Narasaka, *Chem. Lett*. **2000**, 168; (c) M. Yamane, Y. Ishibashi, H. Sakurai, K. Narasaka, *Chem. Lett*. **2000**, 174; (d) J. Barluenga, L. A. López, O. Löber, M. Tomás, S. García-Granda, C. Álvarez-Rúa, J. Borge, *Angew. Chem. Int. Ed.* **2001**, *40*, 3392; (e) R. Aumann, I. Göttker-Schnetmann, R. Fröhlich, O. Meyer, *Eur. J. Org. Chem.* **1999**, 2545; (f) R. Aumann, I. Göttker-Schnetmann, R. Fröhlich, O. Meyer, *Eur. J. Org. Chem.* **1999**, 3209; (g) I. Göttker-Schnetmann, R. Aumann, *Organometallics* **2001**, *20,* 346; (h) I. Göttker-Schnetmann, R. Aumann, K. Bergander, *Organometallics* **2001**, *20*, 3574; (i) C. Albéniz, P. Espinet, R. Manrique, A. Pérez-Mateo, *Angew. Chem. Int. Ed.* **2002**, *41*, 2363; (j) J. Barluenga, P. Barrio, L. A. López, M. Tomás, S. García-Granda, C. Álvarez-Rúa, *Angew. Chem. Int. Ed.* **2003**, *42*, 3008; (k) J. Barluenga, R. Vicente, L. A. López, E. Rubio, M. Tomás, C. Álvarez-Rúa, *J. Am. Chem. Soc.* **2004**, *126*, 470.

[4] M. A. Sierra, I. Fernández, M. J. Mancheño, M. Gómez-Gallego, M. R. Torres, F. P. Cossío, A. Arrieta, B. Lecea, A. Poveda, J. Jiménez-Barbero, *J. Am. Chem. Soc.* **2003**, *125*, 9572.

nucleophiles to α,β-unsaturated carbene complexes have been recently shown to occur by pathways more complex than a simple addition to the metal.[1k,1n,5]

The initial proposal by Hegedus in 1988 that the irradiation of chromium(0) carbene complexes promotes a carbonylation process to produce ketene-like species,[6] systematized the photochemistry of group 6 carbene complexes in the presence of nucleophiles, and opened gates to a varied and efficient entry to ketene derived products.[1d,h,j] Despite the synthetic efficiency of these reactions, very little is still known about the intimacies of the mechanism of the main photochemical process. In this work "some light will be seed" about this fundamental process of group 6 metal carbene complexes.

The UV-visible spectra of Fischer metal-carbene complexes[7] shows three well defined absorptions: a forbidden metal-ligand charge transfer (MLCT) absorption around 500 nm, the allowed low energy ligand-field (LF) absorption in the range of 350-450 nm and the high energy LF absorption in the range of 300-450 nm. The two LF absorptions generally overlap. These absorptions are attributable to electronic transitions from the higher nonbonding metal centered b_2 occupied orbital to the empty carbene centered $2b_1$ (MLCT), $2a_1$ (low energy LF) and $3a_1$ (high energy LF) orbitals, respectively (Figure 1).

[5] Recent examples from our laboratories: (a) M. A. Sierra, M. J. Mancheño, J. C. del Amo, I. Fernández, M. Gómez-Gallego, *Chem. Eur. J.* **2003**, *9*, 4943; (b) P. Ramírez-López, M. Gómez-Gallego, M. J. Mancheño, M. A. Sierra, M. Bilurbina, S. Ricart, *J. Org. Chem.* **2003**, *68*, 3538; (c) M. A. Sierra, P. Ramírez, M. Gómez-Gallego, T. Lejon, M. J. Mancheño, *Angew. Chem. Int. Ed.* **2002**, *41*, 3442.
[6] L. S. Hegedus, G. deWeck, S. D'Andrea, *J. Am. Chem. Soc.* **1988**, *110*, 2122.
[7] H. C. Foley, L. M. Strubinger, T. S. Targos, G. L. Geoffroy, *J. Am. Chem. Soc.* **1983**, *105*, 3064.

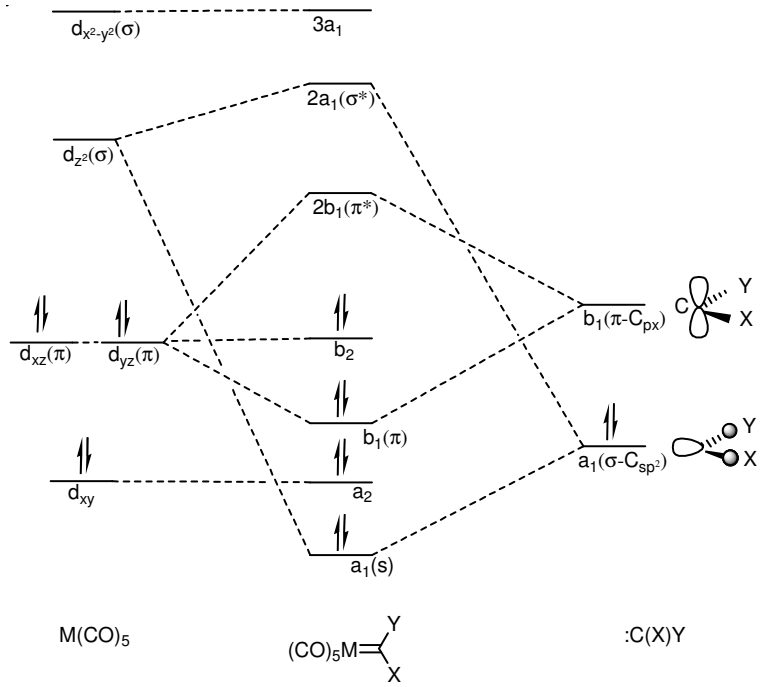

Figure 1. Canonical molecular orbitals corresponding to the octahedral structure of Fischer carbenes at the ground state.

Most of the mechanistic photochemical studies carried on this kind of complexes focused on the irradiation on LF bands. These photo-processes usually result in the extrusion of a CO ligand. Thus, activation of the high energy LF band of the $[(CO)_5W{=}C(OMe)Ph]$ results in the dissociation of one of the four *cis*-CO ligands,[7] while the irradiation of the low energy LF band provokes the lost of the *trans*-CO ligand.[8] CO-Photoextrusion leads to a long-life intermediate having a tetracarbonylcarbene structure (Scheme 1, equation a). It has been proposed that the free coordination site of these species is blocked by an agostic interaction with a C–H bond of the neighbor alkoxy-group (curved arrow in Scheme 1).[9] Matrix photolysis studies on the MLCT band of Cr and W Fischer carbene complexes resulted in the isomerization from the most stable *anti*-isomer to the less stable *syn*-isomer (Scheme 1, equation b).[10] None of these processes have found application in the chemical synthesis of relevant compounds.

---

[8] P. C. Servaas, D. J. Stufkens, A. Oskam, *J. Organomet. Chem.* **1990**, *390*, 61.

[9] (a) J. N. Bechara, S. E. J. Bell, J. J. McGarvey, A. D. Rooney, *J. Chem. Soc., Chem. Commun*. **1986**, 1785; (b) S. E. J. Bell, K. C. Gordon, J. J. McGarvey, *J. Am. Chem. Soc*. **1988**, *110*, 3107.

[10] (a) A. D. Rooney, J. J. McGarvey, K. C. Gordon, R. A. McNicholl, U. Schubert, W. Hepp, *Organometallics* **1993**, *12*, 1277; (b) A. D. Rooney, J. J. McGarvey, K. C. Gordon, *Organometallics* **1995**, *14*, 107; (c) For a complete theoretical discussion on the *anti-syn* isomerization of group 6 metal carbene complexes, see: I. Fernández, F. P. Cossío, A. Arrieta, B. Lecea, M. J. Mancheño, M. A. Sierra, *Organometallics* **2004**, *23*, 1065.

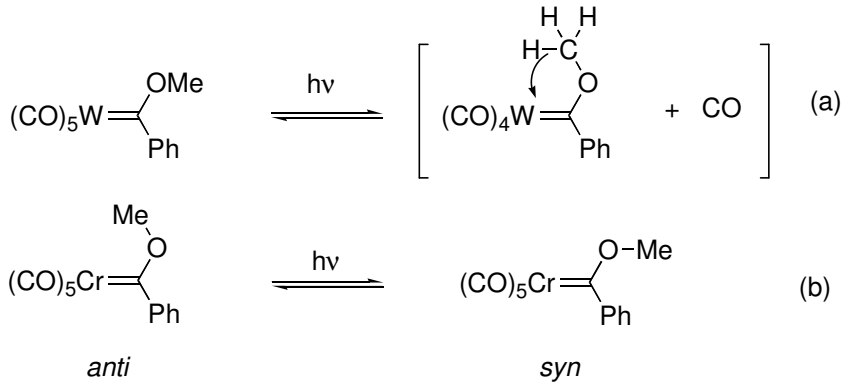

Scheme 1

The seminal finding by McGuire and Hegedus[11] demonstrating that Cr and Mo (but not W) Fischer carbene complexes when exposed to sun light in the presence of an imine formed a β-lactam in almost quantitative yield turned out to be a general reaction. As stated above the intermediacy of ketene-like species formed by the reversible insertion of a *cis*-CO ligand onto the M=C bond was postulated by Hegedus in 1988 on the basis of indirect evidences.[6] This hypothesis is reasonable since the irradiation on the MLCT band should promote one electron from the metal-centered HOMO orbital to the carbene-carbon centered LUMO orbital. Formally, this is the one-electron oxidation of the metal which is known to facilitate the CO-insertion on M–C bonds.[12] However, and despite the synthetic usefulness of this process, the many efforts directed to experimentally detect these ketene-like species have been up to date fruitless.[13] Strikingly, the reverse isomerization metal-bonded ketene to carbene complexes has been reported by Gröthjan on an Ir-nucleus (Scheme 2).[14]

---

[11] (a) M. A. McGuire, L. S. Hegedus, *J. Am. Chem. Soc.* **1982**, *104*, 5538; (b) L. S. Hegedus, M. A. McGuire, L. M. Schultze, C. Yijun, O. P. Anderson, *J. Am. Chem. Soc.* **1984**, *106*, 2680.

[12] J. P. Collman, L. S. Hegedus, J. R. Norton, R. G. Finke, *Principles and Applications of Organotransition Metal Chemistry*, University Science Books, Mill Vlley (CA), 1987, pp. 373-375.

[13] (a) H. Gut, N. Welte, U. Link, H. Fischer, U. E. Steiner *Organometallics*, **2000**, *19*, 2354; (b) M. L. Gallagher, J. B. Greene, A. D. Rooney, *Organometallics*, **1997**, *16*, 5260; (c) K. O. Doyle, M. L. Gallagher, M. T. Pryce, A. D. Rooney, *J. Organomet. Chem.* **2001**, *617-618*, 269.

[14] (a) D. B. Gröthjan, G. A. Bikzhanova, L. S. B. Collins, T. Concolino, K. C. Lam, A. L. Rheingold, *J. Am. Chem. Soc.* **2000**, *122,* 5222; (b) H. Urtel, G. A. Bikzhanova, D. B. Gröthjan, P. Hofmann, *Organometallics*, **2001**, *20*, 3938; (c) D. B. Gröthjan, L. S. B. Collins, M. Wolpert, G. A. Bikzhanova, H. C. Lo, D. Combs, J. L. Hubbard, *J. Am. Chem. Soc.* **2001**, *123,* 8260.

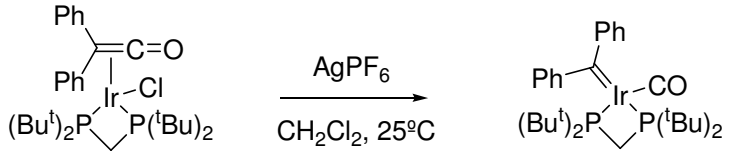

Scheme 2

Our preliminary contribution to understand the mechanisms of photochemical reactivity of chromium(0) carbene complexes and imines by using a combination of experimental and theoretical methods,[15] assumed as the starting point of the reaction a preformed metallo-ketene. DFT-Calculations carried out in three different model carbenes including methylene, dihydroxymethylenepentacarbonyl and methylenephosphinetetracarbonylchromium(0) complexes, show that the effect of the ligands on the carbonylation process is a reasonable probe to study this fundamental organometallic reaction. Reported herein is a detailed DFT-study of the carbonylation of group 6 metal-carbene complexes promoted by light. Experimental support for the main conclusions will be presented, together with theoretical arguments that explain the difficulties in the experimental detection of the photo-generated intermediates.

2.2.2. Computational Details

All the calculations reported in this paper were obtained with the GAUSSIAN 98 suite of programs.[16] Electron correlation has been partially taken into account using the hybrid functional usually denoted as B3LYP[17] and the standard 6-31G* or 6-31+G* basis sets[18] for hydrogen, carbon, oxygen, nitrogen, and phosphorus, and the Hay-Wadt small-core effective core potential (ECP) including a double-ξ valence basis set[19] for chromium or tungsten (LANL2DZ keyword). We shall denote these basis sets schemes

---

[15] A. Arrieta, F. P. Cossío, I. Fernández, M. Gómez-Gallego, B. Lecea, M. J. Mancheño, M. A. Sierra, *J. Am. Chem. Soc.* **2000**, *122*, 11509.

[16] Gaussian 98, Revision A.11.3, M. J. Frisch, G. W. Trucks, H. B. Schlegel, G. E. Scuseria, M. A.Robb, J. R. Cheeseman, V. G. Zakrzewski, J. A. Montgomery, Jr.,R. E. Stratmann, J. C. Burant, S.Dapprich, J. M. Millam, A. D. Daniels, K. N. Kudin, M. C. Strain, O. Farkas, J. Tomasi, V. Barone, M. Cossi,R. Cammi, B. Mennucci, C. Pomelli, C. Adamo,S. Clifford, J. Ochterski, G. A. Petersson, P. Y. Ayala, Q. Cui, K. Morokuma, N. Rega, P. Salvador, J. J. Dannenberg, D. K. Malick, A. D. Rabuck, K. Raghavachari, J. B.Foresman, J. Cioslowski, J. V. Ortiz, A. G. Baboul, B. B. Stefanov, G. Liu, A. Liashenko, P. Piskorz, I.Komaromi, R. Gomperts, R. L. Martin, D. J. Fox, T. Keith, M. A. Al-Laham, C. Y. Peng, A. Nanayakkara, M.Challacombe, P. M. W. Gill, B. Johnson, W. Chen, M. W. Wong, J. L. Andres,C. Gonzalez, M. Head-Gordon, E. S. Replogle, and J. A. Pople,Gaussian, Inc., Pittsburgh PA, 2002.

[17] (a) A. D. Becke, *J. Chem. Phys.* **1993**, *98*, 5648; (b) C. Lee, W. Yang, R. G. Parr, *Phys. Rev. B* **1998**, *37*, 785; (c) S. H. Vosko, L. Wilk, M. Nusair, *Can. J. Phys.* **1980**, *58*, 1200.

[18] W. J. Hehre, L. Radom, P. v. R. Scheleyer, J. A. Pople, *Ab Initio Molecular Orbital Theory*; Wiley: New York, 1986, page 76 and references therein.

[19] P. J. Hay, W. R. Wadt, *J. Chem. Phys.* **1985**, *82*, 299.

as LANL2DZ&6-31G(d) and LANL2DZ&6-31+G(d) respectively. Zero point vibrational energy (ZPVE) corrections have been computed at the same level and have not been corrected. Excited states were located at the CIS level[20] and triplets were optimized at the uB3LYP level. Stationary points were characterized by frequency calculations[21] and have positive defined Hessian matrices. Transition structures (TSs) show only one negative eigenvalue in their diagonalized force constant matrices, and their associated eigenvectors were confirmed to correspond to the motion along the reaction coordinate under consideration. Bond orders and atomic charges have been computed using the Natural Bond Order (NBO)[22] method.

2.2.3. Results and Discussion

Model complex **1a** was used to tune up our theoretical model. The different excited states of complex **1a** were computed by using the configuration interaction method at the CIS level. The S_0 geometry of complex **1a** was optimized at the B3LYP/LANL2DZ&6-31+G(d) level. The most stable excited state of complex **1a** is a triplet (T_1) having the vertical excitation energy of 1.06 eV, with the first singlet (S_1) resting 1.42 eV above T_1. The structure of this first triplet was optimized at the UB3LYP/LANL2DZ&6-31+G(d) level leading to the structure **2a** which lies 22.0 kcal mol^{-1} (0.95 eV) above S_0. An additional S_0 stationary point denoted as **1a'** was also optimized. In this case the methylene moiety is co-planar with two co-linear equatorial CO-groups whilst **1a** has the CH_2-moiety bisecting the plane defined by two adjacent equatorial CO-groups. According to our results, **1a'** has an imaginary frequency associated with the rotation of the CH_2-fragment around the Cr–C bond and lays only 0.3 kcal mol^{-1} above **1a**. Distortion of the symmetry group of **1a'** coupled to the optimization of the resulting triplet state produced structure **3a**. Triplet **3a** is 17.4 kcal mol^{-1} more stable than **2a** (the triplet derived from **1a**) and is only 4.6 kcal mol^{-1} above the S_0 of **1a** (Figure 2). It is worthy to note that the triplet **3a** corresponds with the chromacyclopropanone (or chromium-coordinated ketene) proposed by Hegedus to

[20] These computations were preformed at the configuration interaction singles (CIS) level of theory starting from the HF wave-function. See: J. B. Foresman, M. Hedd-Gordon, J. A. Pople, M. J. Frisch, *J. Phys. Chem.* **1992**, *96*, 135.
[21] J. W. McIver, A. K. Komornicki, *J. Am. Chem. Soc.* **1972**, *94*, 2625.
[22] (a) J. P. Foster, F. Weinhold, *J. Am. Chem. Soc*. **1980**, *102*, 7211; (b) A. E. Reed, F. J. Weinhold, *J. Chem. Phys*. **1985**, *83*, 1736; (c) A. E. Reed, R. B. Weinstock, F. Weinhold, *J. Chem. Phys*. **1985**, *83*, 735; (d) A. E. Reed, L. A. Curtiss, F. Weinhold, *Chem. Rev*. **1988**, *88*, 899.

explain the reaction products obtained in the photochemical reaction of chromium(0) carbene complexes.

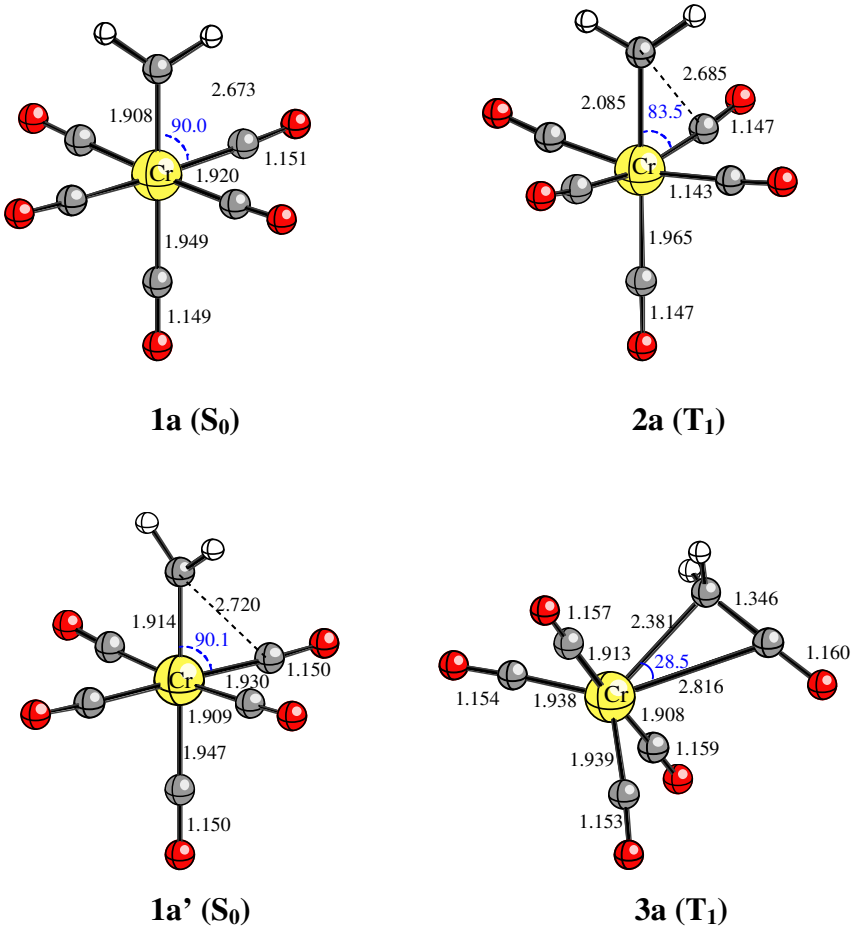

Figure 2. Ball and stick representations of complexes **1a**,**a'**-**3a**. S_0 and T_1 denote the ground and first triplet states, respectively. All S_0 and T_1 structures correspond to fully optimized B3LYP/LANL2DZ & 6-31+G(d) and UB3LYP/LANL2DZ & 6-31+G(d) geometries, respectively. Bond distances and angles are given in Å and deg., respectively. Unless otherwise stated, white, grey and red colors denote hydrogen, carbon and oxygen atoms, respectively.

The results obtained with the model compound **1a** encouraged us to study complex **1b**. A theoretical study of the structure and conformational behavior of this complex has been recently reported by us.[10c] According to our results, compound **1b** may exist in two conformers ***anti*-1b** and ***syn*-1b**, ***anti*-1b** being 1.8 kcal mol^{-1} more stable than the *syn*-conformer. Both isomers have the [C(OMe)Me] moiety bisecting the plane defined by two contiguous equatorial CO-ligands. CIS method was again used to determine the different excited states of both isomers of **1b**. The most stable excited state of ***anti*-1b** is a triplet with a vertical excitation energy of 2.85 eV, whilst the first singlet S_1 is 1.17 eV above this T_1. These results agree with the order of energy levels

that is characteristic of d^6-metal in a strong ligand field.[23] The geometry of the triplets derived from both isomers of **1b** was computed again at the UB3LYP/LANL2DZ&6-31G(d) level and converged to the corresponding cyclopropanone chromium complexes **3b** (from ***anti*-1b**) and **3c** (from ***syn*-1b**) (Figure 3). The species **3c** is 37.9 kcal mol^{-1} above ***syn*-1b** while the species **3b** is 41.8 kcal mol^{-1} above ***anti*-1b**. Therefore, **3c** is 2.1 kcal mol^{-1} more stable than **3b**, which is the opposite order of stability found for both isomers in the S_0 state.

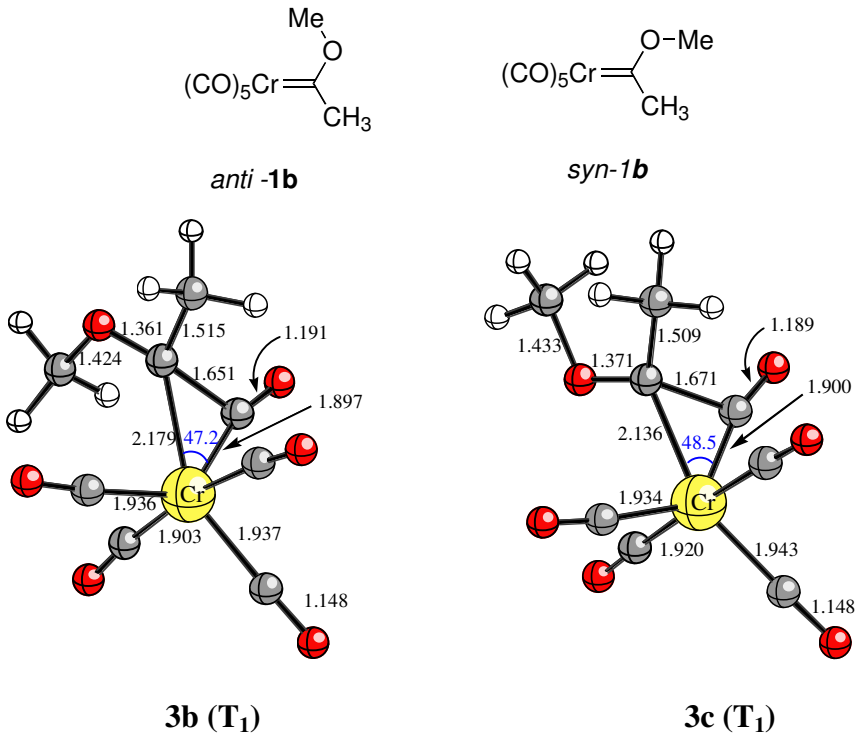

3b (T_1) **3c (T_1)**

Figure 3. Fully optimized structures (UB3LYP/LANL2DZ&6-31G(d) level of theory, see text) of the first excited triplet states of Fischer carbenes ***anti*-** and ***syn*-1b** (Structures **3b** and **3c**, respectively). See Figure 2 caption for additional details.

It can be reasoned from the above exposed results that the irradiation of alkoxychromium(0) carbene complexes, either in the LF band followed by relaxation to the MLCT band,[23] or directly in the MLCT band, results in the excitation of these complexes to the S_1 state, which readily decays to T_1 by intersystem crossing (ISC) due to spin-orbit coupling. This is a general phenomenon in group 6 metal-carbonyls (Figure 4).[24]

[23] G. J. Ferraudy, *Elements of Inorganic Photochemistry*; Wiley: New York, 1988; pages 168-171.
[24] (a) N. J. Turro, *Modern Molecular Photochemistry*, University Science Books: Sausalito-California, 1991, pages 164-170; (b) M. Wrighton, *Chem. Rev*. **1974**, *74*, 401.

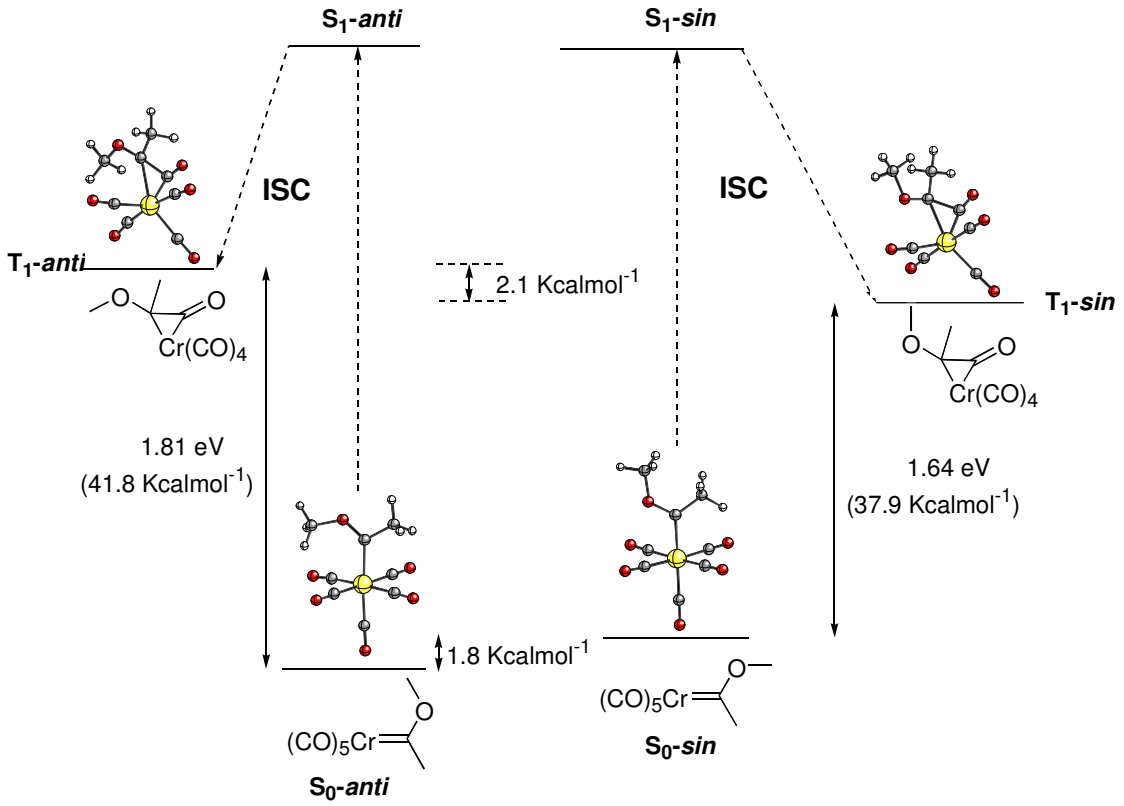

Figure 4

The Cr-calculated spin densities are 0.95 au for **3b** and 0.96 au for **3c**, while the C-calculated spin densities are 0.43 au for **3b** and 0.46 au for **3c** respectively. These values indicate that the chromacyclopropanone triplet species **3b** and **3c** have a biradical character (Figure 5).

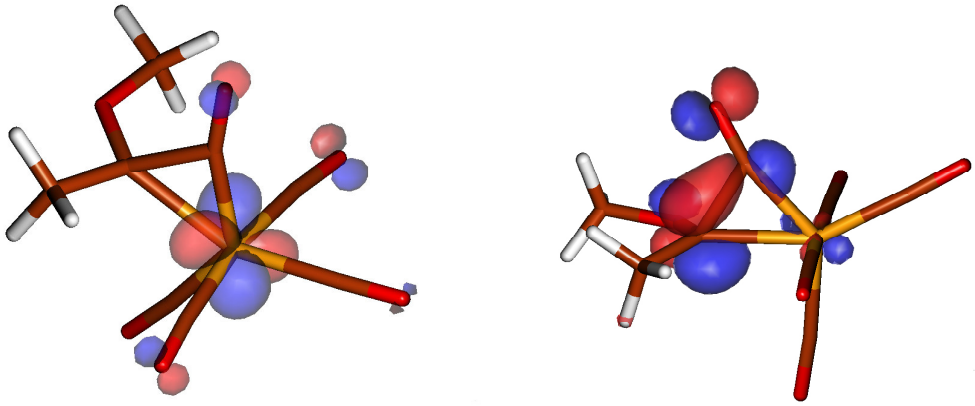

Figure 5. Canonical SOMOs of the first excited triplet state of metallocyclopropanone **3b**.[25]

[25] Orbital plot made with MOLDEN: G. Schaftenaar, J. H. Noordik , "Molden : a pre- and post-processing program for molecular and electronic structures", *J. Comput.-Aided Mol. Design* **2000**, *14*, 123.

We have previously proposed[15] that the reaction of photo-generated chromacyclopropanone species and nucleophiles to form ketene-derived products occurs on the S_0 hypersurface. Therefore, species **3** should change their multiplicity prior to evolve to the ketene derived products. This is accomplished by filling the free vacant of species **3** with a molecule of solvent (water in our model, as a computational equivalent of a coordinating solvent such as diethyl ether) in the apical position. The optimization of the geometry of this new structure at its S_0 state was effected from **3b** and **3c** leading in both cases to the structure **4** in which the methoxy group is outside the carbonyl plane (Figure 6).

From **4**, ketene-derived products can now be formed in the presence of ketenofiles, while in their absence the species **4** should revert to the starting complex **1b**. It is well known that alkoxychromium(0) complexes are photochemically stable for days in the absence of nucleophiles. Furthermore, this ketene-chromium to carbene-chromium complex reversion[26] has to occur on the S_0 hypersurface. The reversion of **4** to ***syn*-1b** is strongly exothermic[27] (ΔE = -30.6 kcal mol^{-1}) on this hypersurface and occurs through the 16-electron intermediate **5** formed by elimination of the solvent molecule (in this case H_2O). Intermediate **5** evolves to complex ***syn*-1b** by breaking of the carbene-CO bond (Figure 6). So far we have been unable to found a transition state connecting **4** to **5** or **5** to **1b**. Therefore, it is likely that this process occur without any measurable energy of activation,[26] which is in agreement with the computed exothermicity of the reaction.

[26] The ketene→carbene reversion should be analogous to that reported by Gröthjan on an Ir-nucleus. See reference 14.
[27] This strongly exothermic reaction may account for the *anti* to *syn* isomerization observed by different authors in the absence of ketenophiles.

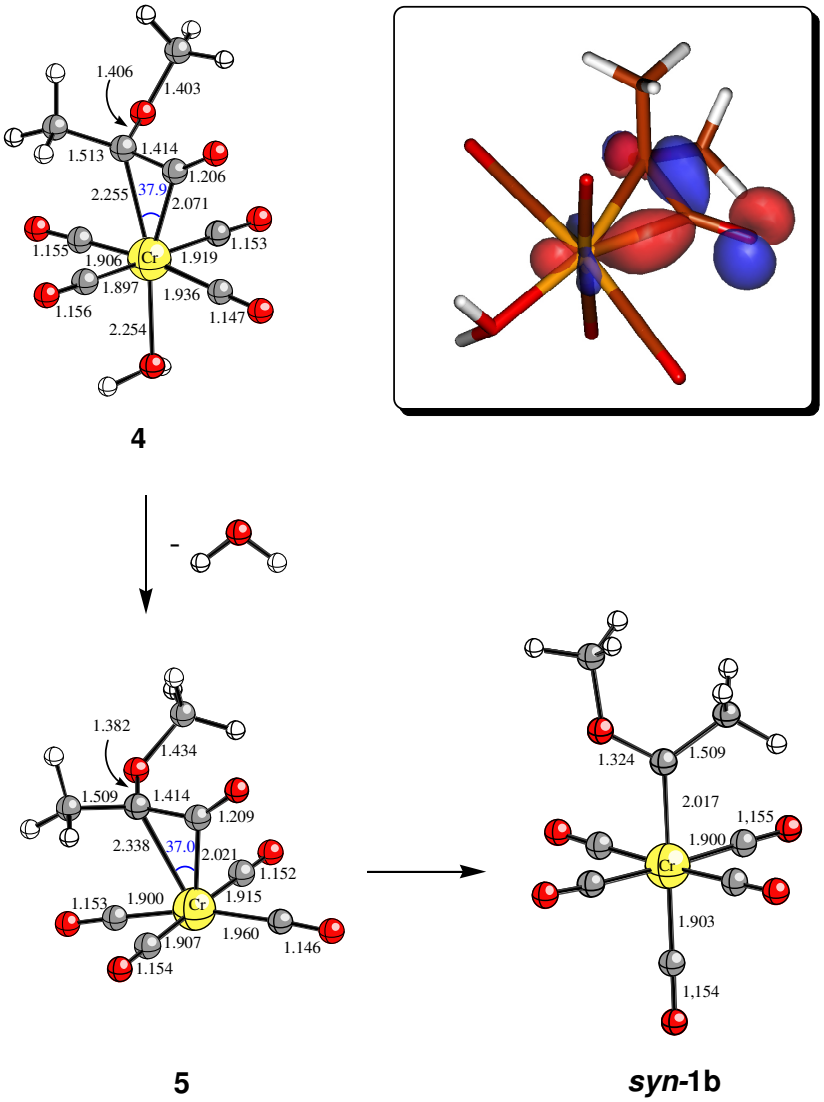

Figure 6. Fully optimized geometries (B3LYP/LANL2DZ&6-31G(d) level, see text) of stationary points associated with the **4**→***syn*-1b** transformation on the S_0 energy hypersurface. See Figure 2 caption for additional details. The boxed drawn corresponds to the HOMO of **4**. Structural data of ***syn*-1b** have been taken from ref. 10c.

The structures of the metallacyclopropanone species **3**-**4** deserve further analysis. The T_1 species **3a**-**c** have elongated [Cr–$C_{carbene}$] bonds (up to 0.12 Å) compared to the starting carbene complex **1b**. The [Cr–C]=O bond distances are around 1.9 Å, and the C=O bond of the inserted CO ligand is about 0.03 Å longer than the CO in **1b**, which makes this group a truly C=O bond. The new bond formed between the former carbene carbon and the inserted CO is approximately 1.65 Å, which makes the species **3** truly metallocyclopropanones. However, S_0 complex **4** has the distance between the Cr and the former carbene carbon and the [Cr-C]=O moiety elongated with respect to those in their corresponding T_1 structures **3b**,**c**. Similarly, in **4** the [C–C]=O distance has a value of 1.414 Å, which is considerably shorter than those of **3b** or **3c**.

Therefore, the structure of the S_0 ketene complexes of chromium corresponds to a ketene species coordinated to chromium with a highly polarized Cr–C (former carbene C) bond. NBO calculated bond orders for complexes **3b**-**c** and **4** validate the above discussion (Table 1). In fact, NBO analyses carried out on **4** give a charge value of -0.962 for the chromium atom and +0.158 for the former carbene atom. It can be concluded that the S_0 species **4** has a larger acylchromate character than **3b**,**c**, the latter structures having a comparatively larger metallacyclopropanone character (Table 1 and Figures 3 and 7).

Table 1. Selected bond distances (r(X-Y), in Å), angles (in degrees) and bond orders (B(X-Y), in a.u., in parentheses) for complexes **1b** and intermediates **3b**-**c** and **4**.

	***anti*-1b**[10c]	***syn*-1b**[10c]	**3b** (T_1)	**3c** (T_1)	**4** (S_0)
r(Cr-C) / Å	2.060	2.017	2.179	2.136	2.254
			(0.38)	(0.40)	(0.40)
r(Cr-C=O) / Å	1.904	1.900	1.897	1.900	2.071
			(0.68)	(0.66)	(0.52)
r(C-C=O) / Å	2.739	2.753	1.651	1.671	1.414
			(0.75)	(0.71)	(1.22)
r(C=O) / Å	1.153	1.155	1.191	1.189	1.206
			(1.87)	(1.88)	(1.85)
C-Cr-C(=O)	87.3	89.3	47.2	48.5	37.9

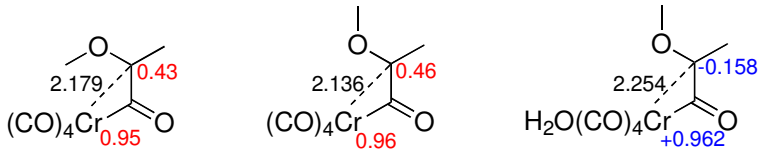

3b **3c** **4**

Figure 7. Calculated spin densities (red, a.u.) and NBO charges (blue, a.u.) for species **3b**-**c** and **4**.

According to the theoretical model developed above, the reaction of complex **6** (Scheme 3) with imines in different solvents would be a good probe to test the sequence carbene complex (S_0)→chromacyclopropanone (T_1)→acylchromate (S_0). In fact, deinsertion of CO from ketene-complexes **4** (through unsaturated complexes **5**) will be disfavored by strongly coordinating ligands. Furthermore, these strongly coordinating

ligands will favor the decay of the T_1 species **3** to S_0 species **4**, which is necessary to the subsequent reaction with nucleophiles. Therefore, the yield of the reaction between a carbene complex such as **6** and imine **7** (Scheme 3) must be dependent on the nucleophilicity of the solvent used. A series of experiments were carried out using a variety of solvents ranging in polarity from hexane to MeCN. A clear relationship between the donor number (DN) of the solvent and the yield of the reaction was found as predicted by our model. Thus, good coordinating solvents such as THF or MeCN gave very high yields of the mixture of *cis-trans* β-lactams **8**, but the yields are poorer in non-coordinating solvents such as hexane or benzene (Table 2, Scheme 3). Formation of β-lactams **8** in non-coordinating solvents may be explained by deactivation of the T_1 chromacyclopropanone **3** by coordination with the lone pair of the imine nitrogen.[28]

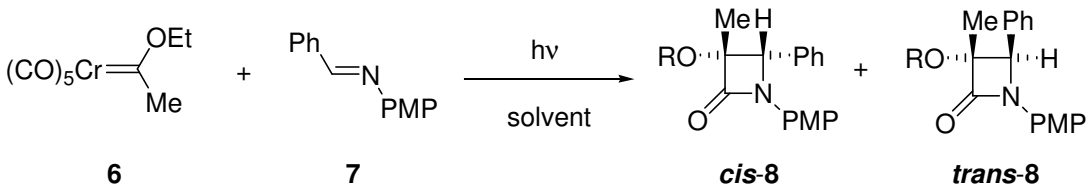

6 **7** ***cis*-8** ***trans*-8**

Scheme 3

Table 2. Photochemical Reactions of Complex **6** and Imine **7** in Different Solvents.

Entry[a]	Solvent/T[b]	DN[c]	Conversion[d]	*cis* **8**/*trans* **8**[e]
1	Hexanes / rt	–	32	7.3:1
2	Benzene / rt	–	55	3.2:1
3	CH_2Cl_2 / rt.	0.00	69	4.4:1
4	THF / rt	0.52	85	1:1
5	MeCN / rt	0.36	90	6.3:1

[a] All the experiments were carried out using a 10^{-2} M concentration of solvent. [b] rt refers to the temperature in the inside of the light box (monitorized by using an external probe) in the range of 26-30 ˚C. [c] Values for donor number (DN)[29] are refered to 1,2-dichloroethane. [d] The value of conversion is calculated based on the amount of unreacted imine observed after 8h of irradiation (^{1}H NMR). All the experiments were effected simultaneously to ensure identical reaction conditions and repeated twice. The given values are the media of both experiments. [e] Determined by integration of the signals corresponding to H4 in the NMR spectra of the crude reaction mixtures.

[28] A theoretical-experimental model to account for the torquoselectivity in the photochemical reactions of chromium(0)carbene complexes and imines will be reported in due time.
[29] C. Reichardt, *Solvents and Solvent Effects in Organic Chemistry*, 3rd Ed., VCH Publishers, Weinheim, 2003.

As stated above, the effect of the substitution of one or two CO ligands of the pentacarbonylchromium(0) carbene complexes by phosphines on the photochemical reaction with imines was reported by our group.[15] With a model for the carbonylation of alkoxypentacarbonylchromium(0) carbene complexes in hand, we studied the far more complicated situation of PH_3 substituted complexes. Now the number of possible starting situations for a determined complex is higher, since the PH_3 ligand can be either *cis*- or *trans*- to the carbene ligand, and for each isomer two possible *syn*- and *anti*-isomers of the carbene ligands are also likely. Therefore, we have calculated all the stationary points on the S_0 hypersurface for all the possible combinations shown in Figure 8.

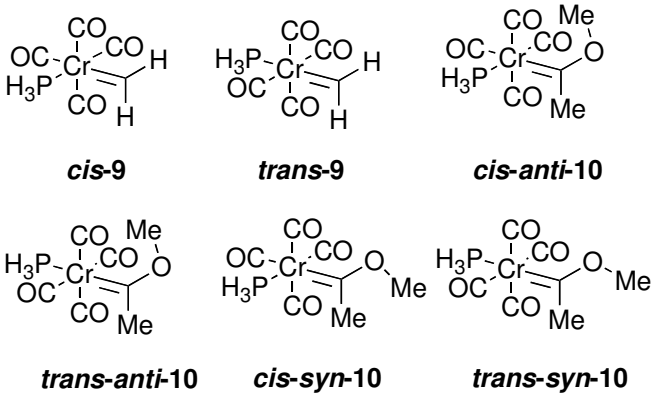

Figure 8. Possible isomers resulting from substitution of one CO unit of carbenes **1a** and **1b** by one PH_3 ligand to yield structures **9** and **10**, respectively.

We considered, on the first place, the model complexes ***cis*-9** and ***trans*-9** having the phosphine ligand *cis*- and *trans*- to the methylene ligand, respectively. The introduction of a strong σ-donor ligand in the sphere of coordination of chromium has a heavy impact in the geometry of the complexes **9**, respect to the parent complex **1a**. This effect is stronger for the *cis*- than for the *trans*- geometry. Thus, the [Cr–C]=O bond is shortened by 0.04 Å for ***cis*-9** and by 0.01 Å for ***trans*-9**. Furthermore, now the methylene fragment of ***cis*-9** is coplanar with two co-linear equatorial CO groups (like in **1a'**, see above), while the methylene fragment of ***trans*-9** bisects the plane defined by two contiguous CO-groups (like in **1a**, see above). In the S_0 state complex ***trans*-9** is 0.9 kcal mol^{-1} more stable than ***cis*-9** (Figure 9). From these model Fischer carbenes, the corresponding T_1 states for ***cis*-9** and ***trans*-9** were optimized as above leading to structures **11** and **12**, respectively (Figure 9). Species **11** and **12** are 20.0 kcal mol^{-1} and 21.5 kcal mol^{-1} higher in energy than ***cis*-9** and ***trans*-9**, respectively. Neither **11** nor **12**

have a chromacyclopropanone structure, in contrast with the optimized T_1 states derived from complexes **1**. Therefore, it can be assumed that the photocarbonylation of complexes **9** is hampered by the PH_3 group. These calculations demonstrate that an increment on the σ-donating ability of the PH_3 ligand results in the increment of the π-back electron-donating ability of the chromium, making stronger Cr–CO bonds and therefore, in the excited state, less susceptible to the nucleophilic intramolecular attack by the carbene carbon that is required for the formation of the corresponding chromacyclopropanone.

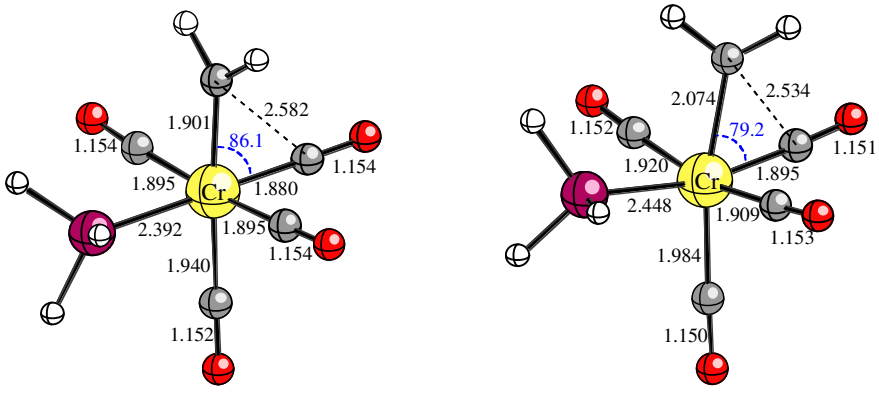

***cis*-9 (S_0)** **11 (T_1)**

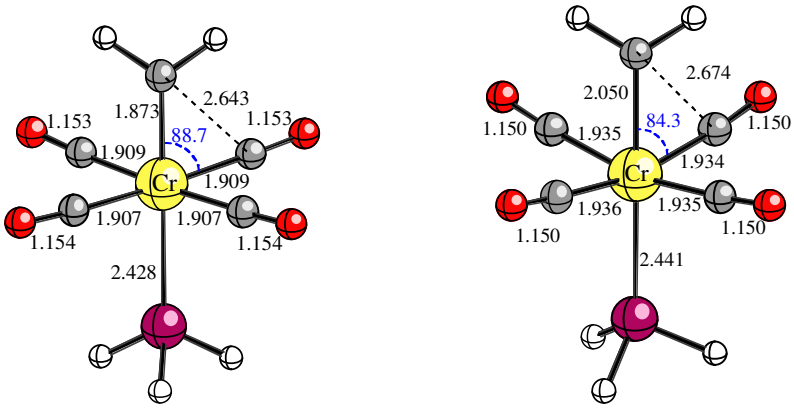

***trans*-9 (S_0)** **12 (T_1)**

Figure 9. Fully optimized B3LYP/LANL2DZ&6-31G(d) structures of complexes ***cis-*** and ***trans*-9** at the S_0 state and UB3LYP/LANL2DZ&6-31G(d) converged geometries of the corresponding compounds at the first excited triplet state T_1 (**11** and **12**, respectively). Phosphorus atoms are represented in pink. See Figure 2 caption for additional details.

This model should be an extreme situation of reactivity, since the effect of σ-donation of the PH_3 on the carbene ligand is not compensated by the π-donation from the heteroatom to the carbene carbon. In fact, we have previously demonstrated that phospine-substituted alkoxychromium(0) Fischer carbene complexes are

photochemically active towards imines in coordinating solvents.[15] Therefore, the model study was extended to complexes **10** having σ-donor alkoxy moieties bonded to the carbene carbon. Calculations were pursued with the two more stable forms of both complexes, namely ***cis-syn*-10** and ***trans-anti*-10** isomers (in both cases the [C(OMe)Me] fragment bisects the plane defined by the two equatorial CO ligands, like their analogous complexes **1b**). The optimization of the corresponding T_1 structures on the respective hypersurfaces was effected at the UB3LYP/LANL2DZ&6-31G(d) level as described above and the structures **13** and **14** were obtained in both cases. The species **13** is 36.9 kcal mol^{-1} higher in energy than ***trans-anti*-10** while **14** is 33.8 kcal mol^{-1} above ***cis-syn*-10**. Both T_1 species show the chromacyclopropanone structure analogous to **3**. It is therefore proven that the presence of the methoxy substituents in complexes **10** makes the carbene carbon more nucleophilic (in the excited state) allowing for the CO-insertion to occur (Figure 10). As in species **3**, the calculated spin density for the Cr in **13** is 1.02 au and for the former carbene carbon is 0.42 au (the spin density values for **14** are 1.06 au and 0.52 au, respectively). Therefore, both **13** and **14** have a biradical character.

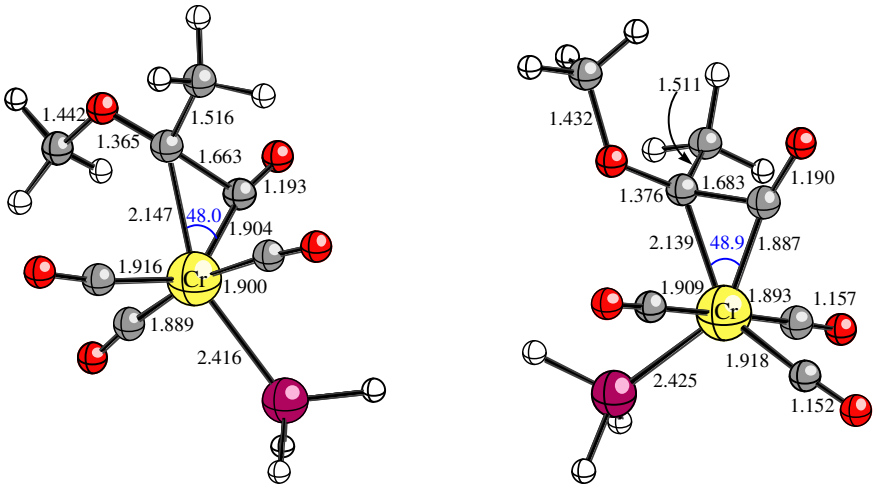

13 (T_1) **14 (T_1)**

Figure 10. Fully optimized triplet structures **13** and **14** (UB3LYP/LANL2DZ&6-31G(d) level). See Figures 2 and 9 captions for additional details.

The chief geometric data for complexes **10**-**14** are collected in Table 3. These results demonstrate that while for pentacarbonylchromium(0) carbene complexes **1** carbonylation occurs both in the presence of an alkoxy group bonded to the carbene carbon (**1b**) and in its absence (**1a**), the presence of σ-donors such as alkoxy groups in

phosphine complexes is needed for the insertion of the CO. Moreover, the presence of a PH_3 ligand in alkoxychromium(0) carbenes has no effect on the nature of the structures on the T_1 hypersurface, exception made of the narrowing of the S_0-T_1 gap. Both T_1 structures **13** and **14** were deactivated to the S_0 hypersurface by coordination with a molecule of water as a model for an ethereal solvent. The S_0 active species **15** is analogous to that obtained from pentacarbonylchromium(0) carbene complexes **4**. NBO analysis of **15** gives values of –0.881 au for Cr and +0.194 au for the former carbene carbon. Again, **15** is a highly polarized species with a strong acylchromate character. The Cr-C (former carbene) distance is larger than that of its analog **4** due to the donor effect of the phosphine ligand that makes the metal less prone to accept charge from the acyl ligand (Table 3, Figure 11).

Table 3. Selected bond distances (r(X-Y), in Å), angles (in degrees)and bond orders (B(X-Y), in a.u., in parentheses) for complexes **10** and intermediates **13**,**14** and **15**.

	***cis-syn*-10**	***trans-anti*-10**	**13**	**14**	**15**
r(Cr-C)	1.991	2.003	2.147	2.139	2.310
			(0.25)	(0.39)	(0.77)
r(Cr-C=O)	1.899	1.858	1.904	1.887	2.039
			(0.31)	(0.73)	(0.57)
r(C-C=O)	2.676	2.704	1.663	1.683	1.421
			(0.81)	(0.70)	(1.20)
r(C=O)	1.157	1.160	1.193	1.190	1.215
			(2.23)	(1.86)	(1.81)
r(Cr-P)	2.381	2.382	2.416	2.425	2.417
			(0.26)	(0.36)	(0.38)
C-Cr-C(=O)	86.9	88.8	48.0	48.9	37.5

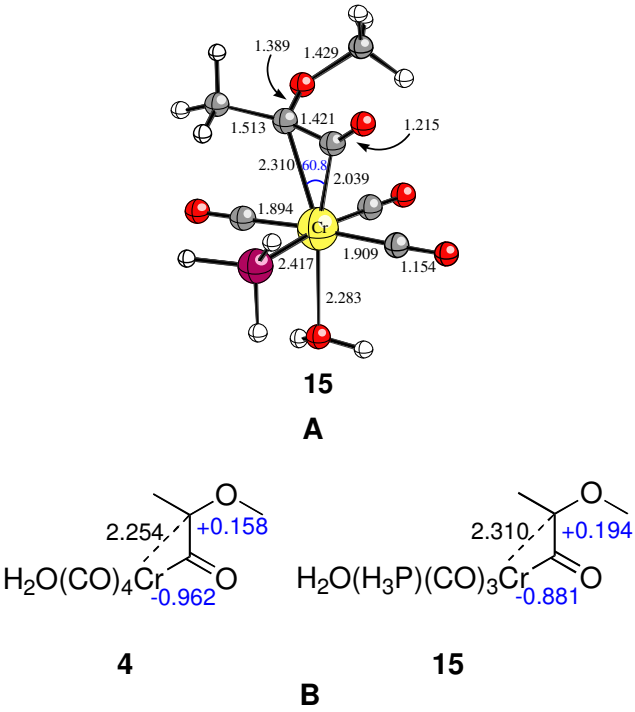

Figure 11. A: Fully optimized structure **15** at the S_0 state (B3LYP/LANL2DZ&6-31G(d) level). See Figures 2 and 7 captions for additional details. B: NBO charges (blue, in a.u.) of species **4** and **15**. Numbers in black refer to bond distances in Å.

The effect of diphosphine substitution in the carbonylation process was checked in model diphos-like complex **16**. Calculations carried on compound **16** resulted again in the finding of a stable triplet **17** having vertical excitation energy of 1.58 eV (36.4 kcal mol^{-1}). The optimized structure of **17** is again a chromacyclopropanone of biradical character (spin densities for Cr = 1.24 au and C = 0.48). Therefore, no significant differences with carbene complexes possessing only one phosphine unit were encountered (Figure 12).

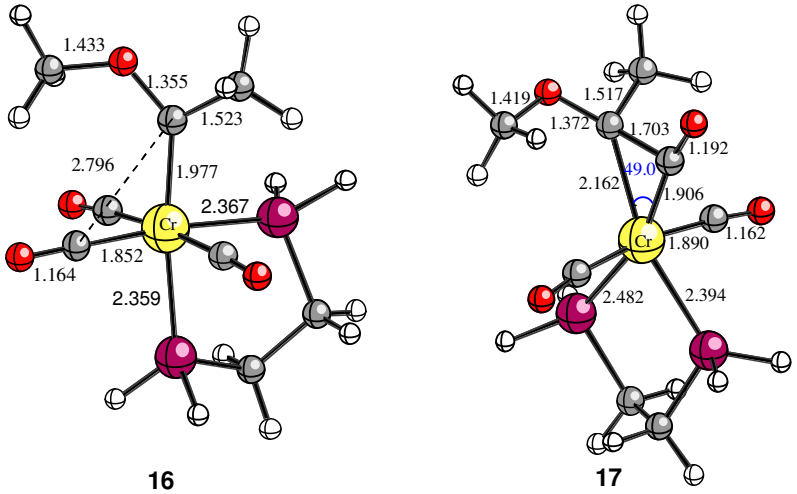

Figure 12. Fully optimized structures **16** (B3LYP/LANL2DZ&6-31G(d) level, S_0 state) and **17** (UB3LYP/LANL2DZ&6-31G(d) level, T_1 state, see text). See Figures 2 and 9 captions for additional details.

Finally, our model was tested against alkoxytungsten(0) carbene complexes that, until today, have proven inert towards photocarbonylation. We carried out calculations on pentacarbonyl[methoxymethylcarbene]tungsten(0) **18**. The geometry and conformational behavior of this complex have been previously calculated by us.[10c] Calculations carried out at the CIS level on the more stable ***anti*-18** conformer resulted again in the finding of a stable triplet state having a vertical excitation energy of 3.60 eV. However, in this case S_1 is located only 0.23 eV above T_1. The geometry of both triplets derived from ***anti*-18** and its isomer ***syn*-18** were optimized at the UB3LYP/LANL2DZ&6-31G(d). The optimization resulted in complexes **19** and **20**, respectively. Complex **19** is 54.0 kcal mol^{-1} above ***anti*-18**, while ***syn*-18** is 51.3 kcal mol^{-1} above **20**. Both triplets **19** and **20** differ only in 0.1 kcal mol^{-1}. Contrary to the behavior of their chromium counterparts **3b-c**, neither **19** nor **20** have a tungstenacyclopropanone structure. Thus, the bond distances between carbene C atoms and the closest CO groups are 2.716 Å and 2.567 Å respectively, without any measurable bond order between both atom pairs. Therefore, no ketene-like species are formed by excitation of an alkoxypentacarbonyltungsten(0) carbene complex (Figure 13). Thence, our model is in good accord with the experimentally observed photochemical lack of reactivity tungsten(0) carbenes.

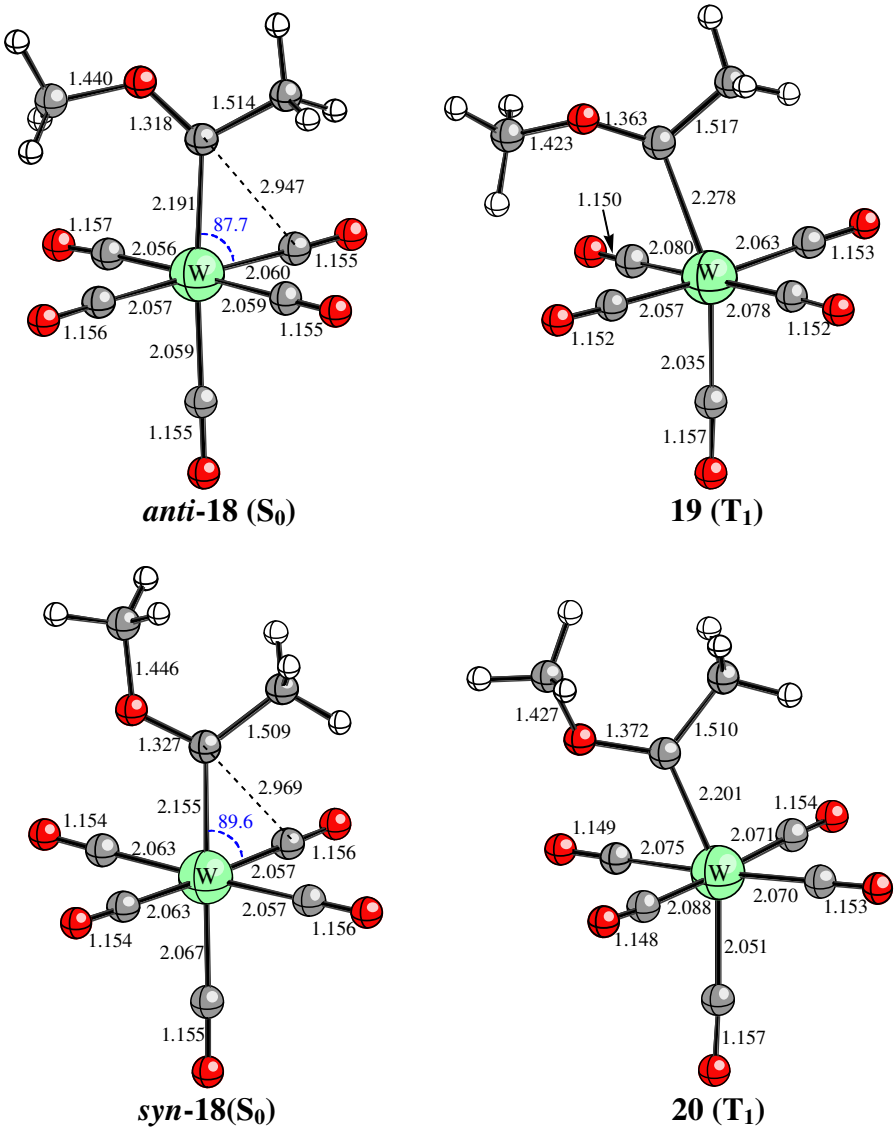

Figure 13. Fully optimized (B3LYP/LANL2DZ&6-31G(d) level) structures of tungsten (0) carbenes ***syn-*** and **anti-18** at their ground state. The corresponding excited T_1 structures **19** and **20**, optimized at the UB3LYP/LANL2DZ&6-31G(d) level, are also shown. See Figure 2 caption for additional details.

Based on the calculations effected above we can attribute the inertia of tungsten(0) carbene complexes to a stronger W–C(=O) bonding respect to Cr-C(=O), together with a decreased in the nucleophilicity of the carbene carbon in the excited state. In fact, NBO calculated bond orders range from 0.81-0.82 for *cis*-W-C(=O) in complexes **18** and from 0.71-0.74 for *cis*-Cr-C(=O) in complexes **1b**. The effect would be similar but exacerbated to the one observed with PH_3 substituted chromium(0) carbenes respect to their pentacarbonylchromium(0) carbene parent compounds.

2.2.4. Experimental Section

Photochemical reactions. General procedure. All photochemical reactions were conducted by using a 450W-medium pressure mercury lamp through a Pyrex filter. All the reactions were carried out in the specified solvent, dry and degassed (vacuum-Ar, four cycles) in a rubber septum-sealed Pyrex tube filled with argon. For all cases pentacarbonyl[(ethoxy)(methyl)carbene]chromium(0), **6**, was reacted with *N*-(4-methoxylphenyl)benzylideneimine **7**. In a typical experiment a solution of 53 mg (0.20 mmol) of the carbene complex and 42 mg (0.20 mmol) of imine **7** in 20 mL of the indicated solvent was irradiated for 8 h. The solvent was removed *in vacuo* and the residue was dissolved in a mixture of hexane:AcOEt (1:1) and exposed to direct sunlight until a clear solution was obtained. The solution was filtered through a short pad of celite, the solvent eliminated and the isomeric composition of the β-lactam mixture was checked by ^{1}H-NMR (see text). The reaction conversion was estimated by integration of well-resolved signals of the imine proton at 8.4 ppm. The isomers ratio was determined by comparison of the signals at 4.85 and 5.01 ppm for compound ***trans*-8** and 4.78 and 5.03 ppm for ***cis*-8** respectively.

Hexanes: following the general procedure, 48 mg of a reaction mixture were obtained. The *cis/trans*-β-lactam **8** ratio was 7.3:1.

Benzene: following the general procedure, 52 mg of a reaction mixture were obtained. The *cis/trans*-β-lactam **8** ratio was 3.2:1.

Dichloromethane: following the general procedure, 56 mg of a reaction mixture were obtained. The *cis/trans*-β-lactam **8** ratio was 4.4:1.

Tetrahydrofuran: following the general procedure, 59 mg of a reaction mixture were obtained. The *cis/trans*-β-lactam **8** ratio was 1:1.

Acetonitrile: following the general procedure, 60 mg of a reaction mixture were obtained. The *cis/trans*-β-lactam **8** ratio was 6.3:1.

2.2.5. Conclusions

The photocarbonylation reaction of group 6 Fischer carbene complexes has been studied by DFT and experimental procedures. The process occurs by ISC from the lowest excited singlet state (S_1) to the lowest triplet state (T_1). The structure of the triplet is decisive for the outcome of the reaction. Methylene pentacarbonylchromium(0) complexes, alkoxypentacarbonylchromium(0) carbene complexes and alkoxyphosphinetetracarbonyl-chromium(0) carbene complexes have coordinatively unsaturated chromacyclopropanone T_1 structures with a significant biradical character. The evolution of these species takes place by an additional ISC to the S_0 hypersurface (spin inversion) by coordination of a molecule of the solvent. In the presence of ketenophiles, ketene-derived products are formed but in their absence, the reversion to the carbene complex takes place. This step is highly exothermic and is responsible for the experimentally observed *anti→syn* isomerization of chromium(0) carbene complexes in the absence of nucleophiles. On the contrary, the excitation of methylene phosphinetetracarbonylchromium(0)complexes does not lead to T_1 species with metallacyclopropanone structures. This behavior is analogous to that observed for pentacarbonyltungsten(0) carbene complexes that do not carbonylate. Following these conclusions, the photoreactivity of group 6 carbene complexes is strongly related to the coordinating ability of the solvent. Thus, coordinating solvents facilitate the reaction by favoring the deactivation of the T_1 species. This prediction of our model has been tested experimentally in the reaction of alkoxypentacarbonylchromium(0) complexes and imines.

2.3. A Theoretical-Experimental Approach to the Mechanism of the Photocarbonylation of Chromium(0) (Fischer)-Carbene Complexes and Their Reaction with Imines

2.3. A Theoretical-Experimental Approach to the Mechanism of the Photocarbonylation of Chromium(0) (Fischer)-Carbene Complexes and Their Reaction with Imines

Irradiation of a chromium-carbene complex (visible light) is thought to promote the reversible insertion of a CO-ligand into the Cr-carbene bond to form a Cr-ketene complex.[1] This ketene-like behavior is one of the paradigmatic processes of these complexes[2] and has resulted in exceptionally efficient synthesis of compounds such as β-lactams, cyclobutanones, amino acids and peptides, polinuclear hydrocarbons, allenes, etc.[3] Despite the close parallelism between the photoreactivity of these complexes and free ketenes, the sole reported attempt made to directly detect the intermediacy of ketene species occurred with no success.[4] Moreover, a goodly number of questions associated with these synthetically useful processes remain unanswered. For example, although it is known that the reactivity of carbene complexes is strongly affected by the substitution at the carbene ligand, there are no data to establish the influence of ligands different than CO bonded to the chromium center. Thus, α,β-unsaturated chromium metal-carbene complexes and complexes having two heteroatoms bonded to the carbene carbon are listed as photochemically unreactive.[3a,5] In this communication we have focussed on three aspects of the photocarbonylation reaction of chromium carbene complexes and imines: the effect of substituents on the complex on the photocarbonylation step, the nature of the intermediate resulting from this carbonylation and the mechanism of the reaction of chromium carbene complexes and imines.

---

[1] Hegedus, L. S.; de Weck, G.; D'Andrea, S. *J. Am. Chem. Soc.* **1988**, *110*, 2122.

[2] The synthesis and synthetic applications of Fischer metal-carbene complexes has been profusely reviewed. See, among others: (a) Dötz, K. H.; Fischer, H.; Hofmann, P.; Kreissel, R.; Schubert, U.; Weiss, K. *Transition Metal Carbene Complexes*, Verlag Chemie: Deerfield Beach, Florida, 1983. (b) Dötz, K. H. *Angew. Chem. Int. Ed. Eng.* **1984**, *23*, 587. (c) Wulff, W. D. in *Comprehensive Organometallic Chemistry II,* Abel, E. W.; Stone, F. G. A.; Wilkinson, G.; Eds. Pergamon: Oxford. 1995; vol. 12, p. 470. (d) Harvey, D. F.; Sigano, D. M. *Chem. Rev.* **1996**, *96*, 271. (e) Aumann, R.; Nienaber, H. *Adv. Organomet. Chem.* **1997**, *41*, 163.

[3] Reviews: (a) Hegedus, L. S. *Tetrahedron* **1997**, *53*, 4105. (b) Hegedus, L. S. in *Comprehensive Organometallic Chemistry II,* Abel, E. W.; Stone, F. G. A.; Wilkinson, G.; Eds. Pergamon: Oxford. 1995; vol. 12, p. 549. (c) Hegedus, L. S. *Acc. Chem. Res.* **1995**, *28*, 299.

[4] Gallagher, M. L.; Greene, J. B.; Rooney. A. D. *Organometallics* **1997**, *16*, 5260.

[5] Complexes having good π-acceptor groups on the carbene carbon (e.g. PhCH=CH, PhC≡C-) have been considered that fail to undergo photochemical reactions when subjected to visible light. However, they are photochemical sources of carbenes at temperatures near to 0° C, forming cyclopropanes in the presence of electron-deficient olefins, see: Sierra, M. A.; del Amo, J. C.; Mancheño, M. J.; Gómez-Gallego, M. *Tetrahedron Lett.* **2001**, *42*, 5345.

The behavior of chromium-carbene complexes having ligands different from CO in the photocarbonylation was studied first using their reaction with imines to form 2-azetidinones. The compounds employed in this study are collected in Chart 1. Chromium carbene complex **1a** was selected as reference. Introduction of Ph_3P and Bu_3P ligands was achieved by heating complex **1a** in the presence of the corresponding phosphines,[6] to yield compounds **2** that were used as models for complexes having soft and strong σ-donor ligands, respectively.[7] Complex **3** was prepared analogously from *diphos* and **1a** and used to study the additive effect of two σ-donors in the photocarbonylation reaction.

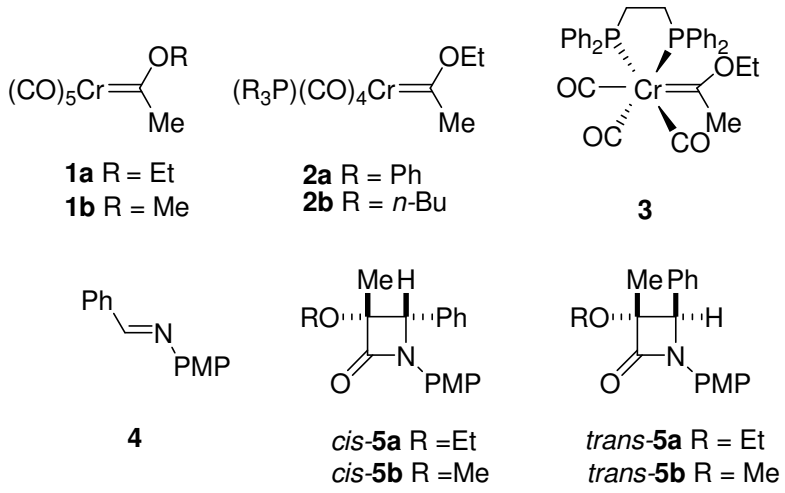

Chart 1

Irradiation (visible light) of complexes **1a** and **2a** in the presence of imine **4** gave the expected 2-azetidinones **5a**. Traces of compounds **5a** were obtained from complexes **2b** and **3**. Strikingly, β-lactam **5a** was obtained as a *cis*/*trans*-mixture in all cases (Table 1), while the analogous reaction between complex **1b** and imine **4** was reported to yield a single *cis*-diastereomer.[8] We then effected the reaction of complex **1b** and imine **4** and consistently obtained a mixture of *cis*- and *trans*-2-azetidinones **5b**, independently of the reagent concentration used.[9] As listed in the Table 1, the *cis/trans* ratio of β-lactams **5** depends on the nature of the ligands attached to the metal center, and it is strongly affected by the reaction temperature. The presence of a strong σ-donor (Bu_3P) bonded

[6] Xu, Y.-Ch.; Wulff, W. D. *J. Org. Chem.*. **1987**, *52*, 3263.
[7] Collman, J. P.; Hegedus, L. S.; Norton, J. R.; Finke, R. G. *Principles and Applications of Organotransition Metal Chemistry*, University Science Books, Mill Valley, California, 1987.
[8] Hegedus, L. S.; McGuire, M. A.; Schultze, L. M.; Yijun, C.; Anderson, O. P. *J. Am. Chem. Soc.* **1984**, *106*, 2680.
[9] See the Experimental Section for the experimental procedures used through this work.

to the chromium (complex **2b**) inhibits the photocarbonylation, while softer σ-donors (Ph_3P) are compatible with the reaction (complex **2a)**. Furthermore, the bonding of two σ-donor ligands (complex **3)** to the chromium center, results also in the almost complete inhibition of the process.

Table 1.

Entry	Complex	Conversion[a]	*cis/trans* ratio[b]	Solvent/T[c]	Concentration of complex
1	**1a**	100	6.1:1	MeCN/RT	10^{-2} M
2	**2a**	71	10.5:1	MeCN/RT	10^{-2} M
3	**2b**	< 5		MeCN/RT	10^{-2} M
4	**2b**	< 5		Et_2O/RT	10^{-2} M
5	**3**	< 5		MeCN/RT	10^{-2} M
6	**3**	< 5		Et_2O/RT	10^{-2} M
7	**1b**	100	5.0:1	MeCN/RT	$4\ 10^{-2}$ M
8	**1b**	100	4.7:1	MeCN/RT	$2\ 10^{-2}$ M
9	**1b**	100	6.3:1	MeCN/RT	10^{-2} M
10	**1b**	100	5.7:1	MeCN/RT	$2.5\ 10^{-2}$ M[e]
11	**1a**	100	2.7:1	MeCN/0 °C[d]	10^{-2} M
12	**1a**	100	6.3:1	MeCN/30 °C[d]	10^{-2} M
13	**1a**	100	12.0:1	MeCN/60 °C[d]	10^{-2} M

[a] Referred to unreacted imine. Experiments under entries 1-6, and 7-10 were carried out simultaneously in two different batches to ensure identical reaction conditions. Conversions listed as < 5 % means that only traces of signals attributable to the 2-azetidinone **5** could be observed in the ^{1}H NMR spectra of the reaction mixtures. [b] Determined by integration of the well resolved signals corresponding to the C4 hydrogen in the ^{1}H NMR spectra of the reaction mixtures. [c] RT refers to the temperature in the interior of the light box (26 to 30 °C). [d] The Pyrex tube was introduced in a thermostatic bath at the indicated temperature. [e] Concentration used in reference 8.

Due to the difficulties of experimental characterization of the possible reaction intermediates, we have studied several model compounds, by using computational tools.[10] All calculations[11] have been performed at the B3LYP[12] level, using the standard 6-31G* basis set[13] for hydrogen, carbon, oxygen, and nitrogen, and the Hay-Wadt

[10] Frenking, G.; Wagener, T. In *Encyclopedia of Computational Chemistry*. Schleyer, P. v. R., Ed. Wiley: Chichester, 1999; Vol. 5, pp 3073-3084.

[11] Gaussian 98, Revision A.5, Frisch, M. J.; Trucks, G. W.; Schlegel, H. B.; Scuseria, G. E.; Robb, M. A.; Cheeseman, J. R.; Zakrzewski, V. G.; Montgomery, Jr., J. A.;. Stratmann, R. E.; Burant, J. C.; Dapprich, S.; Millam, J. M.; Daniels, A. D.; Kudin, K. N.; Strain, M. C.; Farkas, O.; Tomasi, J.; Barone, V.; Cossi, M.; Cammi, R.;. Mennucci, B.; Pomelli, C.; Adamo, C.; Clifford, S.; Ochterski, J.; Petersson, G. A.; Ayala, P. Y.;. Cui, Q.; Morokuma, K.; Malick, D. K.; Rabuck, A. D.; Raghavachari, K.;.Foresman, J. B.; Cioslowski, J.; Ortiz, J. V.; Stefanov, B. B.; Liu, G.; Liashenko, A.; Piskorz, P.; Komaromi, I.; Gomperts, R.; Martin, R. L.; Fox, D. J.; Keith, T.; Al-Laham, M. A.; Peng, C. Y.; Nanayakkara, A.; Challacombe, M.; Gill, P. M. W.; Johnson, B.; Chen, W.; Wong, M. W.; Andres, J. L.; González, C.; Head-Gordon, M.; Replogle, E. S.; Pople, J. A., Gaussian, Inc., Pittsburgh PA, 1998.

[12] (a) Becke, A. D. *J. Chem. Phys.* **1993**, *98*, 5648. (b) Lee, C.; Yang, W.; Parr, R. G. *Phys. Rev. B* **1988**, *37*, 785. (c) Vosko, S. H.; Wilk, L.; Nusair, M. *Can. J. Phys.* **1980**, *58*, 1200.

[13] Hehre, W. J.; Radom, L.; Schleyer, P. v. R.; Pople, J. A. *Ab Initio Molecular Orbital Theory;* Wiley: New York, 1986, p 76 and references therein.

small-core effective core potential (ECP) including a double-zeta valence basis set[14] for chromium. Substitution of one CO unit in $(CO)_5Cr{=}CH_2$, **7**, by PH_3 resulted in an enlargement of the C-Cr-L angle (from 90.0 ° for L = CO to 93.6 ° for L = PH_3) and in a larger HOMO-LUMO gap ($\Delta\Delta E_g$= 0.97 kcal/mol for L = PH_3, respect to L = CO). Assuming that this transition is involved in the photocarbonylation reaction, chromium carbene complexes having trialkylphosphines should be much less reactive than their carbonylated analogs, as it was found for complex **2b**. Arylphosphine ligands in turn, should yield photoreactive complexes due to their larger π-donor character, that should reduce the HOMO-LUMO gap. For *diphos*, we should be in the lower limit of reactivity with the additive effect of two arylphospines resulting in a more difficult carbonylation step. This model could also explain the inertia of chromium carbene complexes having two π-donating substituents attached to the carbene carbon. In those cases, the b_2 symmetric LUMO has two π_1^* interactions, one between one d-orbital of chromium and the central p-AO of the carbene, and the other resulting from the antibonding combination between the carbene and the two filled p-AOs of the heteroatoms. Thus, our B3LYP calculation on the model $(CO)_5Cr{=}C(OH)_2$ complex yielded $\Delta\Delta E_g$ = 33.5 kcal/mol with respect to $(CO)_5Cr{=}CH_2$, **7** (Figure 1).

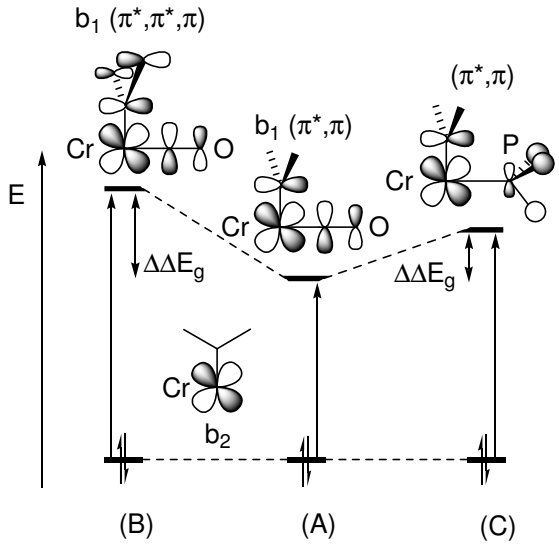

Figure 1

[14] Hay, P. J.; Wadt, W. R. *J. Chem. Phys.* **1985**, *82*, 299. In this scheme, the ECP includes the 10 internal electrons of chromium, whereas the $3s^2 3p^6 4s^1 3d^5$ electrons are explicitly described by means of a double-zeta basis set, as implemented in the Gaussian98 package (LANL2DZ keyword).

Once having defined the structural requisites for the carbonylation process to occur, we turned our attention to the structure of the complex derived from the carbonylation of **7**. Since previous experimental work[3] indicates that the stereochemistry of [2+2] cycloadditions involving these ketene-like compounds is identical to that found in the equivalent thermal nonmetallated cycloadditions, the calculations on **7** and on following stationary points were performed in the S_0 state. Either η^2-Cr **A** or chromacyclopropanone **B** structures have been proposed[3a] for the product of carbonylation of **7** (Figure 2). Our results, however, are in agreement with structure **C**, with η^1-coordination of the ketene to the metallic center. This mode of coordination should enhance the contribution of **E**, the polar mesomer form of the ketene **D**. The computed structure for the complex corresponds to a square base pyramid **8**, the ketene moiety occupying the apical position. Since **8** is a 16-electron complex, the coordination sphere of chromium was saturated by addition of one molecule of H_2O to model a coordinating solvent. Thus, the octahedral 18-electron complex **9**, with the ketene and the solvent in the axial positions, was obtained. Strikingly, in **9**, the coordination of the ketene is the same as in type **B** structure (Figure 2).

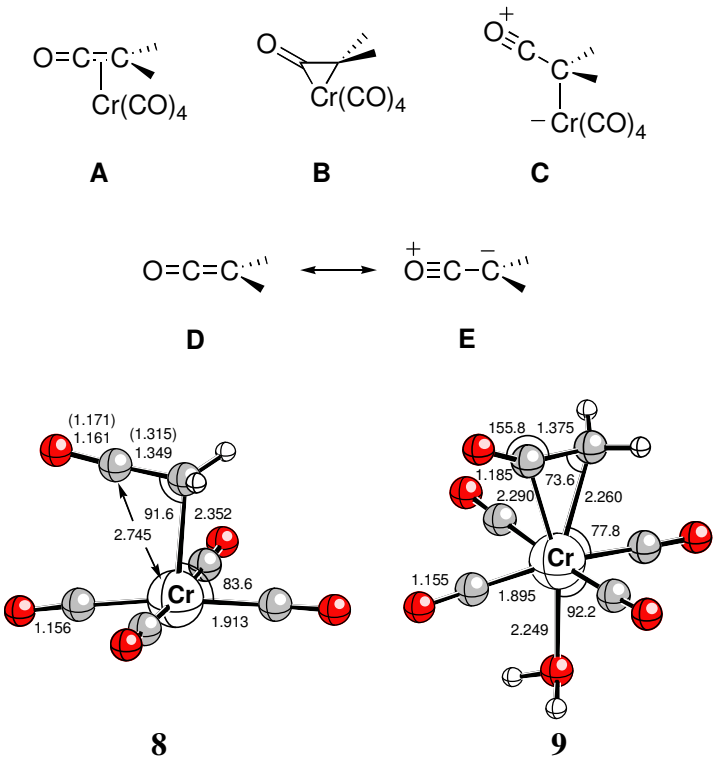

Figure 2

The reaction between complex **9** and methanimine CH_2=NH **10**, to yield the cycloadduct **11** (Scheme 1) was studied next.

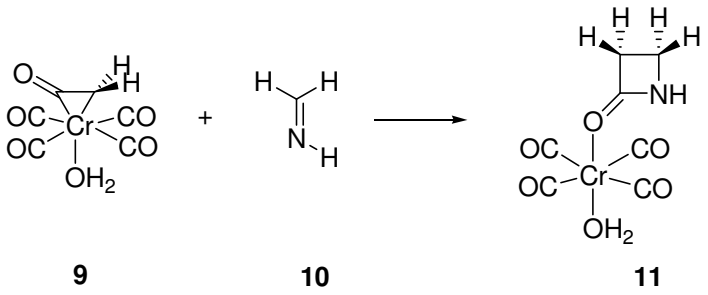

9 **10** **11**

Scheme 1

As in the classical Staudinger reaction between ketenes and imines,[15] a stepwise mechanism was obtained instead of the [$\pi 2_s+\pi 2_a$] or [$\pi 2_s+(\pi 2_s+\pi 2_s)$] pathways. However, the reaction profile is even more complex than that previously found for the unmetalated version.[16] We have located the orientation complex **INT1** before the formation of the C-N bond. This reaction intermediate lies 3.21 kcal/mol below the separate reagents and the ketene moiety is coordinated to the chromium center through the carbon atom, as in unsaturated complex **8**. In this way, the non-coordinated atoms of the ketene are positively charged and have a Coulombic stabilizing interaction with the imine nitrogen. The resulting ketene is more electrophilic and the first transition structure (**TS1** in Figure 3), lies only 1.72 kcal/mol above **INT1**. The C1···N2 distance is quite large in this saddle point, as would be expected for an early transition state. The next reaction intermediate is **INT2**, in which the C1-N2 bond is already formed and the C3 atom is bound to the chromium center. We have found another reaction intermediate denoted as **INT3** in Figure 3, which is 4.15 kcal/mol less stable than **INT2**. In this local minimum, the O5 atom is bound to chromium and in consequence, the C2-C3 and N1-C2 bond distances are shorter than in **INT2**. Therefore, **INT3** can be considered as a chromium enolate–iminium zwitterionic complex. Since formation of the C3-C4 bond is required to complete the reaction, a 1,3-chromium shift has to occur to form the

[15] (a) Staudinger, N. *Liebigs Ann. Chem*. **1907**, *356*, 51. (b) Georg, G. I. Ed. *The Organic Chemistry of β-lactams*. VCH Publishers: New York, 1993; p 295. (c) Tidwell, T. T. *Ketenes*; Wiley: New York, 1995; p 518.

[16] (a) Cossío, F. P.; Ugalde, J. M.; López, X.; Lecea, B.; Palomo, C. *J. Am. Chem. Soc.* **1993**, *115*, 995. (b) Cossío, F. P.; Arrieta, A.; Lecea, B.; Ugalde, J. M. *J. Am. Chem. Soc.* **1994**, *116*, 2085. (c) Lecea, B.; Arrastia, I.; Arrieta, A.; Roa, G.; López, X.; Arriortua, M. A.; Ugalde, J. M.; Cossío, F. P. *J. Org. Chem*. **1996**, *61*, 3070. (d) Arrieta, A.; Lecea, B.; Cossío, F. P. *J. Org. Chem*. **1998**, *63*, 5869.

cycloadduct.[17] We have located the saddle point **TS2** which connects **INT2** and **INT3**, the corresponding energy barrier being *ca.* 15 kcal/mol larger that that associated with formation of the N1-C2 bond. The next transition structure **TS3** corresponds to the formation of the C3-C4 bond. The geometry and the harmonic analysis of this saddle point indicate that it corresponds to a conrotatory ring closure and therefore is subjected to torquoelectronic effects.[18] According to our results, the second barrier of the reaction is substantially larger than the first one. This explains the correlation found by Hegedus[19] between the stereochemistry of the reaction and the torquoelectronic effects computed[16,20] for the nonmetallated version of the reaction. Finally, **TS3** connects **INT3** with the reaction product **11**, which is *ca.* 33 kcal/mol more stable than the separate reagents. Cycloadduct **11** has the O5 atom bound to the chromium atom, with a negative charge of –0.334 on the metallic center. It is expected, being that the chromium is bonded to the reagents during the whole reaction, the effect of ligand changes would be reflected in the reaction selectivity, probably by influence over the charge distribution and steric effects in **TS1** and in **INT3**.

In conclusion, theoretical models to explain the photocarbonylation of chromium carbene complexes and their reaction with imines have been developed. Additionally, the nature of the chromium-ketene intermediate has been studied. The theoretical results are fully consistent with the experimental data about these reactions, including the influence of the chromium ligands and substituents at the carbene carbon in the reactivity. Efforts to fully develop a general theoretical model and to gain a deeper experimental insight into these amazing processes are now underway.

[17] A similar rearrangement was proposed in the reaction of α,β-unsaturated chromium (Fischer) carbenes with different nucleophiles. These results suggest that this kind of shift is a general feature of the chemistry of these compounds. (a) Mancheño, M. J.; Sierra, M. A.; Gómez-Gallego, M.; Ramírez, P. *Organometallics* **1999**, *18*, 3252. (b) Gómez-Gallego, M.; Mancheño, M. J.; Ramírez, P.; Piñar, C.; Sierra, M. A. *Tetrahedron* **2000**, *56*, 4893. (c) Barluenga, J.; Rubio, E.; López-Pelegrin, J. A.; Tomás, M. *Angew. Chem. Int. Ed.* **1999**, *38*, 1091 and related references therein.

[18] (a) Niwayama, S.; Kallel, E. A.; Spellmeyer, D. C.; Sheu, C.; Houk, K. N. *J. Org. Chem.* **1996**, *61*, 2813. (b) Dolbier, W. R., Jr.; Korionak, H.; Houk, K. N.; Sheu, C. *Acc. Chem.Res.* **1996**, *29*, 471 and previous references therein.

[19] Dumas, S.; Hegedus, L. S. *J. Org. Chem*. **1994**, *59*, 4967.

[20] López, R.; Sordo, T. L.; Sordo, J. A.; González, J. *J. Org. Chem*. **1993**, *58*, 7063.

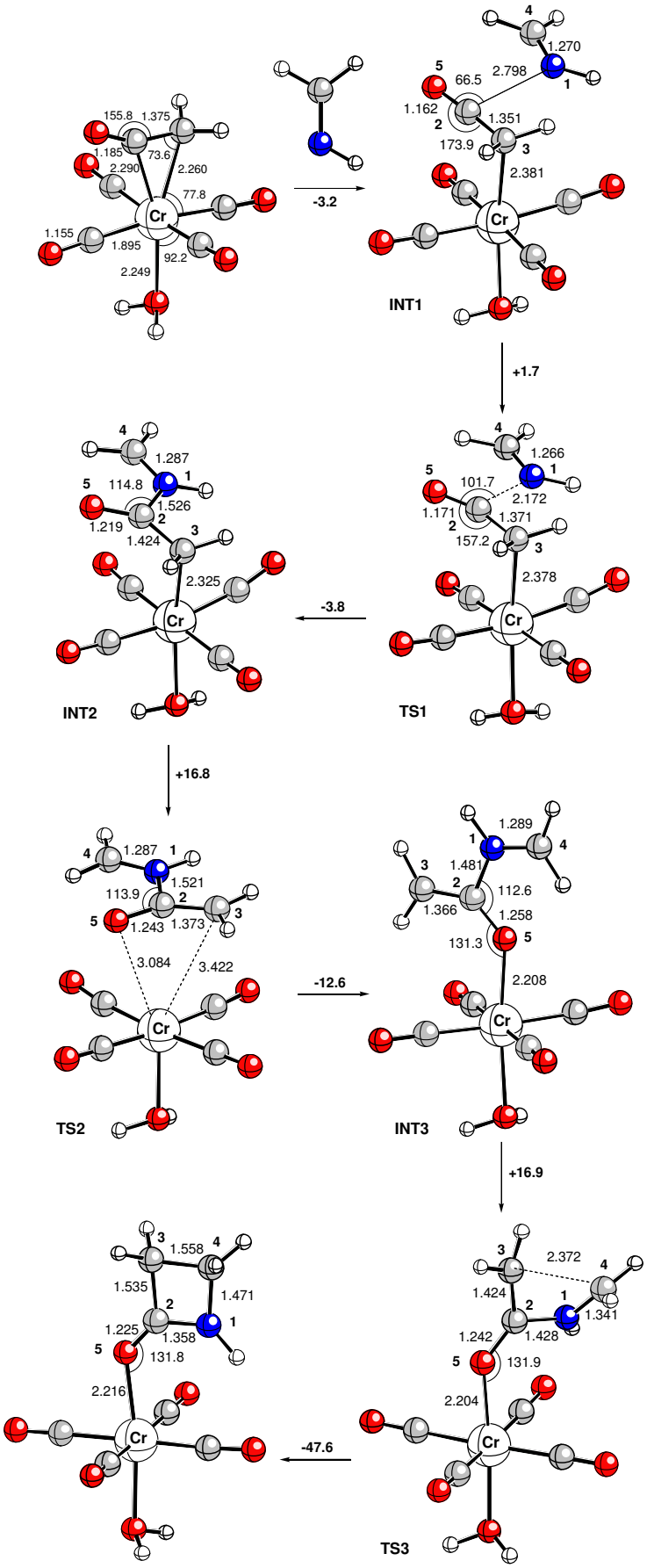

Figure 3

Experimental Section

General. ^{1}H NMR and ^{13}C NMR spectra were recorded in $CDCl_3$, on a Varian XL-300S (299.94 MHz for ^{1}H and 75.43 MHz for ^{13}C), a Bruker 250-AC (250.13 MHz for ^{1}H and 62.90 MHz for ^{13}C), a Bruker 200-AC (200.13 MHz for ^{1}H and 50.03 for ^{13}C MHz) and a Bruker Avance-300 (300.13 MHz for ^{1}H and 75.48 for ^{13}C MHz) spectrometers. Chemical shifts are given in ppm relative to TMS (^{1}H, 0.0 ppm), or $CDCl_3$ (^{13}C, 77.0 ppm). IR spectra were taken on a Perkin-Elmer 781 spectrometer. Flame-dried glassware and standard Schlenck techniques were used for all the reactions. Merck silica-gel (230-400 Mesh) was used as the stationary phase for purification of crude reaction mixtures by flash chromatography. Identification of products was made by TLC (Kiesegel 60F-254), UV light (λ = 254 nm), phosphomolibdic acid solution in 95% EtOH and iodine were also used to develop the plates. All commercially available compounds were used without further purification. The next starting carbene-chromiun complexes were prepared according to literature methods: pentacarbonyl[(ethoxy)(methyl)carbene]chromium(0) (**1a**),[21] pentacarbonyl[(methoxy) (methyl)carbene]chromium(0) (**1b**).[22]

General procedure for the synthesis of compounds 2-3

The synthesis was carried out following the general method described by Fischer.[23] A solution of carbene complex **1a** (0.8 g, 3.03 mmol) and the corresponding phosphine (3.33 mmol) in 20 mL of benzene/hexane (1:1) was heated at reflux overnight (unless otherwise specified). The solvents were removed under reduced pressure and the residue was submitted to flash column chromatography (SiO_2, Hexane: AcOEt) under argon atmosphere to give pure compounds.

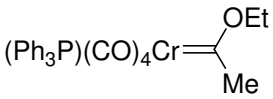

2a

[(Ethoxy)(methyl)carbene](triphenylphosphine)(tetracarbonyl)chromium(0) 2a. Following the general procedure, from 0.8 g (3.03 mmol) of complex **1a** and 0.87 g (3.33 mmol) of triphenylphosphine was obtained **2a** as a *cis:trans* mixture of isomers (4.8:1 ratio). Isomerization was observed after column chromatography to yield 1.15 g (83 %) of the *cis:trans* mixture (11:1 ratio) of **2a** as an orange solid. *cis*-**2a**: ^{1}H NMR δ 1.36 (s, 3H), 2.63 (s, 3H), 4.35 (br s, 2H), 6.90-7.56 (m, 15H); ^{13}C NMR δ 14.6, 45.5, 72.9, 128.2 (d, J_{C-P} = 9.2 Hz), 129.5, 133.4 (d, J_{C-P} = 11.6 Hz), 136.4 (d, J_{C-P} = 32.3 Hz), 221.1 (d, J_{C-P} = 13.4 Hz), 226.6 (d, J_{C-P} = 5.5 Hz), 230.1 (d, J_{C-P} = 11.6 Hz), 357.7 (d, J_{C-P} = 11.6 Hz); IR (KBr) 2004, 1925, 1892, 1867 cm^{-1}. *trans*-**2a**: ^{1}H NMR δ 1.58 (s, 3H), 3.00 (s, 3H), 5.17 (br s, 2H), 6.90-7.56 (m, 15H).

[21] Hegedus, L.S.; McGuire, M.A:; Schultze, L. M. *Organic Syntheses*; Wiley: New York, Collect. Vol. VIII, p 217.
[22] Fischer, E. O., Maasböl, A. *Chem Ber,* **1967**, *100*, 2445.
[23] Fischer, E. O., Fischer, H. *Chem Ber,* **1974**, *107*, 657.

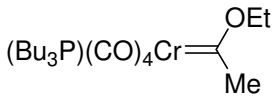

2b

[(Ethoxy)(methyl)carbene](tri-*n*-butylphosphine)(tetracarbonyl)chromium(0) 2b. Following the general procedure starting from 0.8 g (3.03 mmol) of carbene **1a** and 0.67 g (3.3 mmol) of tri-*n*-butylphosphine, was obtained **2b** (0.9 g, 68%), as a red oil and identified as a *cis:trans* mixture of isomers (1:3.4 ratio). *cis*-**2b**: ^{1}H NMR δ 0.86-0.97 (m, 9H), 1.35-1.40 (m, 12H), 1.64-1.72 (m, 8H), 2.86 (s, 3H), 4.62 (q, 2H, J = 6.9 Hz). The ^{1}H NMR data for *trans*-isomer are indistinguishable from that of *cis*-isomer with the exception of the signal assigned to the ethoxy group at 4.93 ppm. *cis*-**2b**: ^{13}C NMR δ 13.6, 14.9, 24.4 (d, $J_{C\text{-}P}$ = 12.2 Hz), 25.2, 28.0 (d, $J_{C\text{-}P}$ = 18.9 Hz), 46.1, 72.5, 221.9 (d, $J_{C\text{-}P}$ = 15.3 Hz), 226.1 (d, $J_{C\text{-}P}$ = 7.3 Hz), 230.9 (d, $J_{C\text{-}P}$ = 12.8), 356.7 (d, $J_{C\text{-}P}$ = 13.4 Hz). *trans*-**2b**: ^{13}C NMR δ 13.6, 15.3, 24.1 (d, $J_{C\text{-}P}$ = 13.2 Hz), 28.4 (d, $J_{C\text{-}P}$ = 20.1 Hz), 48.6, 73.5, 223.5 (d, $J_{C\text{-}P}$ = 12.3 Hz), 226.1 (d, $J_{C\text{-}P}$ = 7.3 Hz), 230.9 (d, $J_{C\text{-}P}$ = 12.21), 349.3 (d, $J_{C\text{-}P}$ = 11.0 Hz); IR (film) 2004, 1878 (br) cm^{-1}.

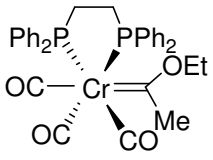

3

***fac*-[(Ethoxy)(methyl)carbene](1,2-bis(diphenylphosphino)ethane)](tricarbonyl)-chromium(0) 3**. Following the general procedure from 0.8 g (3.03 mmol) of carbene **1a** and 1.37 g (3.33 mmol) of 1,2-bis(diphenylphosphino)ethane, compound **3** (1.7 g, 97%) was obtained after 17 h as a red-orange solid. **3**: ^{1}H NMR δ 0.085 (t, J = 7.2 Hz, 3H), 1.53 (s br, 3H), 2.49-2.56 (m, 2H), 2.60 (s, 3H), 2.75-2.87 (m, 4H), 7.18-7.55 (m, 20H); ^{13}C NMR δ 12.8, 26.5 (t, $J_{C\text{-}P}$ = 19.6 Hz), 41.5, 67.8, 127.9 (t, $J_{C\text{-}P}$ = 4.2 Hz), 128.2 (t, $J_{C\text{-}P}$ = 4.2 Hz), 128.4 (t, $J_{C\text{-}P}$ = 3.5 Hz), 128.7 (t, $J_{C\text{-}P}$ = 6.9 Hz), 130.9 (t, $J_{C\text{-}P}$ = 5.4 Hz), 131.2 (t, $J_{C\text{-}P}$ = 5.2 Hz), 132.7 (t, $J_{C\text{-}P}$ = 9.2 Hz), 138.5 (m), 235. 6 (t, $J_{C\text{-}P}$ = 5.5 Hz), 235.2 (t, $J_{C\text{-}P}$ = 5.6 Hz), 354.4 (t, $J_{C\text{-}P}$ = 17.3 Hz); IR (KBr) 1919, 1840, 1815 cm^{-1}.

Photochemical reactions. General procedure. All photochemical reactions were conducted by using a 450W-medium pressure mercury lamp through a Pyrex filter. All the reactions were carried out in dry degassed CH_3CN or Et_2O in a sealed pyrex tube filled with argon. For all cases *N*-(4-methoxylphenyl)benzylideneimine **4** was used. In a typical experiment a solution of the carbene complex (0.20 mmol) and 42 mg (0.20 mmol) of imine **4** in 20 mL of CH_3CN was irradiated for 14 h. The solvent was removed *in vacuo* and the residue was dissolved in a mixture of hexane:AcOEt (1:1) and exposed to direct sunlight until a clear solution was obtained. The solution was filtered through a short pad of celite, the solvent eliminated and the desired *β*-lactam was purified by flash column accomplished by crystallization from hexane to yield pure compounds. Reaction conversion was estimated by integration of well-resolved signals of the imine proton at 8.4 ppm. Isomers ratio was determined by comparison of the signals at 4.85 and 5.01 ppm for compound **5a** and 4.78 and 5.03 ppm for **5b** respectively.

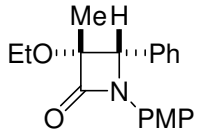

cis-**5a**

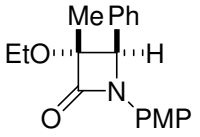

trans-**5a**

Irradiation of 1a. Following the general procedure a solution of carbene complex **1a** (53 mg, 0.20 mmol) and 42 mg (0.20 mmol) of imine **4** in 20 mL of CH_3CN was irradiated under the same conditions using different reaction temperatures, the obtained *cis:trans* isomers ratio of **5a** and the temperature used are specified below: (temp = 0 ˚C, 2.7:1 ratio), (temp = 30 ˚C, 6.3:1 ratio), (T = 60 ˚C, 12:1 ratio). *cis*-**5a**: ^{1}H NMR δ 0.74 (t, J = 7.0 Hz, 3H), 1.66 (s, 3H), 3.14 (dq, ^3J = 7.0 Hz, ^2J = 8.8 Hz, 1H), 3.39 (dq, ^3J = 7.0 Hz, ^2J = 8.8 Hz, 1H), 3.71 (s, 3H), 4.85 (s, 1H), 6.74-6.78 (m, 2H), 7.22-7.31 (m, 7H); ^{13}C NMR δ 15.0, 19.3, 55.4, 61.3, 68.4, 88.2, 114.3, 118.8, 128.2, 128.3, 131.0, 134.4, 156.3, 166.3; IR (KBr) 1742, 1518 cm^{-1}. Analysis calculated for $C_{19}H_{21}NO_3$: C, 73,29; H.6.80, N; 4.50. Found: C, 73.40; H, 6.92; N, 4.60. *trans*-**5a** (from an enriched mixture): ^{1}H NMR δ 1.2 (t, J = 7.0 Hz, 3H), 3.66 (s, 3H and m, 2H), 5.01 (s, 3H), 6.74-6.78 (m, 2H), 7.22-7.31 (m, 7H); ^{13}C NMR δ 15.5, 16.1, 60.9, 65.6, 90.8, 114.3, 118.9, 126.7, 128.3, 131.0, 134.6, 156.3, 166.5.

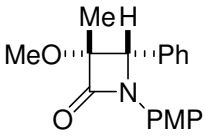

cis-**5b**

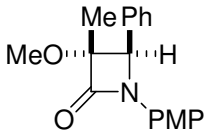

trans-**5b**

Irradiation of 1b. Following the general procedure carbene complex **1b** was irradiated using different concentrations:

a) a solution of carbene complex **1b** (50 mg, 0.20 mmol) and 42 mg (0.20 mmol) of imine **4** in 5 mL of CH_3CN was irradiated for 14 h. The analysis of the crude reaction by ^{1}H NMR reveals the presence of **5b** as a *cis:trans* mixture of isomers (5.0:1 ratio);

b) a solution of carbene complex **1b** (50 mg, 0.20 mmol) and 42 mg (0.20 mmol) of imine **4** in 10 mL of CH_3CN was irradiated for 14 h. The analysis of the crude reaction by ^{1}H NMR reveals the presence of **5b** as a *cis:trans* mixture of isomers (4.7:1 ratio);

c) a solution of carbene complex **1b** (50 mg, 0.20 mmol) and 42 mg (0.20 mmol) of imine **4** in 20 mL of CH_3CN was irradiated for 14 h. The analysis of the crude reaction by ^{1}H NMR reveals the presence of **5b** as a *cis:trans* mixture of isomers (6.3:1 ratio);

d) a solution of carbene complex **1b** (50 mg, 0.20 mmol) and 42 mg (0.20 mmol) of imine **4** in 8 mL of CH_3CN was irradiated for 14 h. The analysis of the crude reaction by ^{1}H NMR reveals the presence of **5b** as a *cis:trans* mixture of isomers (5.7:1 ratio). *cis*-**5b**[4]: ^{1}H NMR δ 1.64 (s, 3H), 3.04 (s, 3H), 3.68 (s, 3H), 4.78 (s, 1H), 6.80-6.82 (m, 2H), 7.14-7.44 (m, 7H). ^{13}C NMR δ 18.3, 55.4, 68.4, 88.0, 114.3, 118.8, 127.7, 128.7, 130.9, 134.1, 156.3, 166.1. *trans*-**5b**: ^{1}H NMR δ 1.01 (s, 3H), 3.49 (s, 3H), 3.68 (s, 3H), 5.03 (s, 1H), 6.80-6.82 (m, 2H), 7.14-7.44 (m, 7H). ^{13}C NMR δ 15.6, 53.3, 65.1, 91.3, 114.4, 119.1, 126.7, 128.33, 130.9, 134.6, 156.3, 166.2; IR (KBr) 1740 cm^{-1}.

Irradiation of compounds 1a, 2a, 2b and 3. Following the general procedure all the irradiations were carried out under the same conditions and for the same time as specified below.

a) Irradiation of **1a**: (53 mg, 0.20 mmol, 14 h, 100% conversion) gave compound **5a** as a *cis:trans*-isomers mixture, ratio (6.1:1).

b) Irradiation of **2a**: (100 mg, 0.20 mmol, 14 h, 71% conversion) gave compound **5a** as a *cis:trans*-isomers mixture, ratio (10.5:1).

c) Irradiation of **2b**: (121 mg, 0.20 mmol, 14 h, <5 % conversion,) gave only traces of compound **5a**.

d) Irradiation of **3**: (88 mg, 0.20 mmol, 14 h, <5 % conversion) gave only traces of **5a**.

e) Irradiation of **2b** and **3** was also carried out in 20 mL of diethyl ether to give similar results (<5 % conversion, only traces of **5a** was detected).

El estudio anterior demuestra que la fotorreactividad de complejos metal-carbeno frente a cetenófilos depende claramente de la densidad electrónica sobre el núcleo metálico. En la Tabla 2 se recogen los valores de conversión en un experimento de control transcurridas 6h de reacción, para evitar conversión total, y proporción de β-lactamas *cis/trans* en la reacción de los complejos **1a**, **2a**-**b** y **3** con la imina **4**.

Tabla 2.

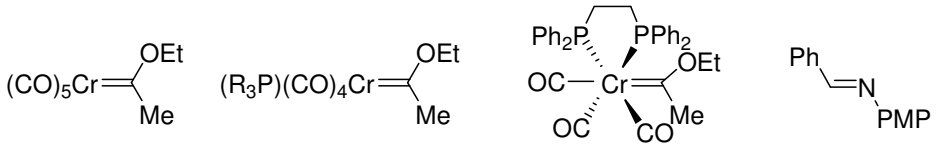

1a | **2a** R = Ph, **2b** R = *n*-Bu | **3** | **4**

Entrada	Complejo	Conversión[a]	Relación *cis/trans*[b]	Disolvente[c]
1	**1a**	81	2.8:1	MeCN
2	**2a**	73	7.3:1	MeCN
3	**2b**	5	3.6:1	MeCN
4	**3**	20	4.5:1	MeCN
5	**1a**	79	1.4:1	THF
6	**2a**	71	2.5:1	THF
7	**2b**	10	2.3:1	THF
8	**3**	30	1.3:1	THF

[a] Referida a la imina sin reaccionar. Los experimentos se llevaron a cabo a 30ºC, de manera simultánea las entradas 1-4 y 5-8 para asegurar las mismas condiciones de reacción. [b] Determinada por integración de las señales correspondientes al hidrógeno unido a C4 de la β-lactama en el espectro de ^{1}H-RMN del crudo de reacción. [c] Todos los experimentos se llevaron a cabo a una concentración de complejo de 10^{-2} M.

Como se puede observar, la sustitución de ligandos en la esfera de coordinación del metal provoca cambios importantes de la reactividad con iminas para producir β-lactamas. Así, el efecto de la sustitución de un ligando CO por un ligando σ-dador débil como es la PPh_3 (complejo **2a**, entradas 2 y 6) es poco importante. Las conversiones en la correspondiente β-lactama, son algo menores que para el complejo de referencia **1a**, pero del mismo orden de magnitud. El efecto es mucho más acusado para ligandos bidentados (complejo **3**, entradas 4 y 8). En esta caso, la reactividad es mucho menor que en **1a** para tiempos iguales de reacción. Por último, el intercambio de un ligando CO por un ligando fuertemente σ-dador como es la PBu_3 (complejo **2b**, entradas 3 y 7) provoca la práctica inhibición de la formación de β-lactamas.

Podemos concluir, entonces, que el proceso de formación de β-lactamas es más eficaz en complejos con ligandos π-aceptores, tipo CO, en su esfera de coordinación. La eficacia del proceso es menor si intercambiamos ligandos de ese tipo por ligandos σ-dadores, disminuyendo drásticamente la reactividad al incrementarse el carácter dador del/los ligando/s. Las conclusiones obtenidas en el Capítulo 2.2 para el proceso de fotocarbonilación parecen contradecirse con este orden de reactividad observado experimentalmente en la reacción con iminas, puesto que la diferencia de energía entre el estado fundamental S_0 y el triplete de carbonilación T_1 es menor para complejos con ligandos σ-dadores (PH_3 en el modelo).[24] Desde un punto de vista sencillo, esto significaría que una vez suministrada la energía necesaria para alcanzar el estado excitado S_1, el estado T_1 más estable es aquel que posee mayor número de grupos σ-dadores, lo que es coherente con la estructura de metalaciclopropanona propuesta. Por tanto, las diferencias de reactividad no deben encontrarse en el proceso de fotocarbonilación, sino en una etapa posterior del proceso de reacción de la metalacetena con el cetenófilo. De esta forma, podemos concluir que la fotocarbonilación no es la etapa determinante de estas reacciones.

Basándonos en el mecanismo propuesto en la Figura 3, hemos calculado de nuevo la coordenada de reacción (B3LYP/6-31G*&LanL2DZ)[25] para los complejos **12** y **13** (Figura 4) y la imina **10** con el fin de comparar las distintas energías de activación del proceso. Ahora, el modelo usado se aproxima más a la realidad, ya que considera el grupo metoxi sobre el complejo metal-carbeno.

[24] No se puede descartar que la discrepancia observada se deba a la utilización de un modelo demasiado sencillo para el ligando σ-dador (PH_3) en los cálculos realizados en el Capítulo 2.2.
[25] Se ha obviado el cálculo de **TS1** (asociado al ataque de la imina al carbonilo de la metalacetena) debido a su escasa contribución energética.

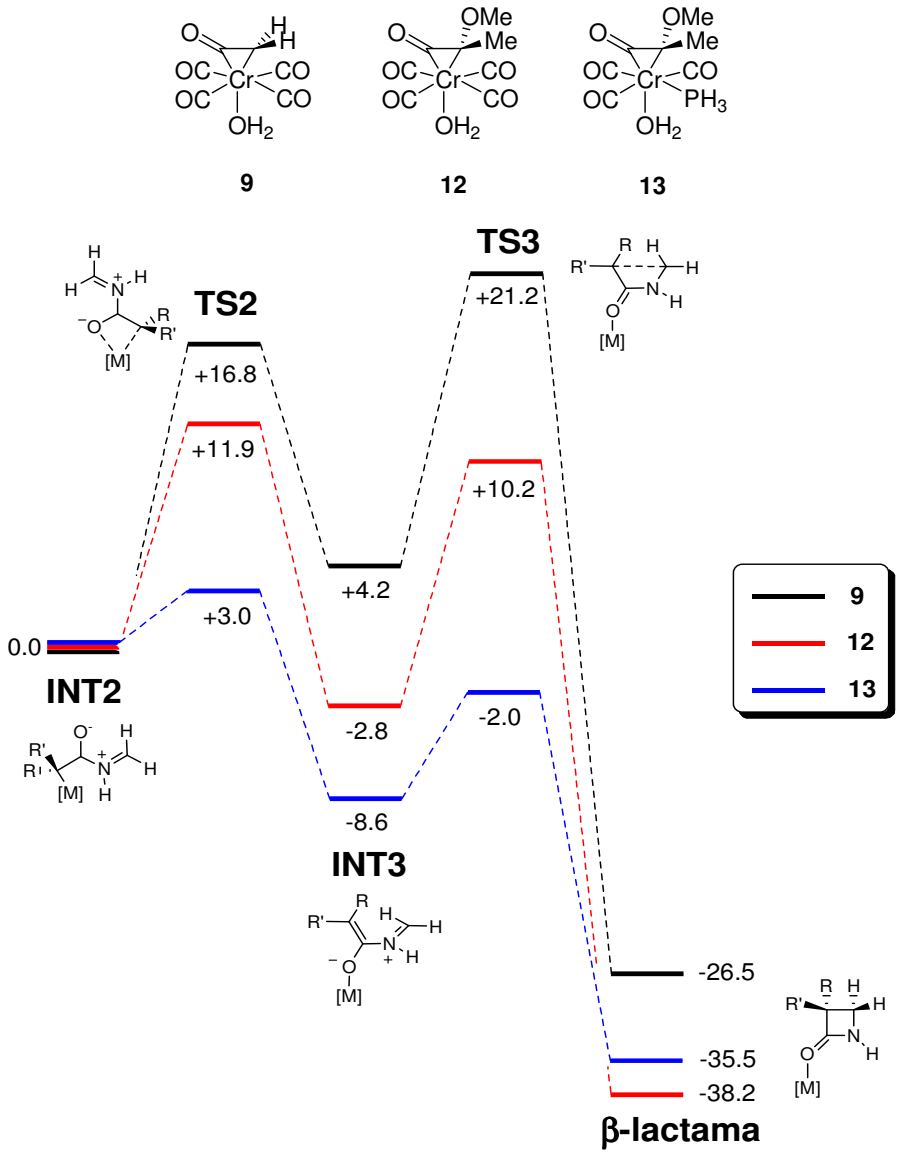

Figura 4

Como se puede ver, tanto la barrera que conecta **INT2** con **INT3**, correspondiente a la migración 1,3- de cromo, como la que conecta **INT3** con la *β*-lactama coordinada al metal son inferiores cuando tenemos un ligando *σ*-dador (PH_3 en el modelo) en la esfera de coordinación del metal. Estos resultados indican que la reacción entre los complejos **2** e iminas debe estar favorecida respecto a la misma reacción empleando los complejos **1**, en los que no se ha producido ningún intercambio de ligando. De nuevo, este resultado computacional no justifica los resultados experimentales observados.

Los datos experimentales de la Tabla 2 demuestran que realmente son los complejos **1** los que generan conversiones mayores en la fotorreacción con iminas a

tiempos iguales de reacción. Por lo tanto, es clara la discrepancia entre los resultados experimentales y teóricos.

Llegados a este punto, se puede proponer un curso de reacción diferente al considerado hasta este momento. Podemos asumir que, antes de que ocurra el ataque desde el nitrógeno de la imina al carbono carbonílico (camino **INT1→TS1→INT2**, Figura 3), las especies **12**-**15**, con gran carácter de acil-cromato, experimentarían un proceso de reordenamiento a una cetena coordinada a metal por el átomo de oxígeno (especies **16**-**19**) a través del estado de transición, $\mathbf{TS_{reor}}$, correspondiente (Esquema 2) y en la hipersuperficie S_0. Una vez formadas, las cetenas reaccionarían del modo usual con la imina para llegar al intermedio **INT3** coincidente con el mecanismo original.

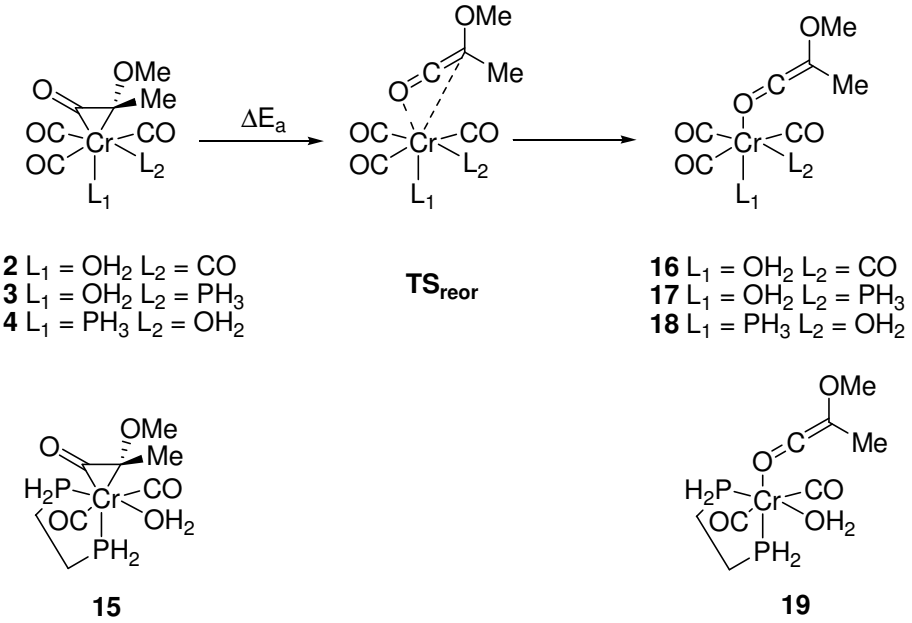

Esquema 2

La Tabla 3 recoge los valores de energía de activación (ΔE_a) y energía de reacción (ΔE_r) para el reordenamiento propuesto.

Tabla 3.

Entrada	Complejo	ΔE_a / kcal mol^{-1}	ΔE_r / kcal mol^{-1}
1	**12**	+10.7	+6.4
2	**13**	+8.3	+6.8
3	**14**	+15.0	+13.9
4	**15**	+21.8	+17.2

Como se puede apreciar, para el complejo modelo **12** (análogo al complejo real **1b**) y para el complejo **13** (en el que se ha sustituido un ligando CO en posición *cis* por un ligando PH_3), tanto ΔE_a como ΔE_r son muy similares. En concreto, ΔE_a es 2.4 kcal mol^{-1} menor para **13** que para **12**, lo que indica, de nuevo, que la reacción debería estar favorecida en complejos que poseen un ligando σ-dador en su esfera de coordinación. Estas diferencias se incrementan cuando sustituimos el ligando fosfina en posición *trans* o cuando introducimos dos ligandos σ-dadores ($\Delta\Delta E_a$ = 4.3 kcal mol^{-1} y $\Delta\Delta E_a$ = 11.1 kcal mol^{-1} respectivamente), lo que podría justificar la diferencia de reactividad observada. Sin embargo, puesto que en todos los casos este proceso de reordenamiento es endotérmico, puede argumentarse que el camino favorecido debería ser el propuesto inicialmente (Figura 3). Por tanto, las razones últimas que justifican las diferencias de reactividad en función del ligando observadas experimentalmente continúan todavía sin esclarecerse totalmente.[26]

La irradiación del complejo **2c** constituye una prueba adicional para apoyar la presencia del metal durante toda la coordenada de reacción que lleva a la formación de β-lactamas. Dicho complejo se prepara fácilmente por reacción entre el complejo **1a** y la fosfina quiral **20** siguiendo el método estándar (Esquema 3).[27]

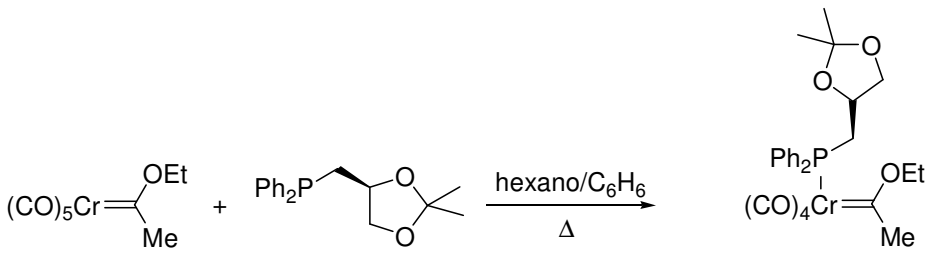

1a **20** **2c** (83%)

Esquema 3

Al irradiar **2c** en presencia de la imina **4** se obtienen las correspondientes β-lactamas como mezcla *cis/trans* en relación 3.5:1. Tras separación cromatográfica de ambos diastereoisómeros, mediante espectroscopia de ^{1}H-RMN usando (+)-tris[3-

[26] En estos momentos se está abordando el estudio de este reordenamiento en la hipersuperficie triplete, antes de que ocurra la saturación de la vacante de coordinación por una molécula de disolvente coordinante (ver Capítulo 2.2). Resultados no incluidos.
[27] Brunner, H.; Leyerer H. *J. Organomet. Chem.* **1987**, *334*, 369.

(heptafluoropropilhidroximetilen)canforato] de Eu(III),[28] se determinó que el diastereómero ***cis*-5a** se obtiene con un 14% *ee* = (Figura 5).[29]

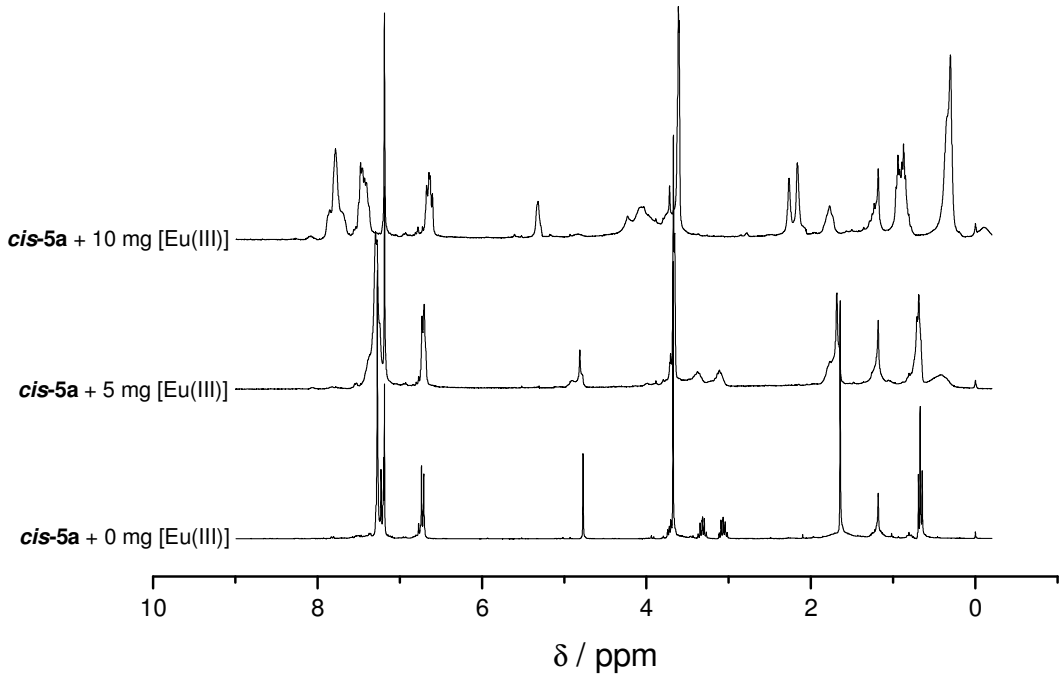

Figura 5

La discriminación quiral es baja debido, probablemente, a la lejanía del auxiliar quiral respecto del sistema reactivo en la etapa en que se produce ésta, pero demuestra de manera inequívoca que el metal permanece unido al sistema reactivo durante todo el proceso. A pesar de esto, siempre es posible pensar que la discriminación se deba a un proceso de organocatálisis provocada por el auxiliar quiral desprendido de la esfera de coordinación del metal, antes de producirse esta discriminación. Para confirmar que esto no ocurre así, irradiamos de nuevo el complejo **2c** con la imina **4** en atmósfera de CO (90 psi), lo que garantiza la eyección del auxiliar quiral y su intercambio por un ligando CO. En estas condiciones de reacción no hubo ningún *ee* (determinado nuevamente por RMN). Estos resultados confirman la presencia del metal (y de su esfera de coordinación) durante toda la coordenada de reacción o, al menos, en aquellas etapas en las que se produce la discriminación quiral (Esquema 4). En este último caso la

[28] Sievers, R. E.: *Nuclear Magnetic Resonance Shift Reagents*. New York: Academic Press, 1973.
[29] El valor de *ee* se obtuvo por integración de la señal correspondiente al resto metilo unido a C3 (δ = 1.66 ppm) desdoblado en dos singletes a δ = 2.16 y δ = 2.27 ppm, respectivamente (Figura 5)

conversión obtenida fue mayor puesto que los procesos de fotocarbonilación ocurren mejor bajo presiones moderadas de CO.

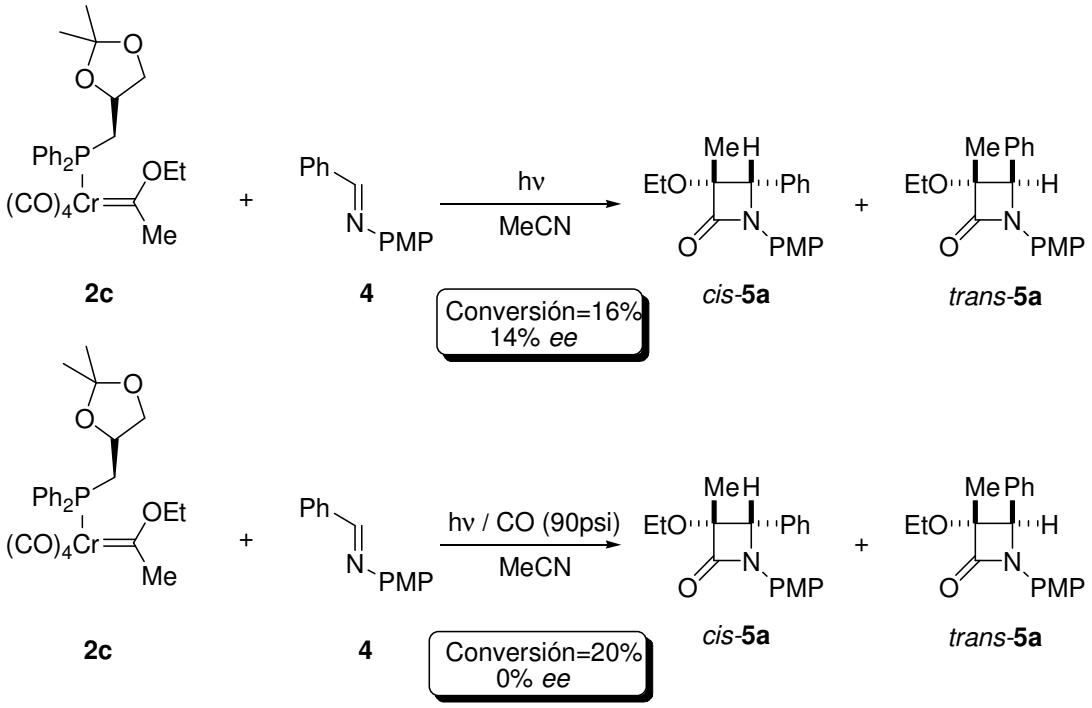

Esquema 4

Estudio teórico del proceso de diastereoselección en el cierre conrotatorio de cromoenolatos

Un aspecto interesante del estudio sistemático de la reacción fotoquímica de complejos metal-carbeno de tipo Fischer e iminas para formar β-lactamas, es establecer, desde un punto de vista teórico, la influencia del centro metálico en la diastereoselección observada en este proceso.

El mecanismo de la reacción clásica entre una cetena y una imina (reacción de Staudinger) no está totalmente esclarecido. Existen numerosos y variados factores que intervienen en la reacción. Además de la estructura y tamaño de los sustituyentes, y de que la cetena suele generarse *in situ* introduciendo una base en el medio de reacción, la presencia de intermedios cargados hace que el disolvente sea un factor muy importante a tener en cuenta. También influyen factores como el orden de adición de los reactivos[30] o la temperatura. En general, cuando el cloruro de ácido se adiciona (preferentemente a baja temperatura) sobre una disolución de la imina y la amina terciaria (comúnmente trietilamina) se obtiene el aducto *cis* de forma mayoritaria o exclusiva. Por el contrario, cuando la base se añade sobre una mezcla de la imina y el cloruro de ácido, se obtienen mezclas *cis*/*trans* en las que el isómero *trans* es mayoritario. Adicionalmente, se ha demostrado que, en las condiciones de reacción utilizadas, no se produce la isomerización de las β-lactamas *cis* ya formadas a sus correspondientes isómeros *trans* (termodinámicamente más estables). En la actualidad se acepta que la formación de 2-azetidinonas ocurre a través del ion dipolar **22** (Esquema 5).

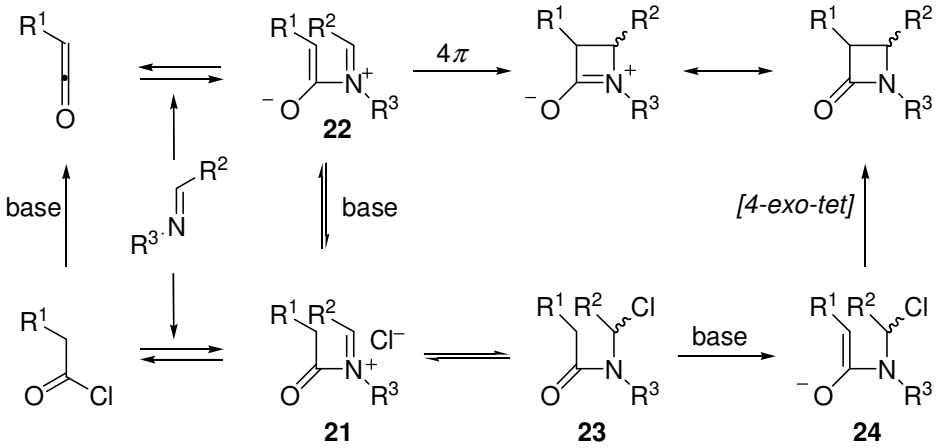

Esquema 5

[30] (a) Bose, A. K.; Anjanayulu, B.; Bhattachayara, S. K.; Manhas, M. S. *Tetrahedron* **1967**, *23*, 4769. (b) Wells, J. N.; Lee, R. E. *J. Org. Chem*. **1969**, *34*, 1477. (c) Lecea, B.; Palomo, C. *J. Chem. Soc., Perkin Trans. 1* **1987**, 875.

La formación de estos intermedios puede ocurrir, además, por dos caminos de reacción diferentes. Por un lado, el ataque de la cetena formada *in situ* sobre la imina formaría un ion dipolar que conduciría a la β-lactama por cierre conrotatorio. Alternativamente, la acilación de la imina por el cloruro de ácido produciría una sal de iminio **21**, que posteriormente evolucionaría al ion dipolar **22** por acción de la base presente en el medio de reacción. Se ha propuesto que la formación del ion dipolar **22** ocurra por ataque del HOMO de la imina al LUMO de la cetena en una disposición ortogonal. Este ion dipolar experimenta posteriormente un cierre conrotatorio formando la β-lactama. El segundo estado de transición que da lugar al cierre de anillo parece ser la etapa limitante de la velocidad del proceso. Adicionalmente, existe una amplia evidencia en contra de un mecanismo concertado cetena-imina [$_\pi 2_s$ + $_\pi 2_a$] del tipo del propuesto para la cicloadición cetena-olefina.[31] El grupo de Sordo, ha demostrado teóricamente la presencia de un intermedio zwitteriónico en la reacción de Staudinger.[32] Otros estudios, sin embargo, sugieren que en ausencia de base, el intermedio **21** puede sufrir un ataque nucleófilo para dar la amida **23** (que se ha aislado en algunos casos).[33] Seguidamente, la captura de un protón conduce al enolato **24**, el cual puede ciclar mediante un proceso S_N2 intramolecular. Este último paso supone un proceso de ciclación *4-exo-tet* que está favorecido según las reglas de Baldwin.[34]

Por otra parte, Lynch ha examinado la reacción de cloruros de ácido e iminas en presencia de bases, a baja temperatura, por espectroscopia IR de transformada de Fourier.[35] La medida de las constantes de formación de la cetena a partir del cloruro de ácido y de la base, y de su reacción con la imina, permitió concluir que las 2-azetidinonas proceden de la reacción de la cetena generada *in situ* y no de la acilación directa de la imina por el cloruro de ácido. Según Brady,[36] el ataque nucleófilo de los electrones no enlazantes del nitrógeno de la imina sobre la cetena se da por el lado que determine el volumen de sus sustituyentes. Así, el sustituyente de la imina se sitúa hacia dentro (inward), debido a la preferencia por la configuración *trans* de la misma. El

[31] Wang, X.; Houk, K. N. *J. Am. Chem. Soc*. **1990**, *112*, 2106.
[32] (a) Sordo, J. A.; González, J.; Sordo, T. L. *J. Am. Chem. Soc*. **1992**, *114*, 6249. (b) López, R.; Sordo, T. L.; Sordo, J. A.; González, J. *J. Org. Chem*. **1993**, *58*, 7036.
[33] (a) Nelson, D. A. *J. Org. Chem*. **1972**, *37*, 1447. (b) Bose, A. K.; Spiegelman, G.; Manhas, M. S. *Tetrahedron Lett*. **1971**, 3167. (c) Duran, F.; Ghosez, L. *Tetrahedron Lett*. **1970**, 245. (d) Moore, H. W.; Hernández, L.; Chambers, R. *J. Am. Chem. Soc*. **1978**, *100*, 2245.
[34] Baldwin, J. E. *J. Chem. Soc., Chem. Commun*. **1976**, 735.
[35] Lynch, J. E.; Riseman, S. M.; Laswell, W. L.; Volante, R. P.; Smith, G. B.; Shinkai, I. *J. Org. Chem*. **1989**, *54*, 3792.
[36] Brady, W. T.; Gu, Y. Q. *J. Org. Chem*. **1989**, *54*, 2838.

orbital p del carbono con hibridación sp de la cetena interacciona entonces con el par de electrones sin compartir de la imina.[37] El cierre conrotatorio del ion dipolar inicialmente formado conduciría a la β-lactama *cis*, menos estable termodinámicamente (Esquema 6, camino a).

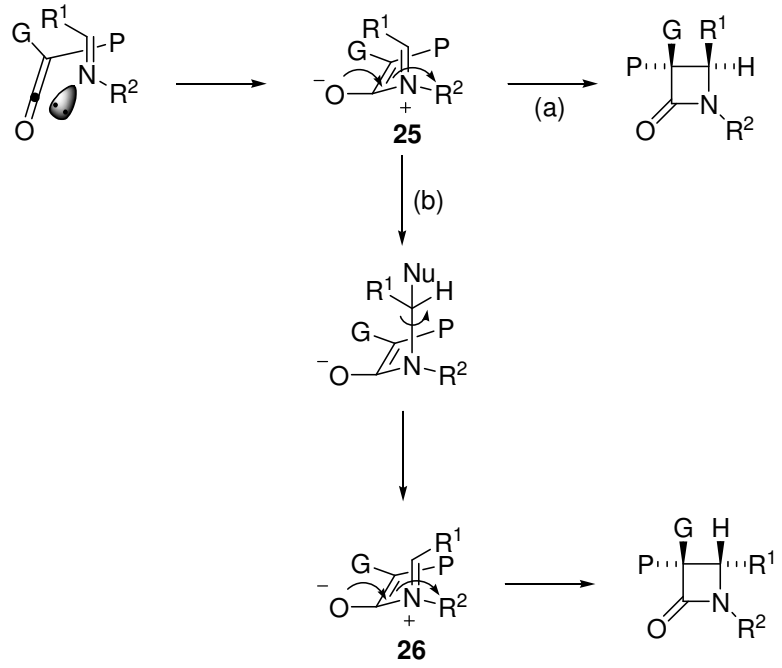

Esquema 6

La formación de β-lactamas *trans* o de mezclas *cis-trans* puede explicarse por dos caminos diferentes. Por un lado, la adición de un nucleófilo al intermedio zwitteriónico **25** (Esquema 6, camino b), permitiría el giro del enlace imínico, dando como resultado la isomerización del ion dipolar a un nuevo intermedio **26**, que evolucionaría posteriormente a la β-lactama *trans*. Por otro lado, y para sustratos como los imidatos, algunas *C*-ariliminas y *C*-alquiliminas, que tienen preferencia por la formación de producto *trans*, se postula que estos grupos, al estabilizar la carga positiva del ion dipolar intermedio, favorecen la isomerización de **25** a **26** originando así, tras el cierre conrotatorio, la β-lactama *trans*.[38]

En cuanto al segundo camino de reacción postulado, la acilación directa de la imina por el cloruro de ácido formaría el cloruro de *N*-aciliminio **27**. Si la base presente en el medio captura un protón, este intermedio puede evolucionar al ion dipolar **28** que

[37] Baigrie, L .M.; Siklay, H. R.; Tidwell, T. T. *J. Am. Chem. Soc*. **1985**, *107*, 5391.
[38] (a) Hegedus, L. S.; Montgomery, J.; Narukawa, Y.; Snustad, D. C. *J. Am. Chem. Soc*. **1991**, *113*, 2085. (b) Dumas, S.; Hegedus, L. S. *J. Org. Chem*. **1994**, *59*, 4967.

cicla conrotatoriamente a la β-lactama. Dependiendo de la geometría del enolato inicialmente formado, se obtendrían los productos *cis* o *trans*. Alternativamente, podría producirse la isomerización del enlace imínico por adición-eliminación de un nucleófilo en el ion dipolar intermedio **27** lo que conduciría, finalmente, al compuesto más estable, la β-lactama *trans* (Esquema 7).[39]

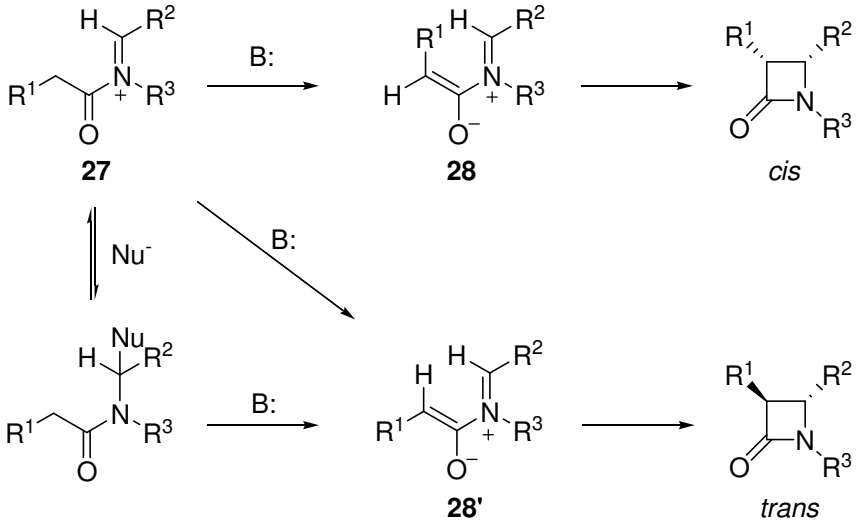

Esquema 7

Un estudio reciente realizado por Cossío[40] ha puesto de manifiesto la tendencia del proceso S_N2 a dar las 2-azetidinonas *trans*. Por otra parte, el camino que supone el cierre conrotatorio favorece la formación de los productos *cis* debido, principalmente a la estereoquímica *E* de la imina y a la interacción electrónica existente entre el orbital ocupado del sustituyente en posición 3 y el orbital $\sigma^*_{3,4}$.

Como se ha comentado anteriormente, la reacción entre metalacetenas derivadas de complejos metal-carbeno e iminas transcurre en tres etapas con una clara diferencia con la reacción clásica: la migración 1,3- de cromo (Figura 3, página 188) entre las especies **INT2** e **INT3**.

Debido a la similitud entre ambos mecanismos (el clásico y el derivado de metalacetenas), en una primera aproximación hemos calculado la diferencia de energía entre los dos posibles estados de transición (**TS3*cis*** y **TS3*trans***) que conducen, tras cierre conrotatorio de anillo, a las β-lactamas *cis* y *trans* respectivamente (Esquema 8).

[39] (a) Arrieta, A.; Lecea, B.; Palomo, C. *Tetrahedron Lett*. **1985**, *26*, 3041. (b) Doyle, T. W.; Belleau, B.; Luh, B.; Ferrari, C. F.; Cunningham, M. P. *Can. J. Chem*. **1977**, *55*, 468.
[40] Arrieta, A.; Lecea, B.; Cossío, F. P. *J. Org. Chem*. **1998**, *63*, 5869.

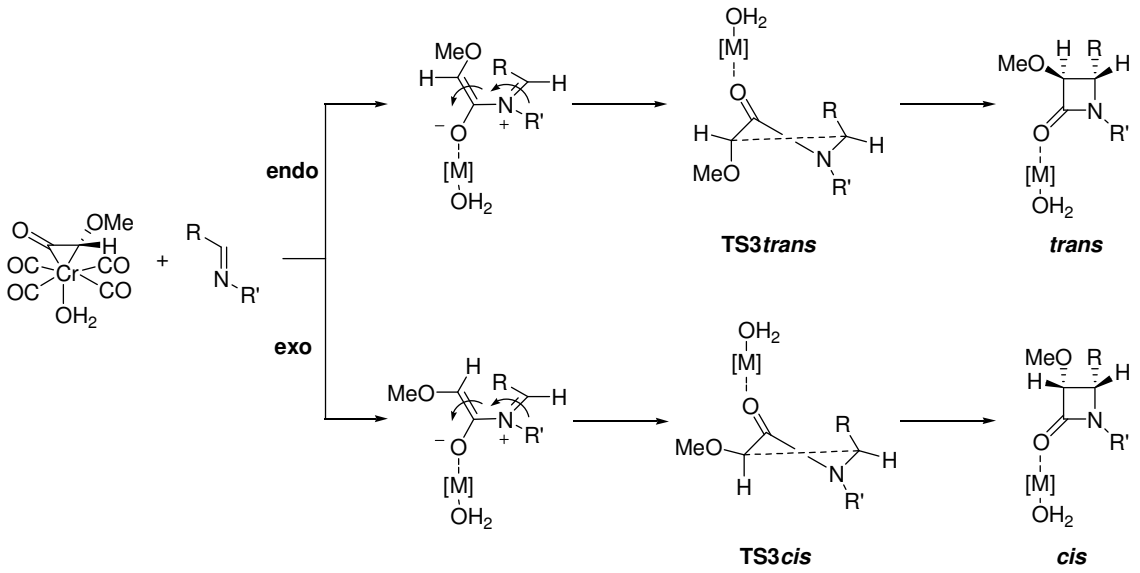

Esquema 8

La Tabla 4 recoge los valores de $\Delta\Delta E^{\ddagger}_{(cis-trans)}$ (que se corresponde con la diferencia de energía **TS3*trans*-TS3*cis***) calculados a nivel B3LYP/6-31G*&LANL2DZ para la versión clásica y metalada de la reacción entre cetenas e iminas.

Tabla 4.

Entrada	R	R'	$\Delta\Delta E^{\ddagger}$/ kcal mol^{-1}
		[M] = —	
1	H	H	+15.2
2	Me	Me	+14.4
3	Me	H	+10.8
4	Ph	Me	+12.5
		[M] = $Cr(CO)_4$	
5	H	H	+12.8
6	Me	Me	+14.3
7	Me	H	+13.7
8	Ph	Me	+13.8
		[M] = $Cr(CO)_3L$, L= PH_3*cis*	
9	H	H	+9.8
10	Me	H	+12.8

Los valores de $\Delta\Delta E^{\ddagger}$ obtenidos para el cierre conrotatorio indican que no existen diferencias significativas entre ambas versiones de la reacción entre cetenas e iminas, ni siquiera cuando introducimos un ligando σ-dador en la esfera de coordinación del metal. En todos los casos, la reacción debe producir mayoritariamente, o de forma casi exclusiva, *cis*-β-lactamas.[41] Por consiguiente, podemos concluir que el efecto del metal en la diastereoselección de este proceso es prácticamente despreciable. Sin embargo, los datos de las Tablas 1 y 2 demuestran que la relación *cis/trans* depende de las condiciones de reacción y del complejo utilizado, lo cual constituye una prueba adicional de la presencia del metal durante todo el proceso de reacción. En cualquier caso, la fotorreación entre complejos metal-carbeno e iminas, aun siendo *cis*-selectiva, produce en muchos casos cantidades apreciables de *trans*-β-lactamas. Puesto que según nuestros cálculos, el cierre conrotatorio de la última etapa de reacción debería conducir únicamente a *cis*-β-lactamas, es necesario suponer que la diastereoselección se deba a una discriminación facial en una etapa previa. De hecho, sólo existen dos puntos en los que dicha discriminación pueda producirse: el ataque *endo* o *exo* de la imina a la metalacetena en el primer paso de la reacción (**INT1→TS1→INT2** en el mecanismo de la Figura 3) o durante el proceso de migración 1,3 de cromo (**INT2→TS2→INT3**).

La Figura 6 muestra los caminos de evolución de los dos posibles intermedios **INT2** que conducen los zwitteriones **INT3** tras ataque de la imina a la metalacetena mediante una aproximación *exo* (es decir, por el lado opuesto al sustituyente OMe de la metalacetena; color rojo en la figura) o *endo* (por el mismo lado del sustituyente OMe; color negro en la figura).

[41] En general, las iminas *E* conducen a *cis*-β-lactamas mientras que las iminas *Z* conducen predominantemente a los isómeros *trans*. Ver referencia 16a.

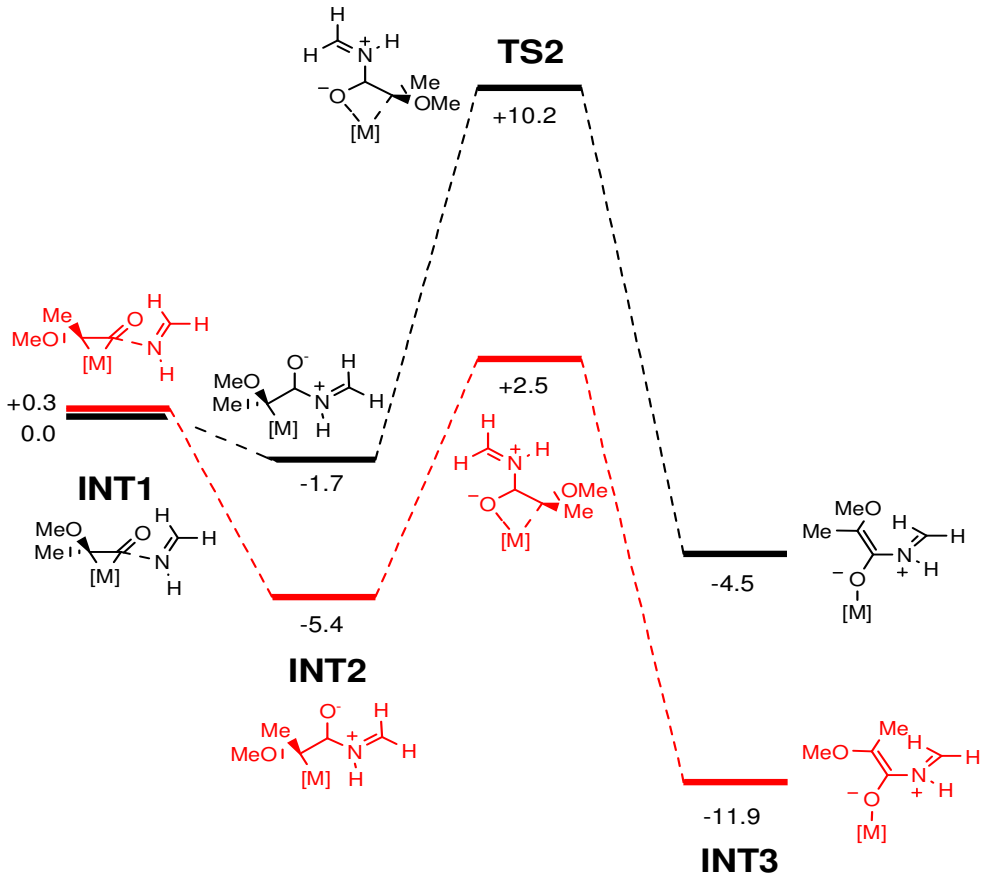

Figura 6

En este modelo de reacción, se puede apreciar claramente que el camino que conecta **INT2** con **INT3** transcurre con una energía de activación menor para el aducto *exo* que para el *endo* ($\Delta\Delta E_a$ = -4.0 kcal mol^{-1}), siendo además un proceso más exotérmico ($\Delta\Delta E_r$(**INT2**→**INT3**)$_{exo\text{-}endo}$ = -3.7 kcal mol^{-1}). Estos resultados indican de nuevo que el proceso sería diastereoselectivo y que preferentemente debería conducir a *cis*-β-lactamas. Sin embargo, puesto que el valor de $\Delta\Delta E_a$ no es demasiado elevado, es de esperar que el proceso produzca una cierta cantidad de *trans*-β-lactamas, como realmente ocurre experimentalmente. Podemos predecir que cambios en la densidad electrónica del metal van a provocar cambios importantes en el valor de $\Delta\Delta E_a$ para este proceso.

Si consideramos en este punto que el esquema cinético de las etapas iniciales de este proceso se puede representar según la ecuación:

$$\textbf{INT1} \rightleftharpoons \textbf{INT2} \longrightarrow \textbf{INT3}$$

como se deduce de las energías relativas representadas en la propuesta representada en las Figuras 3 y 5, la discriminación facial debe producirse realmente en la migración

metalotrópica ($\Delta\Delta E_{\mathbf{TS2}}$ = 7.7 kcal mol^{-1}) favoreciendo la formación de la especie **INT3** procedente del ataque *exo*. Si tenemos en cuenta que, adicionalmente, el ataque *exo* de la imina sobre la metalacetena inicial (**INT1→INT2**) es 4.0 kcal mol^{-1} más exotérmico que el ataque *endo*, ambos resultados deben favorecer la formación de los productos *cis* observados experimentalmente.

El estudio de la diastereoselección de este proceso de la química de complejos metal-carbeno es preliminar. En el momento de redactar esta memoria, se está completando el mismo teniendo en cuenta, tanto los efectos de los sustituyentes en la imina como el efecto de la densidad electrónica sobre el metal, para ajustar mejor los datos teóricos con los resultados experimentales obtenidos.

2.4. Light-Induced Aminocarbene to Imine Dyotropic Rearrangement in a Chromium(0) Center: An Unprecedented Reaction Pathway

2.4. Light-Induced Aminocarbene to Imine Dyotropic Rearrangement in a Chromium(0) Center: An Unprecedented Reaction Pathway

Photochemistry of chromium(0) carbene complexes[1] is one of the fundamental pillars on which the synthetic versatility[2] of these compounds is based. The usefulness of the light-induced reactions of these complexes stems from their ability to reversibly generate ketene-like intermediates,[3] initially postulated in 1988 by D'Andrea and Hegedus. Since then, the different efforts directed toward the detection of these elusive intermediates have been fruitless.[4,5] Recently, we reported a theoretical-experimental study on the mechanism of the photoreaction of group 6 alkoxychromium(0)carbene complexes with imines.[6] Further work by our group resulted in the light-induced carbene transfer from group 6 carbene complexes to olefins.[7,8] We have now studied the photochemistry of complexes **1** having the carbene heteroatom substitutent tethered to the metal nucleus by a phosphine ligand and a carbon chain of variable length and rigidity. Reported herein is the discovery of a new photochemical aminocarbene to imine dyotropic rearrangement.

Complexes **1** were prepared by intramolecular ligand displacement on aminocarbene complexes **2** (boiling hexanes/benzene, 1:1 mixtures).[9] These latter compounds were obtained by aminolysis of pentacarbony[methoxymethyl-carbene]chromium(0), **3**, with the corresponding aminophosphines **4** (Scheme 1).

---

[1] For reviews in the photochemistry of group 6 metal-carbene complexes, see: (a) Hegedus, L. S. *Tetrahedron* **1997**, *53*, 4105. (b) Hegedus, L. S. in *Comprehensive Organometallic Chemistry II,* Abel, E. W.; Stone, F. G. A.; Wilkinson, G., Eds.; Pergamon: Oxford, 1995; vol. 12, p. 549. (c) Schwindt, M. A.; Miller, J. R.; Hegedus, L. S. *J. Organomet. Chem.* **1991**, *413*, 143.

[2] Selected Reviews: (a) Dötz, K. H. *Angew. Chem., Int. Ed. Eng.* **1984**, *23*, 587. (b) Wulff, W. D. in *Comprehensive Organic Synthesis,* Trost, B. M.; Fleming, I., Eds.; Pergamon: Oxford, 1991; vol. 5, p. 1065. (c) Wulff, W. D. in *Comprehensive Organometallic Chemistry II,* Abel, E. W.; Stone, F. G. A.; Wilkinson, G., Eds.; Pergamon: Oxford, 1995; vol. 12, p. 470. (d) Harvey, D. F.; Sigano, D. M. *Chem. Rev.* **1996**, *96*, 271. (e) Aumann, R.; Nienaber, H. *Adv. Organomet. Chem.* **1997**, *41*, 163. (f) Sierra, M. A. *Chem. Rev.* **2000,** *100*, 3591. (g) de Meijere, A.; Schirmer, H.; Duetsch, M. *Angew. Chem., Int. Ed.* **2000**, *39*, 3964.

[3] Hegedus, L. S.; de Weck, G.; D'Andrea, S. *J. Am. Chem. Soc.* **1988**, *110*, 2122.

[4] Gallager, M. L.; Greene, J. B.; Rooney, A. D. *Organometallics* **1997**, *16*, 5260.

[5] The first ketene to carbene isomerizations have been recently reported by Grötjahn in an Ir nucleus. See: (a) Grötjahn, D. B.; Bikzhanova, G. A.; Collins, L. S. B.; Concolino, T.; Lam, K. C.; Rheingold, A. L. *J. Am. Chem. Soc.* **2000**, *122*, 5222. (b) Urtel, H.; Bikzhanova, G. A.; Grötjahn, D. B.; Hofmann, P. *Organometallics* **2001**, *20*, 3938. (c) Grötjahn, D. B.; Collins, L. S. B.; Wolpert, M.; Bikzhanova, G. A.; Lo, H. C.; Combs, D.; Hubbard, J. L. *J. Am. Chem. Soc.* **2001**, *123*, 8260.

[6] Arrieta, A.; Cossío, F. P.; Fernández, I.; Gómez-Gallego, M.; Lecea, B.; Mancheño, M. J.; Sierra, M. A. *J. Am. Chem. Soc.* **2000**, *122*, 11509.

[7] Sierra, M. A.; del Amo, J. C.; Mancheño, M. J.; Gómez-Gallego, M. *Tetrahedron Lett.* **2001**, *42*, 5345.

[8] The irradiation of group 6 metal carbene complexes with UV-light produced CO extrusion and *syn-anti* isomerization of the group tethered to the ligand. See: Doyle, K. O.; Gallagher, M. L.; Pryce, M. T.; Rooney, A. D. *J. Organomet. Chem.* **2001**, *617*, 269.

[9] See the Experimental Section for a full experimental procedure.

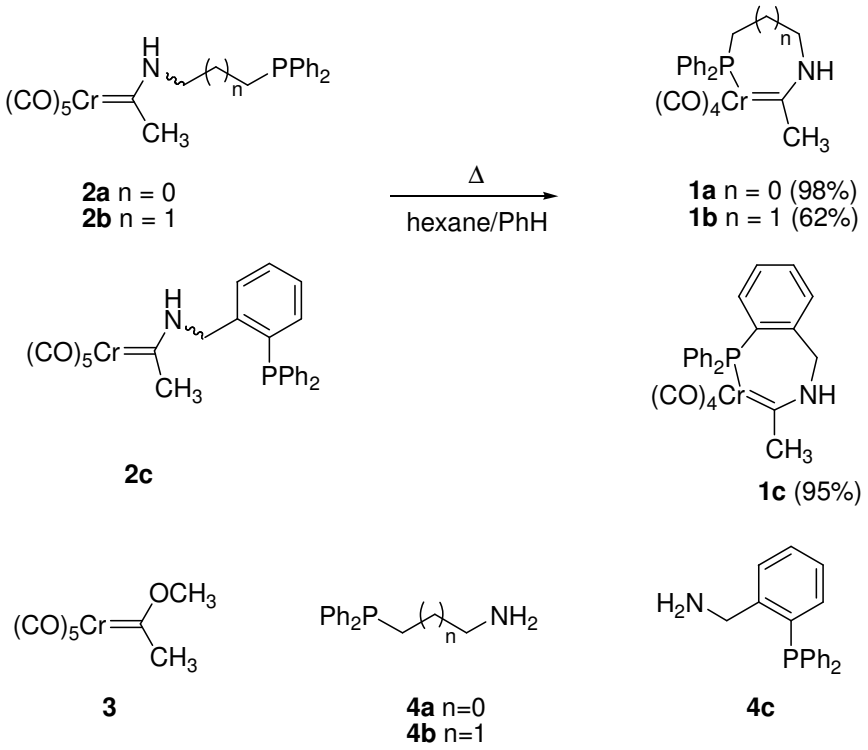

Scheme 1

Irradiation (450 W Hg-medium pressure lamp, Pyrex filter, and Pyrex well) of complexes **1** in MeCN/MeOH solutions resulted in their smooth conversion to new organometallic compounds that lacked the carbene moiety (Scheme 2).

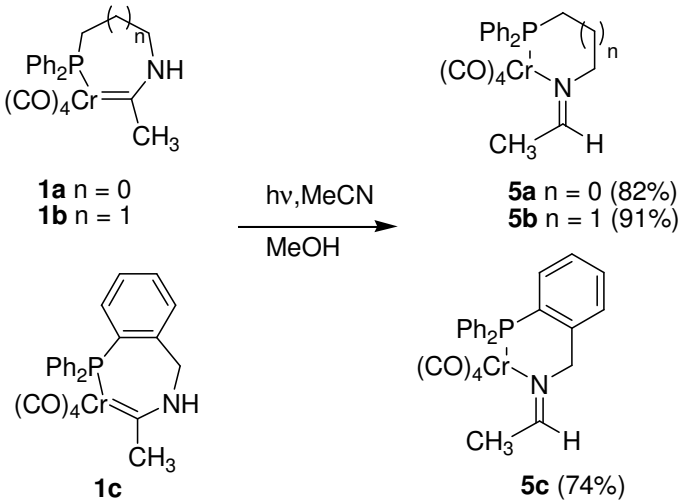

Scheme 2

A combination of 1D- and 2D-homonuclear (COSY and NOESY) and heteronuclear (^{1}H-^{13}C HSQC, ^{1}H-^{13}C HMBC,^{1}H-^{31}P HMBC and ^{1}H-^{15}N HSQC) experiments was performed to assign most of the ^{1}H, ^{13}C and ^{31}P signals of compounds

5b and **5c**.[9] The structure of the reaction products was finally resolved by X-ray diffraction analysis carried out in a single monocrystal of **5c** (Figure 1). Thus, instead of the photocarbonylation process, a new carbene to imine rearrangement has occurred. The reaction occurs with tethers of different lengths (**4a**,**b)** and rigidities (**4c**), showing that the rearrangement process is general.

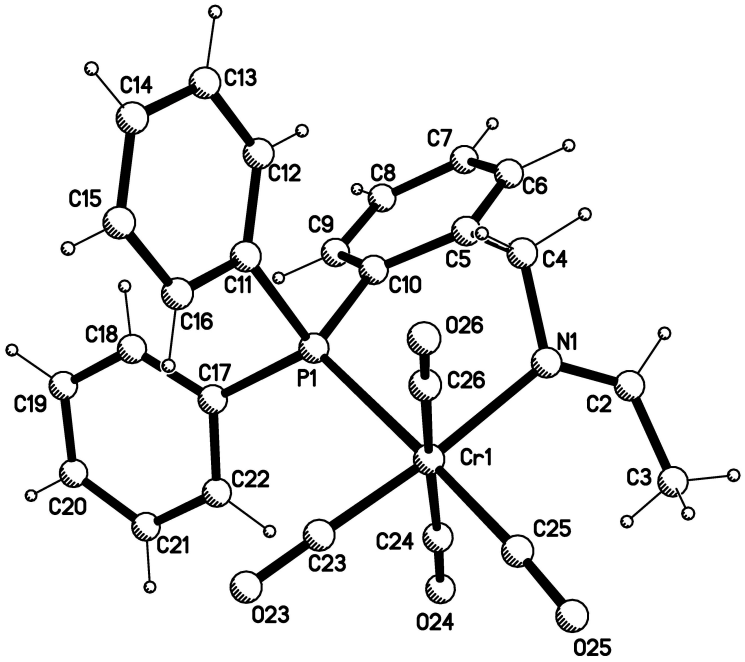

Figure 1. Crystal structure of **5c** (ORTEP, 30% probability ellipsoids). Selected bond lengths [Å]: Cr1-C23···1.804(8), Cr1-C24···1.792(4), Cr1-C25···1.827(10)), Cr1-C26···1.828(4), Cr1-P1···2.410(2), Cr1-N1···2.154(5), N1-C2···1.283(8).

Experimental results above indicate that chromium(0)carbenes **1a**-**c** are transformed upon irradiation into *N*-metalated imines **5a**-**c** instead of in the usually proposed ketenes.[1] This transformation is formally a 1,2-dyotropic rearrangement of type 1 according to the definition proposed by Reetz.[10] Both C-Cr and N-H bonds migrate and the Cr and H atoms interchange their positions, the C=N moiety (structure II contributes significantly to the description of the complex) being the static scaffold (Squemes 3 and 4).

[10] (a) Reetz, M. T. *Angew. Chem., Int. Ed. Engl.* **1972**, *11*, 129. (b) Reetz, M. T. *Tetrahedron* **1973**, *29*, 2189.

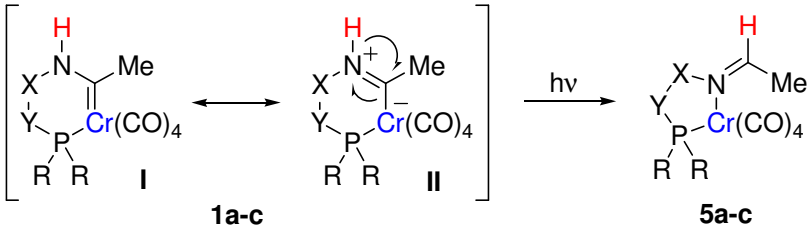

Scheme 3

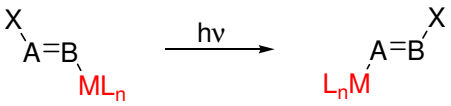

Scheme 4

Computational studies[11,12,13] on the transformation of model chromium(0) carbene **1d** into coordinated imine **5d** showed that the **1d**→**5d** reaction is exothermic by 14.7 kcal/mol at the ground state S_0 (Figure 2).

[11] All calculations were carried out using the GAUSSIAN 98 suite of programs. Gaussian 98, Revision A.5, Frisch, M. J. et al. Gaussian, Inc., Pittsburgh PA, 1998.
[12] All calculations were performed at the UB3LYP level of theory. See: (a) Becke, A. D. *J. Chem. Phys.* **1993**, *98*, 5648. (b) Lee, C.; Yang, W.; Parr, R. G. *Phys. Rev. B* **1988**, *37*, 785. (c) Vosko, S. H.; Wilk, L.; Nusair, M. *Can. J. Phys.* **1980**, *58*, 1200.
[13] The LANL2 DZ effective core potential and basis set were used for chromium during the optimizations and harmonic analysis to compute zero point vibrational energies (not corrected). In order to obtain more accurate energies, the basis set for the explicit electrons of chromium was augmented with a set of *f*-polarization functions. See: (a) Hay, P. J.; Wadt, W. R. *J. Chem. Phys.* **1985**, *82*, 299. (b) Ehlers, A. W.; Böhme, M.; Dapprich, S.; Gobbi, A.; Höllwarth, A.; Jonas, V.; Köhler, K. F.; Stegman, R.; Veldkam, A.; Frenking, G. *Chem. Phys. Lett.* **1993**, *208*, 111. The remaining elements were described with the standard 6-31+G* basis set. See: Hehre, W. J.; Radom, L.; Schleyer, P.v.R.; Pople, J. A. *Ab Initio Molecular Orbital Theory*; Wiley: New York, 1986, p. 76 and references therein.

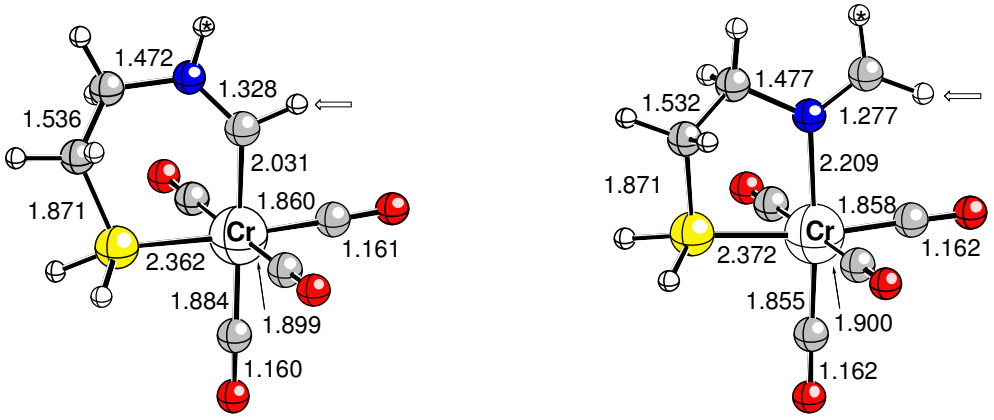

1d (S_0) **5d (S_0)**

Figure 2

Because in the experimentally studied imines **5a**-**c** the methyl group is always *syn* to the chromium atom, we have calculated the structures and energies of both *syn*- and ***anti*-5e** (Figure 3). Our calculations indicate that the *syn* stereoisomer is 0.8 kcal/mol more stable than its *anti* analogue.[9] Therefore, both the 1,2-dyotropic transformations and the double inversion stereochemistry are thermodynamically favored processes.

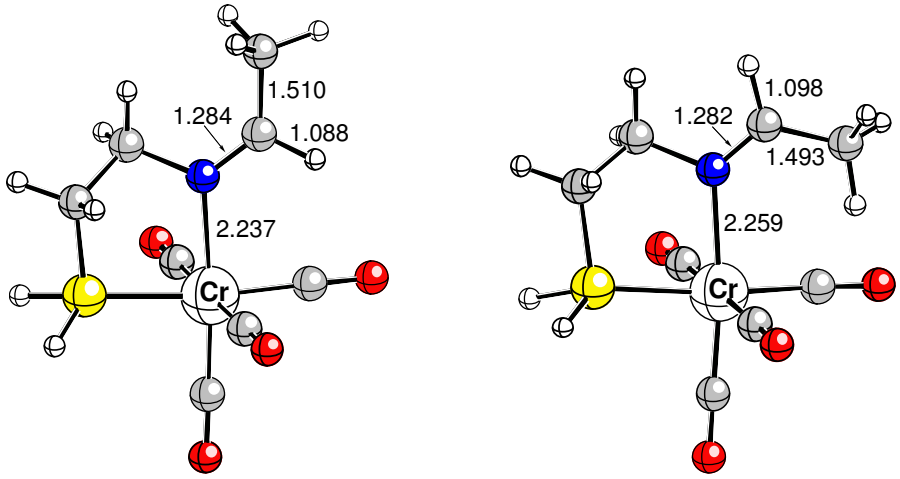

***anti*-5e** ***syn*-5e**

Figure 3

We have found[14] that the lowest energy excited state of **1d** is a triplet, with a vertical excitation energy of 2.66 eV (465.5 nm). The first excited singlet state S_1 lays 0.80 eV above the triplet. It can be assumed that the dyotropic reaction starts with a short-lived triplet state T_1, formed after initial photoexcitation of the singlet ground state S_0 to the excited singlet state S_1.[15,16] The triplet state of **1d** has a C-Cr distance *ca.* 0.2Å larger than that found at the S_0 state. In addition, the spin densities of both centers are 0.582 and 1.675 a.u. respectively, thus indicating that in this excited state there is a significant contribution of the biradical structure depicted in Scheme 5.

We have not been able so far to locate and characterize a concerted transition structure that connects **1d** and **5d** in either the S_0 or T_1 potential energy hypersurfaces. Instead, we have found a stepwise mechanism whose first transition structure (**TS1** in Scheme 5) is associated with the 1,2-migration of the chromium atom from the carbene to the nitrogen, with an activation energy of 19.7 kcal/mol. Efforts to locate **TS1** in the S_0 manifold meet with no success. An Intrinsic Reaction Coordinate (IRC)[17] study from **TS1** at the T_1 state led to the uncoordinated triplet carbene **6**, in which the spin density of the carbene center is 1.887 a.u. This carbene can be transformed into **5d** at the T_1 state by means of **TS2** (a saddle point associated with the migration of the hydrogen atom from the nitrogen atom to the carbene moiety). This step has an activation energy of 35.9 kcal/mol (Figure 4). However, if the **1d**→**5d** transformation should take place along the **TS1**-**6**-**TS2** pathway, the stereochemistry of the reaction should be the contrary to that experimentally observed.

[14] These computations were performed at the configuration interaction singles (CIS) level of theory starting from the HF wavefunction. See: Foresman, J. B.; Head-Gordon, M.; Pople, J. A.; Frisch, M. J. *J. Phys. Chem.* **1992**, *96*, 135.

[15] (a) Zimmermann, H. E.; Sebek, P.; Zhu, Z. *J. Am. Chem. Soc.* **1998**, *120*, 8549. (b) Dauben, W. G.; Hecht, S. *J. Org. Chem.* **1998**, *63*, 6102. (c) Gómez, I.; Olivella, S.; Reguero, M.; Riera, A.; Solé, A. *J. Am. Chem. Soc.* **2002**, *124*, 15375.

[16] It has been reported experimentally that in photochemical reactions of organometallic carbenes such as bis(tricyclohexylphosphine) benzylidene ruthenium dichloride (Grubbs's catalyst) the reactive excited state is a triplet. See: Kunkely, H.; Vogler, A. *Inorg. Chim. Acta* **2001**, *325*, 179.

[17] González, C.; Schlegel, H. B. *J. Phys. Chem.* **1990**, *94*, 5523.

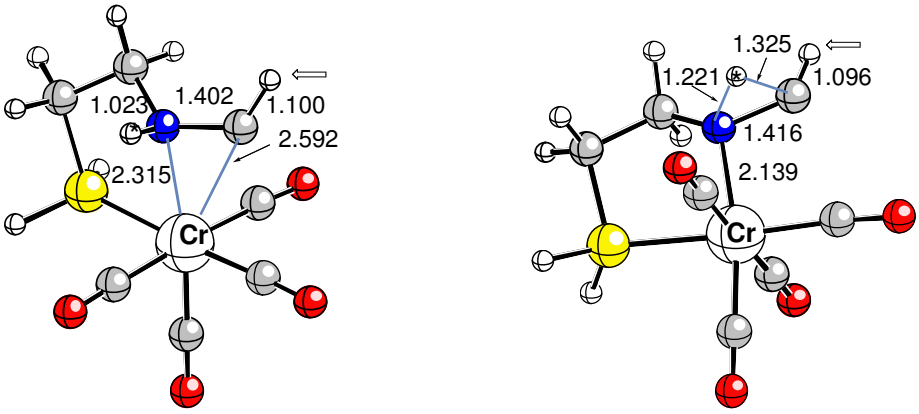

TS1 (T_1) **TS2 (T_1)**

Figure 4

Triplet carbene **6** can isomerize to intermediate **7** through transition structure **TS3** with an associated activation energy of 13.4 kcal/mol. In addition, **7** is 0.9 kcal/mol more stable than its stereoisomer **6** at the T_1 state. Conversion of **7** into **5d** takes place *via* **TS4**, with activation energy of 3.2 kcal/mol lower than that computed for conversion of **6** into **5d**, thus indicating that the **7**→**5d** reaction pathway is kinetically favored. Therefore, this pathway is in full agreement with the experimental data (Figure 5).

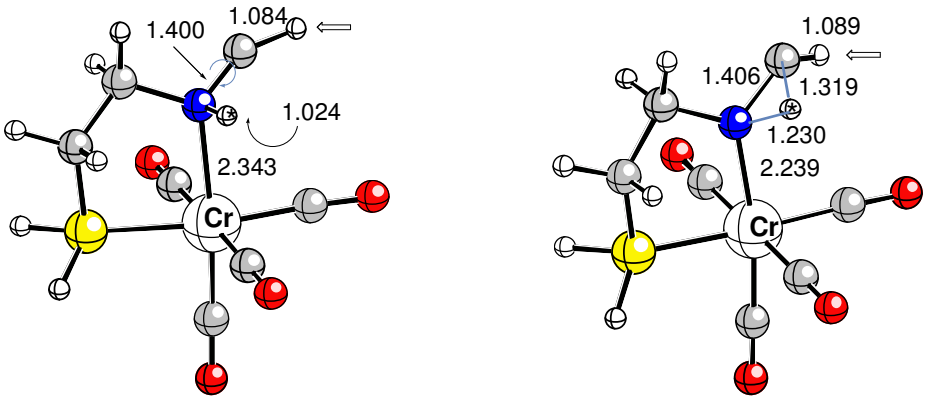

TS3 (T_1) **TS4 (T_1)**

Figure 5

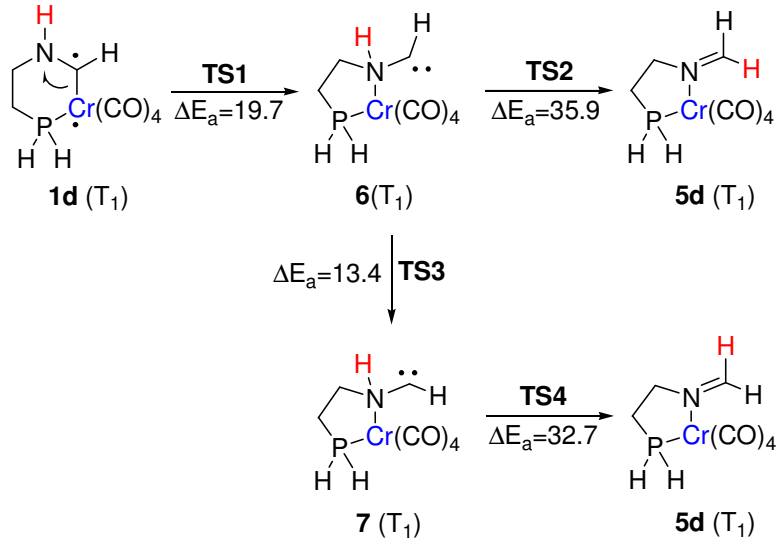

Scheme 5

The rigidity imposed by the cyclic structure of complexes **1** is not the responsible for this new photochemical reaction because the irradiation of complex **8** produced the unstable imino chromium complex **9** in 86% yield (Scheme 6).

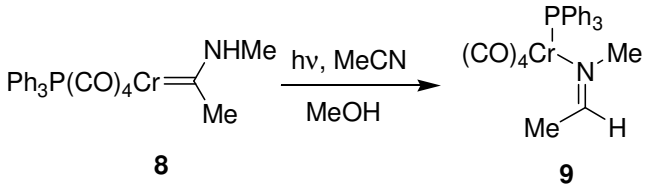

Scheme 6

In conclusion, an unprecedented photochemical pathway alternative to the now classical Hegedus's photocarbonylation has been disclosed. Both theoretical and experimental results are in full agreement with this new dyotropic rearrangement[18] of the carbene ligand to an imine ligand in complexes **1**. Efforts directed to fully understand the general mechanism of the photochemistry of group 6 metal carbene complexes are now deeply active in our laboratories.

[18] Another very interesting experimental and theoretical study of a stepwise dyotropic rearrangement has been reported while this paper was under revision. See: Zhang, X.; Houk, K. N.; Lin, S.; Danishefsky, S. J. *J. Am. Chem. Soc.* **2003**, *125*, 5111.

Experimental Section

General procedure for the synthesis of carbene complexes 2. A solution of pentacarbonyl[ethoxy(methyl)carbene]chromium(0) and the corresponding amine in stochiometric amounts in dry CH_2Cl_2 was stirred at room temperature. The mixture was stirred until the disappearance of the starting material (checked by TLC). Then the solvent was removed and the product was purified by flash column chromatography to yield pure compounds.

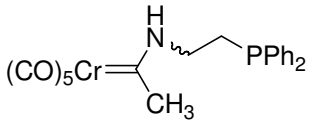

2a

2a (*syn-anti* mixture 1:1): 42%, yellow oil. ^{1}H NMR δ 2.26-2.46 (m, 4H, (*syn*+*anti*)), 2.48 (s, 6H, (*syn*+*anti*)), 3.42 (m, 2H), 4.05 (m, 2H), 7.33-7.39 (m, 20H, ArH, (*syn*+*anti*)), 8.55 (br s, 1H), 8.86 (br s, 1H). ^{13}C NMR δ 27.9 (d, $J_{C\text{-}P}$ = 16.5 Hz), 28.3 (d, $J_{C\text{-}P}$ = 15.3 Hz), 35.6, 45.1 (d, $J_{C\text{-}P}$ = 19.1 Hz), 45.3, 50.4 (d, $J_{C\text{-}P}$ = 16.5 Hz), 128.9 (d, $J_{C\text{-}P}$ = 7.6 Hz), 129.4, 132.6 (d, $J_{C\text{-}P}$ = 19.1 Hz), 132.7 (d, $J_{C\text{-}P}$ = 19.1 Hz), 136.2 (d, $J_{C\text{-}P}$ = 11.4 Hz), 136.5 (d, $J_{C\text{-}P}$ = 11.4 Hz), 217.7, 222.7, 223.1, 276.5, 282.5. IR (CCl_4) 3369, 2054, 1929 cm^{-1}. $C_{21}H_{18}CrNO_5P$: Calcd C 56.38, H 4.06, N 3.13. Found C 56.52, H 3.91, N 3.25.

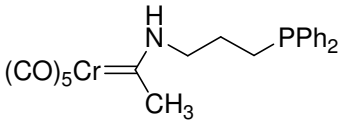

2b

2b: 51%, yellow solid. ^{1}H NMR δ 1.79 (m, 2H), 2.07 (t, 2H, J = 8.1 Hz), 2.53 (s, 3H), 3.44 (m, 2H), 7.29-7.37 (m, 10H, ArH), 8.67 (br s, 1H). ^{13}C NMR δ 25.0 (d, $J_{C\text{-}P}$ = 13.4 Hz), 25.2 (d, $J_{C\text{-}P}$ = 17.7 Hz), 35.5, 48.2 (d, $J_{C\text{-}P}$ = 12.8 Hz), 128.7 (d, $J_{C\text{-}P}$ = 6.7 Hz), 129.1, 132.6 (d, $J_{C\text{-}P}$ = 18.3 Hz), 137.4 (d, $J_{C\text{-}P}$ = 11.6 Hz), 217.8, 222.7, 282.3. IR (KBr) 2054, 1969, 1913 cm^{-1}. $C_{22}H_{20}CrNO_5P$: Calcd C 57.29, H 4.37, N 3.04. Found C 57.08, H 4.15, N 3.16.

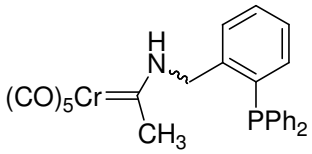

2c

2c (*syn-anti* mixture 1:1): 80%, yellow solid: ^{1}H NMR δ 2.20 (s, 3H), 2.55 (s, 3H), 4.70 (d, 2H, J = 5.6 Hz), 5.22 (d, 2H, J = 5.0 Hz), 6.92 (m, 2H, (*syn*+*anti*)), 7.16-7.37 (m, 26H, ArH, (*syn*+*anti*)), 8.18 (br s, 1H), 9.04 (br s, 1H). ^{13}C NMR δ 35.9, 44.9, 50.8 (d, $J_{C\text{-}P}$ = 24.2 Hz), 56.4 (d, $J_{C\text{-}P}$ = 20.3 Hz), 128.1 (d, $J_{C\text{-}P}$ = 3.8 Hz), 128.9, 128.9, 129.0, 129.1, 129.2, 129.5 (d, $J_{C\text{-}P}$ = 2.5 Hz), 129.9 (d, $J_{C\text{-}P}$ = 5.1 Hz), 130.4 (d, $J_{C\text{-}P}$ = 3.8 Hz), 133.8 (d, $J_{C\text{-}P}$ = 11.4 Hz), 134.2 (d, $J_{C\text{-}P}$ = 11.4 Hz), 134.7 (d, $J_{C\text{-}P}$ = 8.9 Hz),

135.1 (d, $J_{C\text{-}P}$ = 8.9 Hz), 136.4 (d, $J_{C\text{-}P}$ = 15.3 Hz), 137.4, 137.9 (d, $J_{C\text{-}P}$ = 11.4 Hz), 138.3 (d, $J_{C\text{-}P}$ = 10.2 Hz), 138.7, 217.7, 217.8, 222.8, 223.2, 275.9, 282.8. IR (KBr) 3377, 3256, 2054, 1965, 1909, 1528 cm^{-1}. $C_{26}H_{20}CrNO_5P$: Calcd C 61.30, H 3.96, N 2.75. Found C 61.57, H 3.69, N 2.84.

General Procedure for the synthesis of complexes 1: The synthesis was carried out following the general method described by Fischer. A solution of the (phosphino)aminocarbene complex was heated at reflux in benzene/hexane (1:1) for the time specify below. The solvents were removed under reduced pressure to yield pure compounds (unless otherwise specified).

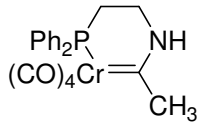

1a

1a: 98%, yellow solid. ^{1}H NMR δ 2.29 (br s, 2H), 2.27 (br s, 3H), 3.89 (br s, 2H), 7.29-7.49 (m, 10H, ArH), 9.20 (br s, 1H). ^{13}C NMR δ 25.1 (d, $J_{C\text{-}P}$ = 18.4 Hz), 31.6, 44.7 (d, $J_{C\text{-}P}$ = 54.2 Hz), 128.2 (d, $J_{C\text{-}P}$ = 8.5 Hz), 129.3, 131.5 (d, $J_{C\text{-}P}$ = 10.9 Hz), 137.7 (d, $J_{C\text{-}P}$ = 33.8 Hz), 221.6 (d, $J_{C\text{-}P}$ = 12.9 Hz), 229.0, 232.8 (d, $J_{C\text{-}P}$ = 15.3 Hz), 283.0 (d, $J_{C\text{-}P}$ = 15.2 Hz). IR (KBr) 3306, 1994, 1870, 1844 cm^{-1}. $C_{20}H_{18}CrNO_4P$: Calcd C 57.29, H 4.33, N 3.34. Found C 57.01, H 4.60, N 3.22.

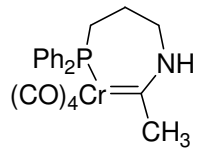

1b

1b: 62%, yellow solid. ^{1}HMR δ 1.89 (m, 2H), 2.43 (m, 2H), 2.78 (s, 3H), 3.97 (m, 2H), 7.28-7.46 (m, 10H, ArH), 8.81 (br s, 1H). ^{13}C NMR (acetone-d_6) δ 24.4, 26.3 (d, $J_{C\text{-}P}$ = 16.0 Hz), 42.6 (d, $J_{C\text{-}P}$ = 3.8 Hz), 49.2 (d, $J_{C\text{-}P}$ = 8.4 Hz), 128.6 (d, $J_{C\text{-}P}$ = 8.4 Hz), 129.6, 132.1 (d, $J_{C\text{-}P}$ = 10.7 Hz), 138.7 (d, $J_{C\text{-}P}$ = 32.0 Hz), 223.1 (d, $J_{C\text{-}P}$ = 12.2 Hz), 229.4 (d, $J_{C\text{-}P}$ = 3.1 Hz), 229.8 (d, $J_{C\text{-}P}$ = 15.3 Hz), 280.5 (d, $J_{C\text{-}P}$ = 14.5 Hz). IR (KBr) 3288, 1998, 1906, 1878 cm^{-1}. $C_{21}H_{20}CrNO_4P$: Calcd C 58.20, H 4.65, N 3.23. Found C 58.46, H 4.59, N 3.29.

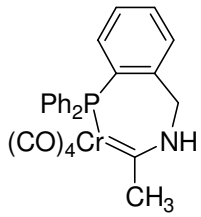

1c

1c: 95%, yellow solid. ^{1}H NMR δ 2.73 (s, 3H), 4.81 (br s, 2H), 6.76 (t, 1H, J = 7.7 Hz), 7.20-7.55 (m, 13H, ArH), 9.12 (br s, 1H). ^{13}C NMR (acetone-d_6) δ 43.3 (d, $J_{C\text{-}P}$ = 3.8 Hz), 54.7 (d, $J_{C\text{-}P}$ = 10.2 Hz), 129.2 (d, $J_{C\text{-}P}$ = 8.9 Hz), 130.1 (d, $J_{C\text{-}P}$ = 5.1 Hz), 130.6, 131.7, 132.0, 133.4, 133.9 (d, $J_{C\text{-}P}$ = 10.2 Hz), 137.1 (d, $J_{C\text{-}P}$ = 34.3 Hz), 142.5 (d, $J_{C\text{-}P}$ =

14.0 Hz), 223.9 (d, $J_{C\text{-}P}$ = 12.7 Hz), 229.9, (d, $J_{C\text{-}P}$ = 2.5 Hz) 230.9 (d, $J_{C\text{-}P}$ = 15.3 Hz), 279.6 (d, $J_{C\text{-}P}$ = 12.7 Hz). IR (KBr) 3292, 2000, 1880, 1834 cm^{-1}. $C_{25}H_{20}CrNO_4P$: Calcd C 62.37, H 4.19, N 2.91. Found C 62.15, H 4.43, N 3.02.

General Procedure for the photochemical reactions of complexes 1 and 8. Photochemical reactions were conducted by using a 450W-medium pressure Hg-lamp, through a Pyrex filter in dry degassed CH_3CN containing CH_3OH in a sealed pyrex tube filled with argon. In a typical experiment, after irradiation for 30 h the solution was filtered through a short pad of celite, the solvent was removed under reduced pressure and the crude was submitted to flash chromatography to give pure complexes **5** and **9**.

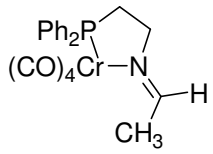

5a

5a: 82%, yellow solid. ^{1}H NMR δ 2.31 (d, 3H, *J* = 5.2 Hz), 2.39 (m, 2H), 3.69 (dm, 2H), 7.39-7.61 (m, 10H, ArH), 8.03 (q, 1H, *J* = 5.2 Hz). ^{13}C NMR δ 23.8, 29.2 (d, $J_{C\text{-}P}$ = 15.9 Hz), 66.9 (d, $J_{C\text{-}P}$ = 15.9 Hz), 128.7 (d, $J_{C\text{-}P}$ = 9.4 Hz), 129.8 (d, $J_{C\text{-}P}$ = 1.5 Hz), 131.4 (d, $J_{C\text{-}P}$ = 19.6 Hz), 136.3 (d, $J_{C\text{-}P}$ = 35.3 Hz), 172.0, 219.0 (d, $J_{C\text{-}P}$ = 13.6 Hz), 227.7, 229.1 (d, $J_{C\text{-}P}$ = 14.3 Hz). IR (KBr) 2006, 1878, 1830 cm^{-1}. $C_{20}H_{18}CrNO_4P$: Calcd C 57.29, H 4.33, N 3.34. Found C 57.48, H 4.49, N 3.21.

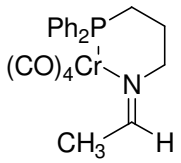

5b

5b: 91%, yellow solid. ^{1}H NMR δ 1.72 (m, 2H), 2.38 (d, 3H, *J* = 5.2 Hz), 2.44 (m, 2H), 3.81 (m, 2H), 7.32-7.51 (m, 10H, ArH), 7.85 (q, 1H, *J* = 5.2 Hz). ^{13}C NMR δ 24.0, 26.2, 29.2 (d, $J_{C\text{-}P}$ = 18.7 Hz), 71.1, 128.4 (d, $J_{C\text{-}P}$ = 9.8 Hz), 129.6, 131.9 (d, $J_{C\text{-}P}$ = 10.4 Hz), 136.3 (d, $J_{C\text{-}P}$ = 33.2 Hz), 173.1, 219.0 (d, $J_{C\text{-}P}$ = 13.6 Hz), 227.7, 229.1 (d, $J_{C\text{-}P}$ = 14.3 Hz). IR (KBr) 2004, 1867, 1834 cm^{-1}. $C_{21}H_{20}CrNO_4P$: Calcd C 58.20, H 4.65, N 3.23. Found C 58.01, H 4.45, N 3.31.

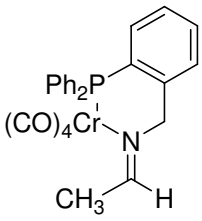

5c

5c: 74%, yellow solid. ^{1}H NMR δ 2.31 (d, 3H, *J* = 5.3 Hz), 4.51 (d, 2H, *J* = 2.5 Hz), 6.90 (t, 1H, *J* = 9.0 Hz), 7.13-7.40 (m, 13H, ArH), 7.96 (q, 1H, *J* = 5.3 Hz). ^{13}C NMR δ 24.0, 75.1 (d, $J_{C\text{-}P}$ = 12.5 Hz), 128.5 (d, $J_{C\text{-}P}$ = 9.7 Hz), 129.0 (d, $J_{C\text{-}P}$ = 8.3 Hz), 129.4

(d, $J_{C\text{-}P}$ = 4,2 Hz), 129.9, 130.9, 132.5, 132.9 (d, $J_{C\text{-}P}$ = 11.1 Hz), 133.0 (d, $J_{C\text{-}P}$ = 21.0 Hz), 134.5 (d, $J_{C\text{-}P}$ = 37.5 Hz), 142.4 (d, $J_{C\text{-}P}$ = 18.0 Hz), 173.9, 219.3 (d, $J_{C\text{-}P}$ = 14.3 Hz), 225.0, 226.5 (d, $J_{C\text{-}P}$ = 12.0 Hz). IR (KBr) 2008, 1892, 1861 cm^{-1}. $C_{25}H_{20}CrNO_4P$: Calcd C 62.37, H 4.19, N 2.91. Found C 62.12, H 4.06, N 2.84.

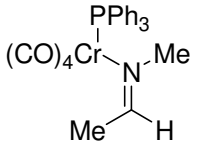

9

9: 86%, Unstable yellow solid. ^{1}H NMR δ 2.29 (s, 3H), 2.57 (d, 3H, J = 4.2 Hz), 7.26-7.63 (m, 15H, ArH), 7.94 (q, 1H, J = 4.2 Hz). ^{13}C NMR δ 29.7, 34.5 (d, $J_{C\text{-}P}$ = 16.6 Hz), 128.5 (d, $J_{C\text{-}P}$ = 11.1 Hz), 131.9, 132.1 (d, $J_{C\text{-}P}$ = 8.3 Hz), 133.7 (d, $J_{C\text{-}P}$ = 20.8 Hz), 184.2, 216.8 (d, $J_{C\text{-}P}$ = 13.9 Hz), 221.7 (d, $J_{C\text{-}P}$ = 13.9 Hz), 228.4. IR (CCl_4): 2054, 1929, 1888 cm^{-1}.

NMR study for compounds 5b,c

Table 1

		5b		5c	
		δ (ppm)	*J* (Hz)	δ (ppm)	*J* (Hz)
CH_3	**^{1}H**	2.45	4.5 J^3(H-H)	2.40	5.6 J^3(H-H)
	^{13}C	23.9		24.7*	
CH	**^{1}H**	7.9	4.5 J^3(H-H)	8	5.6 J^3(H-H)
	^{13}C	173	3 J^3(C-P)	174*	
N-$\underline{CH_2}$	**^{1}H**	3.9		4.6	
	^{13}C	71	4.5 J^3(C-P)	75.3*	
N-CH_2-$\underline{CH_2}$	**^{1}H**	1.8			
	^{13}C	26.2		n.d.	
-$\underline{CH_2}$-P	**^{1}H**	2.5			
	^{13}C	29	15.6 J^1(C-P)	n.d.	
Ph	**^{1}H**	7.5 (o) 7.4 (m,p)		n.d.	
	^{13}C	136.2 131.9 (o) 129.6 (m) 128.4 (p)	32.7 J^1(C-P) 10.9 J^2(C-P) - 8.6 J^4(C-P)	n.d.	
CO	**^{13}C**	226.5 225 219.3	12 J^2(C-Cr-P) - 14.3 J^2(C-Cr-P)	n.d.	
	^{31}P	42		48	

* data obtained from HSQC experiments
** data obtained from HMBC experiments

For all compounds, a combination of 1D and of 2D-homonuclear (COSY and NOESY) and heteronuclear (^{1}H-^{13}C HSQC, ^{1}H-^{13}C HMBC and ^{1}H-^{31}P HMBC) experiments were performed to assign most of the ^{1}H, ^{13}C and ^{31}P signals of the different molecules. No indication of protons directly attached to nitrogen atoms was observed. Indeed, an overnight ^{1}H-^{15}N HSQC experiment showed no signals at all. Four carbonyl signals were deduced for these compounds, two of them splitted by coupling to phosphorus.
The COSY experiments permitted to assign those signals pertaining to the trimethylene moiety of **5b** as well as to clearly identify one proton at δ 7.9 ppm attached to a carbon atom at δ 173.0 ppm. This carbon signal is a doublet in the broadband decoupled ^{13}C spectrum, with probably a J_{CP} 3 Hz. In turn, this δ 7.9 ppm proton was shown to hold an either geminal or *cis*-disposition with regard to a methyl group (J = 4.7 Hz for **5b** and 5.6 Hz for **5c**). A NOE cross peak was also observed between the corresponding protons signals in the NOESY spectra of both compounds.
The HSQC and HMBC experiments permitted to unambiguously identify the corresponding ^{13}C atoms for the tri-methylene and aromatic moieties. No regular olefinic fragments were deduced. Indeed, only the δ 7.9 / 173.0 (**5b**) and 8.0 / 174.0 ppm (**5c**) atom pairs indicated the presence of a double bond, although not between two

carbon atoms. Indication of a methylene group attached to a heteroatom (δ 3.9 / 71.0) was deduced.

The NOESY experiment of **5b** and **5c** showed a cross peak between the δ 7.9 ppm proton and the CH_2 protons of the methylene group attached to the heteroatom, indicating a close distance between them. A variety of mixing times in the NOESY experiments (from 0.4 to 1.5 s) were used to try to identify additional cross peaks. In all cases, only the above mentioned non trivial NOEs were detected. No NOEs between the methyl group and any of the methylene or aromatic moieties were observed, and no cross peaks were detected between the 7.9 ppm and the aromatic protons. The aromatic protons showed NOE cross peaks to the methylene protons of the carbon atom attached to the phosphorus as well as to its contiguous methylene moiety.

The NOESY experiments carried out for **5c** permitted to assign a cross peak between the δ 8.0 ppm proton and some of the aromatic protons and between the δ 8.0 ppm proton and those of the only methylene moiety of the molecule (δ 4.6 ppm). This methylene group has also to be directly attached to a heteroatom (δ 75.3 ppm).

Additional indications of the relative orientations of the groups came from the HMBC experiments. The ^{1}H-^{13}C HMBC of **5b** permitted to relate the δ 7.9 ppm proton with the δ 71.0 ppm carbon and the δ 3.9 ppm methylene protons with the δ 173.0 ppm carbon. Analogous correlations were deduced for **5c**. The ^{1}H-^{31}P HMBC of **5b** and **5c** permitted to deduce a direct connection between the δ 29.2 ppm methylene carbon and the phosphorus atom ($J_{C\text{-}P}$>15 Hz). With all these data at hand, the structure that fitted the experimental observations was an imine-type of compound with the δ 7.9-8.0 ppm proton in geminal orientation to the methyl group, and in *cis*- relationship to the methylene group (δ 71.0 / 3.9 ppm) or (δ 75.3 / 4.6 ppm). This methylene is directly attached to the imine nitrogen, which in turn is coupled to the chromium. The other side of the trimethylene group of **5b** is directly attached to the phosphorus (δ 29.2 ppm carbon and $J_{C\text{-}P}$>15 Hz). In the case of **5c**, the methylene moiety attached to phosphorus is replaced by one phenyl group.

Para aproximar nuestro modelo teórico a los resultados experimentales, se calculó toda la coordenada de reacción (B3LYP/6-31+G*&LanL2DZ) desde el complejo **1e**, análogo al complejo metal-carbeno inicial **1a**. La diferencia más notable entre el modelo **1e** y el complejo real **1a** es la sustitución de los grupos fenilo en la fosfina por átomos de hidrógeno. Si observamos detenidamente los caminos de reacción obtenidos para el modelo más simple **1d** (Esquema 5) y para el modelo que se aproxima más a **1e** (Esquema 7), se comprueba que no existen diferencias significativas entre las coordenadas de reacción calculadas para ambos complejos modelo.

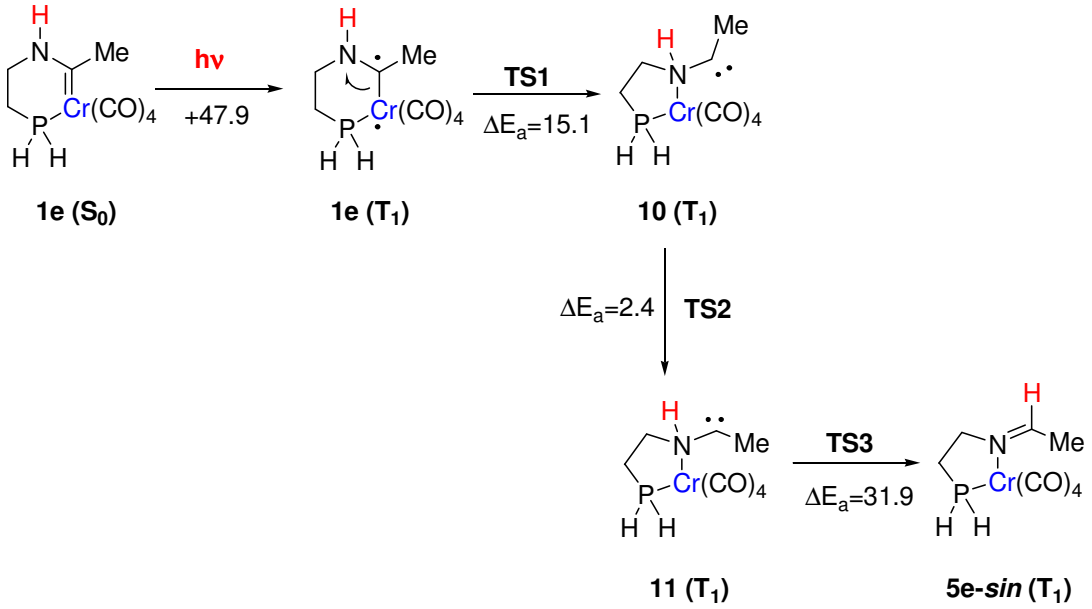

Esquema 7

Existe una clara posibilidad de que, si bien los complejos de wolframio son inertes frente a la fotocarbonilación, no lo sean frente a este nuevo proceso fotoquímico. Por ello, siguiendo la metodología sintética empleada para preparar los complejos de cromo **1a-c**, se obtuvieron los complejos **1f-h** con rendimientos similares (Esquema 8). En estos casos se requiere elevar la temperatura para efectuar la sustitución intramolecular de ligando, empleando tolueno como disolvente, debido a la menor labilidad del enlace W-CO respecto al enlace Cr-CO.

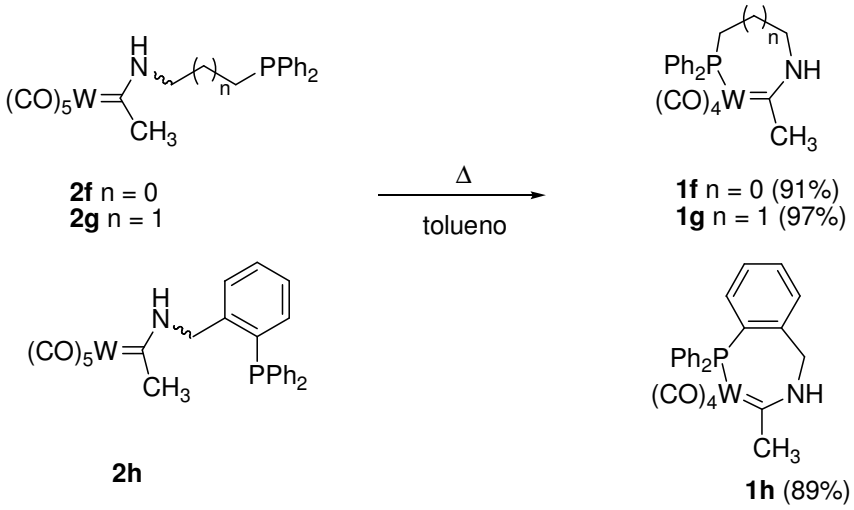

Esquema 8

La irradiación de los complejos **1f**-**h** en mezcla MeCN/MeOH (10:1) conduce a la formación de iminas *sin*-*N*-metaladas **5f**-**h**, con rendimientos que van de moderados a buenos y en tiempos de reacción algo menores que en el caso de los complejos análogos de cromo (Esquema 9).

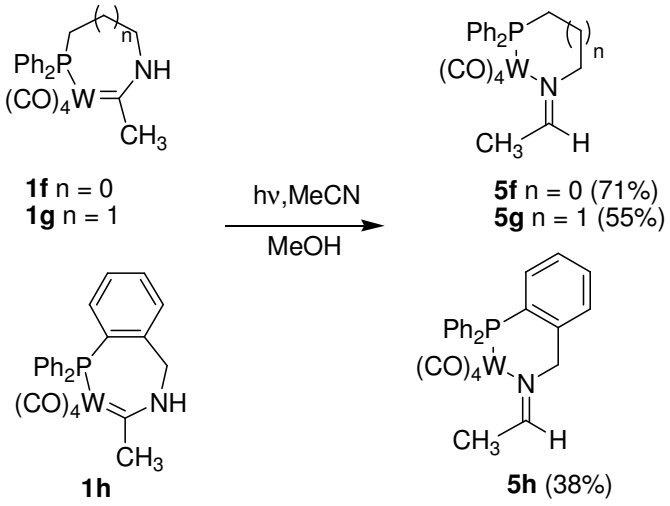

Esquema 9

Como se puede ver, el proceso de reordenamiento fotoquímico es perfectamente compatible con complejos metal-carbeno de wolframio de tipo Fischer, *lo cual constituye el primer ejemplo descrito en la literatura química de reactividad fotoquímica de un metalacarbeno de wolframio*. Puede concluirse que este proceso es

incluso más general que el proceso de fotocarbonilación, puesto que engloba a todos los complejos metal-carbeno del grupo 6.[19]

Se calculó (B3LYP/6-31+G*&LanL2DZ) el camino de reacción que seguiría el complejo modelo **1i**, análogo al complejo real **1f**, en su evolución hacia el complejo ***5i-sin*** (Esquema 10). Como era de esperar, el camino de reacción consiste en un reordenamiento 1,2-diotrópico de tipo I que transcurre por etapas y en la hipersuperficie triplete. Las energías de activación calculadas en este caso son prácticamente las mismas que las obtenidas para el modelo análogo de cromo **1e**, lo que constituye una prueba adicional que demuestra la generalidad del proceso de reordenamiento.

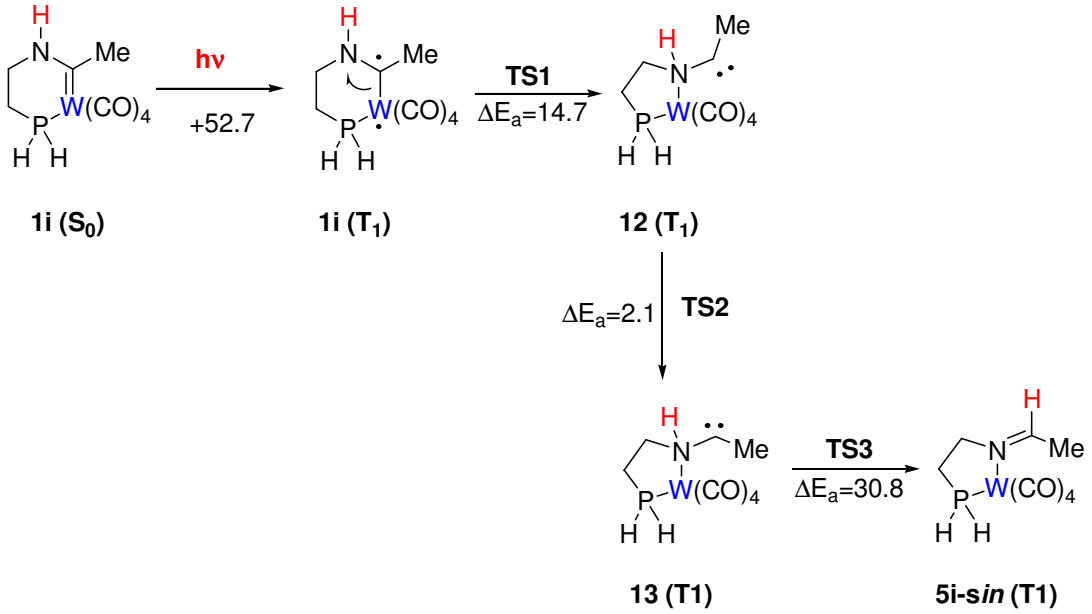

Esquema 10

Con el objetivo de profundizar en la intimidad de este proceso fotoquímico se estudió el efecto de la sustitución en el átomo de nitrógeno directamente unido al carbono carbenoide en los complejos **1**. Los complejos *N*-sustituidos **14** se prepararon por reacción de los complejos **1** con el haluro de alquilo correspondiente en presencia de Cs_2CO_3 y a temperatura ambiente. De esta forma, se obtuvieron los complejos **14** de manera prácticamente cuantitativa (Esquema 11).

[19] Los complejos metal-carbeno de molibdeno se están estudiando en estos momentos.

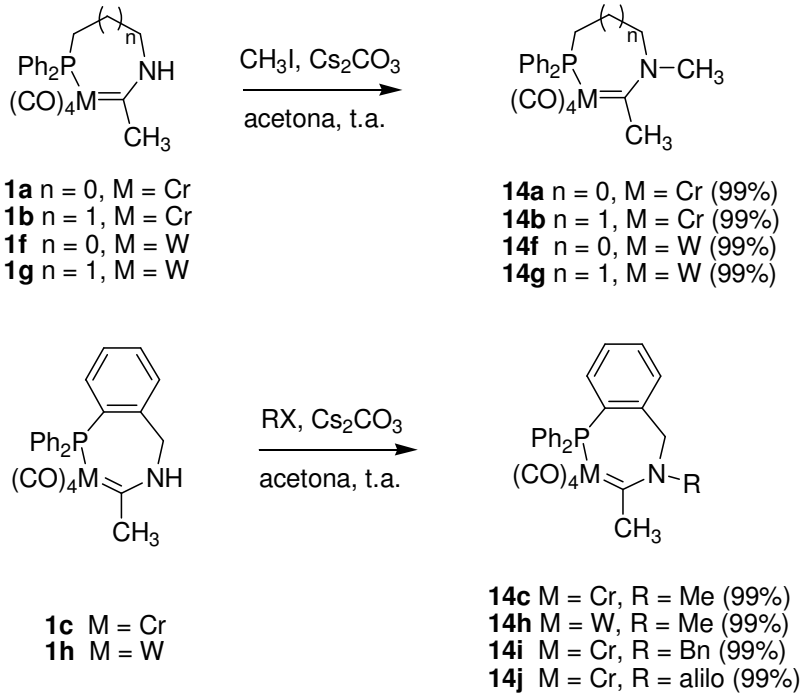

1a n = 0, M = Cr
1b n = 1, M = Cr
1f n = 0, M = W
1g n = 1, M = W

14a n = 0, M = Cr (99%)
14b n = 1, M = Cr (99%)
14f n = 0, M = W (99%)
14g n = 1, M = W (99%)

1c M = Cr
1h M = W

14c M = Cr, R = Me (99%)
14h M = W, R = Me (99%)
14i M = Cr, R = Bn (99%)
14j M = Cr, R = alilo (99%)

Esquema 11

La irradiación de los complejos **14** en mezclas MeCN/MeOH (10:1) o MeCN/THF/MeOH (5:5:1) no condujo en ningún caso a los productos derivados de un proceso de reordenamiento 1,2-diotrópico de tipo I. De hecho, se obtienen, según el caso, mezclas separables de dos compuestos principalmente: ésteres **15**, derivados de un proceso de fotocarbonilación junto con un complejo organometálico, **16**, derivado de un nuevo proceso fotoquímico (Esquema 12). Los fosfinoésteres **15** se caracterizaron completamente utilizando las técnicas espectroscópicas habituales. Los espectros de ^{13}C-RMN muestran una única señal en torno a δ = 174 ppm correspondiente al carbono cuaternario del éster metílico. Para determinar el estado de oxidación del átomo de fósforo (fosfinas u óxidos de fosfinas) utilizamos espectroscopia ^{31}P-RMN (utilizando como referencia interna H_3PO_4, δ = 0.0 ppm). Así, las fosfinas **15c**,**i**,**j** muestran una única señal en el rango δ = -12.6–-14.8 ppm mientras que en los óxidos de fosfina, **15b**,**h**, la señal correspondiente al núcleo de fósforo aparece a campo más bajo, $\delta \approx 34$ ppm. La estructura de los óxidos de fosfina **15b**,**h** se estableció adicionalmente utilizando espectrometría de masas ESI-MS, encontrando los picos *m/z* = 359 y *m/z* = 407, correspondientes a los iones moleculares de **15b** y **15h**, respectivamente. Los distintos espectros de ^{13}C-RMN de los complejos **16** muestran la ausencia del ligando carbeno en su estructura junto con una esfera de coordinación para el metal de tipo [M(CO)$_4$]. Los datos anteriores nos han permitido asignar a este tipo de complejos una

estructura de tipo fosfinoamina coordinada a metal. Como podemos ver, nos encontramos ante otro nuevo proceso fotoquímico para complejos metal-carbeno de tipo Fischer del grupo 6. Parece claro, por tanto, que pequeños cambios en la estructura electrónica del complejo provocan fuertes diferencias en la reactividad fotoquímica del mismo.[20]

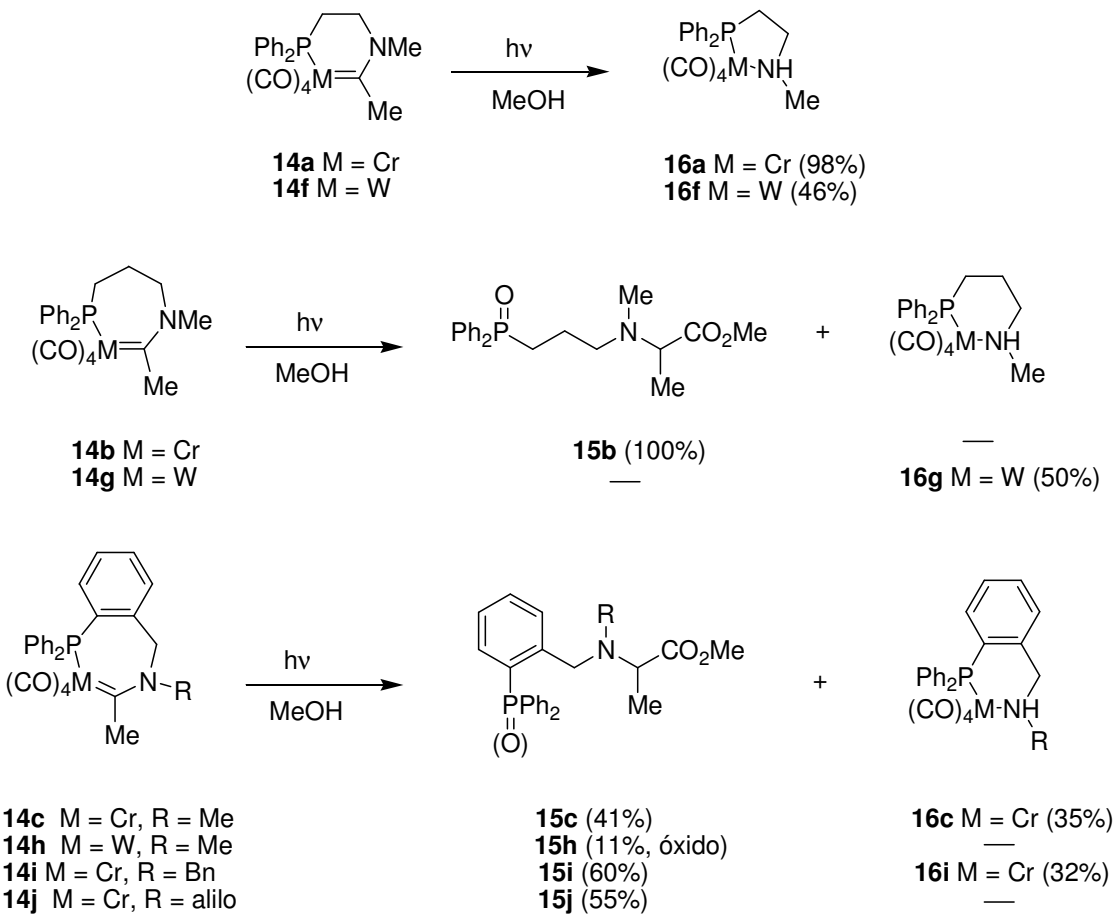

Esquema 12

Aún más interesante que encontrar un tercer proceso fotoquímico, el hecho más relevante es la formación del producto **15h**, ya que *constituye el primer ejemplo de fotocarbonilación en un complejo metal-carbeno de wolframio*. A pesar del escaso rendimiento del proceso, este hecho abre las puertas al diseño de nuevos complejos de wolframio, capaces de insertar fotoquímicamente CO en el enlace metal-carbeno y producir así toda la reactividad estudiada para sus análogos de cromo.

[20] A simple vista podría pensarse que las aminas **16** son los productos de hidrólisis de los complejos procedentes del reordenamiento 1,2-diotrópico. Sin embargo, debe notarse que de ser éste el caso, el nitrógeno amínico no estaría sustituido.

Este nuevo proceso fotoquímico se ha estudiado computacionalmente (B3LYP/6-31+G*&LanL2DZ) sobre el modelo **14d**, análogo al complejo real **14a**. El estado excitado de menor energía del complejo **14d** es un triplete con una excitación vertical de 45.1 kcal mol^{-1}, formado tras la fotoexcitación inicial al primer singlete excitado (S_1) y posterior ISC. La distancia Cr-C es *ca*. 0.14 Å mayor que la encontrada en el estado fundamental S_0. Las densidades de espín calculadas en el átomo de cromo y en el carbono carbenoide inicial son 1.727 y 0.627 u.a. respectivamente, por lo que nos encontramos con una especie de naturaleza birradicálica, **14d(T_1)**, análoga al triplete inicial desde donde se produce el proceso 1,2-diotrópico para los complejos **1**. Al igual que sucedía con el reordenamiento diotrópico discutido anteriormente, no hemos encontrado ningún camino de reacción que conecte de manera concertada **14d** con la amina metalada **16d**, ni en la hipersuperficie singlete ni en la triplete. Sin embargo, hemos localizado un estado de transición, **TS-Cr**, en la hipersuperficie triplete, cuya única frecuencia imaginaria se encuentra asociada, según demuestra el cálculo IRC, a la migración de un protón desde el resto metilo unido al carbono carbenoide hasta dicho carbono. Esta migración conduce a la enamina **17** en el estado triplete, la cual, tras posterior hidrólisis y complejación del nitrógeno al metal, produce a la amina metalada **16d** (Esquema 13).

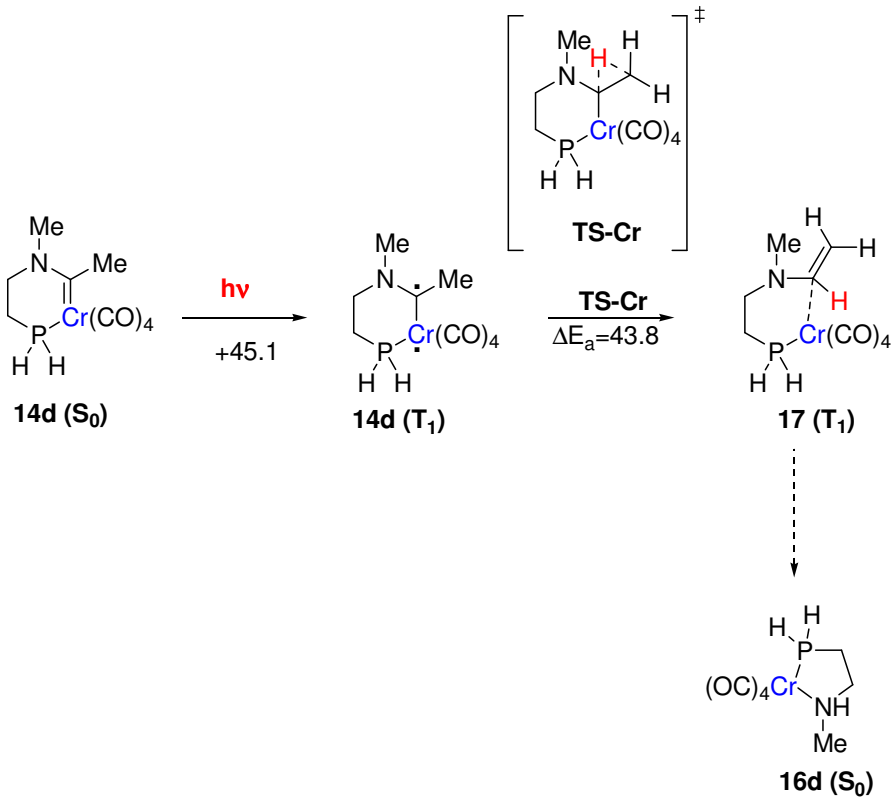

Esquema 13

Hemos calculado esta nueva coordenada de reacción para el carbeno de wolframio modelo **14e**, análogo al complejo **14f** (Esquema 14). De nuevo, no se observan diferencias significativas con el camino calculado para el modelo de cromo **14d**. Del mismo modo, el proceso comienza desde un triplete de naturaleza birradicálica (densidades de espín calculadas: W = 0.56 y C = 0.74 u.a.) y evoluciona a través del estado de transición **TS-W** hacia la enamina **18** que se transforma posteriormente en la amina *N*-metalada **16e**.

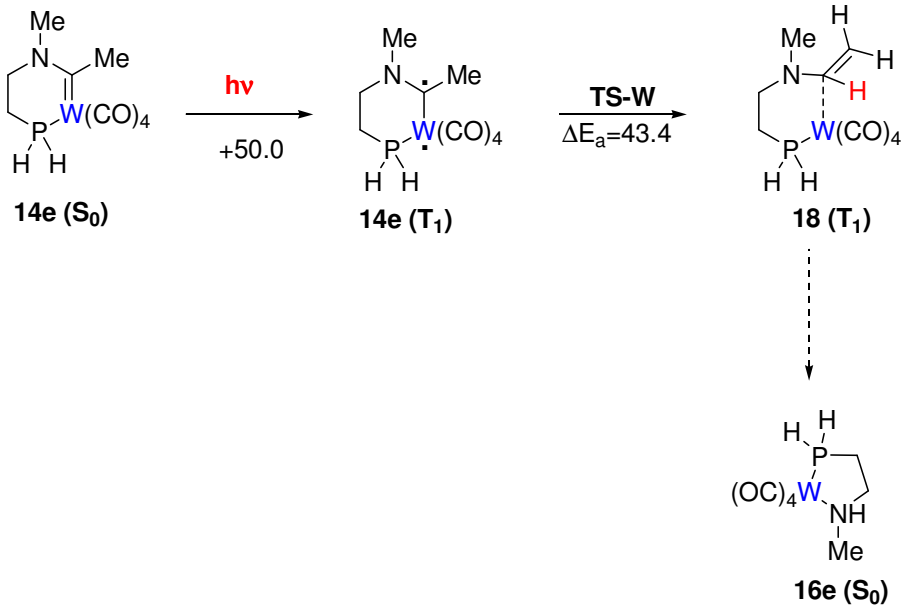

Esquema 14

Como ya se ha dicho, las reacciones de los complejos **14** conducen simultáneamente a los productos de fotocarbonilación **15** y los derivados **16**. Los cálculos DFT (uB3LYP/6-31+G*&LanL2DZ) realizados sobre los modelos **14d** y **14e** muestran la coexistencia de dos especies triplete para cada compuesto: **14d(T_1)** y **14d(T_2)** para **14d** y **14e(T_1)** y **14e(T_2)** para **14e**. Estas especies son, respectivamente, la que deriva de un proceso de fotocarbonilación, T_2, y la resultante del proceso *pseudodiotrópico*, T_1 (Esquema 15).

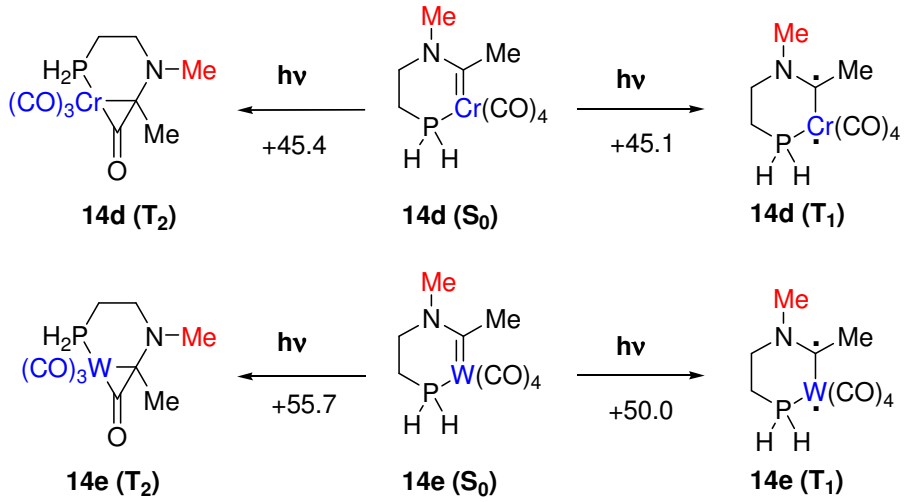

Esquema 15

Las especies T_2 poseen una estructura de tipo metalacetena. En el caso del complejo de cromo modelo **14d**, ambas especies triplete son prácticamente isoenergéticas ($\Delta E_{T2\text{-}T1}$ = 0.3 kcal mol^{-1}), mientras que la especie de fotocarbonilación **14e(T_2)** derivada de wolframio es considerablemente más energética que el triplete pseudodiotrópico T_1 ($\Delta_{ET2\text{-}T1}$ = 5.7 kcal mol^{-1}). Estos resultados justifican la escasa reactividad de los complejos wolframio-carbeno frente al proceso de fotocarbonilación y su preferencia hacia la formación de las aminas *N*-metaladas **16**. Aún así, puesto que la diferencia de energía no es muy grande, es posible encontrar casos en los que la fotocarbonilación sea el camino preferido (caso del complejo **14h**). Por otro lado, en el caso de los cromocarbenos, la coexistencia de dos especies triplete prácticamente isoenergéticas hace que se produzcan mezclas de reacción, justificándose de nuevo los resultados experimentales.

En conclusión, podemos diseñar complejos metal-carbeno de manera que seamos capaces, en principio, de controlar a voluntad su reactividad fotoquímica. El estudio computacional, además de ayudarnos a interpretar los distintos caminos de reacción por los que el experimento transcurre, nos permite predecir qué requisitos estructurales y electrónicos necesita un complejo metal-carbeno para evolucionar fotoquímicamente por al menos uno de los tres caminos de reacción posibles: fotocarbonilación, reordenamiento 1,2-diotrópico de tipo I y reordenamiento *pseudo-diotrópico*.

Parte Experimental

Procedimiento general para la síntesis de los complejos 2f-h: La síntesis de los complejos de wolframio se lleva a cabo siguiendo el procedimiento general descrito anteriormente para los complejos **2** basados en cromo pero utilizando el complejo pentacarbonil[etoxi(metil)]wolframio(0) carbeno.

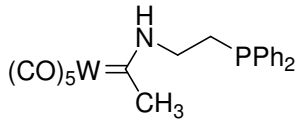

2f

2f: 58%, aceite amarillo. ^{1}H RMN (300 MHz, $CDCl_3$) δ = 1.75 (m, 2H), 2.56 (s, 3H), 3.95 (m, 2H), 7.32-7.72 (m, 10H), 8.46 (br s, 1H, NH). ^{13}C RMN (50 MHz, $CDCl_3$) δ= 28.1 (d, $J_{C\text{-}P}$ = 15.3 Hz), 47.1, 52.7 (d, $J_{C\text{-}P}$ = 16.5 Hz), 128.9 (d, $J_{C\text{-}P}$ = 6.4 Hz), 129.4, 132.7 (d, $J_{C\text{-}P}$ = 19.1 Hz), 136.5 (d, $J_{C\text{-}P}$ = 11.4 Hz), 198.2, 203.2, 255.6. IR (CCl_4) 2062, 1965, 1927 cm^{-1}. $C_{21}H_{18}NO_5PW$: Calc. C 43.55, H 3.13, N 2.42. Encontrado C 43.69, H 3.00, N 2.28.

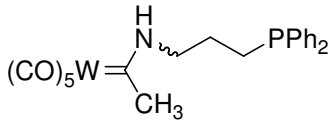

2g

2g: (mezcla *sin-anti* **1:3.6**): 40%, aciete amarillo. ^{1}H RMN (300 MHz, $CDCl_3$) δ = 1.76 (m, 4H, (M+m)), 2.05 (m, 4H, (M+m)), 2.53 (s, 3H), 2.66 (s, 3H), 3.33 (m, 2H), 3.78 (m, 2H), 7.24-7.33 (m, 20H, ArH), 8.48 (br s, 1H, NH), 8.67 (br s, 1H, NH). ^{13}C RMN (75.5 MHz, $CDCl_3$) δ = 25.0 (d, $J_{C\text{-}P}$ = 12.1 Hz), 25.6 (d, $J_{C\text{-}P}$ = 16.8 Hz), 37.3, 47.1, 48.4 (d, $J_{C\text{-}P}$ = 12.9 Hz), 56.3 (d, $J_{C\text{-}P}$ = 11.9 Hz), 128.6 (d, $J_{C\text{-}P}$ = 5.6 Hz), 128.9, 132.6 (d, $J_{C\text{-}P}$ = 10.3 Hz), 137.4 (d, $J_{C\text{-}P}$ = 11.1 Hz), 198.3, 198.8, 203.3, 254.8, 255.4. IR (CCl_4) 2062, 1965, 1925 cm^{-1}. $C_{22}H_{20}NO_5PW$: Calc. C 44.54, H 3.40, N 2.36. Encontrado C 44.39, H 3.22, N 2.27.

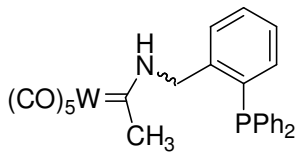

2h

2h (mezcla *sin-anti* **1:5.5**)**:** 62%, sólido amarillo: ^{1}H RMN (300 MHz, $CDCl_3$) δ = 2.09 (s, 3H), 2.28 (s, 3H), 4.63 (d, 2H, J = 5.6 Hz), 5.10 (d, 2H, J = 4.9 Hz), 6.93 (m, 2H, ArH, (M+m)), 7.17-7.36 (m, 26H, ArH, (M+m)), 8.05 (br s, 1H, NH), 8.91 (br s, 1H, NH). ^{13}C RMN (75.5 MHz, $CDCl_3$) δ = 46.7, 58.7 (d, $J_{C\text{-}P}$ = 19.8 Hz), 129.0 (d, $J_{C\text{-}P}$ = 7.0 Hz), 129.3, 129.5, 129.8, 130.4 (d, $J_{C\text{-}P}$ = 4.1 Hz), 133.7, 134.1, 134.1 (d, $J_{C\text{-}P}$ = 19.6 Hz), 135.1 (d, $J_{C\text{-}P}$ = 8.8 Hz), 137.6 (d, $J_{C\text{-}P}$ = 15.2 Hz), 138.3 (d, $J_{C\text{-}P}$ = 25.5 Hz), 198.3, 198.7, 203.2, 255.1. IR (KBr) 2062, 1960, 1898 cm^{-1}. $C_{26}H_{20}NO_5PW$: Calc. C 48.70, H 3.14, N 2.18. Encontrado C 48.52, H 3.31, N 2.26.

Procedimiento general para la síntesis de los complejos 1f-h: La síntesis de los complejos de wolframio se lleva a cabo siguiendo el procedimiento general descrito anteriormente para los complejos **1** basados en cromo pero utilizando tolueno como disolvente para provocar la sustitución intramolecular de ligando.

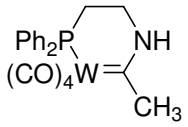

1f

1f: 91%, sólido amarillo. ^{1}H RMN (300 MHz, $CDCl_3$) δ = 2.36 (m, 2H), 2.77 (s, 3H), 3.85 (m, 1H), 3.92 (m, 1H), 7.30-7.52 (m, 10H, ArH), 8.92 (s, 1H, NH). ^{13}C RMN (75.5 MHz, $CDCl_3$) δ = 25.2 (d, $J_{C\text{-}P}$ = 23.6 Hz), 46.6 (d, $J_{C\text{-}P}$ = 4.1 Hz), 48.9 (d, $J_{C\text{-}P}$ = 6.1 Hz), 128.5 (d, $J_{C\text{-}P}$ = 9.3 Hz), 129.8 (d, $J_{C\text{-}P}$ = 1.4 Hz), 131.9 (d, $J_{C\text{-}P}$ = 12.0 Hz), 137.0 (d, $J_{C\text{-}P}$ = 38.3 Hz), 203.2 (d, $J_{C\text{-}P}$ = 7.0 Hz), 209.2 (d, $J_{C\text{-}P}$ = 26.8 Hz), 213.4 (d, $J_{C\text{-}P}$ = 7.3 Hz), 261.4 (d, $J_{C\text{-}P}$ = 9.6 Hz). IR (KBr) 3304, 2002, 1875, 1838 cm^{-1}. $C_{20}H_{18}NO_4PW$: Calc. C 43.58, H 3.29, N 2.54. Encontrado C 43.74, H 3.51, N 2.70

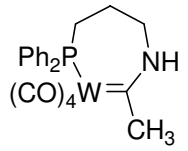

1g

1g: 97%, sólido amarillo. ^{1}H RMN (300 MHz, $CDCl_3$) δ = 1.91 (m, 2H), 2.63 (m, 2H), 2.75 (s, 3H), 3.91 (m, 2H), 7.10-7.46 (m, 10H, ArH), 8.77 (s, 1H, NH). ^{13}C RMN (75.5 MHz, $CDCl_3$) δ = 24.1, 26.5 (d, $J_{C\text{-}P}$ = 21.1 Hz), 46.0 (d, $J_{C\text{-}P}$ = 3.7 Hz), 50.5 (d, $J_{C\text{-}P}$ = 8.6 Hz), 128.4 (d, $J_{C\text{-}P}$ = 9.1 Hz), 129.6, 131.9 (d, $J_{C\text{-}P}$ = 11.3 Hz), 137.8, 203.8 (d, $J_{C\text{-}P}$ = 6.1 Hz), 209.3 (d, $J_{C\text{-}P}$ = 26.6 Hz), 212.3 (d, $J_{C\text{-}P}$ = 7.2 Hz), 264.3 (d, $J_{C\text{-}P}$ = 8.4 Hz). ^{31}P RMN (121MHz, $CDCl_3$) δ= –2.4. IR (KBr) 3288, 2006, 1909, 1871, 1836 cm^{-1}. $C_{21}H_{20}NO_4PW$: Calc. C 44.63, H 3.57, N 2.48. Encontrado C 44.55, H 3.69, N 2.59.

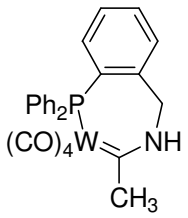

1h

1h: 89%, sólido amarillo. ^{1}H RMN (300 MHz, $CDCl_3$) δ = 2.75 (s, 3H), 4.83 (m, 2H), 6.67 (m, 1H, ArH), 7.19-7.42 (m, 13H, ArH), 8.88 (s, 1H, NH). ^{13}C RMN (50.0 MHz, acetona-d_6) δ = 45.0 (d, $J_{C\text{-}P}$ = 3.8 Hz), 56.2 (d, $J_{C\text{-}P}$ = 11.4 Hz), 129.3 (d, $J_{C\text{-}P}$ = 8.9 Hz), 130.1 (d, $J_{C\text{-}P}$ = 5.1 Hz), 130.9, 131.8, 132.3 (d, $J_{C\text{-}P}$ = 6.4 Hz), 133.5, 134.2 (d, $J_{C\text{-}P}$ = 11.4 Hz), 136.9 (d, $J_{C\text{-}P}$ = 39.4 Hz), 142.2 (d, $J_{C\text{-}P}$ = 12.7 Hz), 205.5 (d, $J_{C\text{-}P}$ = 7.6 Hz), 207.0 (d, $J_{C\text{-}P}$ = 7.6 Hz), 209.7 (d, $J_{C\text{-}P}$ = 28.0 Hz) 213.1 (d, $J_{C\text{-}P}$ = 7.6 Hz), 258.7 (d, $J_{C\text{-}P}$ = 7.6 Hz). IR (KBr) 3292, 2010, 1878, 1830 cm^{-1}. $C_{25}H_{20}NO_4PW$: Calc. C 48.96, H 3.29, N 2.28. Encontrado C 49.06, H 3.40, N 2.46.

Procedimiento general para la síntesis de los complejos 14: A una disolución del complejo **1** correspondiente en acetona desoxigenada (0.025 M) se le añaden 2 equivalentes del correspondiente haluro de alquilo, 3 equivalentes Cs_2CO_3 y varias gotas de agua. La mezcla se agita durante 16 h a temperatura ambiente y el crudo se filtra a través de un lecho de celita. El disolvente se elimina a presión reducida para producir productos puros.[21]

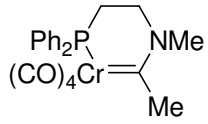

14a

14a: 99%, sólido amarillo. ^{1}H RMN (300 MHz, $CDCl_3$) δ= 2.26 (m, 2H), 2.67 (s, 3H), 3.31 (d, 3H, J = 1.0 Hz), 4.04 (m, 1H), 4.13 (m, 1H), 7.26-7.47 (m, 10H, ArH). ^{13}C RMN (75.5 MHz, $CDCl_3$) δ = 25.3 (d, $J_{C\text{-}P}$ = 18.9 Hz), 29.2, 40.3 (d, $J_{C\text{-}P}$ = 3.5 Hz), 57.8 (d, $J_{C\text{-}P}$ = 6.2 Hz), 128.4 (d, $J_{C\text{-}P}$ = 8.5 Hz), 129.4 (d, $J_{C\text{-}P}$ = 1.5Hz), 131.5 (d, $J_{C\text{-}P}$ = 11.0 Hz), 138.1 (d, $J_{C\text{-}P}$ = 33.3 Hz), 222.9 (d, $J_{C\text{-}P}$ = 13.0 Hz), 228.8 (d, $J_{C\text{-}P}$ = 1.7 Hz), 231.1 (d, $J_{C\text{-}P}$ = 14.6 Hz), 281.1 (d, $J_{C\text{-}P}$ = 16.1 Hz). IR (KBr) 1992, 1900, 1863, 1844 cm^{-1}. $C_{21}H_{20}CrNO_4P$: Calc. C 58.20, H 4.65, N 3.23. Encontrado C 58.45, H 4.78, N 3.33.

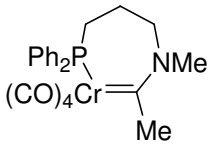

14b

14b: 99%, sólido amarillo. ^{1}H RMN (300 MHz, $CDCl_3$) δ= 2.72 (s, 3H), 3.21 (s, 3H), 7.18-7.71 (m, 10H, ArH). ^{13}C RMN (75.5 MHz, $CDCl_3$) δ = 22.1, 25.8 (d, $J_{C\text{-}P}$ = 15.6 Hz), 39.6, 40.4, 61.1 (d, $J_{C\text{-}P}$ = 10.1 Hz), 128.3-133.6 (m), 281.9 (d, $J_{C\text{-}P}$ = 9.2 Hz). IR (KBr) 1990, 1901, 1871, 1832 cm^{-1}. $C_{22}H_{22}CrNO_4P$: Calc. C 59.06, H 4.96, N 3.13. Encontrado C 58.87, H 4.84, N 2.99.

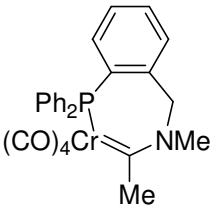

14c

14c: 99%, sólido amarillo. ^{1}H RMN (300 MHz, $CDCl_3$) δ= 2.70 (s, 3H), 3.34 (s, 3H), 4.23 (m, 1H), 6.05 (m, 1H), 6.88 (m, 1H, ArH), 7.30-7.56 (m, 13H, ArH). ^{13}C RMN (75.5 MHz, $CDCl_3$) δ= 40.2 (d, $J_{C\text{-}P}$ = 3.7 Hz), 40.9, 65.9 (d, $J_{C\text{-}P}$ = 12.5 Hz), 128.2 (d, $J_{C\text{-}P}$ = 8.9 Hz), 129.5, 129.5(d, $J_{C\text{-}P}$ = 5.3 Hz), 129.7, 130.2 (d, $J_{C\text{-}P}$ = 1.6 Hz), 133.0 (d, $J_{C\text{-}P}$ = 10.9 Hz), 133.6 (d, $J_{C\text{-}P}$ = 18.5 Hz), 133.7, 136.0 (d, $J_{C\text{-}P}$ = 34.2 Hz), 140.0 (d, $J_{C\text{-}P}$ = 14.0 Hz), 222.2 (d, $J_{C\text{-}P}$ = 10.1 Hz), 228.4, 229.7 (d, $J_{C\text{-}P}$ = 15.6 Hz), 280.7 (d, $J_{C\text{-}P}$ =

[21] En el caso de usar como agente alquilante bromuro de bencilo, es necesario, tras evaporación del disolvente, lavar el residuo con hexano un par de veces para eliminar el exceso de agente alquilante.

12.0 Hz). IR (KBr) 1998, 1905, 1877, 1838 cm^{-1}. $C_{26}H_{22}CrNO_4P$: Calc, C 63.03, H 4.48, N 2.83. Encontrado C 63.25, H 4.58, N 2.60.

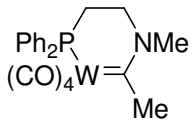

14f

14f: 99%, sólido amarillo. ^{1}H RMN (300 MHz, $CDCl_3$) δ= 2.31 (m, 2H), 2.67 (s, 3H), 3.26 (s, 3H), 4.05 (m, 1H), 4.14 (m, 1H), 7.26-7.46 (m, 10H, ArH). ^{13}C RMN (75.5 MHz, $CDCl_3$) δ = 24.8 (d, $J_{C\text{-}P}$ = 23.6 Hz), 42.0 (d, $J_{C\text{-}P}$ = 37.2 Hz), 53.4, 62.5 (d, $J_{C\text{-}P}$ = 7.1 Hz), 128.5 (d, $J_{C\text{-}P}$ = 9.3 Hz), 129.7 (d, $J_{C\text{-}P}$ = 1.6 Hz), 131.9 (d, $J_{C\text{-}P}$ = 12.0 Hz), 137.3 (d, $J_{C\text{-}P}$ = 38.2 Hz), 203.9 (d, $J_{C\text{-}P}$ = 6.9 Hz), 210.1 (d, $J_{C\text{-}P}$ = 28.1 Hz), 213.0 (d, $J_{C\text{-}P}$ = 6.7 Hz), 259.7 (d, $J_{C\text{-}P}$ = 10.1 Hz). IR (KBr) 2000, 1902, 1857, 1842 cm^{-1}. $C_{21}H_{20}NO_4PW$: Calc. C 44.63, H 3.57, N 2.48. Encontrado C 44.44, H 3.40, N 2.55.

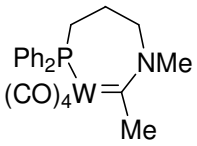

14g

14g: 99%, sólido amarillo. ^{1}H RMN (300 MHz, $CDCl_3$) δ= 2.69 (s, 3H), 3.15 (s, 3H), 7.12-7.81 (m, 10H, ArH). ^{13}C RMN (75.5 MHz, $CDCl_3$) δ = 25.0 (d, $J_{C\text{-}P}$ = 21.0 Hz), 29.0, 41.0 (d, $J_{C\text{-}P}$ = 7.3 Hz), 53.5 (d, $J_{C\text{-}P}$ = 16.3 Hz), 62.6 (d, $J_{C\text{-}P}$ = 9.2 Hz), 128.3-135.6 (m), 209.9 (d, $J_{C\text{-}P}$ = 28.2 Hz), 210.9, 212.4 (d, $J_{C\text{-}P}$ = 6.7 Hz), 261.7 (d, $J_{C\text{-}P}$ = 8.7 Hz). IR (KBr) 2000, 1869, 1838 cm^{-1}. $C_{22}H_{22}NO_4PW$: Calcd C 45.62, H 3.83, N 2.42. Encontrado C 45.45, H 4.04, N 2.55.

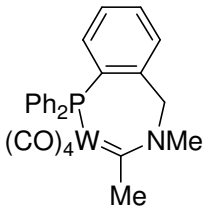

14h

14h: 99%, sólido amarillo. ^{1}H RMN (300 MHz, $CDCl_3$) δ= 2.59 (s, 3H), 3.33 (s, 3H), 4.21 (m, 1H), 6.26 (m, 1H), 6.84 (m, 1H, ArH), 7.24-7.56 (m, 13H, ArH). ^{13}C RMN (75.5 MHz, acetona-d_6) δ= 39.9, 41.8 (d, $J_{C\text{-}P}$ = 3.8 Hz), 67.5 (d, $J_{C\text{-}P}$ = 12.0 Hz), 128.8 (d, $J_{C\text{-}P}$ = 7.7 Hz), 130.0 (d, $J_{C\text{-}P}$ = 5.3 Hz), 131.3, 131.4 (d, $J_{C\text{-}P}$ = 6.7 Hz), 133.1, 133.6 (d, $J_{C\text{-}P}$ = 11.0 Hz), 133.9, 136.7 (d, $J_{C\text{-}P}$ = 38.9 Hz), 140.8 (d, $J_{C\text{-}P}$ = 13.9 Hz), 209.8 (d, $J_{C\text{-}P}$ = 28.8 Hz), 212.6 (d, $J_{C\text{-}P}$ = 6.7 Hz), 258.3 (d, $J_{C\text{-}P}$ = 8.2 Hz). ^{31}P RMN (121 MHz, $CDCl_3$) δ= 4.1. IR (KBr) 2006, 1896, 1869, 1838 cm^{-1}. $C_{26}H_{22}NO_4PW$: Calc. C 49.78, H 3.54, N 2.23. Encontrado C 49.92, H 3.33, N 2.40.

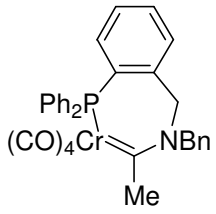

14i

14i: 99%, sólido amarillo. ^{1}H RMN (300 MHz, $CDCl_3$) δ= 2.81 (s, 3H), 4.21 (br s, 1H), 4.62 (br s, 1H), 5.20 (br s, 1H), 5.91 (br s, 1H), 6.89 (m, 1H, ArH), 7.05-7.35 (m, 18H, ArH). ^{13}C RMN (75.5 MHz, $CDCl_3$) δ= 40.2 (d, J_{C-P} = 3.8 Hz), 55.3, 62.5 (d, J_{C-P} = 12.5 Hz), 126.3, 128.1, 128.2 (d, J_{C-P} = 8.3 Hz), 129.4, 129.6 (d, J_{C-P} = 4.2 Hz), 130.1 (d, J_{C-P} = 6.1 Hz), 130.3, 133.0 (d, J_{C-P} = 11.2 Hz), 133.5 (d, J_{C-P} = 6.9 Hz), 134.0 (d, J_{C-P} = 18.6 Hz), 136.0 (d, J_{C-P} = 34.5 Hz), 140.0 (d, J_{C-P} = 14.1 Hz), 222.4 (d, J_{C-P} = 7.4 Hz), 228.4 (d, J_{C-P} = 1.8 Hz), 229.9 (d, J_{C-P} = 16.4 Hz), 282.9 (d, J_{C-P} = 12.6 Hz). IR (KBr) 1994, 1913, 1871, 1840 cm^{-1}. $C_{32}H_{26}CrNO_4P$: Calc. C 67.25, H 4.59, N 2.45. Encontrado C 67.01, H 4.43, N 2.34.

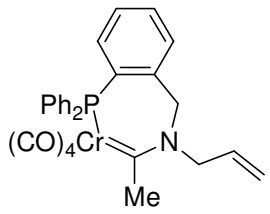

14j

14j: 99%, sólido amarillo. ^{1}H RMN (300 MHz, $CDCl_3$) δ= 2.74 (s, 3H), 4.20 (br s, 2H), 5.11 (br s, 1H), 5.25 (d, 2H, J = 10.2 Hz), 5.72 (m, 1H), 5.94 (br s, 1H), 6.90 (m, 1H, ArH), 7.26-7.54 (m, 13H, ArH). ^{13}C RMN (75.5 MHz, $CDCl_3$) δ= 39.5 (d, J_{C-P} = 4.1 Hz), 54.4, 62.9 (d, J_{C-P} = 12.1 Hz), 117.8, 128.2 (d, J_{C-P} = 9.0 Hz), 129.5, 129.6, 130.1 (d, J_{C-P} = 6.3 Hz), 130.3, 132.9 (m), 133.6, 133.8 (d, J_{C-P} = 18.5 Hz), 136.1 (d, J_{C-P} = 34.2 Hz), 140.1 (d, J_{C-P} = 14.2 Hz), 222.4 (d, J_{C-P} = 10.6 Hz), 228.4 (d, J_{C-P} = 1.7 Hz), 229.8 (d, J_{C-P} = 16.4 Hz), 282.0 (d, J_{C-P} = 12.8 Hz). IR (KBr) 1996, 1894, 1875, 1846 cm^{-1}. $C_{28}H_{24}CrNO_4P$: Calc. C 64.49, H 4.64, N 2.69. Encontrado C 64.61, H 4.73, N 2.41.

Procedimiento general para las reacciones fotoquímicas de los complejos 2f-h y 14. Las distintas irradiaciones se llevaron a cabo siguiendo el procedimiento experimental indicado en las irradiaciones de los complejos **1a-c**. En un típico experimento tras 10h de irradiación, la disolución (0.015 M) se filtra a través de un lecho de celita, se eliminan los disolventes a presión reducida y el crudo, salvo que se indique otro procedimiento, se somete a purificación por cromatografía en columna (hexano/AcOEt, 3:1).

Irradiación de 2f. Siguiendo el procedimiento general se obtiene el complejo **5f**.

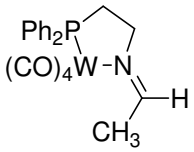

5f

5f: 71%, sólido amarillo. ^{1}H RMN (300 MHz, $CDCl_3$) δ = 2.28 (d, 3H, *J* = 5.2 Hz), 2.46 (m, 2H), 3.85 (m, 1H), 3.93 (m, 1H), 7.34-7.59 (m, 10H, ArH), 7.86 (q, 1H, *J* = 5.2 Hz). ^{13}C RMN (75.5 MHz, $CDCl_3$) δ = 26.0, 30.7 (d, J_{C-P} = 21.2 Hz), 69.6 (d, J_{C-P} = 10.1 Hz), 128.8 (d, J_{C-P} = 9.9 Hz), 130.2 (d, J_{C-P} = 1.7 Hz), 131.9 (d, J_{C-P} = 12.2 Hz), 135.5 (d, J_{C-P} = 40.4 Hz), 172.9, 203.0 (d, J_{C-P} = 7.0 Hz), 210.1 (d, J_{C-P} = 32.0 Hz), 211.6 (d, J_{C-P} = 5.1 Hz). IR (KBr) 2008, 1867, 1838 cm^{-1}. $C_{20}H_{18}NO_4PW$: Calc. C 43.58, H 3.29, N 2.54. Encontrado C 43.39, H 3.33, N 2.41.

Irradiación de 2g. Siguiendo el procedimiento general se obtiene el complejo **5g**.

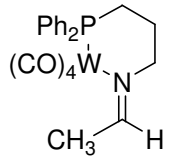

5g

5g: 55%, sólido amarillo. ^{1}H RMN (300 MHz, $CDCl_3$) δ= 1.87 (m, 2H), 2.28 (d, 3H, *J* = 5.3 Hz), 2.60 (m, 2H), 4.02 (m, 2H), 7.33-7.49 (m, 10H, ArH), 7.72 (q, 1H, *J* = 5.3 Hz). ^{13}C RMN (75.5 MHz, $CDCl_3$) δ = 26.0, 26.7 (d, J_{C-P} = 1.2 Hz), 29.7 (d, J_{C-P} = 5.9 Hz), 71.5 (d, J_{C-P} = 9.0 Hz), 128.5 (d, J_{C-P} = 9.3 Hz), 129.9 (d, J_{C-P} = 1.1 Hz), 132.1 (d, J_{C-P} = 11.8 Hz), 135.6 (d, J_{C-P} = 38.6 Hz), 173.7, 204.1 (d, J_{C-P} = 6.8 Hz), 204.5 (d, J_{C-P} = 8.2 Hz), 208.3, 208.5 (d, J_{C-P} = 5.6 Hz). ^{31}P RMN (121 MHz, $CDCl_3$) δ= 12.5. IR (KBr) 2010, 1869, 1836 cm^{-1}. $C_{21}H_{20}NO_4PW$: Calc. C 44.63, H 3.57, N 2.48. Encontrado C 44.81, H 3.60, N 2.61.

Irradiación de 2h. Siguiendo el procedimiento general se obtiene el complejo **5h**.

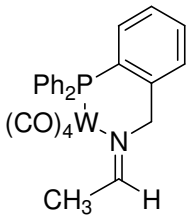

5h

5h: 38%, sólido amarillo. ^{1}H RMN (500 MHz, $CDCl_3$) δ= 2.35 (d, 3H, *J* = 5.3 Hz), 4.95 (d, 2H, *J* = 2.1 Hz), 6.93 (m, 1H, ArH), 7.29-7.50 (m, 13H, ArH), 7.96 (q, 1H, *J* = 5.3 Hz). ^{13}C RMN (125 MHz, $CDCl_3$) δ= 26.2, 75.6 (d, J_{C-P} = 11.7 Hz), 128.6 (d, J_{C-P} = 9.6 Hz), 129.3 (d, J_{C-P} = 7.9 Hz), 129.6 (d, J_{C-P} = 3.9 Hz), 130.1, 131.3, 132.0, 132.8 (d, J_{C-P} = 19.9 Hz), 133.1 (d, J_{C-P} = 11.7 Hz), 134.2 (d, J_{C-P} = 38.5 Hz), 142.4 (d, J_{C-P} = 12.9 Hz), 173.4, 204.0 (d, J_{C-P} = 9.9 Hz), 208.3, 210.1 (d, J_{C-P} = 5.7 Hz). IR (KBr) 2009, 1869, 1838 cm^{-1}. $C_{25}H_{20}NO_4PW$: Calc. C 48.96, H 3.29, N 2.28. Encontrado C 49.11, H 3.36, N 2.14.

Irradiación de 14. Siguiendo el procedimiento general se obtiene el complejo **16a**.

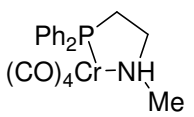

16a

16a: 98%, sólido amarillo. ^{1}H RMN (300 MHz, $CDCl_3$) δ= 2.03 (m, 1H), 2.22 (m, 1H), 2.58 (d, 3H, *J* = 4.1 Hz), 2.69 (m, 1H), 2.69 (m, 1H), 2.96 (m, 1H), 7.31-7.60 (m, 10H, ArH). ^{13}C RMN (75.5 MHz, $CDCl_3$) δ = 28.1 (d, J_{C-P} = 16.1 Hz), 46.1, 54.0 (d, J_{C-P} = 11.8 Hz), 128.7 (d, J_{C-P} = 9.3 Hz), 128.8 (d, J_{C-P} = 9.1 Hz), 129.9 (d, J_{C-P} = 1.6 Hz), 130.0 (d, J_{C-P} = 1.7 Hz), 131.1 (d, J_{C-P} = 11.7 Hz), 131.6 (d, J_{C-P} = 11.8 Hz), 135.7 (d, J_{C-P} = 17.6 Hz), 136.2 (d, J_{C-P} = 14.6 Hz), 218.1 (d, J_{C-P} = 13.7 Hz), 218.4 (d, J_{C-P} = 14.1 Hz), 226.6 (d, J_{C-P} = 2.6 Hz), 228.0 (d, J_{C-P} = 12.8 Hz). IR (CCl_4): 2012, 1954, 1888 cm^{-1}. $C_{19}H_{18}CrNO_4P$: Calc. C 56.03, H 4.45, N 3.44. Encontrado C 56.28, H 4.59, N 3.27.

Irradiación de 14b. Siguiendo el procedimiento general, tras irradiación en MeCN/THF/MeOH (5:5:1) durante 10h y posterior exposición a la luz solar hasta conseguir una disolución transparente, se obtiene, tras purificación en columna, el compuesto **15b**.

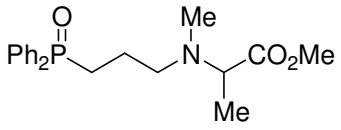

15b

15b: rendimiento cuantitativo, aceite amarillo pálido. ^{1}H RMN (300 MHz, $CDCl_3$) δ = 1.17 (d, 3H, *J* = 7.0 Hz), 1.17 (m, 2H), 2.16 (s, 3H), 2.21 (m, 2H), 2.50 (m, 2H), 3.28 (q, 1H, *J* = 7.0 Hz), 3.60 (s, 3H), 7.38-7.71 (m, 10H, ArH). ^{13}C RMN (75.5 MHz, $CDCl_3$) δ = 14.4, 19.7 (d, J_{C-P} = 3.3 Hz), 27.0 (d, J_{C-P} = 73.1 Hz), 37.5, 51.1, 54.2 (d, J_{C-P} = 15.4 Hz), 61.1, 128.5 (d, J_{C-P} = 11.5 Hz), 130.7 (d, J_{C-P} = 9.2 Hz), 131.6 (d, J_{C-P} = 2.6 Hz), 133.0 (d, J_{C-P} = 98.3 Hz), 173.6. ^{31}P RMN (121, MHz, $CDCl_3$) δ= 34.1. IR (CCl_4): 1936, 1732, 1437, 1215. cm^{-1}. ESI-MS m/z = 359. $C_{20}H_{26}NO_3P$: Calc. C 66.84, H 7.29, N 3.90. Encontrado C 66.67, H 7.05, N 4.09.

Irradiación de 14c. Siguiendo el procedimiento general, tras irradiación en MeCN/THF/MeOH (5:5:1) durante 10h y posterior purificación por cromatografía en columna se obtienen los compuestos **15c** y **16c**.

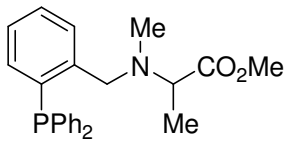

15c

15c: 41%, sólido amarillo. ^{1}H RMN (300 MHz, $CDCl_3$) δ = 0.84 (d, 3H, *J* = 7.1 Hz), 2.00 (s, 3H), 3.32 (q, 1H, *J* = 7.1 Hz), 3.59 (s, 3H), 3.83 (qd, 2H, J_1 = 6.0 Hz, J_2 = 1.7 Hz), 6.86 (m, 1H, ArH), 7.10-7.37 (m, 13H, ArH). ^{13}C RMN (75.5 MHz, $CDCl_3$) δ = 14.4, 35.5, 51.0, 58.2 (d, J_{C-P} = 18.2 Hz), 59.7, 127.2, 128.1, 128.3 (d, J_{C-P} = 10.3 Hz), 128.3 (d, J_{C-P} = 6.9 Hz), 128.6, 129.3 (d, J_{C-P} = 5.7 Hz), 133.4 (d, J_{C-P} = 19.3 Hz), 133.7 (d, J_{C-P} = 22.3 Hz), 134.4, 136.7 (d, J_{C-P} = 15.5 Hz), 137.8 (d, J_{C-P} = 10.3 Hz), 137.9 (d, J_{C-P} = 10.0 Hz), 144.2 (d, J_{C-P} = 23.6 Hz), 173.9. ^{31}P RMN (121, MHz, $CDCl_3$) δ= -12.6. IR (CCl_4): 1942, 1736, 1433. cm^{-1}. $C_{24}H_{26}NO_2P$: Calc. C 73.64, H 6.69, N 3.58. Encontrado C 73.89, H 6.48, N 3.37.

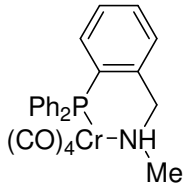

16c

16c: 35%, sólido amarillo. ^{1}H RMN (300 MHz, $CDCl_3$) δ = 2.41 (d, 3H, J = 6.3 Hz), 2.98 (br s, 1H), 3.43 (m, 2H), 6.74 (m, 1H, ArH), 7.28-7.42 (m, 13H, ArH). ^{13}C RMN (75.5 MHz, $CDCl_3$) δ = 46.1, 60.7 (d, $J_{C\text{-}P}$ = 12.7 Hz), 128.5 (d, $J_{C\text{-}P}$ = 1.8 Hz), 128.7 (d, $J_{C\text{-}P}$ = 2.0 Hz), 129.9, 130.2 (d, $J_{C\text{-}P}$ = 13.6 Hz), 131.1 (d, $J_{C\text{-}P}$ = 22.6 Hz), 131.5, 132.0 (d, $J_{C\text{-}P}$ = 7.4 Hz), 132.9 (d, $J_{C\text{-}P}$ = 11.5 Hz), 134.1 (d, $J_{C\text{-}P}$ = 34.8 Hz), 138.7 (d, $J_{C\text{-}P}$ = 17.1 Hz), 218.2 (d, $J_{C\text{-}P}$ = 13.1 Hz), 218.8 (d, $J_{C\text{-}P}$ = 13.1 Hz), 225.1, 226.2 (d, $J_{C\text{-}P}$ = 13.6 Hz). IR (KBr): 3288, 2004, 1878, 1838 cm^{-1}. $C_{24}H_{20}CrNO_4P$: Calc. C 61.41, H 4.29, N 2.98. Encontrado C 61.25, H 4.46, N 3.15.

Irradiación de 14f. Siguiendo el procedimiento general se obtiene el complejo **16f**.

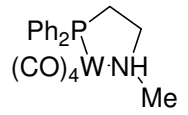

16f

16f: 46%, sólido amarillo. ^{1}H RMN (300 MHz, $CDCl_3$) δ= 2.21 (m, 1H), 2.48 (m, 1H), 2.76 (m, 1H), 2.89 (d, 3H, J = 5.9 Hz), 3.20 (m, 1H), 7.32-7.62 (m, 10H, ArH). ^{13}C RMN (75.5 MHz, $CDCl_3$) δ = 30.0 (d, $J_{C\text{-}P}$ = 21.6 Hz), 48.1, 56.1 (d, $J_{C\text{-}P}$ = 10.2 Hz), 128.7 (d, $J_{C\text{-}P}$ = 3.9 Hz), 128.9 (d, $J_{C\text{-}P}$ = 3.6 Hz), 130.3, 131.7 (d, $J_{C\text{-}P}$ = 12.7 Hz), 132.1 (d, $J_{C\text{-}P}$ = 12.6 Hz), 134.8 (d, $J_{C\text{-}P}$ = 19.9 Hz), 135.3 (d, $J_{C\text{-}P}$ = 22.9 Hz), 202.9 (d, $J_{C\text{-}P}$ = 6.8 Hz), 204.0 (d, $J_{C\text{-}P}$ = 7.8 Hz), 210.2 (d, $J_{C\text{-}P}$ = 31.9 Hz), 210.8 (d, $J_{C\text{-}P}$ = 4.1 Hz). IR (CCl_4): 2012, 1954, 1888 cm^{-1}. $C_{19}H_{18}NO_4PW$: Calc. C 42.33, H 3.37, N 2.60. Encontrado C 42.28, H 3.50, N 2.74.

Irradiación de 14g. Siguiendo el procedimiento general se obtiene el complejo **16g**.

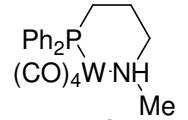

16g

16g: 50%, sólido amarillo. ^{1}H RMN (300 MHz, $CDCl_3$) δ = 1.75 (m, 1H), 2.15 (m, 1H), 2.39 (m, 1H), 2.59 (m, 1H), 2.83 (m, 1H), 2.85 (d, 3H, J = 5.6 Hz), 3.10 (m, 1H), 7.32-7.54 (m, 10H, ArH). ^{13}C RMN (75.5 MHz, $CDCl_3$) δ = 24.2 (d, $J_{C\text{-}P}$ = 3.8 Hz), 28.9 (d, $J_{C\text{-}P}$ = 20.5 Hz), 51.3 (d, $J_{C\text{-}P}$ = 3.5 Hz), 59.6 (d, $J_{C\text{-}P}$ = 2.8 Hz), 128.6 (d, $J_{C\text{-}P}$ = 5.8 Hz), 128.7 (d, $J_{C\text{-}P}$ = 5.7 Hz), 129.8 (d, $J_{C\text{-}P}$ = 1.7 Hz), 130.0 (d, $J_{C\text{-}P}$ = 1.6 Hz), 131.9 (d, $J_{C\text{-}P}$ = 11.8 Hz), 132.1 (d, $J_{C\text{-}P}$ = 11.9 Hz), 135.8 (d, $J_{C\text{-}P}$ = 37.5 Hz), 136.2 (d, $J_{C\text{-}P}$ = 39.7 Hz), 204.0 (d, $J_{C\text{-}P}$ = 7.1 Hz), 204.8 (d, $J_{C\text{-}P}$ = 7.1 Hz), 208.3 (d, $J_{C\text{-}P}$ = 31.0 Hz), 209.0 (d, $J_{C\text{-}P}$ = 6.1 Hz). ^{31}P RMN δ= 12.4. IR (CCl_4): 2012, 1888 cm^{-1}. $C_{20}H_{20}NO_4PW$: Calc. C 43.42, H 3.64, N 2.53. Encontrado C 43.25, H 3.46, N 2.45.

Irradiación de 14h. Siguiendo el procedimiento general, tras 10h de irradiación en mezcla MeCN/THF/MeOH (5:5:1) y posterior exposición a la luz solar hasta conseguir una disolución transparente, se obtiene, tras purificación en columna, el compuesto 1**5h**.

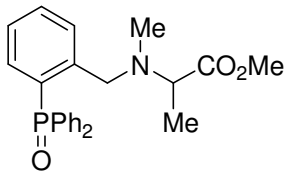

15h

15h: 11%, aceite amarillo pálido. ^{1}H RMN (300 MHz, $CDCl_3$) δ = 0.86 (d, 3H, *J* = 6.9 Hz), 1.91 (s, 3H), 3.31 (q, 1H, *J* = 6.9 Hz), 3.54 (s, 3H), 3.92 (d, 2H, *J* = 10.6 Hz), 6.95-7.59 (m, 14H, ArH). ^{13}C RMN (125 MHz, $CDCl_3$) δ = 14.0, 36.5, 51.1, 56.9, 60.7, 126.1 (d, J_{C-P} = 13.2 Hz), 128.4 (d, J_{C-P} = 9.1 Hz), 130.1, 131.2 (d, J_{C-P} = 9.4 Hz), 131.6, 131.8 (d, J_{C-P} = 8.6 Hz), 132.0, 133.2, 133.6 (d, J_{C-P} = 12.0 Hz), 145.5 (d, J_{C-P} = 9.4 Hz), 174.0. ^{31}P RMN (121 MHz, $CDCl_3$) δ= 34.2. IR (CCl_4): 1736, 1437, 1194, 1159, 1119 cm^{-1}. ESI-MS m/z = 407. $C_{24}H_{26}NO_3P$: Calc. C 70.75, H 6.43, N 3.44. Encontrado C 70.60, H 6.61, N 3.59.

Irradiación de 14i. Siguiendo el procedimiento general, tras irradiación en MeCN/THF/MeOH (5:5:1) durante 10h y posterior purificación por cromatografía en columna se obtienen los compuestos **15i** y **16i**.

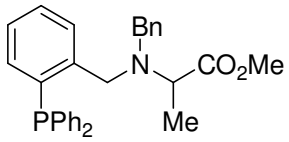

15i

15i: 60%, aceite amarillento. ^{1}H RMN (300 MHz, $CDCl_3$) δ = 1.14 (d, 3H, *J* = 7.1 Hz), 3.38 (q, 1H, *J* = 7.1 Hz), 3.56 (s, 3H), 3.58 (q, 2H, *J* = 14.1 Hz), 3.87 (qd, 2H, J_1 = 17.8 Hz, J_2 = 3.3 Hz), 6.73 (m, 1H, ArH), 7.04-7.29 (m, 17H, ArH), 7.68 (m, 1H, ArH). ^{13}C RMN (75.5 MHz, $CDCl_3$) δ = 14.3, 51.2, 52.1 (d, J_{C-P} = 24.6 Hz), 54.4, 56.5, 126.8 (d, J_{C-P} = 9.2 Hz), 128.1, 128.4, 128.5 (d, J_{C-P} = 3.5 Hz), 128.6 (d, J_{C-P} = 6.6 Hz), 128.7, 128.8 (d, J_{C-P} = 11.5 Hz), 133.1, 133.7 (d, J_{C-P} = 3.5 Hz), 134.0 (d, J_{C-P} = 3.2 Hz), 136.0 (d, J_{C-P} = 14.5 Hz), 136.5 (d, J_{C-P} = 10.6 Hz), 136.8 (d, J_{C-P} = 10.5 Hz), 139.7, 144.0 (d, J_{C-P} = 22.2 Hz), 174.2. ^{31}P RMN (121, MHz, $CDCl_3$) δ= -14.8. IR (CCl_4): 1942, 1736, 1433 cm^{-1}. $C_{30}H_{30}NO_2P$: Calc. C 77.07, H 6.47, N 3.00. Encontrado C 76.89, H 6.66, N 3.12.

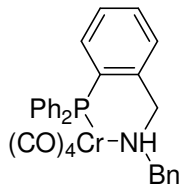

16i

16i: 32%, sólido amarillo. ^{1}H RMN (300 MHz, $CDCl_3$) δ = 3.22-3.45 (m, 4H), 4.08 (d, 1H, *J* = 13.2 Hz), 6.79-6.88 (m, 2H), 7.11-7.45 (m, 17H, ArH). ^{13}C RMN (75.5 MHz, $CDCl_3$) δ = 54.4 (d, J_{C-P} = 12.0 Hz), 60.8, 128.2, 128.4, 128.5 (d, J_{C-P} = 5.3 Hz), 128.6

(d, $J_{C\text{-}P}$ = 5.5 Hz), 129.1, 129.9 (d, $J_{C\text{-}P}$ = 2.7 Hz), 129.9, 130.1, 130.1 (d, $J_{C\text{-}P}$ = 5.5 Hz), 131.6, 131.7, 131.9, 132.2 (d, $J_{C\text{-}P}$ = 7.5 Hz), 132.5, 132.8 (d, $J_{C\text{-}P}$ = 11.5 Hz), 133.2, 133.4 (d, $J_{C\text{-}P}$ = 36.8 Hz), 133.7 (d, $J_{C\text{-}P}$ = 11.6 Hz), 134.2 (d, $J_{C\text{-}P}$ = 34.9 Hz), 136.7, 138.5 (d, $J_{C\text{-}P}$ = 16.5 Hz), 218.2 (d, $J_{C\text{-}P}$ = 12.9 Hz), 219.0 (d, $J_{C\text{-}P}$ = 12.9 Hz), 224.8, 226.4 (d, $J_{C\text{-}P}$ = 13.4 Hz). IR (KBr): 3288, 2004, 1878, 1838 cm^{-1}. $C_{30}H_{24}CrNO_4P$: Calc. C 66.06, H 4.43, N 2.57. Encontrado C 65.87, H 4.66, N 2.45.

Irradiación de 14j. Siguiendo el procedimiento general, tras irradiación en MeCN/THF/MeOH (5:5:1) durante 10h y posterior purificación por cromatografía en columna se obtiene el compuesto **15j**.

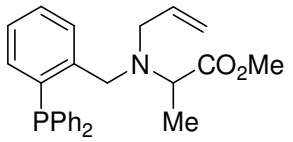

15j

15j: 55%, aceite amarillento. ^{1}H RMN (300 MHz, $CDCl_3$) δ = 1.02 (d, 3H, J = 7.1 Hz), 3.03 (qd, 2H, J_1 = 13.6 Hz, J_2 = 5.6 Hz), 3.38 (q, 1H, J = 7.1 Hz), 3.54 (s, 3H), 3.88 (qd, 2H, J_1 = 15.9 Hz, J_2 = 2.2 Hz), 4.93 (d, 1H, J = 10.1 Hz), 5.02 (dd, 1H, J_1 = 17.2 Hz, J_2 = 1.5 Hz), 5.60 (m, 1H), 6.78 (m, 1H, ArH), 7.06-7.27 (m, 12H, ArH), 7.55 (m, 1H, ArH). ^{13}C RMN (75.5 MHz, $CDCl_3$) δ = 14.5, 51.1, 52.8 (d, $J_{C\text{-}P}$ = 22.4 Hz), 53.4, 57.0, 116.8, 126.9, 128.3, 128.4, 128.5 (d, $J_{C\text{-}P}$ = 3.2 Hz), 128.9 (d, $J_{C\text{-}P}$ = 5.4 Hz), 133.6, 133.7 (d, $J_{C\text{-}P}$ = 10.9 Hz), 133.9 (d, $J_{C\text{-}P}$ = 9.8 Hz), 136.0 (d, $J_{C\text{-}P}$ = 14.7 Hz), 136.6, 136.9 (d, $J_{C\text{-}P}$ = 10.2 Hz), 137.3 (d, $J_{C\text{-}P}$ = 10.9 Hz), 144.3 (d, $J_{C\text{-}P}$ = 22.8 Hz), 174.3. ^{31}P RMN (121, MHz, CDCl3) δ= -13.4. IR (CCl_4): 1942, 1736, 1433 cm^{-1}. $C_{26}H_{28}NO_2P$: Calc. C 78.40, H 6.76, N 3.36. Encontrado C 78.55, H 6.58, N 3.55.

DISCUSIÓN DE RESULTADOS

En este apartado se discuten los aspectos más relevantes de los distintos capítulos tratados anteriormente. Asimismo, se valorará de forma crítica la consecución de los objetivos inicialmente propuestos.

D.1. Capítulo I

D.1.1. Síntesis, estructura y comportamiento electroquímico de complejos metal-carbeno bi- y polimetálicos[1]

El empleo de complejos metal-carbeno de tipo Fischer del grupo 6 permite la construcción de nuevos complejos metal-carbeno con estructuras conformacionalmente restringidas. Concretamente, se ha llevado a cabo con éxito la síntesis de este tipo de complejos con estructuras ciclofánicas y macrocíclicas.

Para la consecución de este objetivo se ha seleccionado la reacción de adición 1,4 de tipo Michael de diferentes bisaminas a complejos de Fischer polimetálicos. Los moldes para la construcción de las distintas estructuras polimetálicas (Figura 1) se han seleccionado en base a que los complejos metal-carbeno α,β-insaturados de tipo Fischer son unos aceptores de Michael excepcionales.[2]

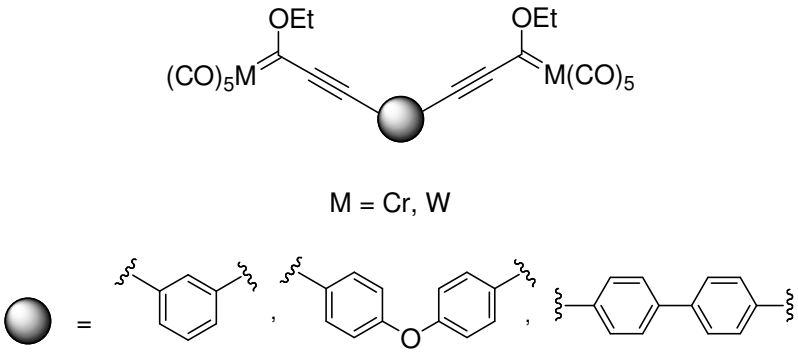

Figura 1

Para la síntesis de complejos ciclofánicos se han usado como nucleófilos diaminas capaces de producir una doble adición 1,4 para conseguir la formación del ciclofano. Las distintas diaminas seleccionadas (Figura 2) tienen la distancia adecuada entre los dos grupos amino para producir esta doble adición 1,4. Así, se han generado

[1] (a) Fernández, I.; Sierra, M. A.; Mancheño, M. J.; Gómez-Gallego, M.; Ricart, S. *Organometallics* **2001**, *20*, 4304. (b) Fernández, I.; Mancheño, M. J.; Gómez-Gallego, M.; Sierra, M. A. *Org. Lett*. **2003**, *5*, 1237.

[2] (a) Aumann, R.; Nienaber,H. *Adv. Organomet. Chem*. **1997**, *41*, 163. (b) de Miejere, A.; Schirmer, H.; Duetsch, M. *Angew. Chem. Int. Ed*. **2000**, *39*, 3964.

complejos bimetálicos con una estructura bastante más sofisticada que la estructura inicial de los moldes empleados.

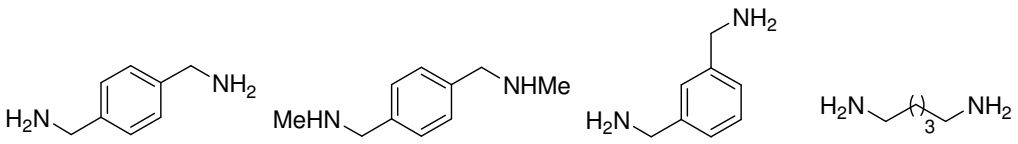

Figura 2

La reacción entre los distintos bisetinil-complejos y bisaminas es siempre una doble adición 1,4 (Esquema 1) y conduce a los distintos complejos ciclofánicos bimetálicos con rendimientos desde buenos a cuantitativos.

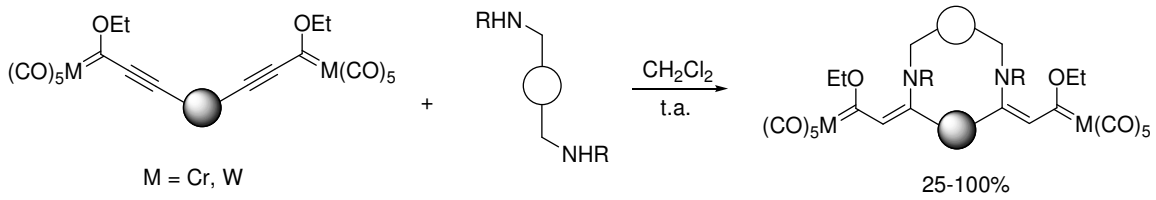

Esquema 1

La única excepción a la reactividad general es la putrescina (1,4-diaminobutano). En este caso, cuando se hace reaccionar dicha amina con el complejo **1**, se obtiene de manera casi inmediata el complejo **2**, resultante de una adición 1,4 sobre el primer centro metálico, seguida de adición 1,2 sobre el segundo centro (Esquema 2). Las razones que justifican la selectividad de esta reacción particular no están claras en este momento.

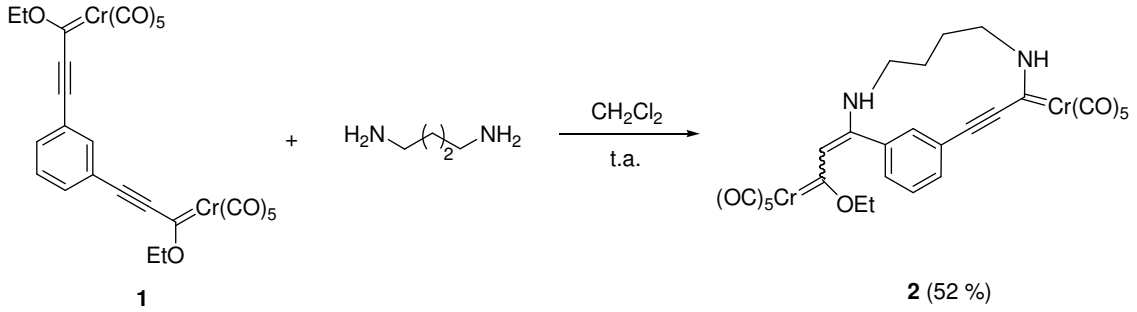

Esquema 2

La estereoquímica de los dos dobles enlaces formados en este proceso general se ha asignado como *Z*,*Z*, por comparación de los datos espectroscópicos de los complejos ciclofánicos obtenidos con los datos publicados para complejos análogos no ciclofánicos.[3] Como confirmación de esta asignación estereoquímica, se preparó el complejo no ciclofánico **3** (Figura 3).[4] Su estructura se determinó mediante difracción de rayos-X y en ella se puede observar la existencia de dos enlaces de hidrógeno entre los hidrógenos unidos a los átomos de nitrógeno y los oxígenos de los grupos etoxi adyacentes. Estos enlaces fijan la estereoquímica de los dos dobles enlaces enamínicos formados durante el proceso de doble adición 1,4. Si admitimos que estas interacciones están presentes en los complejos ciclofánicos análogos, entonces no sólo justifican la estereoquímica de los mismos sino también la excepcional reactividad de los moldes bimetálicos preparados.

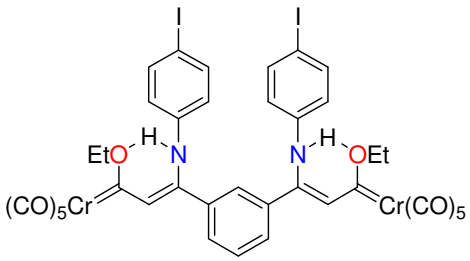

3

Figura 3

Una modificación sencilla del procedimiento empleado para la síntesis de ciclofanos permite la obtención de complejos polimetálicos con estructuras aún más sofisticadas. Concretamente, se pueden obtener complejos ciclofánicos macrocíclicos por reacción de los moldes α,β-insaturados anteriormente diseñados con dos equivalentes de una bisamina aromática (1,4-diaminobenceno o bencidina). Esta reacción conduce a complejos bisenamino-carbeno con estructuras análogas a la del complejo **3** mediante una doble adición 1,4 de Michael. La reacción ocurre de manera prácticamente instantánea y con excelentes rendimientos. Posteriormente, mediante otra nueva doble adición 1,4 entre tales complejos y un nuevo equivalente del complejo α,β-insaturado inicial se produce la reacción de macrociclación de forma eficaz y con muy buenos rendimientos (Esquema 3). El procedimiento descrito también se ha realizado en

[3] Moretó, J. M.; Ricart, S.; Dötz, K. H.; Molins, E. *Organometallics* **2001**, *20*, 62.
[4] Este complejo se prepara siguiendo el procedimiento general para la síntesis de ciclofanos por reacción del complejo **1** con dos equivalentes de 4-yodoanilina.

un único paso de reacción (*one-pot*) usando cantidades equimolares de bisamina y molde bimetálico, obteniéndose los correspondientes macrociclos con rendimientos similares a la síntesis en dos pasos.

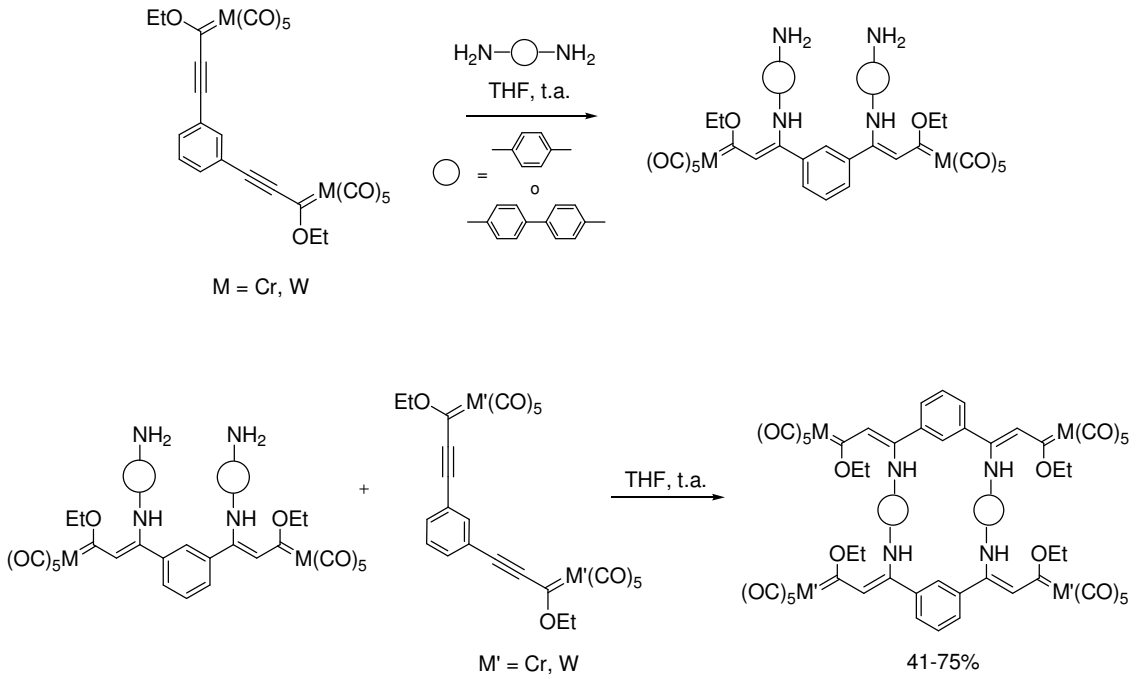

Esquema 3

El procedimiento desarrollado es general y versátil, ya que permite la síntesis de complejos macrocíclicos homo- y heterotetrametálicos. La regioquímica del proceso y la estereoquímica de los dobles enlaces producidos en la reacción se pueden deducir en base a lo discutido anteriormente para la síntesis de los complejos ciclofánicos bimetálicos.

La capacidad de estos nuevos complejos metal-carbeno para funcionar como anfitriones de pequeñas moléculas o átomos está todavía en fase de estudio. Sin embargo, se ha estimado mediante cálculos teóricos llevados a cabo a nivel PM3 sobre el tetraéster modelo **4**, que la cavidad generada en tales complejos permite acomodar a un huésped cuyo tamaño se encuentre en torno a 6Å (Figura 4). El tamaño de dicha cavidad puede variarse a voluntad seleccionando el molde biscarbeno y la bisamina utilizada según nuestras necesidades.[5]

[5] Tesis Doctoral de María Pascual, en realización.

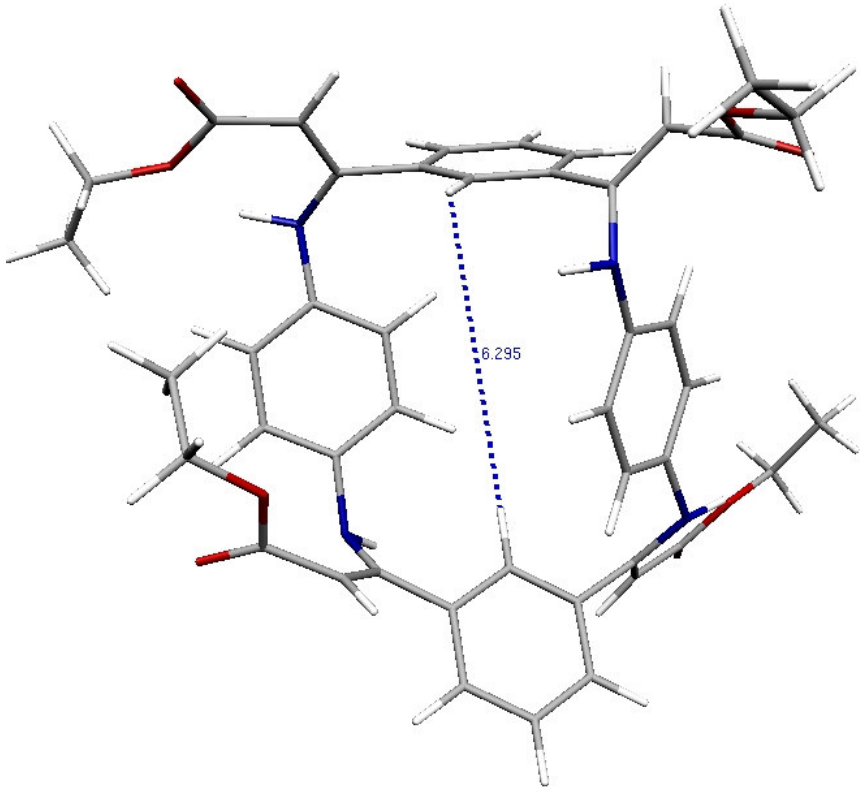

4

Figura 4

El comportamiento electroquímico de los complejos polimetálicos sintetizados, se ha estudio mediante voltamperometría cíclica. Como se ha discutido en el Capítulo I, estos complejos muestran una única onda de oxidación irreversible en el rango de E_{pa} = 0.88−0.92 V para complejos de cromo y de E_{pa} = 1.03−1.04 V para los de wolframio (esta diferencia sigue la tendencia general encontrada en complejos metal-carbeno del grupo 6). Los valores de E_{pa} obtenidos son similares a los encontrados para complejos monometálicos y bimetálicos no ciclofánicos análogos, lo que nos lleva a pensar que los distintos centros metálicos presentes en la moléculas se oxidan a la vez sin que exista prácticamente ningún tipo de interacción entre los mismos.

Puesto que las aminas empleadas tienen potenciales de oxidación más bajos que los encontrados en los distintos complejos sintetizados, podemos decir que dichas aminas actúan en el complejo tetrametálico únicamente como dadores de electrones. Por tanto, un cambio en la bisamina utilizada no provoca cambios significativos en los potenciales de oxidación de los complejos. Este hecho demuestra que dichos complejos

son híbridos de resonancia entre las estructuras **I** y **II**, presentando esta última una elevada contribución a la estructura electrónica real de tales compuestos (Figura 5). Es necesario resaltar que aunque la participación de formas de tipo II en la descripción de β-aminocarbenos se ha propuesto en repetidas ocasiones, ésta es la primera vez en que este hecho se demuestra experimentalmente. Por otra parte, los procesos redox en los que se pierden cuatro electrones simultáneamente como en el caso que nos ocupa, no son, en modo alguno, frecuentes.

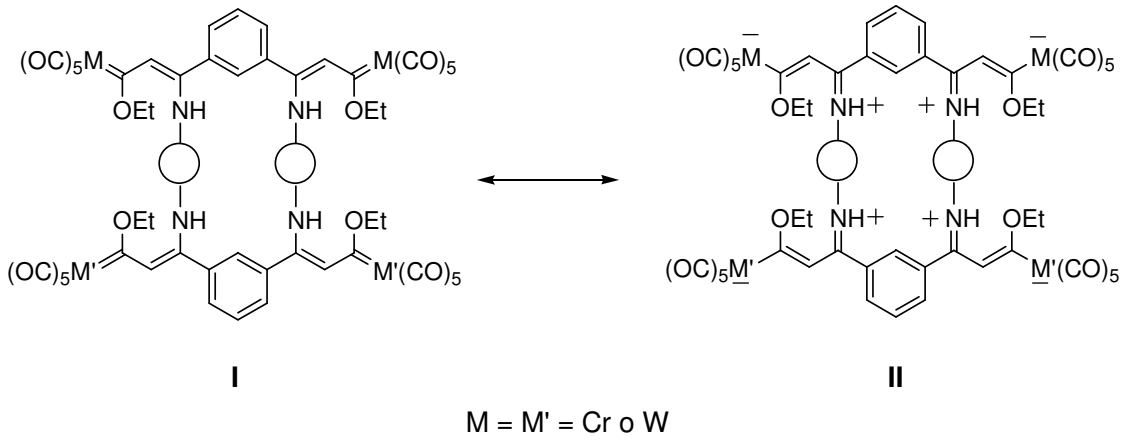

I **II**

M = M' = Cr o W

Figura 5

Por tanto, hemos desarrollado un método general, eficiente y versátil para la síntesis de complejos metal-carbeno bi- y polimetálicos de tipo Fischer del grupo 6 con estructuras conformacionalmente restringidas de tipo ciclofánicas o macrocíclicas. Dicho proceso ocurre a través de adiciones 1,4 de tipo Michael y constituye el primer ejemplo sintético que transcurre con retención de los centros metálicos en los productos finales de reacción.

D.1.2. Nuevas formas de reactividad térmica entre complejos metal-carbeno e iminas[6]

Durante la síntesis de complejos metal-carbeno con un ligando fosfina en la esfera de coordinación del metal, hemos encontrado un nuevo proceso térmico desconocido en la química de estos compuestos. Cuando se calienta en hexano-benceno (1:1) una mezcla equimolar del complejo pentacarbonil[etoximetilcarbeno]cromo(0), **5**, y una iminofosfina de estructura general **6**, se obtienen complejos cromo-imidato, de estructura general **7**, con rendimientos moderados (Esquema 4).

[6] Fernández, I.; Mancheño, M. J.; Gómez-Gallego, M.; Sierra, M. A.; Lejon, T.; Hansen, L. K. *Organometallics* **2004**, *23,* 1851.

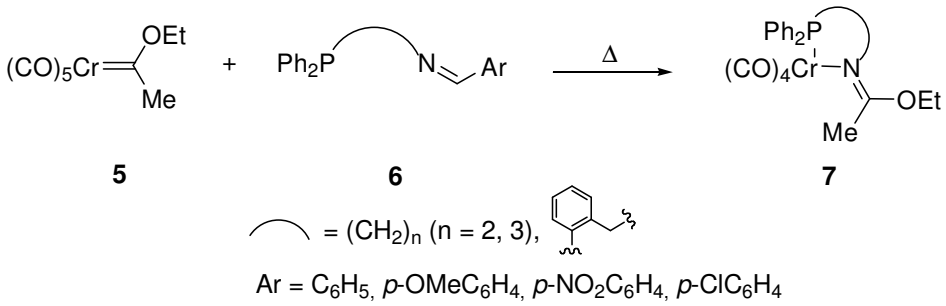

Esquema 4

Este nuevo proceso térmico no es general, dependiendo fuertemente de la longitud del espaciador en la iminofosfina, de la electrofilia de la imina y del volumen estérico de los sustituyentes en la misma. Así, únicamente las iminofosfinas con espaciadores cortos o rígidos, electrófilas y con sustituyentes moderadamente voluminosos son capaces de reaccionar con complejos metal-carbeno de Fischer electrófilos. Por tanto, las iminas voluminosas o carbenos menos electrofilos (como los de wolframio) no son eficaces a la hora de producir la reacción.

Estos hechos se pueden racionalizar en base a la formación del azametalaciclo **9** a partir del zwitterion **8**. La evolución de **8** a **9** sólo es posible cuando tratamos con iminas poco voluminosas y con enlaces C=N bastante electrófilos (con grupos electroatractores en el sustituyente aromático). A partir de **9**, el sistema evoluciona hacia el complejo cromo-imidato final mediante apertura del metalaciclo (en un proceso similar a la metátesis) y posterior complejación del nitrógeno al metal (Esquema 5).

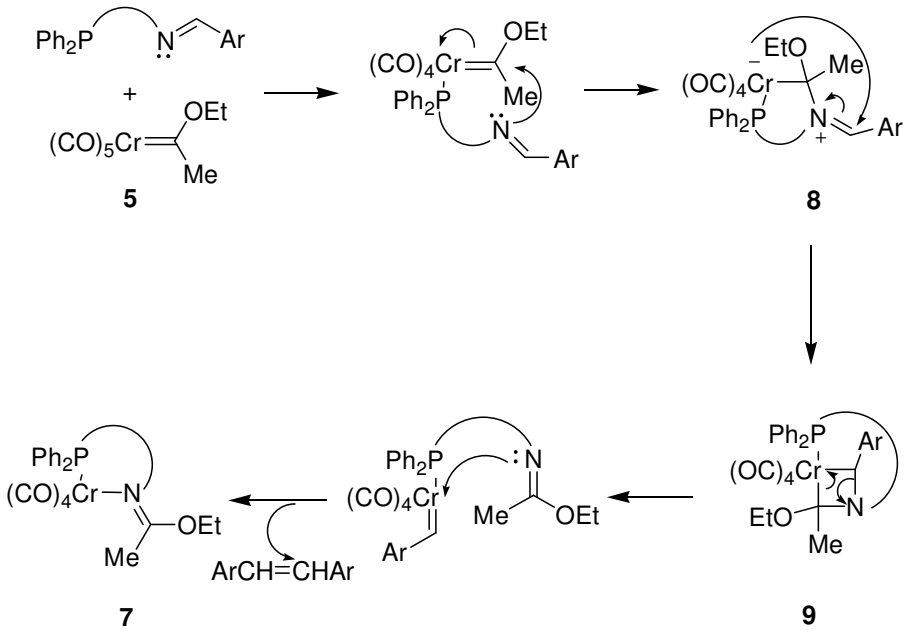

Esquema 5

Si tratamos con iminas voluminosas o poco electrófilas, el azametalaciclo **9** no se formará, por lo que el sistema o bien descompone o bien forma productos de condensación derivados de una reactividad ácido-base.

D.1.3. Espectrometría de masas ESI como herramienta para el estudio de procesos de transferencia electrónica en medios no convencionales

D.1.3.1. Complejos bi- y polimetálicos[7]

El empleo de la espectrometría de masas mediante ionización por electrospray (ESI-MS) constituye una herramienta valiosa para el estudio de procesos de transferencia electrónica (TE) en complejos metal-carbeno bi- y polimetálicos.

Cuando tratamos con complejos metal-carbeno de tipo Fischer con un grupo ferrocenilo unido al ligando carbeno a través de un espaciador π-conjugado (sistema dador-aceptor) no es necesaria la utilización de aditivos tales como la hidroquinona (HQ) para que ocurra la ionización. De hecho, el grupo ferrocenilo, cuya capacidad dadora se conoce bien, es capaz de actuar como un dador interno, aceptando los electrones procedentes de la fuente ESI y transfiriéndolos al aceptor carbeno a través del espaciador, con la consiguiente formación del anión-radical correspondiente (Esquema 6).

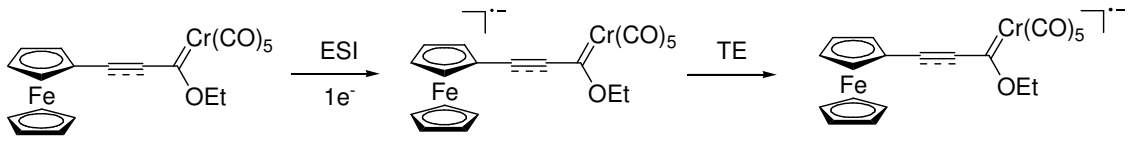

Esquema 6

Si tratamos con complejos en los que el grupo ferrocenilo se encuentra unido directamente al ligando carbeno (complejos **10a**,**b**, Figura 6), la ionización sólo ocurre en presencia de aditivos como la hidroquinona (HQ). De nuevo, la presencia de este grupo en el proceso de TE es indispensable puesto que, funcionando como transportador interno, permite la ionización y por tanto, la detección de tales complejos mediante MS. Este efecto se evidencia cuando sustituimos dicho grupo por un sustituyente fenilo, incapaz de funcionar como transportador. En este caso, la ionización no ocurre ni siquiera en presencia de aditivos.

[7] Martínez-Álvarez, R.; Gómez-Gallego, M.; Fernández, I.; Mancheño, M. J.; Sierra, M. A. *Organometallics* **2004**, *23*, 4647.

El comportamiento de aquellos complejos que poseen dos unidades metal-carbeno conectadas entre sí a través de un espaciador conjugado (complejos **11a**-**c**, Figura 6) es similar al comportamiento de sus análogos monometálicos. Por tanto, dichos complejos sólo se pueden ionizar en presencia de aditivos (HQ o TTF), lo que prueba de nuevo que la posible interacción entre los distintos centros metálicos es prácticamente inexistente.

Uno de los aspectos más relevantes y atractivos de este estudio ha sido comprobar cómo la unidad $Co_2(CO)_6$ se comporta como un sumidero de electrones en procesos de TE de este tipo. Así, cuando este grupo se encuentra presente en un complejo metal-carbeno (complejos **12** y **13**, Figura 6) inhibe el proceso de ionización del complejo. La justificación de este efecto se haya en que una vez que el fragmento $Co_2(CO)_6$ se ha reducido, tanto en condiciones ESI directas o mediante el empleo de aditivos ($HQ^{\bullet-}$), se oxida sin interaccionar con el enlace Cr-C. Este hecho queda probado por la detección de un pico en el espectro de masas (*m/z* 171) correspondiente a la especie $Co(CO)_4^{\bullet-}$. El mismo efecto se observa cuando se registra un experimento ESI-MS de un complejo metal-carbeno en presencia de $Co_2(CO)_8$.

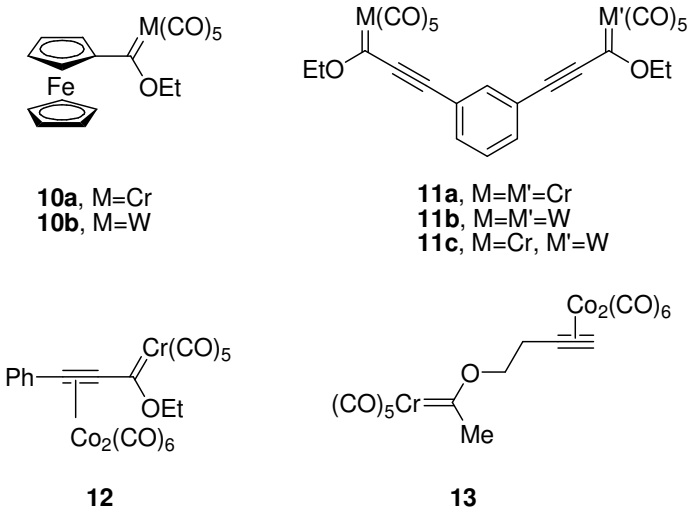

10a, M=Cr
10b, M=W

11a, M=M'=Cr
11b, M=M'=W
11c, M=Cr, M'=W

12

13

Figura 6

D.1.3.2. Mecanismo del proceso ESI-MS para complejos metal-carbeno

Como se ha discutido anteriormente, los complejos metal-carbeno α,β-insaturados como **14** sólo pueden ionizarse en condiciones ESI si están presentes transportadores de electrones. Este proceso se puede racionalizar mediante la captura inicial de un electrón por parte de **14** para formar el intermedio **15**, el cual evoluciona al

anión detectado [M - H]$^-$ por extrusión de un radical hidrógeno, a través de dos posibles caminos de reacción (Esquema 7).

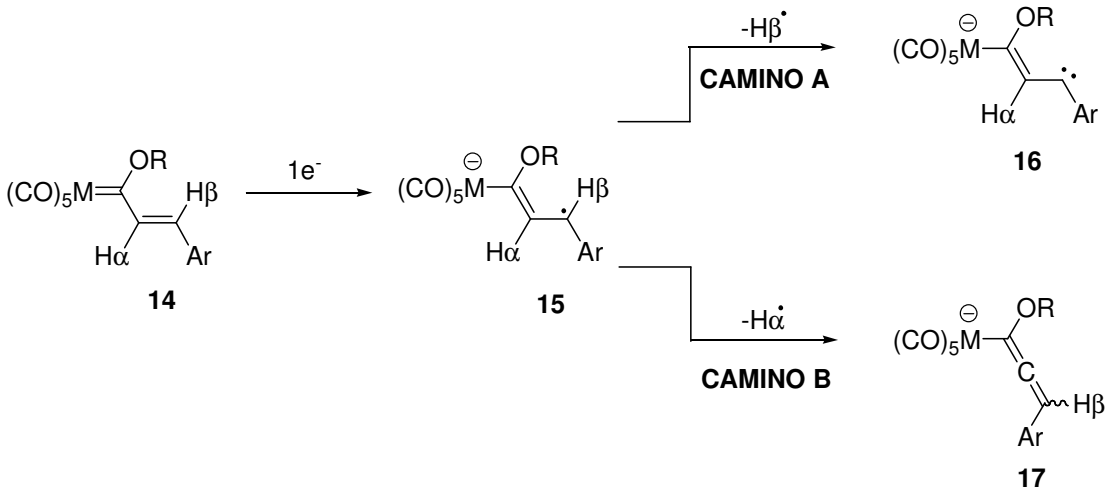

Esquema 7

Para distinguir entre ambos caminos y desarrollar simultáneamente una metodología para estudiar los procesos de TE en medios no convencionales, se sintetizó el complejo **18**. El registro del espectro ESI-MS de **18** en presencia de HQ muestra un ión pseudomolecular a *m/z* 358 correspondiente a [M - H]$^-$ sin que ocurra pérdida de deuterio. Este hecho, nos lleva a pensar que el camino de evolución preferido es la extrusión de Hα. Para confirmar esta hipótesis, también se sometió a las mismas condiciones de ionización al complejo **19** (Figura 7). En este caso, el anión detectado corresponde a la especie [M - D]$^-$ (*m/z* 357), demostrando de forma inequívoca que el camino de evolución del anión-radical **15** es el B.

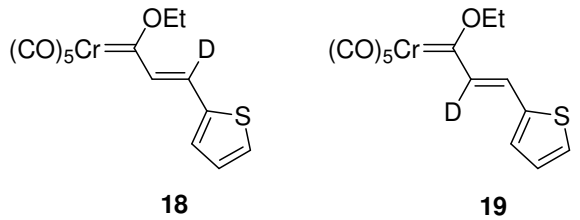

Figura 7

La preferencia por la extrusión de Hα se he establecido en base a la estabilidad relativa de las especies **16** y **17**. Mediante métodos computacionales efectuados a nivel B3LYP/6-31G(d)&LanL2DZ sobre el complejo pentacarbonil[estirilmetoxi]cromo(0) carbeno en fase gas, se comprueba que la especie de tipo aleno (análoga a **17**) es mucho

más estable (ΔE = 34.05 kcal mol^{-1}) que la especie de tipo carbeno (análoga a **16**). Este estudio teórico complementa lo observado en el estudio experimental de deuteración selectiva.

También hemos estudiado el mecanismo de ionización en complejos alquinil-carbeno de tipo **20**. En este caso, utilizando de nuevo la deuteración selectiva, se ha comprobado que la extrusión de hidrógeno ocurre desde el anillo aromático, lo que provoca la formación del alenil-anión detectado posteriormente como [M - D]$^-$ (Esquema 8). Este hecho descarta la posibilidad de una transferencia de hidrógeno desde el grupo etoxi a la especie **21** seguida de extrusión de hidrógeno (camino B).

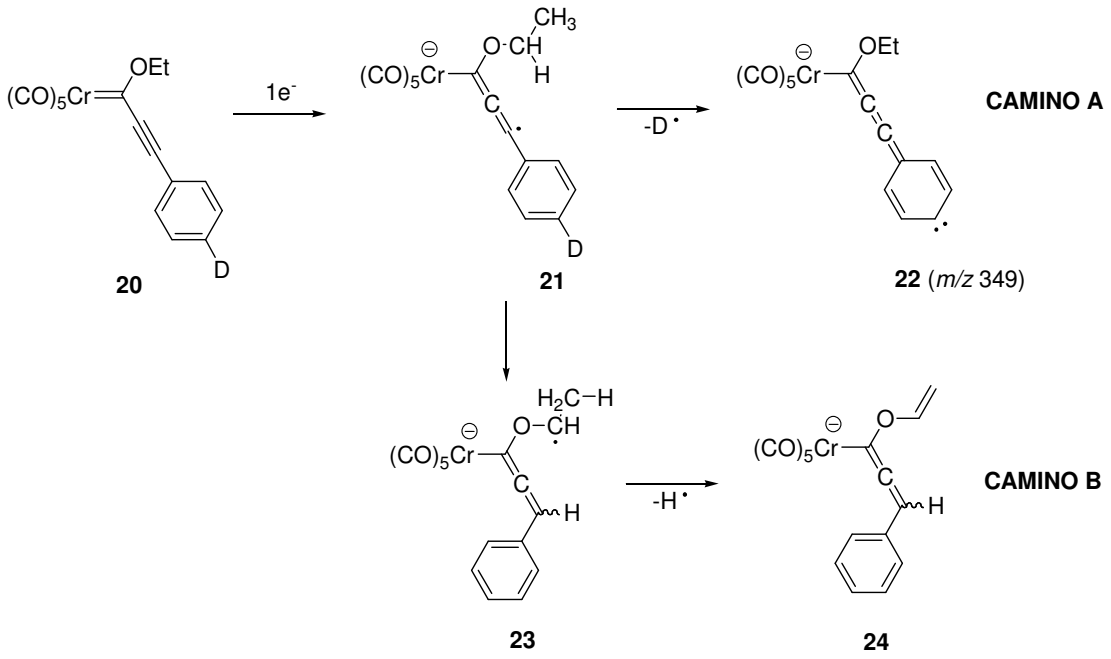

Esquema 8

Por tanto, mediante el empleo de dos técnicas usuales en la determinación de mecanismos de reacción, como son las técnicas de marcaje isotópico y técnicas computacionales, hemos conseguido adentrarnos en la intimidad de una reacción organometálica en fase gas y, así, hemos conseguido proponer un camino de reacción razonable que satisface todos los datos, experimentales y teóricos, encontrados en el proceso de transferencia electrónica en complejos metal-carbeno de tipo Fischer en un medio no convencional como es ESI-MS. Se demuestra, por tanto, que esta aproximación es viable para el estudio de procesos de TE en fase gaseosa.

D.2. Capítulo II

D.2.1. Estructura y conformaciones de complejos alcoximetal-carbeno[8]

Tanto los complejos alcoximetal-carbeno como sus homólogos no metálicos pueden existir en dos conformaciones, la forma *anti* y la forma *sin* (Figura 8), siendo la primera la forma de menor energía.

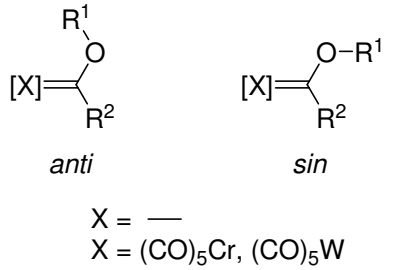

Figura 8

La preferencia por la forma *anti* puede explicarse en base a dos efectos aditivos. El isómero *sin* posee dos interacciones desfavorables: una interacción estérica entre el sustituyente unido al átomo de oxígeno y el sustituyente unido al carbono carbénico y otra, la repulsión electrónica entre el par de electrones del carbeno y los pares de electrones no enlazantes del átomo de oxígeno (Figura 9). Evidentemente, esta última interacción no ocurre en los complejos metálicos puesto que el carbeno se encuentra coordinado al metal.

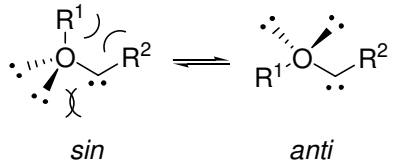

Figura 9

En el caso de complejos metálicos deberíamos encontrar una interacción desestabilizante de tipo estérica entre el sustituyente R^1 y la pared de CO_{cis} de la esfera de coordinación del metal, presente en la forma *anti* pero no en la forma *sin*. Sin embargo, está interacción queda minimizada debido a tres factores: a) alargamiento de la distancia metal-carbono carbenoide en la forma *anti* con respecto a la *sin*, b) adopción de una conformación alternada entre dos grupos CO*cis* que minimiza la repulsión

[8] Fernández, I.; Cossío, F. P.; Arrieta, A.; Lecea, B.; Mancheño, M. J.; Sierra, M. A. *Organometallics* **2004**, *23*, 1065.

estérica y c) interacción estabilizante de tipo estereoelectrónico sólo presente en la forma *anti*. Esta interacción se produce por la donación electrónica desde el orbital σ_{CH} del resto OR^1 al orbital antienlazante π^*_{CO} de un ligando CO, junto a retrodonación desde el orbital π_{CO} al orbital antienlazante σ^*_{CH} (Figura 10).

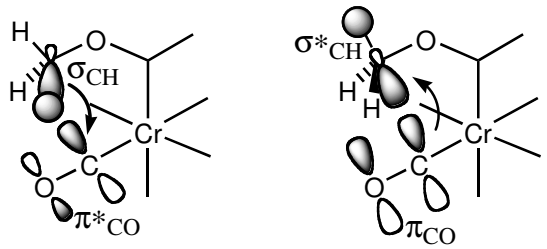

$\Delta E(2)$=-0.21 kcal mol^{-1} $\Delta E(2)$=-0.67 kcal mol^{-1}

Figura 10

La isomerización *anti→sin* en los complejos metal-carbeno ocurre mediante rotación simple del enlace O-C (del sustituyente R^1) sin afectar al ligando carbeno. De hecho, el estado de transición que conecta ambas formas conserva la disposición alternada característica de ambas especies. Por tanto, aunque la diferencia de energía entre ambas especies *sin-anti* en complejos metal-carbeno es menor que la observada entre las formas de los carbenos no metalados, todos estos efectos hacen que la forma *anti* sea la preferida para complejos metal-carbeno del grupo 6. Los datos de rayos-X recogidos en la literatura química para un número elevado de complejos metal-carbeno confirman plenamente el modelo propuesto.

D.2.2. Fotocarbonilación de complejos metal-carbeno

La irradiación (luz visible) de un complejo metal-carbeno supone la promoción de un electrón desde un orbital no enlazante centrado en el metal (HOMO) a un orbital π^* centrado en el carbono carbenoide (orbital p del carbeno, LUMO), por lo que puede considerarse como una oxidación formal del metal que involucra un electrón.

Empleando métodos computacionales, hemos encontrado que la irradiación de complejos alcoxicromo-carbeno, bien sea en la banda LF seguida de relajación a la MLCT o directamente en la banda MLCT, provoca la excitación de los mismos al primer singlete excitado S_1, el cual decae rápidamente al estado triplete T_1 mediante cruce intersistémico (ISC). Este ISC, extremadamente eficiente, se debe al acoplamiento espín-órbita inducido por el átomo de cromo. Este proceso ocurre de la misma manera

tanto desde la forma más estable de este tipo de complejos, *anti,* como desde la forma de mayor contenido energético, *sin* (Figura 11).

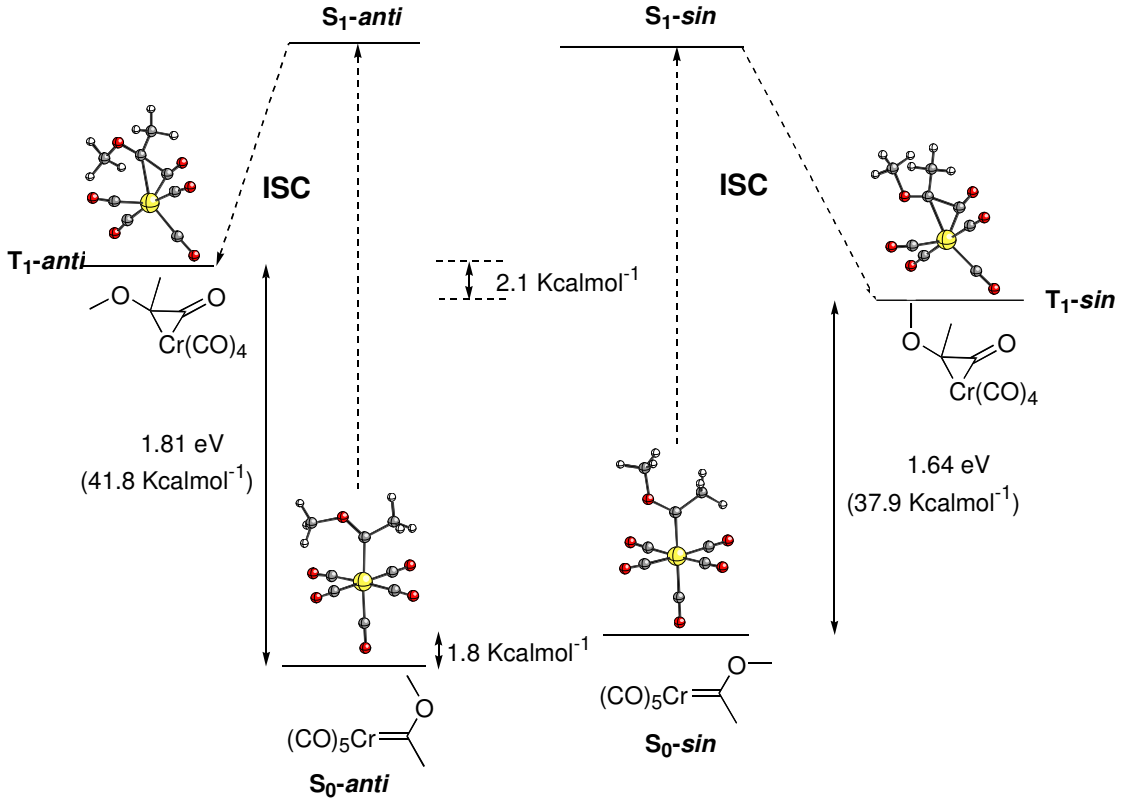

Figura 11

La estructura de los tripletes T_1-*sin* y T_1-*anti* nos indica que nos encontramos ante especies de naturaleza cromaciclopropanona (estructura **III**, Figura 12) como resultado de la inserción de uno de los ligandos CO_{cis} en el enlace cromo-carbeno. Estos complejos son coordinativamente insaturados y se pueden considerar como birradicales teniendo en cuenta los valores de densidad de espín calculados para los mismos (T_1-*sin*: Cr = 0.96 u.a., C = 0.46 u.a.; T_1-*anti*: Cr = 0.95 u.a., C = 0.43 u.a.).

La introducción de una molécula de disolvente en la vacante de coordinación generada en el estado triplete, conduce a la saturación de la misma. La optimización de la geometría de este nuevo estado estacionario singlete condujo, tanto desde la forma *sin* como desde la forma *anti*, a un nuevo complejo en el que el grupo alcoxilo se posiciona hacia fuera del plano de los carbonilos (forma *sin*). La estructura de este complejo nos indica que nos encontramos ante una especie de naturaleza cetena coordinada a metal (estructura **IV**, Figura 12), en la que el enlace metal-carbono (inicialmente el carbono

carbenoide) se encuentra fuertemente polarizado, o lo que es lo mismo, esta especie posee carácter de acilcromato (estructura **V**, Figura 12).

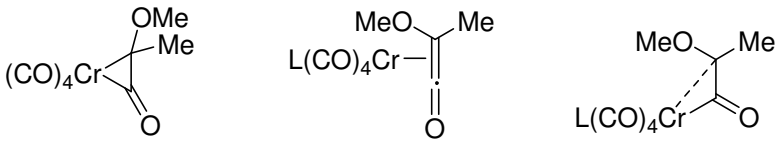

III **IV** **V**

Figura 12

El empleo de un disolvente coordinante en las reacciones fotoquímicas de este tipo de complejos organometálicos es, por tanto, crucial para el devenir de las mismas. Este hecho se ha comprobado experimentalmente, observándose un descenso drástico del rendimiento de la reacción entre complejos metal-carbeno e iminas al utilizar disolventes con números de donación (DN) bajos, o lo que es lo mismo, con poca capacidad coordinativa (Tabla 1).

Tabla 1.

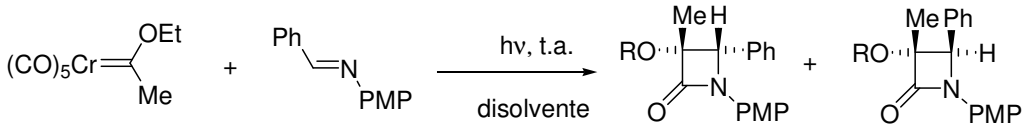

cis ***trans***

Entrada	Disolvente	DN	Conversión	*cis /trans*
1	Hexano	–	32	7.3:1
2	Benceno	–	55	3.2:1
3	CH_2Cl_2	0.00	69	4.4:1
4	THF	0.52	85	1:1
5	MeCN	0.36	90	6.3:1

Desde este punto, y en la hipersuperficie S_0, el sistema evolucionará hacia los productos de reacción si en el medio existen sustratos capaces de reaccionar con cetenas o bien, revertirá hacia la forma *sin* del complejo cromo-carbeno de partida, a través de una ruta fuertemente exotérmica, en ausencia de dichos sustratos. Así, nuestros cálculos justifican la isomerización *anti→sin* encontrada experimentalmente en la irradiación de este tipo de complejos en la banda MLCT en ausencia de cetenófilos.

La reacción de fotocarbonilación así descrita es, teóricamente, compatible con complejos de cromo en los que se ha realizado un intercambio de ligando en la esfera de coordinación. Concretamente, la fotoinserción ocurre cuando introducimos uno, o

incluso dos ligandos σ-dadores de tipo fosfina. Las especies calculadas en estos casos poseen una naturaleza muy similar a la de sus análogos homolépticos; la única diferencia se encuentra en un mayor carácter de acilcromato para la estructura **V** (Figura 13), debido al efecto dador del ligando fosfina que hace al metal menos susceptible de aceptar carga desde el ligando acilo.

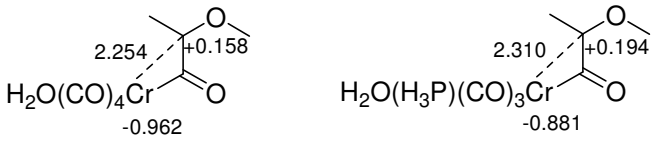

Figura 13

Por otra parte, nuestro modelo explica la inercia frente a la fotocarbonilación de complejos alcoxiwolframio-carbeno encontrada experimentalmente. En este caso, las especies triplete derivadas de carbenos de wolframio no poseen una estructura similar a la que muestran sus análogos de cromo (estructura **III**), o lo que es lo mismo, no ocurre la inserción de CO en el enlace metal-carbeno cuando tratamos con complejos wolframio-carbeno. Este hecho se debe a la mayor fortaleza de enlace metal-carbono (W-C(=O)), junto con la menor nucleofilia del carbono carbenoide en el estado excitado que impiden la fotoinserción del ligando CO.

D.2.3 Mecanismo de la fotorreacción de complejos cromo-carbeno de tipo Fischer con iminas[9]

La reacción entre complejos metal-carbeno e iminas para producir β-lactamas ocurre en la hipersuperficie S_0 desde una especie de naturaleza acilcromato (estructura **V**, Figura 12). Como en la reacción de Staudinger clásica entre cetenas e iminas, el proceso es *cis*-selectivo y transcurre a través de un mecanismo por etapas y no mediante un camino concertado de tipo $[\pi 2_s+\pi 2_a]$ o $[\pi 2_s+(\pi 2_s+\pi 2_s)]$.

Una vez formado el enlace entre el carbono del carbonilo fotoinsertado y el nitrógeno de la imina, **INT2**, ocurre un desplazamiento 1,3- de cromo que conduce a un zwitterion de naturaleza enolato de cromo-iminio, **INT3**, el cual evoluciona mediante cierre conrotatorio, sujeto a efectos torcuoelectrónicos, al producto de reacción (Esquema 9).

[9] Arrieta, A.; Cossío, F. P.; Fernández, I.; Gómez-Gallego, M.; Lecea, B.; Mancheño, M. J.; Sierra, M. A. *J. Am. Chem. Soc.* **2000**, *122*, 11509.

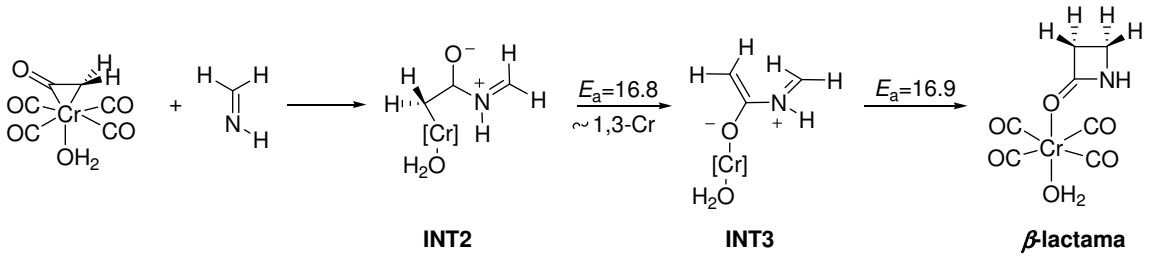

Esquema 9

Quizás el hecho más importante de este mecanismo sea que el metal permanece unido al centro reactivo durante toda la coordenada de reacción. Esto significa que tanto la eficacia como la selectividad de la reacción pueden modularse variando la naturaleza misma del complejo metal-carbeno utilizado. De hecho, se ha demostrado que variaciones en la esfera de coordinación del metal provocan cambios importantes en el rendimiento de la reacción, así como en la proporción de isómeros *cis/trans* de las β-lactamas producidas en la misma.

Concretamente, se ha estudiado el efecto provocado por el intercambio de un ligando CO por un ligando σ-dador de tipo fosfina. En general, podemos decir que este tipo de complejos son menos fotorreactivos que sus análogos homolépticos, disminuyendo drásticamente la conversión del proceso cuanto mayor es el carácter σ-dador del ligando introducido en la esfera de coordinación del complejo. Las razones que justifican este comportamiento no se conocen en este momento y se están estudiando exhaustivamente en la actualidad. En cualquier caso y como predicen los datos computacionales, los complejos metal-carbeno de tipo Fischer que poseen ligandos de tipo fosfina son capaces de insertar fotoquímicamente CO en el enlace metal-carbeno para generar metalacetenas, capaces de reaccionar con cetenófilos tales como iminas.

La reacción fotoquímica entre complejos metal-carbeno e iminas para producir β-lactamas es *cis*-selectiva. A pesar de ello, la proporción de isómeros *cis*/*trans* depende en gran medida de las condiciones de reacción empleadas, sobre todo de la temperatura de reacción y del disolvente empleado. El origen de la diastereoselección observada no se encuentra en el cierre conrotatorio que conduce a las β-lactamas, como ocurre en el mecanismo clásico de esta reacción. Nuestros resultados permiten proponer que el origen de la selectividad se debe encontrar en la migración 1,3- metalotrópica.

D.2.4. Nuevas formas de reactividad fotoquímica en complejos metal-carbeno[10]

Hasta la fecha, la reactividad fotoquímica de complejos metal-carbeno se limitaba a procesos derivados de la fotoinserción de CO en el enlace metal-carbeno. Sin embargo, es posible diseñar metalocarbenos capaces de producir nuevas formas de reactividad fotoquímica. En estos compuestos, el heteroátomo del ligando carbeno queda unido al núcleo metálico a través de un ligando fosfina y una cadena hidrocarbonada de longitud y rigidez variables.

La elección de este tipo especial de complejos (Esquema 10) se hizo atendiendo a los siguientes hechos experimentales: a) se conoce que no todos los complejos amino-carbenoides dan la reacción fotoquímica con iminas para producir β-lactamas; en concreto, complejos de tipo $[(CO)_5Cr{=}C(NMe_2)Me]$, $[(CO)_5Cr{=}C(NBn_2)Me]$ ó $[(CO)_5Cr{=}C(NMe_2)Ph]$ se consideran fotoinertes;[11] b) los complejos cromo-carbeno en los que se ha introducido un ligando σ-dador como una fosfina en la esfera de coordinación del metal, reaccionan con bastante peor eficacia que los complejos análogos sin fosfina;[9] c) los complejos wolframio-carbeno no dan la reacción de fotocarbonilación.

La modificación de la estructura en estos complejos nos ha permitido encontrar nuevas formas de reactividad fotoquímica. Así, la irradiación de los complejos metal–carbeno de estructura general **25** conduce a iminas *N*-metaladas de estructura **26** (Esquema 10).

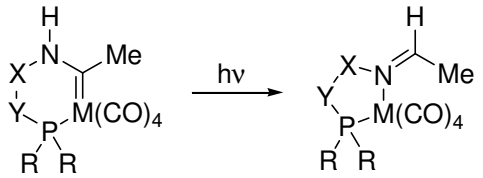

25 **26**

Esquema 10

La formación de tales iminas es un nuevo proceso fotoquímico diferente a la fotocarbonilación. En este caso, ocurre un reordenamiento carbeno→imina sin precedente alguno en la literatura química. Esta reacción ocurre con cadenas hidrocarbonadas de diferente longitud y rigidez, incluso en ausencia de tales cadenas

[10] Sierra, M. A.; Fernández, I.; Mancheño, M. J.; Gómez-Gallego, M.; Torres, M. R.; Cossío, F. P.; Arrieta, A.; Lecea, B.; Poveda, A.; Jiménez-Barbero, J. *J. Am. Chem. Soc.* **2003**, *125*, 9572.
[11] Hafner, A.; Hegedus, L. S.; deWeck, G.; Hawkins, B.; Dötz, K. H. *J. Am. Chem. Soc.* **1988**, *110*, 8413.

(utilizando PPh_3 como ligando) y lo que es más importante, tiene lugar para todo tipo de complejos metal-carbeno del grupo 6, por lo que puede considerarse como un reordenamiento general.

Utilizando métodos computacionales, hemos determinado que esta transformación es un reordenamiento 1,2-diotrópico de tipo I, donde los enlaces M-C y N-H migran y los átomos M y H intercambian sus posiciones, permaneciendo la unidad C=N estática (Esquema 11).

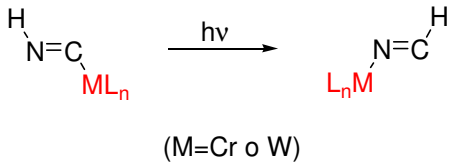

Esquema 11

Al igual que ocurre en el proceso de fotocarbonilación, podemos asumir que la reacción diotrópica comienza desde un triplete de vida corta, formado tras la fotoexcitación vertical del complejo aminocarbeno desde el estado S_0 al estado excitado S_1. La diferencia se encuentra en que en el nuevo birradical formado no ha ocurrido fotoinserción alguna de ningún ligando CO en el enlace metal-carbeno. Desde este punto, el reordenamiento ocurre por etapas[12] y en la hipersuperficie triplete generando iminas *anti-N*-metaladas de manera selectiva y con rendimientos desde buenos a excelentes.

Los perfiles de reacción calculados para complejos de cromo y de wolframio son prácticamente idénticos, con barreras de activación muy similares. Por tanto, podemos decir que el reordenamiento es general e independiente del metal con el que tratemos (Esquema 12). Aún más, *éste constituye el primer ejemplo descrito en el que un complejo metal-carbeno de tipo Fischer de wolframio es capaz de producir un proceso fotoquímico con eficacia*.

[12] Hasta la fecha, sólo existe un único precedente en el que un reordenamiento 1,2-diotrópico ocurre por etapas, ver: Zhang, X.; Houk, K. N.; Lin, S.; Danishefsky, S. J. *J. Am. Chem. Soc.* **2003**, *125*, 5111.

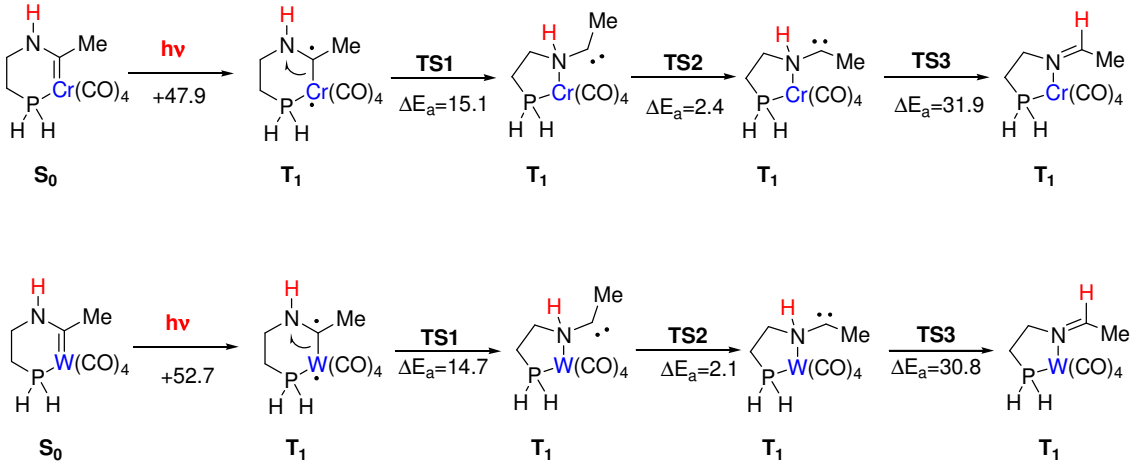

Esquema 12

A pesar del escaso interés sintético que posee esta reacción, su importancia radica en que constituye un proceso totalmente nuevo en la fotoquímica de complejos metal-carbeno y extraordinariamente raro en química organometálica. Se abren así las puertas para encontrar nuevos caminos de reacción y avanzar en el conocimiento de la fotoquímica de especies metálicas. De hecho, un simple cambio en la naturaleza del sustituyente directamente unido al átomo de nitrógeno en este tipo de complejos provoca cambios sustanciales en la reactividad de los mismos.

Según el caso, los complejos de estructura general **27** pueden producir dos tipos diferentes de productos cuando se irradian en presencia de MeOH: ésteres **28**, procedentes de un proceso de fotocarbonilación estándar, y/o aminofosfinas *N*-metaladas **29**, procedentes de un nuevo proceso fotoquímico (Esquema 13).

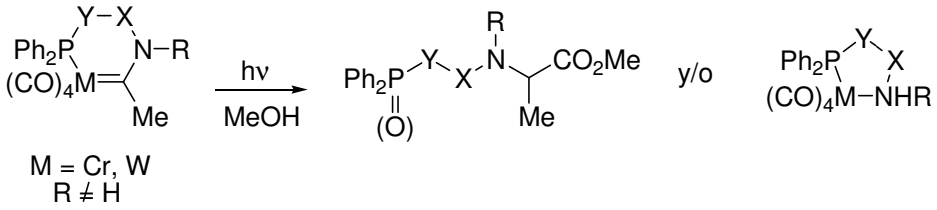

Esquema 13

La formación de los complejos **29** constituye otro nuevo proceso fotoquímico en complejos metal-carbeno de tipo Fischer. Basándonos en métodos computacionales, hemos propuesto un camino de reacción para este proceso. Éste transcurre en la hipersuperficie triplete desde una especie de naturaleza birradicálica similar a la especie desde donde comienza el reordenamiento diotrópico. Sin embargo, debido a la

sustitución en el átomo de nitrógeno, esta especie excitada evoluciona de una manera diferente. Ahora la migración 1,2- de hidrógeno produce metalaenaminas que, tras hidrólisis y posterior complejación del nitrógeno al metal, generan las correspondientes aminofosfinas **29**. De nuevo, los perfiles de reacción calculados para complejos de cromo y de wolframio son prácticamente idénticos, con barreras de activación muy similares (Esquema 14), por lo que este proceso es independiente del metal con el que tratemos.

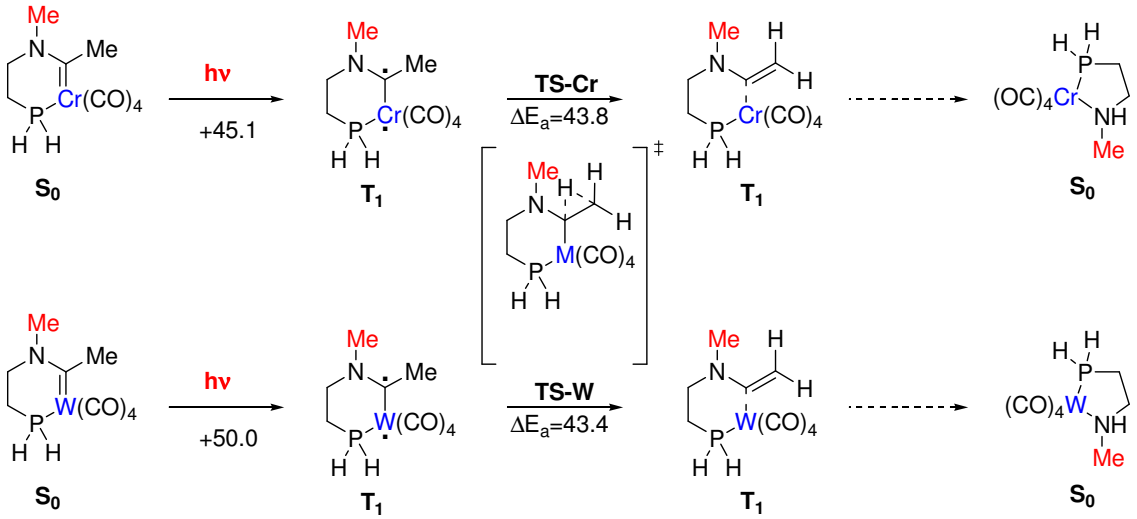

Esquema 14

La formación simultánea en muchos casos de los productos **28** y **29** se explica por a la coexistencia de dos tripletes distintos muy próximos en energía para los complejos **27** tras excitación de los mismos al estado excitado singlete y posterior ISC al estado excitado triplete (Esquema 15).

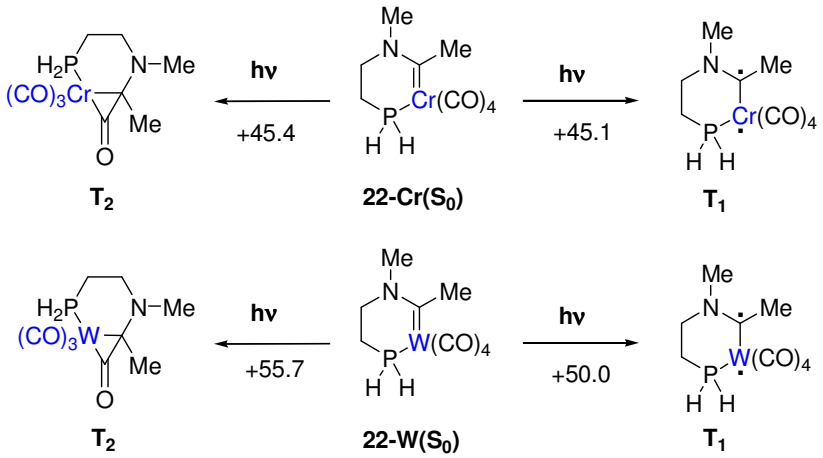

Esquema 15

El primero de ellos posee un estructura de tipo metalaciclopropanona y por tanto conduce a los productos de fotocarbonilación **28**, mientras que el otro es un birradical, de tipo *diotrópico*, que conduce a los complejos **29**. En el caso de complejos de cromo, ambas especies triplete son prácticamente isoenergéticas ($\Delta E_{T2\text{-}T1}$ = 0.3 kcal mol^{-1}), mientras que la especie de fotocarbonilación derivada de wolframio es considerablemente más energética que el triplete pseudodiotrópico ($\Delta_{ET2\text{-}T1}$ = 5.7 kcal mol^{-1}). Estos resultados justifican la escasa reactividad de los complejos wolframio-carbeno frente al proceso de fotocarbonilación y su preferencia hacia la formación de las aminas *N*-metaladas **29**. Aún así, puesto que la diferencia de energía no es muy grande, es posible encontrar casos en los que la fotocarbonilación sea el camino preferido. Por otro lado, en el caso de los cromocarbenos, la coexistencia de dos especies triplete prácticamente isoenergéticas hace que se produzcan mezclas de reacción, justificándose de nuevo los resultados experimentales.

Por tanto, podemos diseñar complejos metal-carbeno de manera que seamos capaces de controlar a voluntad su reactividad fotoquímica. Ligeros cambios en la estructura del complejo provocan cambios drásticos en su reactividad fotoquímica, hasta el extremo de poder efectuar fotocarbonilaciones en complejos de wolframio, compuestos tradicionalmente considerados fotoinertes.

El trabajo realizado hasta el momento ha permitido describir dos nuevos procesos fotoquímicos en complejos metal-carbeno del grupo 6 de tipo Fischer inéditos hasta el momento (reordenamiento 1,2-diotrópico de tipo I y proceso *pseudodiotrópico*) y abre la puerta al estudio de nuevos procesos en la fotoquímica de este tipo concreto de complejos organometálicos.

CONCLUSIONES

C.1. Conclusiones del Capítulo I

- Se ha descrito un procedimiento sencillo y eficaz para la síntesis de complejos metal-carbeno bi- y tetrametálicos con estructuras conformacionalmente restringidas. Este método es el primer ejemplo de síntesis de complejos ciclofánicos y macrocíclicos que transcurre con retención de los fragmentos metálicos en los productos finales de reacción. El control estereoquímico del proceso se produce debido a la existencia de enlaces de hidrógeno entre los hidrógenos unidos a nitrógeno y los oxígenos de los grupos etoxi de los ligandos carbeno. Los complejos formados poseen esteroquímica *Z,Z*.

- El estudio del comportamiento electroquímico de estos complejos muestra que los distintos centros metálicos se oxidan a la vez, comportándose de manera aislada en la molécula sin que exista, por tanto, ningún tipo de interacción entre los distintos núcleos.

- Se ha descrito una nueva reacción térmica entre complejos metal-carbeno e iminas. Este proceso proporciona imidatos de cromo estables con rendimientos moderados mediante un curso de reacción de tipo metátesis por etapas.

- La ionización por electrospray en espectrometría de masas (ESI-MS) demuestra que la ionización directa de complejos metal-carbeno bi- y polimetálicos requiere tanto un grupo dador de electrones, como el ferroceno, como de un espaciador π-conjugado funcionando como canal comunicador con el aceptor. La incorporación del clúster $Co_2(CO)_6$ en la estructura de estos complejos inhibe la ionización incluso en presencia de aditivos externos. Por esta razón, hemos acuñado el término "sumidero de electrones" para tal grupo en las condiciones ESI-MS empleadas.

- Utilizando una combinación de técnicas de marcaje isotópico selectivo y cálculos DFT, se ha diseccionado el mecanismo de ionización de complejos metal-carbeno conjugados de tipo Fischer en condiciones ESI. Los resultados indican que en la fuente ESI, y después de que ocurra el proceso de transferencia electrónica mediado por hidroquinona desde la gota cargada al complejo, se forma un anión radical. Esta especie evoluciona, tras extrusión de un radical hidrógeno, hacia un anión alenilcromo que es la especie detectada en el espectro de masas como $[M - H]^-$. Esta aportación supone uno de los escasos intentos realizados hasta el momento con el fin de entender el proceso de transferencia electrónica en las gotas cargadas.

C.2. Conclusiones del Capítulo II

- Los complejos alcoximetal-carbeno de tipo Fischer del grupo 6 muestran, al igual que los carbenos libres no metalados, una clara preferencia hacia una disposición *anti* del sustituyente directamente unido al átomo de oxígeno. Este comportamiento se debe principalmente a la existencia de una interacción estabilizante de tipo estereoelectrónico sólo presente en la forma *anti* y que consiste en la donación electrónica desde el orbital σ_{CH} del resto alcoxi al orbital antienlazante π^*_{CO} de un ligando CO y retrodonación desde el orbital π_{CO} al orbital antienlazante σ^*_{CH}.

- La irradiación de complejos cromo-carbeno con luz visible provoca la excitación de los mismos al primer singlete excitado S_1, el cual decae rápidamente al estado triplete T_1 mediante cruce intersistémico (ISC) debido al acoplamiento espín-órbita inducido por el átomo de cromo. La estructura de las especies en el estado triplete se corresponde con una metalaciclopropanona. Esta inserción de CO ocurre en complejos metal-carbeno de cromo(0), independientemente de los ligandos en la esfera de coordinación del metal. En carbenos derivados de wolframio(0), la mayor fortaleza del enlace W-CO junto a la menor nucleofilia del carbono carbenoide en el estado excitado impiden la fotoinserción del ligando CO*cis* en enlace W-$C_{carbeno}$.

- Las especies triplete saturan su vacante de coordinación con una molécula de disolvente coordinante. La estructura de estas especies reactivas en la hipersuperficie singlete se corresponde con la de una cetena coordinada a cromo en la que el enlace metal-carbeno original se encuentra muy polarizado (esta polarización todavía es mayor en el caso de intercambiar un ligando CO por una fosfina debido a su gran carácter σ-dador).

- La reacción entre estas metalacetenas e iminas para producir β-lactamas transcurre en la hipersuperficie singlete siguiendo un mecanismo por etapas. Se ha comprobado, tanto experimental como teóricamente, que el metal permanece unido durante toda la coordenada de reacción, existiendo una migración 1,3- de cromo durante el proceso. El proceso es *cis*-selectivo estando la diastereoselectividad de la reacción fuertemente influenciada por el disolvente empleado, la temperatura de reacción y los sustituyentes en la esfera de coordinación del metal.

- La fotoquímica de complejos metal-carbeno de tipo Fischer es susceptible de ser modificada cambiando adecuadamente la estructura del complejo. Los complejos aminocarbeno, tanto de cromo como del fotoinerte wolframio, producen iminas *N*-

metaladas mediante un curso de reacción en el estado triplete que puede ser considerado como un reordenamiento 1,2-diotrópico de tipo I por etapas desconocido al inicio de esta tesis.

- La modificación de los sustituyentes en el nitrógeno de los aminocarbenos conduce a su vez a nuevas formas de reactividad, que van desde la fotocarbonilación a procesos *pseudodiotrópicos*. El estudio computacional detallado de los distintos procesos muestra la coexistencia de dos especies triplete diferentes para estos complejos, cuyas diferencias en energía justifican tanto los distintos cursos de reacción encontrados experimentalmente como el comportamiento diferencial de complejos de cromo(0) y wolframio(0).